



Dipl.-Ing. Bernhard Walzel

Automated Charging of Electric Vehicles with Conductive Standards

DOCTORAL THESIS

to achieve the University Degree of
Doktor der technischen Wissenschaften
submitted to

Graz University of Technology

Assessors:

Assoc.-Prof. Dr.techn. Mario Hirz
Institute of Automotive Engineering

Assoc.-Prof. Dr.techn. Benjamas Panomruttanarug
King Monkut's University of Technology Thonburi, Bangkok, Thailand

Graz, May 2020

Foreword

This doctoral thesis was written during my work as a doctoral student and scientific assistant at the Institute of Automotive Engineering (FTG) at the Graz University of Technology. Topic, objectives and approaches this work deals with are based on research projects in cooperation with the Österreichischer Verein für Kraftfahrzeugtechnik Austrian ÖVK (Association for Automotive Engineering), MAGNA-Steyr, KEBA AG and Bayerische Motoren Werke BMW (Bavarian Motor Works).

First of all, my special thanks go to my doctoral supervisor Associate Prof. Dr. Mario Hirz, at the Institute of Automotive Engineering, who gave me the opportunity of this work. Anytime he supported and guided my way with great understanding and with his fund of scientific and thematic references. I am deeply indebted to him for many valuable expert discussions and suggestions.

For the interest in my work and the constructive suggestions I also would like to thank Associate Prof. Dr. Benjamas Panomruttanarug, who take over my doctor thesis second assessment.

Without the support of numerous individuals and institutions, this work could not have been realized in this form. I would like to take this opportunity to express my sincere thanks for the help provided to my colleagues at the Institute of Automotive Engineering, students of Graz University of Technology and project partners. Technical advice and suggestions as well as results in the context of projects and diploma thesis contributed to the success of this work.

The past few years have been no less stressful for my wife and my family. They have given my work every possible support and motivation throughout the whole time. My deepest gratitude for there patience and encouragement.

Graz, May 2020

Bernhard Walzel

STATUTORY DECLARATION

I declare that I have authored this thesis independently, that I have not used other than the declared sources / resources, and that I have explicitly marked all material which has been quoted either literally or by content from the used sources.

.....

(Date)

.....

(Signature)

Abstract

Charging of electric vehicles is mainly done manually with cables today. Customer comfort demands, as well as autonomous driving and parking functions of electric vehicles, require automated charging technologies. Automated, conductive charging systems enable both the transmission of high charging power as well as comfortable and safe charging processes.

This thesis deals with the investigation of automated electric vehicle charging by conductive standard charging technologies. The research activities range from the identification of technological challenges, boundary conditions and requirements to the development of an automated charging sensor- and actuator system and the evaluation of the introduced approach by experimental studies. The first part of the work examines state-of-the-art concepts in the course of a market- and development-focused benchmark, literature and patent research as well as analyses of published works. Furthermore, an investigation of charging standards, vehicle charging lot positioning, as well as robot- and sensor systems, is done. The focus lies on the determination of challenges and solutions to realize an automated cable connection with standard charging connectors and inlets. The third part of the thesis includes the development of a prototype system, including requirements definition, sensor system development, robot kinematics and control as well as the development of an automated charging procedure. In the introduced approach, the entire docking and undocking process of the charging connector is performed entirely autonomously. One novelty of the work includes the integrated system design of sensor technology, robot system control, and charging procedure. The system enables charging of different vehicle types in various parking positions, while no adaptations on the vehicles themselves are necessary. The last part of the work provides an analysis and interpretation of the prototype tests and a derivation of research-related findings. A conclusion of the research results and an outlook complete this thesis.

Short charging times and convenient charging processes are essential for the successful introduction of electric mobility. The results of this thesis demonstrate the possibilities of charging electric vehicles autonomously by conductive charging standards. Furthermore, challenges and requirements for the successful implementation on a large scale of those systems are presented.

Kurzfassung

Das Laden von Elektrofahrzeugen erfolgt heute zum größten Teil manuell per Ladekabel. Wachsende Komfortansprüche sowie zukünftig autonom fahrende und parkende Elektrofahrzeuge erfordern automatisierte Ladetechnologien, welche sowohl die Übertragung hoher Ladeleistung als auch komfortable und sichere Ladevorgänge ermöglichen.

Die vorliegende Arbeit beschäftigt sich mit automatisiertem Laden von Elektrofahrzeugen mittels standardisierter Kabeltechnologien. Die Forschungsaktivitäten beinhalten die Identifizierung technologischer Herausforderungen, Randbedingungen und Anforderungen, die Entwicklung eines vollautomatischen Ladesystems, sowie die Bewertung der vorgestellten Ansätze durch experimentelle Studien. Im ersten Teil der Arbeit werden Konzepte im Rahmen eines markt- und entwicklungsorientierten Benchmarkings, sowie durch Literatur- und Patentrecherchen publizierter Arbeiten untersucht. Darüber hinaus wird eine Analyse von Ladestandards, der Fahrzeugpositionierung am Ladeparkplatz, sowie von Roboter- und Sensorsystemen durchgeführt. Ein Schwerpunkt der Untersuchungen liegt in der Ermittlung von Herausforderungen und Erarbeitung von Lösungen zur Realisierung eines automatisierten Ladevorgangs. Im dritten Teil der Arbeit werden Prototypen-Ladestation entwickelt und Anforderungen bezüglich der Funktionalität von Sensorik, Roboter-Kinematik und -Steuerung, sowie des automatisierten Ladevorgangs abgeleitet. In dem im Zuge der vorliegenden Arbeit entwickelten Ansatz wird der gesamte An- und Absteckvorgang autonom durchgeführt. Das System ermöglicht das Laden verschiedener Fahrzeugtypen in verschiedenen Parkpositionen, wobei keine Änderungen an den Fahrzeugen selbst erforderlich sind. Der letzte Teil dieser Arbeit beinhaltet eine Analyse und Interpretation der Prototypentests und die Ableitung forschungsbezogener Ergebnisse. Ein Fazit und ein Ausblick auf weitere Forschungstätigkeiten in diesem Themenbereich runden die Arbeit ab.

Komfortable und rasche Ladevorgänge sind ein wesentlicher Faktor für die erfolgreiche Implementierung der Elektromobilität. Die Ergebnisse dieser Arbeit zeigen eine Möglichkeit, Elektrofahrzeuge mit standardisierten Kabeln automatisiert zu laden. Des Weiteren werden Herausforderungen und Anforderungen für die erfolgreiche Einführung solcher Systeme dargestellt und diskutiert.

List of abbreviations

2D	...	Two Dimensional
3D	...	Three Dimensional
AC	...	Alternating Current
ACCS	...	Automated Charging with Conductive Standards
ACD	...	Automated Connection Device
ACD-S	...	Automated Connection Device-Side
ACD-U	...	Automated Connection Device-Underbody
AFID	...	The European Directive for the Development of Alternative Fuels Infrastructure
Ah	...	Ampere hours
BEV	...	Battery Electric Vehicle
Bit	...	Binary digit
CAD	...	Computer Aided Design
Car-IT	...	Vehicle Information Technology
CATIA	...	Computer Aided Three-Dimensional Interactive Application (Dassault Systèmes)
CCD	...	Charge Coupled Device
CCS	...	Combined Charging System
CHaDeMo	...	Charge de Move (electric vehicle charging standard)
DC	...	Direct Current
DXF	...	Drawing Interchange File Format
e.g.	...	For example (Latin "exempli gratia")
EU	...	European Union
EV	...	Electric Vehicles
EVCC	...	Electric Vehicle Communication Controller
FPS	...	Frames Per Second
Fig.	...	Figure
FoV	...	Field of View
GNSS	...	Global Navigation Satellite System (any of the existing or proposed satellite based positioning systems, such as GPS, GLONAS, Galileo and Beidou)
GPRS	...	General Packet Radio Service
GPS	...	Global Positioning System
GSM	...	Global System for Mobile Communication
HALCON	...	Computer Aided Vision Application (MVTEC)
H&C	...	Home and Charge
HEV	...	Hybrid Electric Vehicle
HLC	...	High Level Communication
Hor.	...	Horizontal
HPC	...	High Power Charging

HRC	...	Human Robot Collaboration
ICE	...	Internal Combustion Engine
IEC 61851	...	Electric vehicle charging standard
IEC 61980	...	Electric vehicle charging standard
IFEU	...	Institute of Energy- and Environmental Research
IR	...	Infrared Light
ISO	...	International Organization for Standardization
ISO 15118	...	Communication standard for electric vehicle charging
IT	...	Information Technology
IVI	...	Fraunhofer Institute for Transportation and Infrastructure Systems
LED	...	Light-Emitting Diode
LIDAR	...	Light Detection and Ranging
LPC	...	Low Power Charging
LRR	...	Long-Range-Radar
LTE	...	Long Term Evolution Mobile Communication
Max.	...	Maximum
Min.	...	Minimum
MRR	...	Mid-Range-Radar
N	...	Newton
NEDC	...	New European Drive Cycle
NFER	...	Near Field Electromagnetic Ranging
ns.	...	Not specified
NPE	...	National Platform Electromobility, Germany
OEM	...	Original Equipment Manufacturer
PHEV	...	Plug-in Hybrid Electric Vehicle
Pixel	...	Physical point in a raster image.
PLY	...	Polygon File Format
PoS	...	Point of Sale
R&C	...	Rest and Charge
Radar	...	Radio Detection and Ranging
REEV	...	Range Extender Electric Vehicle
RFID	...	Radio Frequency Identification
S&C	...	Shop and Charge
SAE	...	Society of Automotive Engineers
SAE J1772	...	Electric vehicle charging standard
SCARA	...	Selective Compliance Assembly Robot Arm or Selectively Compliant Articulated Arm
SD	...	Standard Deviation
SECC	...	Supply Equipment Communication Controller
SNR	...	Signal to Noise Ratio
SoC	...	Battery State of Charge

SRR	...	Short-Range-Radar
TCP	...	Transmission Control Protocol
ToF	...	Time-of-Flight
Type 1	...	Electric vehicle charging standard SAE-J1772-2009
Type 2	...	Electric vehicle charging standard EN 62196-2
UMTS	...	Universal Mobile Telecommunications System
US	...	Ultra Sound
USA	...	United States of America
USB	...	Universal Serial Bus
UWB	...	Ultra Wide Band
V2X	...	Vehicle-to-X Communication
VAS	...	Value Added Services
VBM	...	Compact Connection Module
V-Charge	...	Valet Charge
Ver.	...	Vertical
W&C	...	Work and Charge
WLAN	...	Wireless Local Area Network
WLTP	...	Worldwide Harmonized Light Vehicles Test Procedure
WPT	...	Wireless Power Transfer

List of symbols

Mathematical objects within this work are denoted as follows:

a ... scalar,
 \mathbf{a} ... vector,
 $\{A\}$... matrix.

When present, symbols in sub- and superscripts of a variable \mathbf{x} are used in the form

$\frac{1}{2}\mathbf{x}$. The numbers denote the position of the following optional assignments:

- 1 ... Reference coordinate system, e.g. A ,
- 2 ... New coordinate system, e.g. B .

Variables, parameters and constants

A	...	Alternative
AC	...	Accuracy
AR	...	Actuator range
c	...	Benefit analysis criteria
D	...	Distance
D_c	...	Cube diagonal
f	...	Camera focal length
F	...	Force
K	...	Stiffness
l	...	Length
m	...	Mass
P	...	Camera resolution pixel
q_l	...	Weight per meter
R	...	Benefit analysis criteria rating
R_x	...	Rotation around the X -axis.
R_y	...	Rotation around the Y -axis.
R_z	...	Rotation around the Z -axis.
Rot_{RPY}	...	Homogenous rotation matrix with Roll-Pitch-Yaw rotation convention.
$Rot(\alpha, \beta, \gamma)$...	Homogenous rotation matrix
S	...	Score
SR	...	Sensor range
t	...	Time
T	...	Colour depth
$Trans(x, y, z)$...	Homogenous translation matrix
w	...	Cable weight for one meter
W	...	Benefit analysis criteria weighting
α	...	Rotation angle around the X -axis.
β	...	Rotation angle around the Y -axis.
γ	...	Rotation angle around the Z -axis.
μ	...	Mean value
σ	...	Standard deviation

Coordinate systems

- $\{R\}$... Reference coordinate system (frame or pose)
- $\{B\}$... Robot basis coordinate system (frame or pose)
- $\{C1\}$... Camera 1 coordinate system (frame or pose)
- $\{C2\}$... Camera 2 coordinate system (frame or pose)
- $\{C3\}$... Camera 3 coordinate system (frame or pose)
- $\{C\}$... Charging connector coordinate system (frame or pose)
- $\{V\}$... Vehicle coordinate system (frame or pose)

Contents

1. Introduction	1
1.1. Motivation	1
1.2. Initial situation	2
1.3. Aim of work	2
1.4. Methodology	3
1.5. Delimitation of the work	4
1.6. Structure of the work	5
2. State-of-the-art and boundary conditions	7
2.1. Charging technologies	7
2.1.1. Conductive charging	7
2.1.2. Inductive charging	9
2.1.3. Battery swapping	10
2.2. Automated conductive charging	12
2.2.1. Automated connection device-side (ACD-S)	12
2.2.2. Automated connection device-underbody (ACD-U)	16
2.2.3. Pantograph systems	18
2.3. Electric vehicles	19
2.3.1. Battery electric vehicles	20
2.3.2. Plug-in hybrid and range extender electric vehicles	21
2.3.3. ACD integration	22
2.4. Charging standards	23
2.4.1. Charging cables	26
2.4.2. Communication	27
2.5. Charging infrastructure	29
2.5.1. Charging power	29
2.5.2. Charging stations	31
2.5.3. Services	32
2.6. Charging process	33
2.7. Vehicle parking and positioning	37
2.7.1. Manual and automated parking	37
2.7.2. Vehicle position	38
2.7.3. Parking accuracy	39
2.7.4. Vehicle parking aids	41

2.8.	Robotics for automated charging	44
2.8.1.	Architecture and kinematic	45
2.8.2.	Robot control	47
2.8.3.	Safety	52
2.9.	Sensor technologies for automated charging	53
2.9.1.	Positioning sensors	55
2.9.2.	3-dimensional imaging sensor technologies	59
2.9.3.	Vehicle-integrated sensors	60
2.10.	Conclusion of the technology benchmark	63
3.	Prototype development	69
3.1.	Requirements	69
3.1.1.	Use cases	69
3.1.2.	Charging process	70
3.1.3.	Boundary conditions and demands	72
3.1.4.	Supporting ACCS requirements	73
3.2.	System design	74
3.2.1.	Functional concept	74
3.2.2.	Basic layout	75
3.3.	Component requirements	76
3.3.1.	Charging lot	77
3.3.2.	Vehicle detection sensor	77
3.3.3.	Charging start trigger	79
3.3.4.	Inlet detection sensor	79
3.3.5.	Cable handling actuator	86
3.3.6.	System control	90
3.4.	Sensor system selection	91
3.4.1.	Vehicle detection with vehicle-external sensors	92
3.4.2.	Vehicle position detection with vehicle-internal sensors	93
3.4.3.	Inlet position detection	93
3.4.4.	2D-camera specifications	94
3.5.	Recognition process	97
3.6.	Charging process	99
3.7.	Object detection	101
3.7.1.	Vehicle detection	101
3.7.2.	Inlet detection	101
3.8.	Robot control	105
3.9.	Data processing	108
3.10.	Connector system	111
3.11.	Communication	113
3.12.	ACCS prototype	115
3.13.	Conclusion	119

4. Prototype testing and evaluating	121
4.1. Testing plan	121
4.2. Charging process evaluation	123
4.3. Parking and charging	127
4.4. Different vehicles	130
4.5. Outdoor	131
4.6. Conclusion	132
5. Conclusion and outlook	135
5.1. Conclusion	135
5.2. Outlook	137
A. Appendix	139
A.1. Equations	139
A.2. Tables	142
A.3. Test objects and equipment	147
List of Figures	151
List of Tables	159
Bibliography	163

1. Introduction

Motivation and initial situation, as well as the research aim and the related research questions dealt with, are contents of this chapter. Furthermore, the structure of the thesis and an overview of the scientific contributions are presented.

1.1. Motivation

The increasing popularity of *Electric Vehicles* (EVs) and autonomous driving is calling for new solutions regarding battery charging. EVs have to be charged - in other words: Some system has to provide energy to the battery. Today, this is done via conductive or via inductive (wireless) charging. In case of today's conductive charging, it is connected manually, which requires that an operator has to plug-in the charging cable into the charging socket of the car. Rising comfort is expected due to the elimination of the cable connection and disconnection by inductive charging technologies or battery swapping systems. Disadvantages of inductive technologies are the limited charging power as well as specific vehicle adaptations that result in high costs and increased weight of the vehicle. Grid and vehicle integration of battery swapping systems is complicated and expensive.

A further option is automated EV charging by a conductive connection. From a purely technical point of view, automated conductive charging seems to be state-of-the-art, but to date, there is no feasible solution for large scale usage. Concepts presented charging device coupling from the vehicle top, below, front, rear or side, [VOL16], [TES16] and [VOL18b]. The difficulties lie the automated coupling process as well as the charging device integration into vehicles and infrastructure.

Automated charging with conductive standards (ACCS) is beneficial. The performance of widely used standardized coupler systems for manual operation, e.g. *Combined Charging System* (CCS), [COM14a] or *Charge de Move* (ChaDeMo), [COM14b] and [COM14c] is normed and reaches from low up to very high charging power capacities. Compared to other concepts, additional devices, modifications and adaptations can be reduced to a minimum. Furthermore, the presence of a charging connection, which is already used for manual charging is advantageous. Automated charging with standard couplers and the combination of vehicle parking and subsequently automated cable connection are not realized today.

The motivation of this thesis persists in the analyses of ACCS challenges and requirements as well as the development of a sensor and actuator system for automated coupling. The thesis

targets are driven by the realization, technology evaluation and potential assessment of vehicle parking and automated cable connection processes.

1.2. Initial situation

The main idea of automated conductive charging systems includes a straightforward and comfortable charging process. The car parks in the parking bay and the remaining steps are being finished by the automated charging system automatically. That means the system identifies the type of car and recognises thereupon the position of the charging socket. Afterwards, the charging process is carried out by a specific charging strategy. But some obstacles need to be adjusted to realise an automated connection - and for the target to handle standard charging technologies and various vehicle types, the challenges are rising significantly.

Automated charging systems for electric vehicles are in development today. Pilot projects deal in various ways with automated conductive charging. Some concepts have special connectors, [GMR⁺16] and [CON16b]; some concepts deal with the target to integrate standardised charging cables and sockets, [FOR19] and [Ste18]. Furthermore, approaches can be separated into *Automated Connection Device-Underbody* (ACD-U) and *Automated Connection Device-Side* (ACD-S) concepts.

The implementation of automated EV charging by ACCS would be advantageous, but basically, EVs, the infrastructure and standardised cables are not designed for an automated charging process. In this context, various technical-related challenges have to be solved to fulfil the demands of EVs, infrastructure and users.

1.3. Aim of work

The research question of this work focusses on the investigation of how standardized conductive charging technologies can be used for ACD-S charging, so that both vehicle and infrastructure need as less as possible adaptations or new technological developments. For answering the research question, the thesis activities are addressed by the following objectives:

1. Identification and definition of ACCS challenges.
2. Determination of ACCS requirements and boundary conditions.
3. Development and evaluation of an ACCS sensor- and actuator system.
4. Investigation of ACCS vehicle parking and influences of parking aids.
5. Evaluation of the technology and derivation of requirements for a further development of the introduced system.

For the definition of technical requirements for an automated cable connection, objectives are given by the analyses of the ACCS-challenges. The identification and definition of technical requirements represent an important task that has to be solved to enable automated charging of various EV types in different vehicle parking positions. Vehicle design and package, parking lots, user behaviour and -demands as well as parking and charging processes-related factors define ACCS systems. In this context, one main objective at the beginning of the research includes the determination of the demands and requirements to derive recommendations for the successful implementation of ACCS.

A further objective is the development of an ACCS sensor- and actuator system. The sensor system provides the functionalities of vehicle recognition and inlet position detection. Controlled cable movements are carried out by the actuator system. Target is the implementation of the systems into a prototype for autonomous charging of various types of EVs in different parking positions via standard cable-connections. The prototype enables testing and evaluation of the systems in scenarios close to practice.

The fourth aim consists in the analyses of ACCS vehicle parking and the influences of parking aids. This includes prototype tests with various vehicle types, test drivers and vehicle parking positions. The evaluation of these activities provides new findings for ACCS vehicle parking and parking aids.

The last objective includes the provision of recommendations and requirements for further ACCS development. These are derivate from the prototype test results and research findings.

1.4. Methodology

The first step deals with the state-of-the-art of charging technologies and automated conductive charging systems and ACCS boundary conditions. ACCS technical issues and challenges are investigated by literature- and patent research as well as market and development benchmark of published works. Boundary conditions are given by charging infrastructure and EVs, as well as vehicle parking and charging. Besides the determination of future-prove charging standards, it is figured out where, when, and under which boundary conditions vehicles are usually charged. Findings enable the determination of requirements for a successful ACCS implementation. Automated conductive charging systems require a rigid connection of charger and vehicle during energy exchange. In this context, the vehicle parking position plays an important role. Research of parking position accuracy aids provides approaches for improving vehicle parking processes. For the ACCS prototype sensor- and actuator system, state-of-the-art research of sensor and robot technologies is carried out.

In the next step, a robot-based and sensor-controlled charging station prototype is developed for testing selected standard charging connector- and socket technologies. State-of-the-art research and boundary conditions findings, the definition of ACCS charging use cases and findings of the manual charging process analysis enable the definition of prototype requirements. Subsequently, an ACCS system design is developed and serves as the basis for the prototype component

requirements derivation. The prototype development includes charging station layout, vehicle and inlet sensor detection- and robot control processes, data processes and an ACCS charging process that is applicable on different vehicle types.

The evaluation of the prototype functionality is done by different test scenarios. The tests include parking and charging tests with different drivers, various vehicle types and environmental conditions. Parking and automated cable connection processes are recorded and analysed. The analysis contains parking accuracy, vehicle inlet position, drivers parking behaviour and the prototype cable docking and plug-in process.

A summary of the research findings and an outlook of continuative activities to support the implementation of automated charging technologies by the use of conductive standards complete this thesis.

1.5. Delimitation of the work

Automated conductive charging systems are a growing research field. Related to the research activities of this thesis, a state-of-the-art survey in the field results in the following existing approaches:

- a. Concepts with non-standardized charging connectors.
- b. Concepts with conductive standardized systems.
- c. ACD-U and ACD-S coupler concepts.

Related to *b*, the practical implementation of automated cable plug-in and plug-out with different vehicle parking positions is not sufficiently detailed illustrated up to now. IN this context, this work investigates the feasibility of ACD-S with conductive standards. The thesis deals with new approaches regarding the combination of sensor technologies as well as charging station layout, design and control. As an essential aim of the research activities, one novelty of the work includes sensor technology, robot path control and the charging process enabling charging of various vehicle types in different parking positions, while no adaptations on the vehicles themselves are necessary. The content of this work consists of the following delimitations:

- a. The development of the automated charging process is limited to the recognition and plug-in and plug-out procedure by the use of conductive charging standards.
- b. Opening and closing of charging lids as well as removing and repositioning of safety caps are not part of the research.
- c. Vehicle parking and automated cable connection tests are carried out without electrical energy exchange.

1.6. Structure of the work

The structure of this thesis includes three main parts that contain three chapters (figure 1.1). In the following aims, contents and outcomes of the parts are described.

The aims of Part I (Initial situation) include the elaboration of challenges and the identification of boundary conditions and requirements of ACCS. The state-of-the-art survey examines the latest technological solutions in the field of automated charging approaches and concepts. The boundary conditions and requirements are derived from the impact factors EVs, infrastructure, user behaviour, as well as parking- and charging demands. The sensor benchmark study delivers suitable sensor technologies for vehicle identification and inlet position detection. The findings of the robotic-oriented research survey are related to kinematics, control, as well as operational safety issues.

The ACCS prototype development is the aim of Part II (Conceptual design and construction of the prototype). Objectives are the derivation of ACCS requirements and a prototype functional- and ground layout concept. Vehicle and inlet detection sensor systems are evaluated regarding specified prototype requirements and targets. The second target focusses on the realization of an automated cable connection and disconnection strategy and a procedure integrating sensor-based vehicle and inlet position detection and robot path control. Prototype functional targets include an automated inlet position detection and plugging in and off of different vehicles in various parking positions.

Part III (Evaluation and results discussion) evaluates the prototype functionality by different test scenarios and discusses the test results. One objective includes the documentation of the prototype behaviour during automated cable connection procedures under different environmental situations. Further outcomes investigate the influence of vehicle parking of different test drivers on the prototype charging lot.

A conclusion summarizes the research findings of this thesis. An outlook to potential future developments of the treated technologies completes this work.

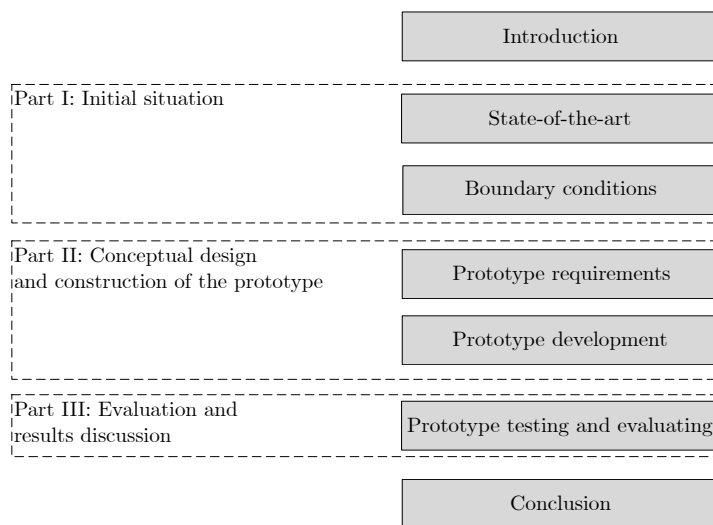


Figure 1.1.: Structure of work.

2. State-of-the-art and boundary conditions

The first part of this chapter investigates charging technologies and the state-of-the-art in the field of *Automated Connection Devices* (ACD) systems. Figure 2.1 shows an overview of the ACCS functional objective and impact fields. The objective is the automation of the cable-based *Charging Process*. Impact fields are *Electric Vehicles*, *Charging Infrastructure*, *Charging Standards* as well as *Vehicle Parking*. The second part of this chapter deals with the analyses of manual cable charging processes and the determination of ACCS tasks and restrictions. Furthermore, ACCS boundary conditions and requirements are derived from the impact fields. The third and last part of the chapter analyses the state-of-the-art in the field of robotics and sensor technologies and presents selected systems for ACCS.

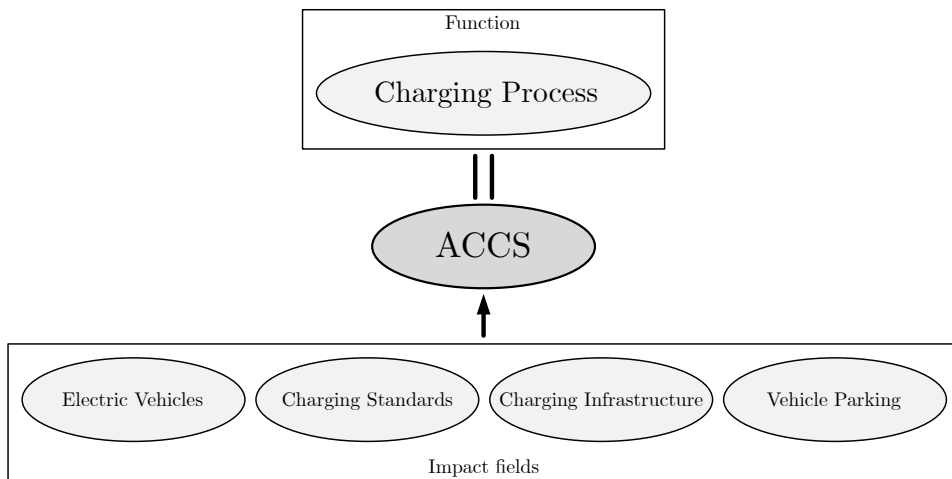


Figure 2.1.: Functional objective and impact fields for automated EV charging with conductive standard technologies (ACCS).

2.1. Charging technologies

Various techniques enable charging of automotive battery systems. In the following, the three most important charging principles for passenger cars are presented. Charging solutions include conductive charging, inductive charging and battery swapping.

2.1.1. Conductive charging

Robert Anderson developed the first electrically driven car in 1832. Practicable EVs have been introduced around the 1870s. With a share of 30% of all vehicles in the USA, EVs reached

2. State-of-the-art and boundary conditions

their high period between 1900 and 1912, [ENE19]. That time charging stations re-filled the batteries in home garages or parking facilities. Figure 2.2 shows images from 1912. Figure 2.2, right, illustrates a woman next to a charging station, also known as "mercury arc rectifier" from the GENERAL ELECTRICS company. This name was given due to the glowing tube on the back of the charger during charging, [Dro19]. Even today, charging by cables is the most common method, but people find the use of cables for recharging the EV energy storage system to be cumbersome. Nevertheless, in comparison to conventional vehicle refuelling, EV charging depends not on special places, e.g. gas filling stations, but can be carried out at home, at work or at public stations.

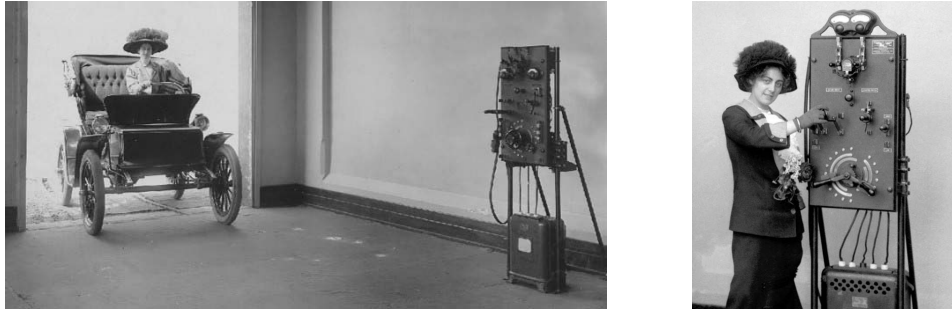


Figure 2.2.: EV charging in 1912. Left: Woman drives the EV into a charging station lot, [MOT19b]. Right: Women next to a charger from GENERAL ELECTRICS, [Dro19].

Today wired, single-phase *Alternating Current* (AC) charging enables power transmissions up to 3.7 kW. Three-phase AC chargers achieve outputs of up to 44 kW. AC charging requires a converter from AC to *Direct Current* (DC) that is located in the vehicle. Significantly more than 50 kW power transmission is made possible by DC charging. An AC/DC converter is not needed, but the high charging voltages and currents require special protection measures, [P. 18].

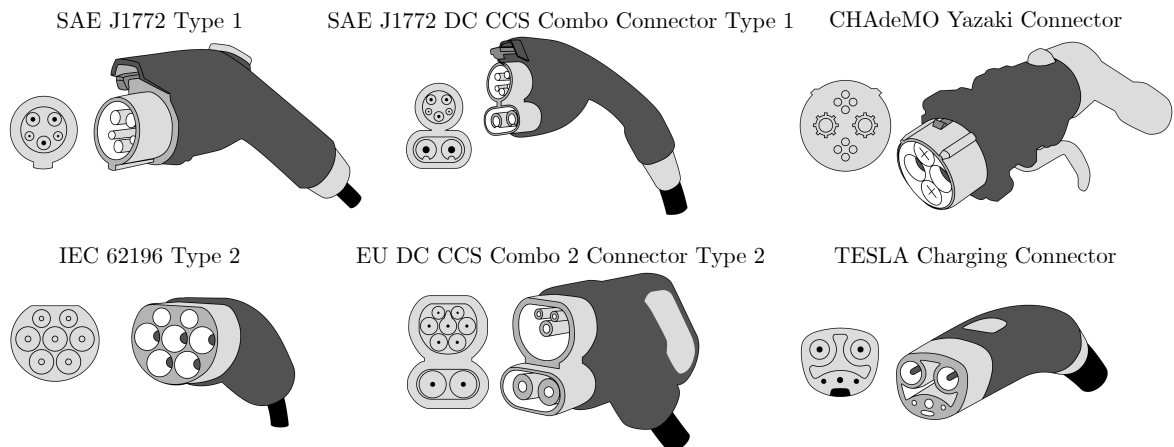


Figure 2.3.: Selection of charging connector standards according to [EI18].

A selection of connector types is shown in figure 2.3, [EI18]. Common norms are the European standards Type 2 and the CCS Type 2 (Combo 2) connector for AC and DC quick charging,

the *CHArge de MOve* (CHAdeMO) as a main standard in Asia and USA, as well as the TESLA standard. The possible charging power ranges reach from widely used low power plugs with household electric charging capacities, up to 500 Ampere and 1000 Volt of CCS Type 2, [CON17].

2.1.2. Inductive charging

Inductive charging or *Wireless Power Transfer* (WPT) is derived from the basic principle techniques of a transformer. The energy transfer takes place via two oppositely directed coils. One device is stationary installed at the designated parking lot (primary coil). The other device is usually mounted at the vehicle's underbody (secondary coil). Advantages of this technology are charging the vehicle without contact and a resulting increase in user comfort because no manual connection or disconnection is necessary. Furthermore, there is a low risk of vandalism because cables can not be damaged or unauthorised disconnected. Nevertheless, inductive charging has challenges. High charging efficiency requires small air gaps and the accurate positioning of the charging pads. Electromagnetic compatibility must be ensured due to the fact that electromagnetic radiation occurs based on high power transfer rates. It must be ensured that humans, animals as well as electric devices in the close environment are not affected negatively. One main challenge is the cost factor because of the expensive technology and effort for vehicle integration. Charging lot have to provide in-the-floor integrated pads and power electronics for high-frequency charging, [Tob16].

The vehicle to ground clearance varies due to different vehicle types. The electromagnetic field distribution varies and hence the resonant frequency, which is needed to optimise the efficiency. To ensure the functionality for a high number of vehicle types, a variable operating frequency of the system is needed, [KH15].

In addition, a mutual misalignment of the oppositely charging pads influences the system efficiency. Studies analysed the efficiency dependency by the misalignment of charging pads with 30 cm diameter. After a misalignment of 10 cm in vehicles longitudinal direction, the efficiency falls under 90% - the transversal direction had a smaller influence. This behaviour lies in the charging coils geometry. Thus, inductive systems typically have a misalignment tolerance of ± 10 cm from their centre point, [BKHC15]. In this context, accurate parking is required for low charging energy losses and to comply with standard specifications, [oAE17]. Inductive charging systems should be as flexible as possible, such that vehicles can be charged on any infrastructure mounted charging pad. National and international standardisation committees are working on such standards, [LFK15].

A study recorded WPT charging user experiences. In comparison to wireless charging, the additional time for wired charging was recorded with 43 seconds. Compared to non-charging, the additional time is 55 seconds. The recorded time includes the parking process, removing the charging cable from the trunk, plugging-in, plugging-out, and stowing the cable. The parking procedure for wireless charging and non-electronic parking aids took an average extra time of 12 seconds. Charging socket and cable position, as well as the complete operating philosophy, have

a significant influence on the time required for cable-bound charging. This differs from vehicle to vehicle due to different charging socket mechanism and -positions. The connection time for WPT depends on parking aid type. Nevertheless, wireless charging is less time-consuming than using a charging cable that has to be carried in the vehicle, [BB11]. A further study investigated the operation and function of WPT. Tests with a one times one-meter charging pad led to the following results, [ENE12]:

- Test drivers were restricted by the charge procedure time.
- The reliability was not sufficient. 30% of the charge processes had to be done by cable.
- More money would be spent for a device that provides fast and battery full charging under 30 minutes.
- Automatic activation of the charging pads was desired.
- There were difficulties in finding an optimal charging parking position.
- The majority desired a different charging pad position, e.g. on the license plate.
- Regarding cable-based charging the cumbersome and time-consuming handling was classified as rather not questionable.
- Due to the problems of inductive charging, users preferred to use conductive technologies.

From a vehicle manufacturer's point of view, every charging system should be as small, as light and cost-efficient as possible and should fulfil all necessary safety standards. Exemplary, a WPT system with 3.6 kW charging power fits, e.g. behind a number plate and is capable of charging a BMW i3 battery with 18.8 kWh like a conductive charging system from empty to full in 3.5 to 7 hours, [Sch13] and [LFK15].

BMW launched the first market-ready WPT system for cars. Prices are approximately 890 Euro for the vehicle module and 2315 Euro for the building-site floor pad, [Bau18]. The pad is installed at the bottom of the parking lot. A coloured display in the vehicle guides the driver to the correct parking position until the vehicle is accurately enough parked over the pad. Charging power is given with 3.2 kW, and a charging efficiency between 80% and 87% is reached, [BMW18].

2.1.3. Battery swapping

An alternative charging concept is battery swapping. The battery unit is decoupled and removed from the EV and replaced by a fully charged battery unit. The system demands are high, e.g. for battery changing facility infrastructure and the provision of electrical power. Several pilot projects have been carried out from BETTERPLACE or TESLA, [P. 18]. Figure 2.4 illustrates two concepts of battery swapping. The empty EV battery unit is replaced by a fully charged battery unit (figure 2.4, left, position 3) by a battery- and vehicle lift system (figure 2.4, left, position 1). Figure 2.4, right, shows the facility concept of BETTERPLACE. Battery storage (position 4) and a unit (position 5 and 6) contains the apparatus for battery

swapping and vehicle moving. BETTERPLACE launched 2007 and was the main driver of this technology that time. In pilot projects, several stations in Israel and Denmark were set up. However, the company failed with its business model and had to declare insolvency 2013. Due to the lack of support from vehicle manufacturers, the concept never really gained public acceptance. For example, RENAULT was one of the few manufacturers, which offered one vehicle type that was compatible with BETTERPLACE’s swapping stations, [ECO16].

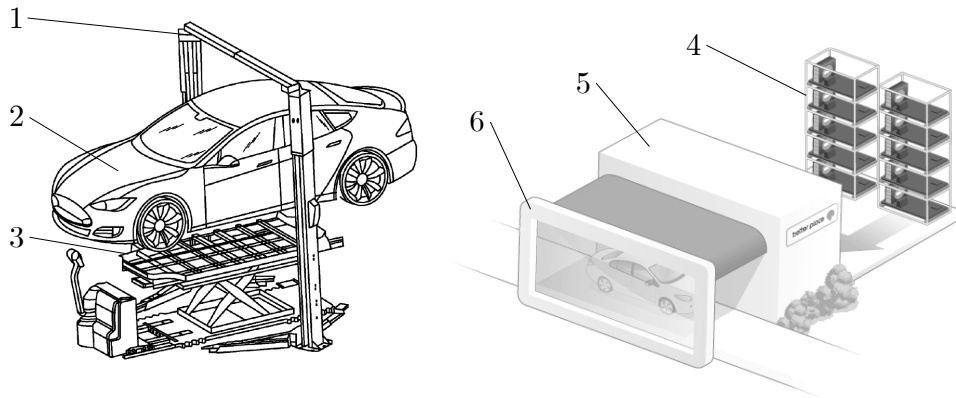


Figure 2.4.: Left: Patent drawing of TESLA’s battery swap system, [TES15]. Right: Concept illustration of the BETTERPLACE battery swap facility, [Jer19].

The Chinese companies NIO and BJEV realized the series implementation of battery swapping. Both operate charging stations for their own vehicle fleet and expand the network. The modular NIO station requires 3 parking lots and stores five battery packs. The whole battery changing process, including vehicle manoeuvring requires around 10 minutes. The total charging station power is given with 300 kW and the 70- and 84 kWh batteries are cooled during charging, [NIO20] and [Bla20]. Vehicle electrics and batteries are checked during every battery swap, which ensures suitable vehicle and battery conditions. In 2019, NIO installed 100 stations in China with the plan to operate 1,100 stations in 2020, [Hal20]. 95% of 9,726 ES8 EVs were delivered with the least battery option that enables battery swapping. The EV manufacturer BJEV invests 1.28 billion Euro in 3000 battery swapping stations with the target to supply a half million EVs at the end of 2022, [Ran20]. The Chinese government supports the implementation of battery swapping standards for enabling charging of every vehicle type at every charging facility, [ELE20].

An empty battery can be swapped within a few minutes. In terms of time, this corresponds approximately to the refuelling process of vehicles with combustion engines. Short EV charging breaks, especially over longer driving distances, mean high driver comfort. New and more powerful generations can easily replace old batteries. Regarding standardization, there are disadvantages. Besides, a battery swap station is associated with significantly higher investment costs compared to a conventional charging station. A further disadvantage regarding costs is the requirement of more than one battery per vehicle, because additionally to the vehicle’s battery, battery packs have to be stored and charged at the swapping stations, [Kle11], [INS10] and [NPE10].

Battery systems influence vehicle packaging and frame structure. For car manufacturers, a standardized battery pack has disadvantages regarding vehicle integration and design and limits the vehicle packaging possibilities. Standardized battery dimensions, electrical connections for power transfer and control systems as well as cooling circuits are challenges for a large number of different vehicle types. In this way, battery swapping might be an interesting technology for selected car manufacturers, but has a low potential for general standardization.

2.2. Automated conductive charging

This chapter deals with the analysis of automated EV charging concepts based on the conductive principle. Due to significant differences concerning vehicle integration and technical implementation, the systems are separated into ACD-S, ACD-U and pantograph coupler. A conclusion and discussion of the presented automated charging technologies are given in Chapter 2.10.

2.2.1. Automated connection device-side (ACD-S)

The designation *Automated Connection Device-Side* (ACD-S) is derived from the type of automated connection between charging device and vehicle. An ACD-S system links charger and vehicle from the vehicle side. This also includes vehicle front and rear side charging plugs, [E.V19].

One reference for this type of technology represents the robot-based project *e-smartconnect* from VW and KUKA from 2015. The charging process starts with the communication between vehicle and charging station. Afterwards, data exchange takes place to guide the autonomous driving and parking vehicle to the charging lot target position. In the published research prototype version (figure 2.5), the charging socket of the vehicle has to be positioned in a target area of 20 by 20 centimetres.



Figure 2.5.: ACCS concept with a KUKA robot arm, gripper and a CCS Type 2 connector, [VOL16].

After charging socket detection, which is processed by a camera on the robot, the robot-gripper picks the DC-connector and connects it to the charging socket of the vehicle. The camera

position detection accuracy is denoted by a millimetre. At the end of the charging process, the robot-gripper unplugs the DC-connector, [VOL16]. The publication does not contain any information regarding the detection of the relative angle or a method for compensating angular misalignments between socket and robot.

Aim of a project at the Technical University of Dortmund was to charge a parked EV without manual driver intervention to increase the comfort of charging processes. The prototype is shown in figure 2.6. The charging system contains a standard energy supply and a wallbox, which is extended by a cost-effective *Compact Connection Module* (VBM). The connection and disconnection process can be started via a smartphone app, [DOR15]. However, the capability and functionality of this concept system are not published in detail.



Figure 2.6.: Automated side coupler concept of the Technical University of Dortmund. The concept includes a special robot arm kinematic, which handles a standard charging plug, [DOR15].

Figure 2.7 shows the prototype head tool of the project *Generic infrastructure for seamless energetic coupling of electric vehicles* (GINKO). The project target was to charge an EV with a robot automatically. Released pictures show a KUKA robot on the robot head equipped with a force sensor from SCHUNK. Especially for automatic-connection and robot-control, solutions in the field of image processing were developed. Before the robot can plug-in the charging cable, the vehicle charging socket position has to be detected. User-friendly navigation both outside and inside buildings, charging control and energy consumption measurement, posed major ch-

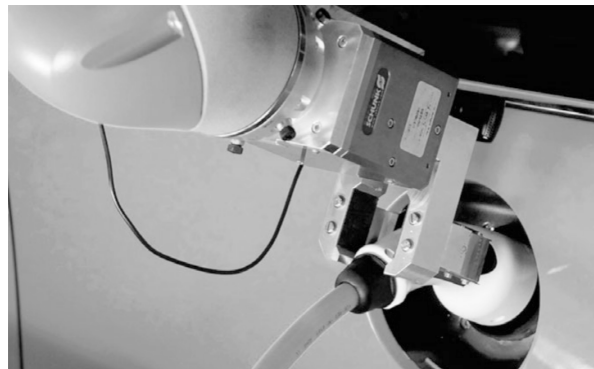


Figure 2.7.: Detailed view on the robot head concept with gripper and a Type 2 connector, [Ste18].

allenges for the project team. In particular, safety in the robot arm movement space was a top priority in the project, so that users, vehicle and robot arm itself are not damaged. Further information of safety function and their implementation are not published yet, [Sch17], and [Ste18].

TESLA developed a snake-like ACCS prototype (figure 2.8) based on TESLA's own connector standard. The system detects the opened charging cover and the prototype robot arm autonomously finds the way to the charging socket. The charging process starts after the connection. The complete connection procedure is applied by the robot. Thus the driver does not have to get out of the car, [TES16] and [MED19]. One system advantage lies in the possibility of charging the own vehicle fleet. Each TESLA vehicle carries the charging socket at same position. Detailed technical information about the vehicle charging socket detection or connector plug positioning processes is not available.

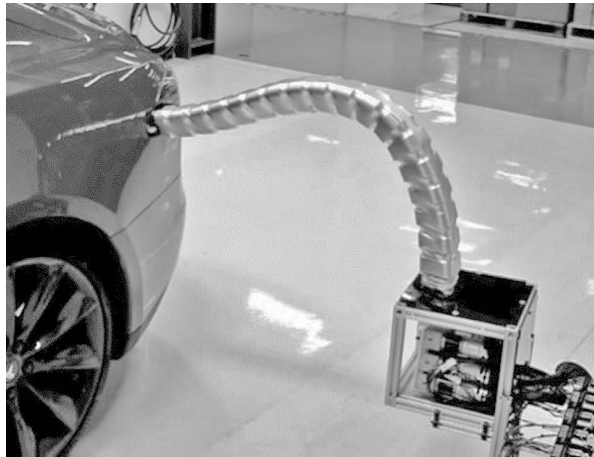


Figure 2.8.: Image section during cable connection from a published video of TESLA's charging snake, [TES16].

FORWARDTTC and KUKA AG are working on an automated cable-based charging assistant for EVs (figure 2.9). The charging assistant is designed not only for companies, public charging stations and vehicle fleets - but also for the home garage. Such a system has to be harmless in every situation as well as easy to be controlled- and affordable. The robot control is carried out by a single-board computer integrated into the robot arm. In this way, the image processing algorithms are specially developed for the application. The system does not need additional safety technologies due to the safe design of the robot's drive trains, [FOR19]. The entire operation can be controlled via a smartphone app. The system has been successfully tested with various vehicle types and presented at the Geneva Motor Show, the Hannover Messe Industrie and the Automechanika in 2019, [FOR19]. Reliability and robustness of the system under different lighting conditions are currently under test. Moreover, software robustness and axis drive loads are evaluated, [Böt19].

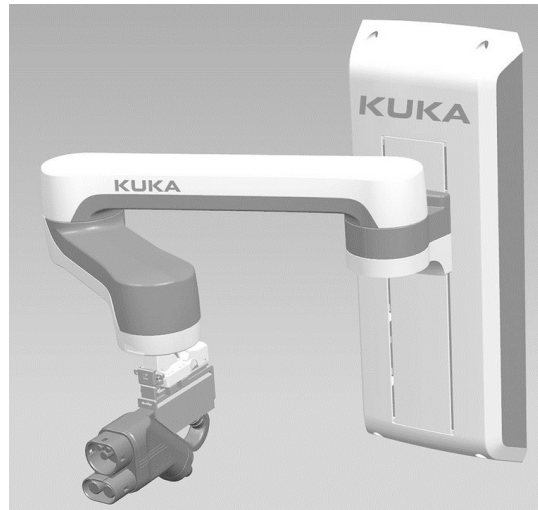


Figure 2.9.: Charging assistent of FORWARDttc, [FOR19]. The system contains a new robot design with a CCS Type 2 connector developed for automated charging.

Figure 2.10 shows further side coupler concepts. A concept introduced by GM is based on a robot arm (figure 2.10, position 1a) that is mounted on a base plate (figure 2.10, position 2a). The robot arm moves the end effector (figure 2.10, position 3a) in three degrees of freedom. The end effector includes electrical contacts for the connection with an electric vehicle charging socket. The charging station robot arm is guided by a controller that receives target information from a camera system (figure 2.10, position 4a), [GMR⁺16].

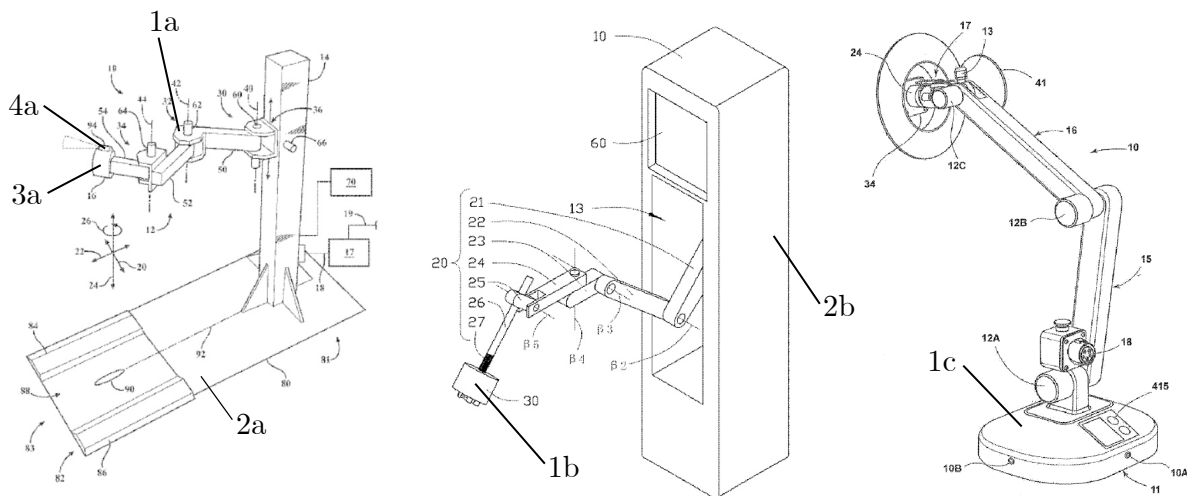


Figure 2.10.: Drawings of selected patented ACD-S concepts. Left: Robot of [GMR⁺16]. Middle: Robot arm coupled to a charging body, [EIL17]. Right: Moveable EV charging robot, [Zho15].

Figure 2.10, right, represents a robot arm on a moveable platform (figure 2.10, position 1c). The concept is designed for SAE 1772 or similar charging standards. The platform enables the robot movement to parked electric vehicles. Opening and closing the inlet lid as well as the charging connector insertion process is carried out by a plug latch system at the robot arm end effector, [Zho15].

The automated docking system of *Hollar* enables convenient EV charging without user intervention. The robotic arm is guided to the charging inlet by cameras and a processor unit. The patent claims the method of an automated charging system including a video device. A video camera sends data to a computing platform that identifies the location of the vehicle charging inlet by a vision-based algorithm, [HH11].

Hayashi introduced a connector system with a feeding coupler on a robot arm that is combined with a receiver coupler at a vehicle. Special features of the feeding coupler are the compensation of charging robot vehicle displacements and a fixing mechanism. The mechanism keeps feeding the receiver coupler during the charging process in position, [HY00].

Examples of patents for the compensation of displacements during the plug-in process are shown in figure 2.11. In *Gao's* concept, a possible fail alignment of the EV and the end effector during the connection process is compensated by a retractable guide (figure 2.11, position 1a) around the charging connector (figure 2.11, position 2a), [GMR⁺16]. The concept of PHEONIX CONTACT describes a device for the compensation of CCS connector position and angle misalignments in relation to the vehicle inlet (figure 2.11, right), [CON16b]. This enables an elastic spring that links the connector housing (figure 2.11, position 1b) and the compensation element housing (figure 2.11, position 2b) of the connector system.

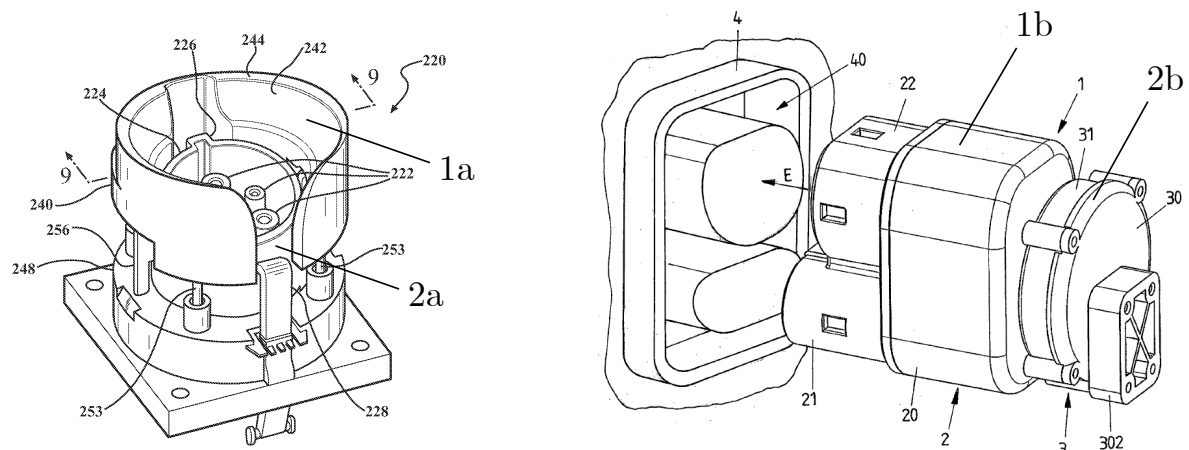


Figure 2.11.: Left: Illustration of a patented coupling unit concept with a retractable guide from GM, [GMR⁺16]. Right: Patent drawing of a connector system with a misalignment compensation module, [CON16b].

2.2.2. Automated connection device-underbody (ACD-U)

As an alternative to conductive side coupler systems, vehicles can be charged from the bottom side. The fundamental idea of VOLTERIO is a system for fast charging that provides a high range of vehicle parking tolerances. The system contains two basic components, a vehicle unit (figure 2.12, position 1), which is mounted in the middle of the car underbody and a base unit (figure 2.12, position 2), which represents the charging robot at the parking area. The base unit automatically starts to communicate with the vehicle unit when an EV approaches the charging lot. The vehicle does not have to park in an exact predefined position. This

process is possible by the conically shaped connection module (figure 2.12, position 3) and the matching counterpart at the vehicle. The system compensates misalignments of up to 0.5 x 0.5 m. Positional errors between vehicle and base module during connection are compensated by allowing the plates to slide into each other. The correct position where an automatic connection is feasible is ensured by an ultrasound-based micro-navigation system that guides the automated arm. After the system checked the authorization, the charging process starts automatically or can be scheduled manually or by an intelligent charging management system. VOLTERIO specifies a charging power of up to 22 kW with a possibility to increase it of up to 400 kW, [VOL18b].

The EASELINK concept describes a conductive matrix-charging system. After authentication via wireless communication, the matrix-connector consisting of vehicle charger and connector (figure 2.12, position 4 and 6) automatically connects to the matrix-charging plate on the floor (figure 2.12, position 5). The selective activation of the contacts (figure 2.12, position 7) for power transmission enables the compensation of parking offsets and allows parking tolerances of up to 400 x 400 mm. The relatively small connector module at the vehicle houses all moving parts. The matrix-charging pad is robust, can be driven over and withstands all weather conditions, [EAS19].

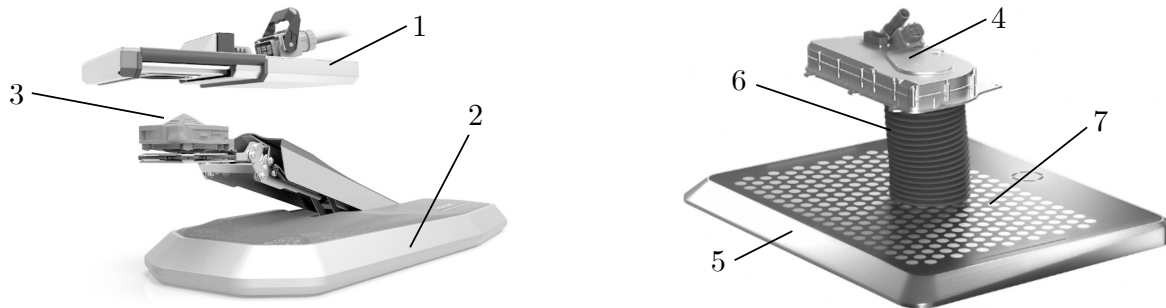


Figure 2.12.: Left: ACD-U charging arm of VOLTERIO, [VOL18b]. Right: Matrix-charging from the company EASELINK, [EAS19].

The concept of *Horvath*, [HJE⁺11] describes ACD-U by a plug apparatus that connects to a vehicle plug adapter. The plug adapter is fixed at the underbody of the car. When a car approaches the charging station, an actuator opens a flap, and the plug apparatus connects to the underbody of the vehicle.

The concept of *Brown* consists of a floor-mounted charging plate (figure 2.13, left, position 1a) that is moved to a vehicle-mounted charging device (figure 2.13, position 2a). A scissors-based kinematics system lifts up the charging plate (figure 2.13, position 3a). The compensation of parking misalignments is not donated [Bro18]. Finally, figure 2.13, right, shows the concept drawing of a floor-integrated charging system. For battery refuelling, the vehicle is positioned above a charging device that is embedded in the ground. A charging arm (figure 2.13, position 1b) is moveable by linear actuators to different positions (figure 2.13, position 2b and 3b), [MVD17].

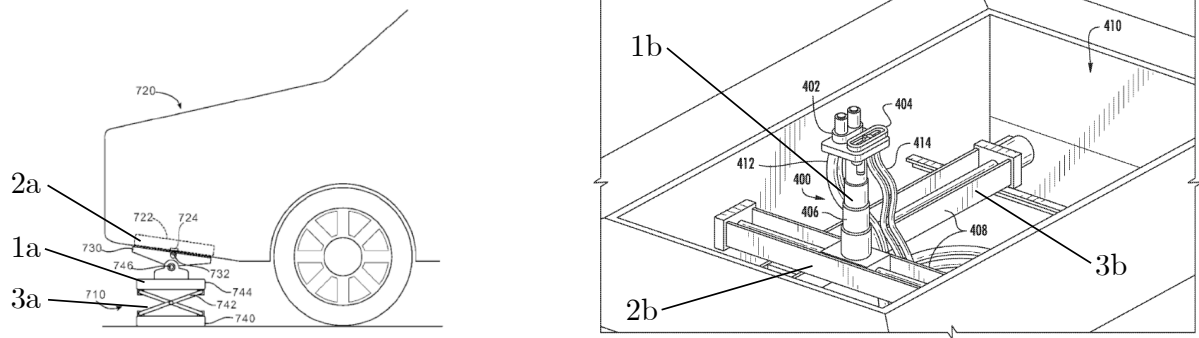


Figure 2.13.: Patent drawings of selected ACD-U concepts, [Bro18] and [MVD17].

2.2.3. Pantograph systems

The company SCHUNK and the *Fraunhofer Institute for Transportation and Infrastructure Systems* (IVI) developed a compact and robust bus charging system with high electrical power transfer capacity. In order to enable automated charging, this system was developed as an alternative to manually plug-in systems. The conductive system consists of a pantograph (figure 2.14, position 1), contact head and a roadside contact hood (figure 2.14, position 2). Apart from the arm lift movement, no actuators are required for positioning the contact head in the contact hood on the roadside. The contact system permits high bus positioning tolerances in relation to the contact hood on the roadside, which can be controlled by the driver. Besides, the contact system compensates lateral movements. The system enables position tolerances of up to 1000 mm in driving direction and 750 mm in vehicle lateral direction as well as charging currents of up to 1000 Ampere and voltages of up to 750 Volt DC. Since May 2016, the system is in practical use at LEIPZIGER VERKEHRSBETRIEBE, where the batteries are charged after each scheduled turn. To minimise infrastructure costs, the charging station is supplied by the rail electricity network, [FRA18].

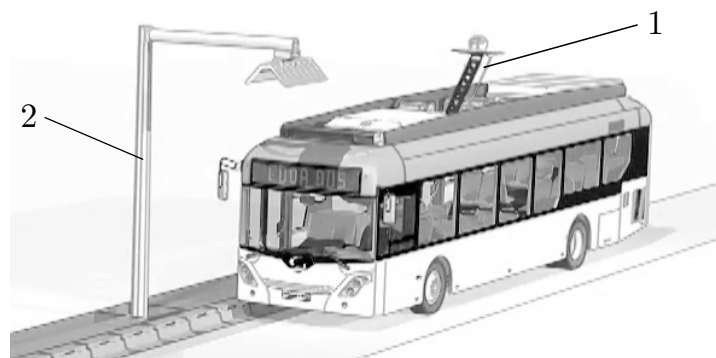


Figure 2.14.: Pantograph charging system for buses, [FRA19].

The company ABB released an automated charging solution for buses named TOSA. A controlled moving arm connects the bus with integrated charging port at the bus stop in less than

one second. Charging takes only 20 seconds, [ABB18]. This is the time buses usually pauses at a bus stop to allow people to enter and leave. This flash charging process offers 600 kW (600 VDC). The operation start was 2017, with 10 equipped buses in 2018. The systems reached 500,000 kilometres driving distance and transported millions of peoples in Geneva within only one year of operation time, [ABB18].

The state-of-the-art research shows different approaches to perform an automated conductive connection. ACD-S concepts for standardized connector systems consist of a robot or a mechanical device to perform the motion sequence. Sensors detect the vehicle charging inlet position. Different previous works introduced mechanical devices with up to 7 axes, to carry out the end effector movements. Some systems include concepts for compensating misalignments during the connection process. Nevertheless, automated connection processes, as well as the functionalities of the systems, are not published in detail yet. For ACD-S that are not based on standard connectors, it is challenging to develop new standards that also enable a manual cable connection. Some conductive systems require equipment of the vehicles with adapters, and others are customized for one specific vehicle model. Vehicle adapters are costly and might increase the vehicle mass. The motion sequences are carried out by the vehicle or charging station module. Furthermore, the vehicle integration of specific adapters, e.g. for underbody charging systems is a challenge and difficult to standardize. Bus systems perform the connection with a pantograph device. The integration of those systems is relatively easy to implement and transferable to different bus types. Because of the limited space and vehicle layout impact, a car application is not feasible.

2.3. Electric vehicles

For many potential customers, the most significant arguments against electric cars are the relatively high purchase price and a too low driving range. The aim of car manufacturers in this context is to provide appropriate customer framework conditions and not dictate customer's behaviour with technical solutions. The big advantage of electric propulsion systems is high efficiency. This denotes relatively low customer costs for energy needed for driving. Compared to conventional driven vehicles, the high price and the uncertain residual value are striking differences. Research and development focus on the enhancement of the driving range and reduction of the battery costs to achieve competitive improvements.

In terms of sales, the forecasts for alternative-powered vehicles are very different. The reason for the diversity lies in the variety of assumptions and influencing parameters such as energy price developments, political boundary conditions or technical developments. In addition to visionary goals with market penetration rates between 40% and 80% by the year 2030, trend and base scenarios show a much smaller market share or EVs between 2.5% and 20%. Besides, TA-SWISS estimates the maximum number of EVs that can be produced on the market, to be able to assess the significance of different forecasts, [SSB⁺14]. The *Center of Automotive Management* estimates a rate of 29% of EVs in Europe and 38% in China in 2030, [MAN18]. Moreover, the online platform STATISTA estimates 25 million EVs in the year 2025. For the

year 2025, leading OEMs plan on putting electric fleets on the market, e.g. VOLKSWAGEN introducing 80 EVs, BMW 12 EVs, HYUNDAI and KIA 14 EVs, [MSH19].

Because of the standardized cable plugging possibility, the major EV concepts for ACCS are pure *Battery Electric Vehicles* (BEVs), *Plug-in Hybrid Electric Vehicles* (PHEVs) as well as *Range Extender Electric Vehicles* (REEVs). Figure 2.15 shows the trends of the percentage share of BEVs and PHEVs of the vehicle class M1 in Austria. From 2014 to 2018, the number of BEVs rose from 0.07% to 0.38%. In the observed period, the percentage of numbers of vehicles that are charged by cable rose from 0.086% (4190 vehicles) to 0.488% (24361 vehicles). In September 2019, the share of newly registered BEVs, Petrol and Diesel PHEVs is recorded with 4.6%, 0.285% and 0.009%, [AUS18].

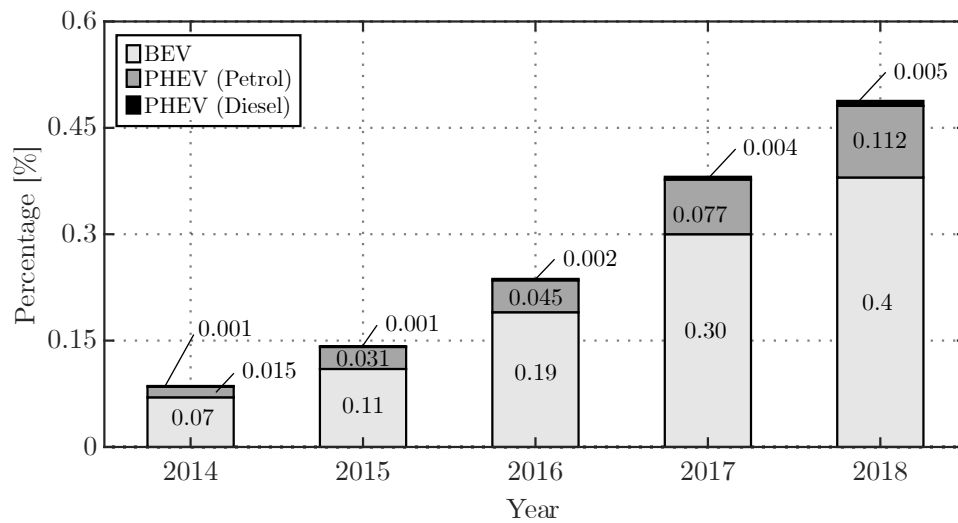


Figure 2.15.: Percentage of numbers of plug-in electric vehicles in Austria, [AUS17].

2.3.1. Battery electric vehicles

A BEV drivetrain consists of a charger, an accumulator, the power electronics for controlling the engine, one or more electric motors and a final drive including gearbox. Depending on driving behaviour, climatic conditions and the associated use of secondary consumers, the driving range of typical EV is between about 70 and 300 km today, [GT12]. State-of-the-art models, e.g. TESLA Model S or AUDI e-tron providing a storage capacity of 95 kWh [AUS19] and 100 kWh [TES20b] are luxury EV with a certain long-distance suitability of more than 400 km. For charging the battery, the AUDI e-tron uses the CCS Type 2 and the TESLA Model S the *Supercharger* charging connector. The TESLA Model 3 Europe version uses the CCS Type 2 standard [TES20b].

Table 2.1 shows a selection of BEVs from 2018. BEVs have reached suitable driving range, not only for the daily work trip but also for longer drives. For several years, vehicles, e.g. TESLA Model S, BMW i3, NISSAN LEAF and RENAULT ZOE have been on the market. Due to the higher battery capacity, the driving range of these vehicles increased considerably. For instance, the early BMW i3 and RENAULT ZOE versions from 2013 were able to drive 190 and 210 km,

according to the *New European Drive Cycle* (NEDC). The latest versions (2019) reach 359 km and 316 km, according to the *Worldwide Harmonized Light Vehicles Rest Procedure* (WLTP). Until now, large driving distances and charging capacities were reserved for TESLA vehicles. With new BEVs, e.g. AUDI e-tron or JAGUAR i-Pace, OEMs follow and produce electrically driven vehicles, which are comparable in performance and comfort with *Internal Combustion Engine* ICE vehicles. Decreasing purchase prices support the distribution of e-mobility and EVs will increasingly replace conventional vehicles.

Table 2.1.: Selection of BEVs in the year 2019 in Austria.

Vehicle	Power [kW]	Battery [kWh]	Charging power [kW]	Range [km]	Price [Euro]
AUDI e-tron, [AUS19]	265 (300 with boost)	95	150	400 (WLTP)	59,990.-
TESLA Model S 100 D, [TES20b]	315	100	145	632 (NEDC)	106,720.-
HYUNDAI Kona Electro, [HYU18b]	150	64	100	<482 (WLTP)	38,190.-
VW e-Golf, [VOL18a]	100	35,8	40	231 (WLTP)	33,990.-
NISSAN LEAF TEKNA, [NIS18]	110	40	50	300 (NEDC)	39,850.-
RENAULT ZOE, [REN19]	80	41	22	316 (WLTP)	21,900.- (without battery)
BMW i3 (120 Ah), [BMW19]	125	37.9	50	359 (WLTP)	40,450.-
JAGUAR i-Pace, [JAG18]	294	90	100	470 (WLTP)	78,380.-

The average energy consumption of a synthetic, typical fleet of electric-powered vehicles at a temperature of 20 °C is 17 kWh per 100km for urban traffic and 34 kWh per 100 km on the highway, [GT12], [GT15], [KH09] and [BH12]. According to the *Institute of Energy- and Environmental Research* (IFEU), an efficiency increase of electrically powered vehicles of 1.2%/p.a. can be assumed, [PGKW13]. A significant influence on the energy consumption of electrically powered vehicles, which is not considered here, is the use of additional consumers such as heating and air conditioning. Accordingly, an average daily commuting traffic drive of almost 50 km [CHA18] leads to about 8.5 kWh energy consumption. On long-haul journeys, stops at 200 km intervals are expected to require about 68 kWh of energy per refilling, provided that the capacity of the electricity storage allows this. An interesting fact is that only 10% of surveyed users travel more than 100 km per day. Moreover, only 1.2% of the respondents stated distances over 250 km per day. Tracks of more than 500 km are driven only 5 times a year, [BNRH13].

2.3.2. Plug-in hybrid and range extender electric vehicles

HEVs are typically equipped with *Electric Motors* (EM) and an *Internal Combustion Engine* (ICE). The drives interact depending on the driving state torque and power requirement, the respective machine efficiency at various operating points and the energy storage level *State*

of Charge (SoC). The goal is to maximize efficiency and reduce fuel consumption. Purely electric driving is limited and only possible over short distances, due to the relatively low battery capacity. The main energy storage system onboard is the fuel tank, supplying the ICE. Charging by a socket is not intended. As a difference, PHEVs allow battery refuelling at a charging socket. Usually, it contains a more powerful electric drive, a larger version of the power storage and a charger. Therefore, purely electric driving is possible over a longer distance. At present, typical electrical driving ranges of PHEV are around 30-60 km, with an electrical storage capacity of approximately 8 to 12 kWh, [GT15]. The integrated ICE and the associated unrestricted driving range, achieved by operating with conventional fuel, increase the attractiveness of the drive concept compared to pure BEVs. In contrast, there are complex propulsion architecture, increased weight and costs.

Another propulsion concept is the REEV. An ICE drives as an electricity generator and charges the empty main battery. Thus, the combustion engine increases the driving range in case of an empty battery. The arrangement of the internal parts corresponds to the concept of serial hybrids - thus mechanical coupling of the combustion engine to the drive wheels is not provided, [WFO10].

2.3.3. ACD integration

The most space-consuming and package-impacting components in EV are battery, wheels with suspension as well as the engine with transmission and propulsion. An example of a typical EV drivetrain and suspension components package is shown in figure 2.16. Because of weight, safety and size, the battery (figure 2.16, position 1) is often built-in between the axles (figure 2.16, position 2) in the vehicle chassis underbody. Engine, transmission and propulsion system (figure 2.16, position 3) are positioned between the wheels and front-, rear- or four-wheel drive is effective to implement by modularization. The vehicle charging system includes an onboard charger and the charging socket (figure 2.16, position 4) for the cable connection. In addition to technical-, space- and safety-related reasons, the socket position often depends on vehicle type and design demands.

The integration of an automated charging system, e.g. charging connectors or pads, requires space and influences the vehicle packaging. Some concepts show the mechanical integration of the WPT charging pad at the vehicle underbody. However, the position is not specified and differs from the front, middle and back of the vehicle, [KH15, p.297-307]. In general, the vehicle underbody offers good preconditions for a charging device positioning. The apparatus is protected, not directly accessible for humans in term of misuse, and the car design is not influenced. However, charging pads and sockets as well as cables require vehicle space and are exposed to dirt and water during driving. Big charging pads have a crucial impact on the vehicle packaging and components, e.g. the main battery. Furthermore, the eventual later installation of an automated charging device has to be considered in the early vehicle development phase. Costs and additional weight are further disadvantages.

In general, most applied are side coupling charging sockets of different standards, e.g. CCS Type 2, Type 2 and CHAdeMO. According to a study of a representative EV fleet, charging sockets are typically located at the height of approximately 70 to 100 cm, [Pan15]. For example, the vehicle front-located charging plug of the RENAULT ZOE is in the height of 70 cm. The BMW i3 has the plug on the left side, over the rear wheel in 95 cm height. In this height, the vehicle body offers enough space for the integration of devices, e.g. a charging inlet. Compared to underbody charging technologies, side-coupler connectors are standard in all electric cars today because of the possibility to charge the car by manual plugging of the cable.

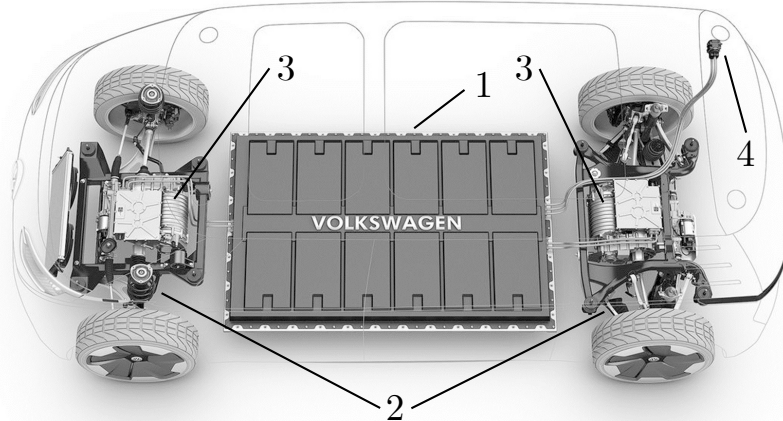


Figure 2.16.: Example of a typical EV component packaging, [VOL19a].

The EV market is rising, and ACCS becomes increasingly interesting to improve the charging comfort of BEVs, PHEVs as well as REEVs. ACCS systems have advantages in the course of vehicle integration. By using standard connector systems, no additional components are necessary, and there are no influences on the vehicle chassis. In terms of costs, the parallel use of the connector system for manual and automated charging is a further advantage. A standardised socket position would support automated charging of a high number of different vehicle types and would simplify parking and cable connection processes. Due to space conditions, suited positions are behind the front wheels and in the rear fenders area, as well as the vehicle front or back. The target of the present research activities is an ACCS system that is capable of serving all types of electric cars with standard charging sockets and all possible positions. The aim is the prevention of vehicle adaptations and interventions in the vehicle architecture for reducing technical effort and costs for automated charging solutions in EVs.

2.4. Charging standards

Standards create consistent and clear rules and ensure that one part fits to the others. ACD charging of a large number of various vehicle types requires the standardization of the charging systems and charging processes. In this context, standards have to enable interoperable charging. However, the creation of standards is difficult and a long process. In addition to

2. State-of-the-art and boundary conditions

the development of technical solutions, demands of various interest groups have to be considered. In this context, the use of existing standards for automated charging provides significant benefits:

1. Reduction of market entry barriers and fast market penetration.
2. Saving costs with regard to charging system technology, infrastructure as well as vehicle adaptation and integration.
3. If required, existing charging standards can be extended for individual automated charging solutions. Cable and inlet standards do not have to be re-developed.

Despite using charging standards, ACD-S is a challenge. Charging standards define connector and inlet design, but there is, for example, no standard for the vehicle charging socket position. An investigation of various EV types regarding the charging socket position shows large differences depending on vehicle brand and type. An overview about various EVs and charging systems is presented in figure 2.17 and table 2.2. Most, *Battery Electric Vehicles* (BEV) and *Plug-in Hybrid Electric Vehicles* (PHEVs) have the charging sockets on the right or left side. Additionally, some vehicles have it on the front or backside. Furthermore, the socket height is not standardized. A second problem can be found in the charging cap mechanism that opens in various ways. Several vehicles have an additional charging inlet security cap that has to be removed for charging the vehicle. Even in this field, there are differences. Some brands have a plastic flap, while others have a rubber plug that has to be unscrewed. Often, the variety of charging systems is based on specific design solutions. Today, the CCS Type 2 connector for DC quick charging and the Type 2 connector for AC are widely used standards in Europe. CCS Type 1, CHAdeMO and the TESLA Supercharger are mainly used in ASIA and the USA. As an example, the charging port of the AUDI e-tron, [AUS19] includes a modern system good prepared for automated charging. The charging lid opens and closes automatically. Vehicles such as the TESLA Model 3, [TES20b] also already meet these requirements.



Figure 2.17.: Examples of various EV charging and security cap systems. Beginning from the top, left: KIA Soul EV (2015), MERCEDES C350 Hybrid (2015), NISSAN Leaf (2010), PEUGEOT iON (2011), PORSCHE Panamera S Hybrid (2013) and BMW i8 (2015).

Table 2.2.: Examples of various EVs and their charging- and security cap system.

Vehicle	Propulsion system	Charging standard	Security cap	Max. charging capacity [kW]	Plug position and height [cm]
Mercedes B-class Electric Drive	BEV	Type 2	Plastic flap	11	Rear, left, 88
KIA Soul EV	BEV	Type 1/ CHAdeMO	Rubber plug	50	Front, middle, 85
BMW i8	PHEV	Type 2	Plastic flap	4.6	Front, left, 81
AUDI e-tron	BEV	CCS	No flap	150	Front, left, 86
BMW i3	BEV/REEV	CCS Type 2/ Type 2	Plastic flap	50 (CCS)	Rear, right, 95
RENAULT ZOE Q210	BEV	Type 2	Plastic flap	43	Front, middle, 76
PEUGEOT iOn	BEV	Type 2	Plastic flap	43	Rear, left, 87
NISSAN Leaf	BEV	Type 1/ CHAdeMO	Plastic cap	43	Front, middle, 75
TESLA Model S	BEV	TESLA Supercharger	No flap	120	Rear, left, 86
VW e-Golf	BEV	CCS Type 2	No flap	40	Rear, right, 88
AUDI A3 e-tron	PHEV	Type 2	Plastic flap	3.7	Rear, right, 85

Figure 2.18 shows the CCS (Combo) charging system in the two variants. The CCS Type 2 (IEC 62196-3 Type 2) (figure 2.18, left) is the EV charging standard in Europe. The CCS Type 1 (figure 2.18, right) was developed for North America according to the standards J1772 and IEC 62196-3 and is also used in Japan. Both variants consist of a DC part with 2 pins for high power charging (figure 2.18, position 1) with up to 500 Ampere and 1000 Volt. For example, the cables from PHOENIX CONTACT allow charging power of up to 500 kW for CCS Type 2 and 200 kW for CCS Type 1. The upper parts correspond to the IEC 62196 Type 2 (figure 2.18, position 2) and SAE J1772-2009 (figure 2.18, position 3) connector shapes, [CON20].

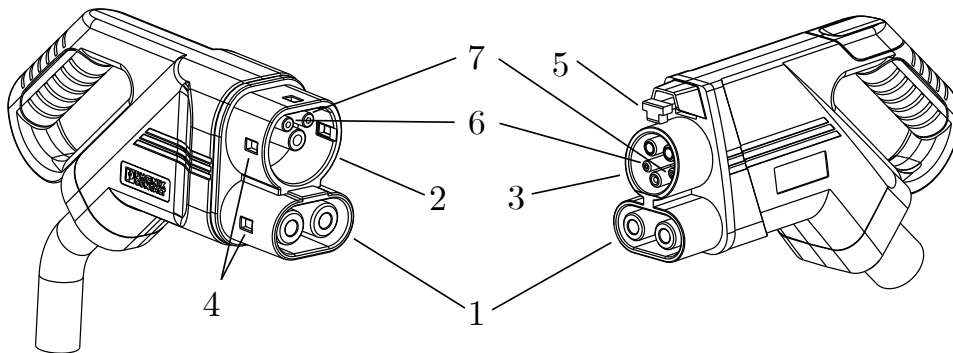


Figure 2.18.: Left: CCS Type 2 connector. The connector contains seven pins - three pins for ground, proximity detection, control pilot and two pins for DC power + and DC power -. Right: CCS Type 1 connector. Five pins are available for AC line 1, AC line 2, ground, proximity detection, control pilot and two pins for DC power +, DC power -, [CON20] and [ELE19]

The upper connector parts consist of a CP pin (figure 2.18, position 7) and PP pin (figure 2.18, position 6) for EV-charging station communication and cable and inlet connection detection.

2. State-of-the-art and boundary conditions

The CCS Type 2 provides of an electromechanical locking mechanism (figure 2.18, position 4), the CCS Type 1 a latch on the upper side (figure 2.18, position 5) for locking, which engages when plugged in that can be released again with a pressure lever. Both mechanisms are preventing the charging plug from being pulled out during the charging process. This ensures plug disconnection only without voltage or power, [GOI20]. [CON20]. In the next years, the stepwise development of the technology through reduced charging sessions and enhanced comfort trough automatization can be expected. Figure 2.19 shows a *big picture* of a possible CCS roadmap that is currently discussed in CharIN e.V., [INI19].

The proposed development step denoted as *CCS basic*, *CCS extended* and *CCS advanced* introduce new CCS charging technologies as well as new charging features to be developed. The interoperability at the interfaces between EVs and charging stations is a crucial aspect of enhancing the acceptance of e-mobility. The parallel interconnected work of different organizations and types of activities (figure 2.19 Level A to E) contributes to the implementation of an interoperable combined charging system, [WHB19c, p.2].

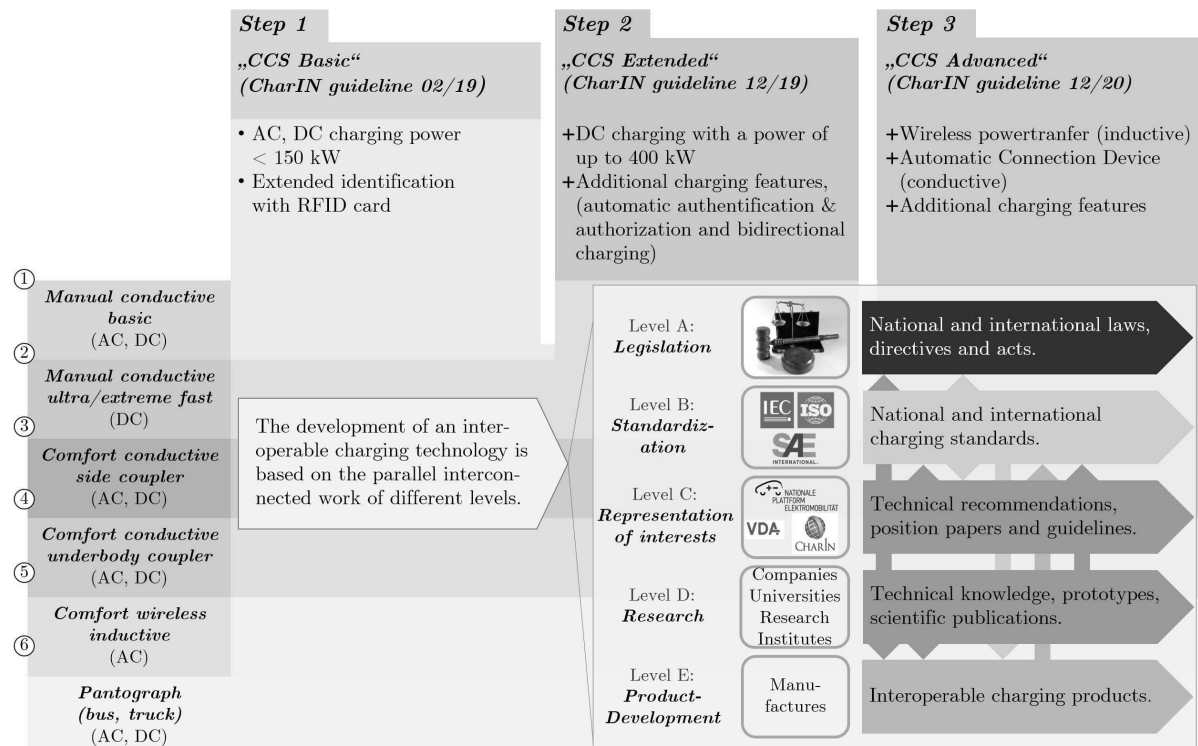


Figure 2.19.: The big picture shows a possible stepwise development of CCS, [INI19].

2.4.1. Charging cables

Table 2.3 gives an overview of standardized EV charging cables. The data are exemplary related to cables with 5-meter length and an opened end for the charging station connection. Increasing the charging power requires charging current and/or voltage enhancement. To prevent the cables from overheating due to the high currents, an increase in the conductive

cable cross-section is necessary, which leads to unwieldy, heavy cables. Cooling the cables is an alternative to decreasing cable diameter and weight. Cooled CCS Type 2 cable (table 2.3, CCS Type 2) enables power currents of up to 500 Ampere DC, under the compliance of temperature guidelines. The maximum allowed cable temperature is specified by 90° Celsius. Several in the HPC system integrated temperature sensors measure the heat in real-time, both directly at the power contacts of the plug and in the cable. [CON20]. Exemplary, the 5 meters cooled CCS-Type 2 charging cable for power capacities of up to 500 kW has a weight of 11.6 kg, carries 5 wires with 25 mm² and 7 wires with 0,75 mm² and has an outer diameter of 35,7 mm², [CON16a].

Table 2.3.: Technical data of different charging cables, [CON20].

Cable	Standard	Voltage [V], current [A]	Charging power [kW]	Insertion/ withdrawal force [N]	Diameter [mm]	Min. bending radius [mm]	Weight, 5 m [kg]
CCS Type 1	SAE J1772, IEC 62196-3	1000 DC, 200	200 DC	<75 / <75	35.3 ±0.4	529.5	13.6
CCS Type 2	IEC 62196-3-1	1000 DC, 500	500 DC	<100 / <100	35.7 ±0.4	535.5	11.6
Type 1	SAE J1772, IEC 62196-2	230 AC, 32	7 AC	<75 / <75	12.8 ±0.4	98	2.1
Type 2	IEC 62196-2	480 AC, 32	26.6 AC	<100 / <100	17 ±0.4	255	2.4
CHAdemo	GB/T 20234.1-2015, GB/T 20234.3-2015	1000 DC, 250	250 DC	<100 / <100	34.9 ±0.4	174.5	17.7

2.4.2. Communication

ACCS requires a communication integrating vehicle and charging infrastructure for authorization, connection, managing the charging process and the possible combination with autonomous vehicle driving functions. However, the charging station is based on inductive or conductive technology. If a vehicle has to be charged, it parks in a free parking lot (manually or autonomously). For the next steps and to perform a successful charging process, the system must gather important data, including driver- and vehicle information. In this way, a communication between car and infrastructure has to be established.

Barrier-free public charging requires communicational and technical compatibility of EVs and charging systems. Since 2015, the standard ISO 15118 also called *Road vehicles and Vehicle to grid communication interface* specifies the communication between charging stations and EVs. The communication is defined by the *Electric Vehicle Communication Controller* (EVCC) and the controller integrated into the charging station *Supply Equipment Communication Controller* (SECC). The standard is not limited to electrically powered cars but is also open to other vehicle classes. The goal is a standardized communication, which is also seen as the key to further business models and prospective use cases. It defines all communication-related issues of smart charging; for example, connection setup, authentication, energy and payment tariffs, charge management and, in the future, consideration of smart grid requirements. ISO 15118 consists of eight parts. The description and content of each part are listed in table 2.4, [INT13].

Table 2.4.: Contents and description of the ISO 15118 standard parts, [INT13].

Standard parts	Content and description
ISO 15118-1	General information and use case definition.
ISO 15118-2	Network and application protocol requirements.
ISO 15118-3	Physical layer and data link layer requirements.
ISO 15118-4	Refers to the conformance tests for requirements specified by ISO 15118-2.
ISO 15118-5	Refers to the conformance tests for requirements defined by ISO 15118-3.
ISO 15118-8	Physical layer and data link layer requirements for wireless communication.
ISO 15118-9	Physical layer and data link layer conformance test for wireless communication.
ISO 15118-20	Second generation network and application protocol requirements.

The current standard drafts of ISO 15118-1 and -8 take into account the requirements for wireless communication, WPT as well as ACD, [INT18a]. The communication between vehicle-internal components, as well as components within the charging station, is not considered. Also, communication with network providers or other subscribers, required for the function of the charging station, is not part of ISO 15118. In this way, the standard provides rules and guidelines exclusively for communication between the EV and the charging station. In summary, ISO 15118 specifies basic conditions and requirements for communication, as well as use cases for conductive and inductive charging systems, aspects that affect the charging process, payment systems, and charging management, [INT13].

Figure 2.20 shows the ISO 15118 process draft for ACD systems. ACD systems adopt the existing standards and regulations for wireless communication. The communication sequence is based on the principle of wireless charging systems and has been extended for ACD. Three new processes *System Status Check*, *AutoConnect* and *AutoDisConnect* have been added. When the driver approaches the charging site area and is in the range of the wireless SECC system, discover and association takes place in the step *Association* (2.20). Parameters are exchanged to check the interoperability of EV and ACD. If the wireless association between EVCC and SECC is successful, *high-level communication* (HLC) services and further use cases steps can start. *VAS* manages the information exchange for future applications and additional services, e.g. reservation of public charging site or the required energy for next usage. The subsequent process *System Status Check* checks the current status of the EV and ACD during the entire charging process, e.g. in case of malfunctions or if the charging station is occupied. In case of an error or an unexpected event, the charging process is aborted. *Fine positioning and Parking* is a procedure where the EV is guided to the ACD until the charging devices are properly aligned. The next step *Pairing* guarantees that the EV is plugged or parked to the right charging supply equipment (ACD). Regarding *Fine Positioning, Parking, Plugging and Pairing*, pairing should start as soon as the EV has reached the parking position. If the parking position is not reached, the driver is requested to drive to the optimal place. The step *AutoConnect* includes the procedure for an automated connection of EV and charger and is controlled through *HLC*. EVCC and SECC exchange messages and data until the connection process is complete. For ACD, the communication standard proposal does not deliver detail information about the exchanged data. Afterwards, the power transmission *Power Transfer* can start. During the unplugging process *AutoDisConnect*, data is exchanged via EVCC and

SECC until the process is completed successfully. The EV is able to request the charger to disconnect the ACD and bring it back to the home position. The ACD has to be moved back in waiting position before the vehicle can leave the charging lot, [INT18a].

For series applications, it is recommended to use the standard proposals for further development of ACCS. (Remark: The proposals are not yet a standard but serve as a guideline). This supports the ACCS compatibility with various EV types, reduces market entry barriers and saves costs. The represented ACD communication process of the ISO 15118 proposal can be transferred as a basis for ACCS. The ACD communication proposals take place wirelessly. Therefore, ACCS requires the implementation of a wireless communication device.

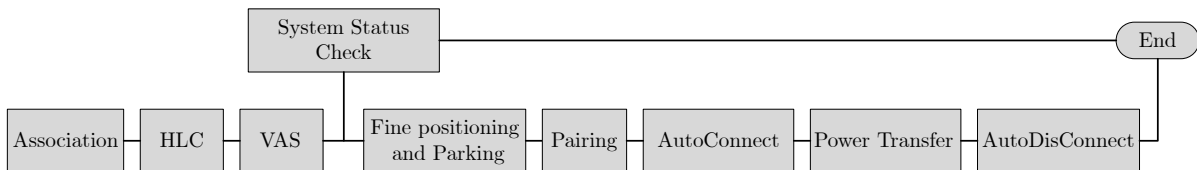


Figure 2.20.: ACD communication sequence draft of the ISO 15118 standard, [INT18a].

2.5. Charging infrastructure

E-mobility requires an area-wide and demand-oriented charging infrastructure. A high number of charging stations should be easily accessible and equipped according to customer demands. A charging power and -services, as well as user demands analysis, provide the basis for the determination of ACCS requirements and boundary conditions.

2.5.1. Charging power

An overview of public EV charging stations in Europe is shown in figure 2.21. From 2010 to 2019, the number of charging stations has increased more than 50 times to 170,149, [OBS20]. TESLA is a pioneer for a long-range charging station infrastructure. Worldwide, at strategically essential mobility intersections 1,804 charging stations with 15,911 chargers enable up to 145

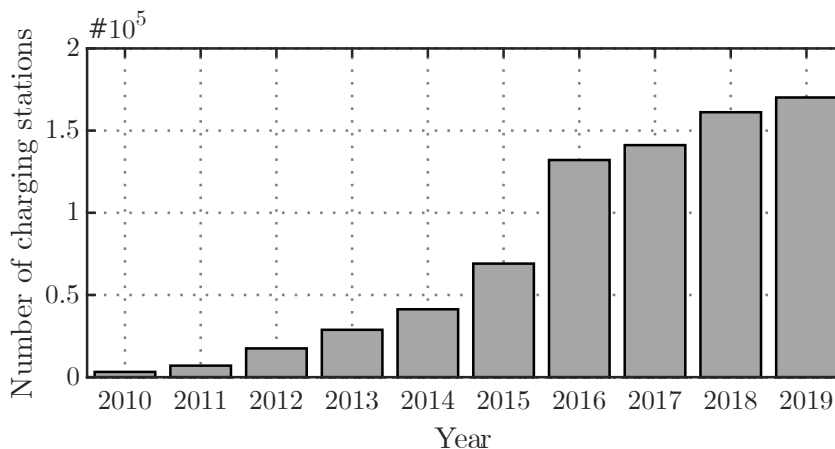


Figure 2.21.: Number of charging stations in Europe from 2010 to 2019, [OBS20].

kW charging power each, [TES20b]. According to the online platform GOINGELECTRIC, Germany offers 1300 charging terminals and Austria 125 with a charging power of more than 100 kW, [GOI20].

The charging infrastructure preparation for the next EVs generation has begun. Although, corresponding vehicles are not on the market yet, 350 kW ultra-high power charging stations have been established in Europe and America, [ION19] and [ELE19]. The high charging power requires a technology step from 400 to 800 or even 1000 Volt. With the increase of charging voltage, there are some more advantages besides the higher charging power. The CCS connector cables are lighter and easier to handle because of the lower cable diameter, due to the lower charging currents. As an example, for the advantages of ultra-fast charging, the trip from a customer from Berlin to Lindau with a driving distance of approximately 720 km can be illustrated. A conventional vehicle needs about 5.5 hours for the route and has to refuel once for about 10 minutes. With the current charging infrastructure, an electric vehicle needs 8 hours for the same route. This is not because of the cruising speed, but because it has to be recharged twice for a total of 160 minutes. The vision of PORSCHE and other premium segment OEMs is to reduce charging time to a customer-friendly level, with less than 17 minutes per charge. This can only be achieved with a significantly higher charging power, [Rec16].

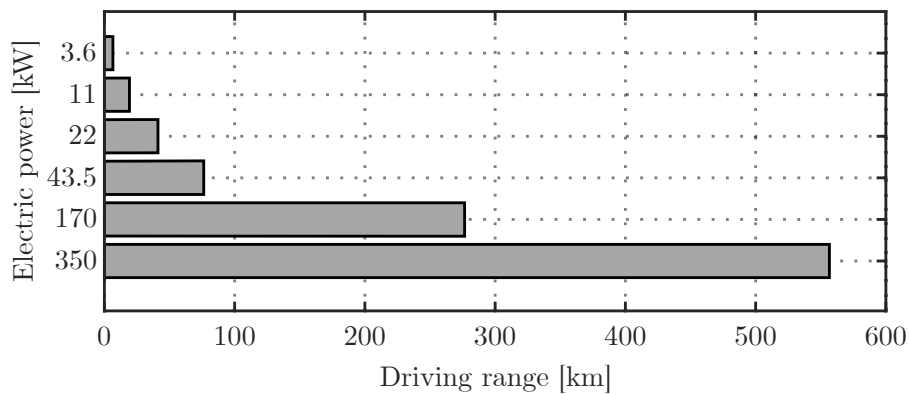


Figure 2.22.: Driving range comparison in case of 15 minutes charging with different charging power levels.

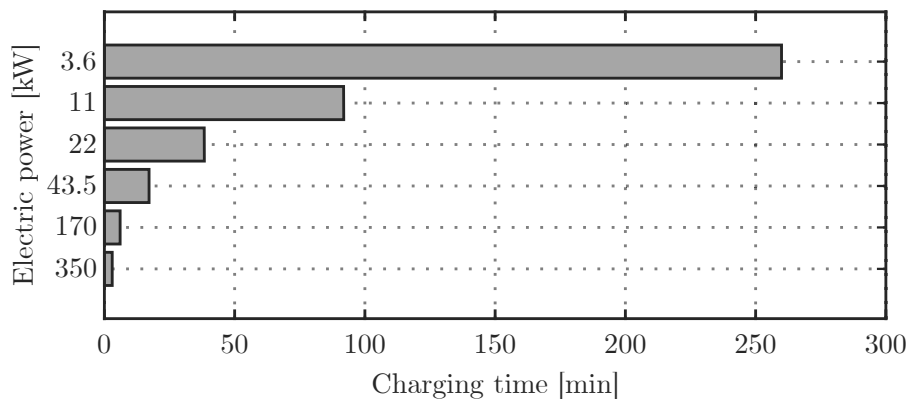


Figure 2.23.: Comparison of the required charging time for a driving range of 100 km with different charging power levels.

Figure 2.22 shows a comparison of the driving range after 15 minutes charging with different charging power levels. In contrast, figure 2.23 depicts the required charging time for 100 km driving range. The calculations are based on the energy consumption of 14.1 kWh for 100 km driving range of a Tesla Model 3 according WLTP, [TES20b]. Charge losses are considered by 10%. The use of perspective high charging capacities of up to 350 kW shows a significant reduction of charging time.

For public charging, ACCS has to provide high charging capacities. In comparison to standard charging cables, HPC cables have more weight and a higher bending radius. The unhandy cables lead to higher ACCS demands, e.g. load capacity and absorption of forces and moments during cable moving. In this context, the target of the research activities is an ACCS actuator system and charging connector path trajectory that fulfil the cable requirements. Fastening, guiding and plugging of the cable must be taken into account for ACCS. This includes the prevention of the limited bending radius as well as high torsion and sharp edges, which can damage the cable.

2.5.2. Charging stations

Besides the charging process itself, essential aspects for customer-friendly vehicle charging are the processes of registration, authentication and payment. Figure 2.24 shows the actual and target state of an experienced EV user survey. With a score from 5.6 to 6.5, all criteria were considered by the subjects to be important or very important. In summary, the result can be interpreted that the practicality and comprehensibility of current charging station processes are far away from the target state. The biggest discrepancy between target and status is an uncomplicated payment system, a functioning roaming and simple authentication. For 82% of the users, the most important criteria is an easy authentication without registration. For find-ability, the charging station positioning, e.g. at supermarkets and shopping centres, is most important. 80% of the respondents assign this as a highly important factor, [VF17].

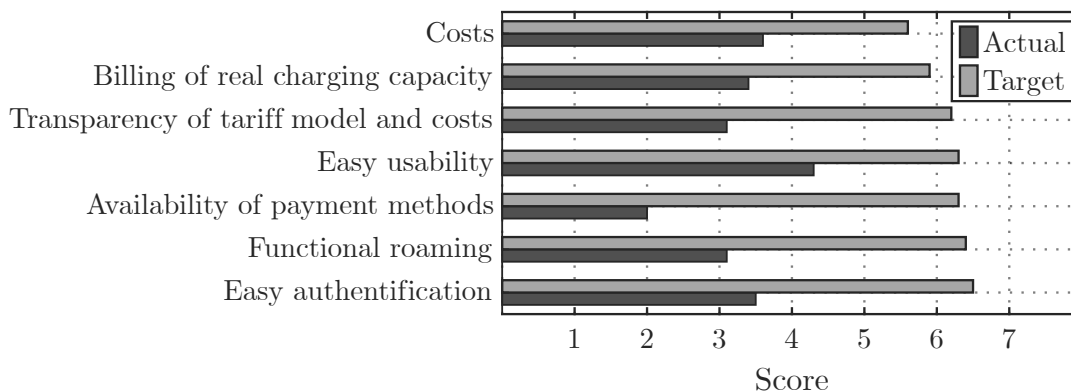


Figure 2.24.: Evaluation of the current and target charging infrastructure with regard to various criteria, [VF17].

For EV-drivers, an unrestricted and straightforward charging station access is essential. In this context, a certain dissatisfaction can be determined. Due to the elimination of cable handling

procedures, ACCS increases the charging comfort for costumers. Nevertheless, easy authentication, as well as billing processes, have to be provided. In this context, the implementation of communication standards, e.g. ISO 15118, into ACCS, has to be considered. The standard enables easy registration, booking and billing for the loading process and already includes information exchange for future applications and additional services (VAS).

2.5.3. Services

The potential to promote new customers through charging infrastructure services appears promising, [VF17]. During the charging process, the drivers can linger in a lounge that offers coffee, *Wireless Local Area Network* (WLAN) as well as charging equipment for tablets and personal computers, [VLO18]. Due to potentially surrounding shopping and relaxing facilities, the EV drivers can use the charging and parking breaks, [Sto15]. The *ChargeLounge* provides an example of an (inter-) urban fast-charging infrastructure. A dedicated business area offers the possibility to hold business meetings, as well as telephone and video conferences, [CHA18].

A study shows the decreasing use of home charging because of the rising charging power and charging points, [WHB16]. Concerning shopping in public institutions, shopping centres play a decisive role in the future. For example, the average length of stay in a supermarket is 20 to 40 minutes, [WH18]. For users, a visit of a *Point of sale* (PoS), e.g. a supermarket, the charging infrastructure is already suitable today. With a rating of at least 6 on a seven-step scale, 74% would change the PoS for a free of charge charging process. Regular public charging infrastructure users have the highest approval, with an average score of 6.2, [VF17].

Figure 2.25 shows a concept proposal of a future shopping centre, providing customer-friendly and innovative service concepts. With the interconnected communication of driver, vehicle and infrastructure, the charging process is automated and combined with self-parking vehicles. The concept is designed from the findings of user behaviour investigations in a shopping centre, [Hir17]. Vehicles autonomously start or carry out various processes without driver intervention, e.g. car washing or battery charging. After arrival, passengers can leave the vehicle at the shop-

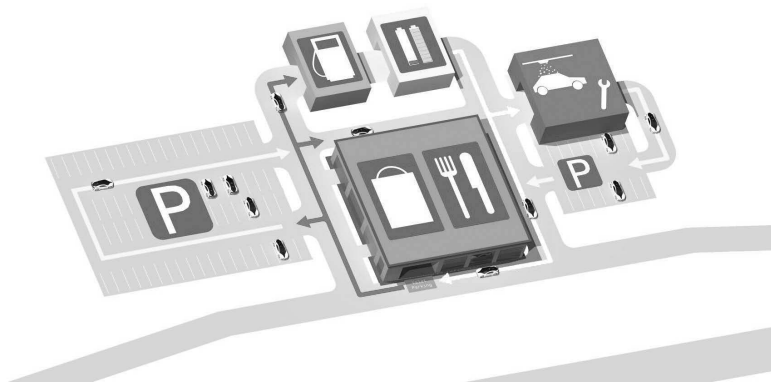


Figure 2.25.: Shopping centre and rest stop concept for the year 2030 with customer-friendly comfort services, [WBH18].

ping centre main entrance. The autonomous car is able to do predefined tasks, e.g. automated electric charging by using an ACCS system, [WBH18]. The time during battery charging can be used for services, e.g. shopping. In this context, ACCS provides a further service application and enhances customer comfort.

2.6. Charging process

In the following, the manual EV charging process is analysed and working tasks and restrictions for ACCS are derived. Figure 2.26 shows the sequence of a manual cable-based charging process. Procedure and duration depend on charging lot, EV type as well as charging station and -standard. *Vehicle pre- and post-processing* includes vehicle parking, -positioning and -unparking. It is impacted by charging lot access as well as charging station- and vehicle charging socket position. *Charging socket pre- and post-processing* prepares the charging socket for cable connection and restores the vehicle to a ready-to-drive condition after disconnected cable. As with the socket position, charging cover mechanism and protective plug(s) differ by vehicle type. *Charging cable handling* includes charging cable plugging and unplugging. Cable moving and insertion depend on the vehicle- and charging station position, cable length and charging standard. Battery charging takes place after successful cable connection and ends with the cable disconnection. The duration of battery charging is given by the charging station power or EV-drivers time constraints.

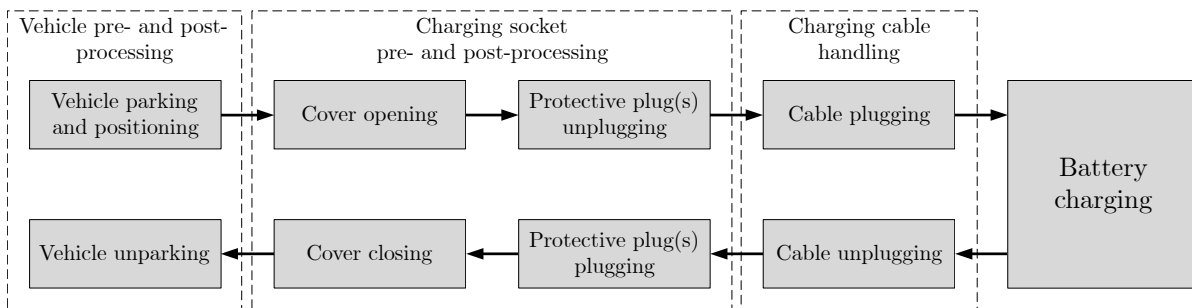


Figure 2.26.: Manual EV charging process with charging cables.

The charging process steps are described by an exemplary charging lot configuration and EV type. Figure 2.27, left, shows a common charging lot with a 11 kW charging station (figure 2.27, CS). The 8 meter Type 2 charging cable (figure 2.27, C) is fixed at the charger and fits to the EV CCS Type 2 inlet standard. At cable-less stations drivers own cables and, if necessary, adapters have to be used. In such cases, cable and adapter have to be unpacked from the vehicle, laid and connected with the charging station and the EV. The exemplary EV (figure 2.27, V and figure 2.28), locates the charging port right, above the rear wheelhouse, at approximately 95 cm height (figure 2.27, left, I).

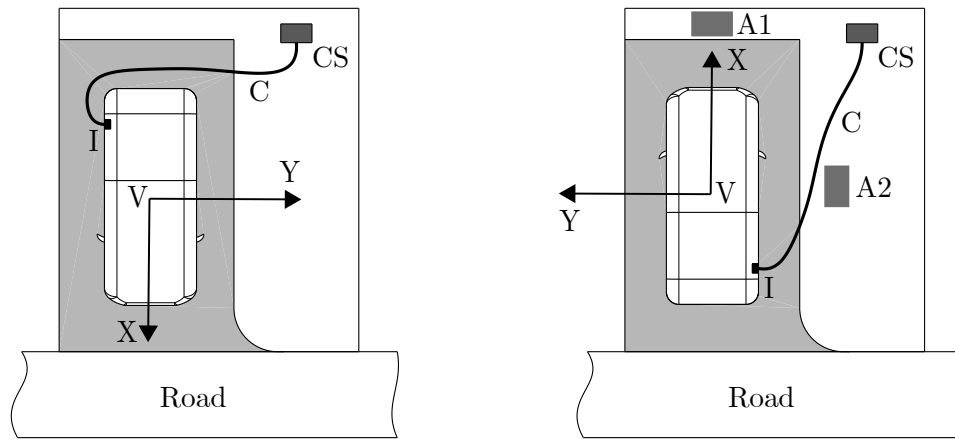


Figure 2.27.: Top view of a charging lot model. Left: Backward parked EV and representation of the charging cable position. Right: Forward parked EV with representation of the charging cable position.

The cable length enables for- (figure 2.27, left) or backward (figure 2.27, right) EV parking. In case of a rear, left side-mounted charging port, only a backward parked EV position would enable a connection due to limited cable length. Figure 2.27, right, A1 and A2 show alternative charger positions. Alternative A1 simplifies cable plugging for EVs with front- and middle charging ports, A2 supports EV-side charging sockets. In the following, the charging process steps are explained in detail:

1. *Vehicle parking and positioning*: The step consists of EV parking and positioning. The EV is parked forward in the charging lot (figure 2.27, right). While entering, the EV position and orientation are adjusted for reaching the targeted position.
2. *Cover opening*: The next step includes cover opening (figure 2.28, left) for providing access to the charging inlet. The charging cover of the exemplary car has a smooth surface and is made of plastic. It must be unlocked by hand, by pressing on the left side of the cover at mid-height. Afterwards, the cover opens automatically and stays in its final position at the right side of the charging inlet (figure 2.28, right).



Figure 2.28.: Left: Side view of a BMW i3 with closed charging socket cover. Middle: View of the CCS Type 2 inlet with unplugged Type 2 inlet plastic flap. Right: View of final cover position and unplugged plastic flaps.

3. *Protective plug(s) unplugging*: Protective and security flap(s) unplugging is done in step 3. For Type 2 (AC) charging the upper flap (figure 2.28, middle) has to be pulled out and fastened at the cover - for DC charging, this also has to be done for the lower plug (figure 2.28, right).
4. *Cable plugging*: The step *Cable plugging* consists of all activities for the connection of charger and EV and can be separated into the following four phases:
 - a) Phase 1: Pre-positioning
 - b) Phase 2: Guiding
 - c) Phase 3: Aligning
 - d) Phase 4: Plugging

Figure 2.29 shows the plugging procedure by a CAD-model sectional view of a CCS Type 2 charging connector and -inlet (figure 2.29, C and I). The first phase *Pre-positioning* (figure 2.29, PP) contains charging station cable removing and towing it to charging socket near. In the second phase *Guiding* (figure 2.29, G), the charging connector (figure 2.29, C, Pos. 1) is guided by hand to the charging inlet. The connector trajectory (figure 2.29, T) is controlled manually. The phase ends with the first contact (figure 2.29, CT) of connector (figure 2.29, C, Pos. 2) and inlet. If the connector does not fit into the conical inlet front, a position correction is made until it slides approximately 3 mm into the inlet. The alignment of connector coordinate system (figure 2.29, CC) and inlet coordinate system (figure 2.29, IC) added the plugging length (figure 2.29, L) in inlets *Z*-direction, defines the third phase *Aligning* (figure 2.29, A). In the fourth phase, the connector is pushed until the connector coordinate system (figure 2.29, CC) and the inlet coordinate system (figure 2.29,) aligns.

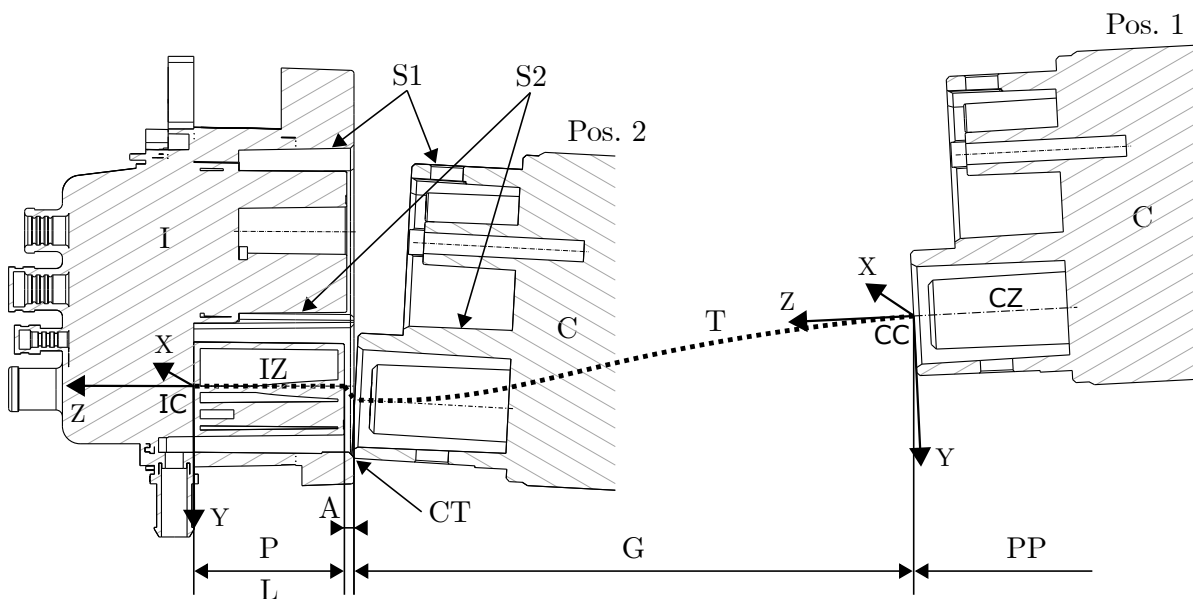


Figure 2.29.: Model of the charging cable plugging process by cut CAD-models of CCS charging inlet and -connector.

2. State-of-the-art and boundary conditions

Inlet- and connector sliding surfaces (figure 2.29, S1 and S2) compensate connector position- and angle misalignments. In phase four, the connector trajectory (figure 2.29, T) is limited controlled manually because of the geometry-based guidance of connector and inlet. In this context, the trajectory path can be influenced minimally, e.g. by shaking the cable. Position and angle misalignments decrease with increasing plug-in length. In plugged position and successfully established vehicle communication, an EV connector lock mechanism ensures holding the charging plug for the next charging phase *Battery charging*.

5. *Battery charging*: Figure 2.30, left, shows the plugged charging connector and figure 2.30, middle, the resulting cable position. Battery charging starts automatically after successfully established communication of EV and charger and locked connector. Alternatively, the charging start requires a trigger, e.g. a start button, user authentication with RFID-card or a smartphone app. The charging process stops after the full battery or can be interrupted by moving the charging connector. In this situation, the power exchange stops and the connector locking mechanism opens.



Figure 2.30.: Left: Side view of the EV with an open charging lid and plugged charging cable. Middle: Side view of the EV during battery charging. Right: 11 kW charging station with two Type 2 charging cables.

6. *Cable unplugging*: The phase includes charging connector unplugging, moving the cable back to the charging station and putting the connector back in its holder.
7. *Protective plug plugging*: After disconnected cable, the protective plug(s) can be returned to their original position.
8. *Cover closing*: The phase includes closing of the socket cover. For the exemplary EV, the cover must be guided from the right side in a quarter circular motion to the left side, until the lock mechanism is triggered, holding the lid in position.
9. *Vehicle unparking*: Vehicle entering and charging lot leaving are the activities in the last phase and completes the EV charging process. For the exemplary charging station (figure 2.27, left) the vehicle has to be driven backwards with a left or right curve into the road.

An ACCS has to perform the manual charging process tasks automatically. ACCS challenges include the compensation of vehicle parking misalignments, the accurate detection of the charging socket and guidance of the charging cable into the charging socket as well as opening and closing of charging lids and handling of security mechanism. The latter leads to particularly high automation effort. The capability of serving a large number of different vehicle types increases the ACCS challenges significantly. Requirements and restriction for ACCS are developed in detail in chapter 3.

2.7. Vehicle parking and positioning

ACCS range and kinematics, e.g. the number of axes and axes rotation angles, depend on EV parking misalignments in relation to the charging station. For the determination of the challenges and requirements, parking processes, -accuracy and -position aids are investigated in the following.

2.7.1. Manual and automated parking

Although most people are generally positive towards car driving, searching for a suitable parking lot and vehicle parking is a stressful situation and reduces driving pleasure. In a study, more than 35% of German vehicle owners identified parking as stressful, [BOS13]. EV owner have to face several challenges in case of unplanned battery refuelling. At first, a near, free and for the vehicle suitable charging station has to be found. Parking starts after reaching the final destination. Depending on the parking lot and charging station layout this can be laborious. Due to the requirement of positioning the charging socket next to the charging station, the vehicle has to be parked properly aligned and accurate. Easy and comfortable EV positioning possibilities, e.g. as it is at petrol stations for conventional vehicle refuelling is rare to find.



Figure 2.31.: Charging park concept with comfortable parking and charging lots, [VF17].

A proposal for quick and comfortable parking and charging similar to conventional vehicle refuelling is shown in figure 2.31. The concept offers different charging station types and charg-

ing connectors with up to 350 kW (600 kW per charging station), aligned on local conditions, [INT18c].

Figure 2.32 depicts the development of automated parking technologies. Mechanical parking systems to sort and park the vehicles efficient and comfortable exist since the beginning of the 20th century. The first modern automated park facilities started in the early 90s. A significant technological jump has been recorded since the start of the 21st century with the introduction of parking robots and automated vehicle carry platforms that enable efficient vehicle sorting. The next significant change is piloted and autonomous parking. Parking and space-saving storage are done by autonomous vehicles that are connected and guided by the user and the infrastructure.

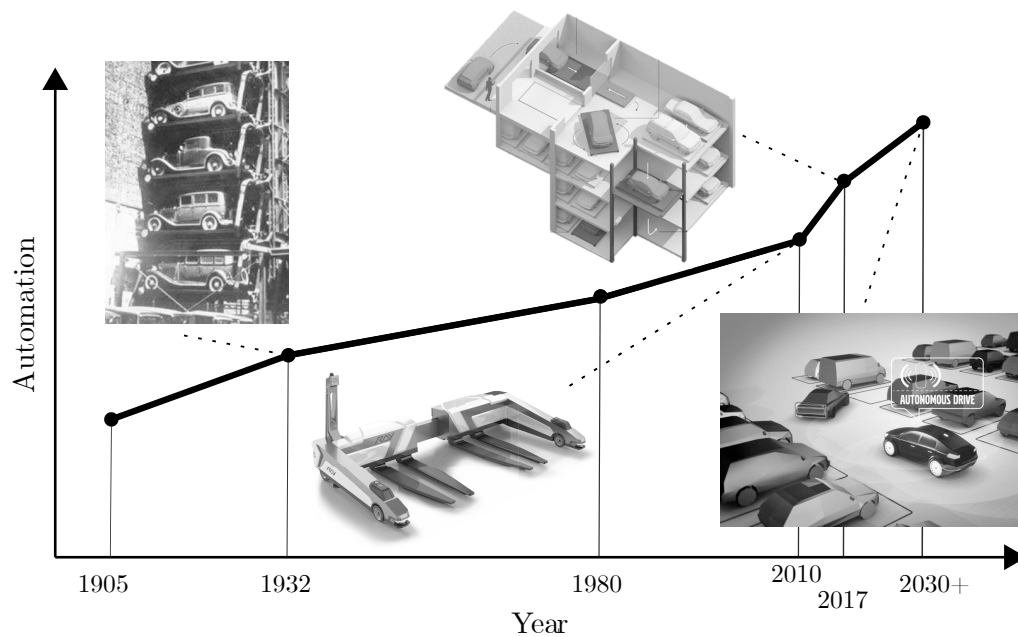


Figure 2.32.: Development steps of the vehicle parking automation, [MOT19a], [Sys19], [Dum15] and [VOL19b]

For ACCS developments, it is essential to consider the whole parking procedure, beginning from targeting the final vehicle charging lot position until reaching it. In addition to parking position accuracy, attention should be paid to simple parking procedures in order to ensure driver comfort. Location, parking lot size as well as vehicle parking processes impact an ACCS charging system. The possible ACCS integration into parking facilities with automated parking vehicle functions has to be taken into account.

2.7.2. Vehicle position

Figure 2.33, left, shows a typical situation of parked vehicles (figure 2.33, left, V_1 , V_2 and V_3) and the resulting different positions of the inlet (figure 2.33, left, I_1 , I_2 and I_3). To enable successful connector and vehicle inlet joining and to avoid tilting during plug-in, exact

positioning of the connector in relation to the inlet is required. The inlet position varies with each parking process. Controlled, exact positioning of the vehicles at the charging station could simplify charging robot systems, but this isn't easy to achieve in real-life applications. Furthermore, different vehicle load situations, wear on chassis and tyres, as well as different tyre pressures lead to variations of the inlet position. From the mechanical point of view, especially robot systems for industrial applications have been used in previous research work, [VOL16] and [Res18] to fulfil the demand of high kinematics and control accuracy for moving the connector into the end position of the inlet. Due to the variable inlet position, systems can not be controlled by a predefined path. In this way, the exact position of the charging inlet has to be determined by a combination of a highly-accurate sensor system and a performant mechatronic system path computation and control.

Figure 2.33, right, shows an exemplary model of a vehicle on a charging lot with body-related coordinate systems as they are common in the field of robotics science. Also referred to as frames $\{F\}$, these consist of 3 translational and 3 rotational components with 6 degrees of freedom, [Wüs04]. For instance, the object-referenced frames of vehicle $\{V\}$, inlet $\{I\}$ and the parking lot reference frame $\{R\}$ can be seen. ACCS should be able to determine the inlet position $\{I\}$ independently from its vehicle location and to compensate vehicle misalignments with respect to the charging station.

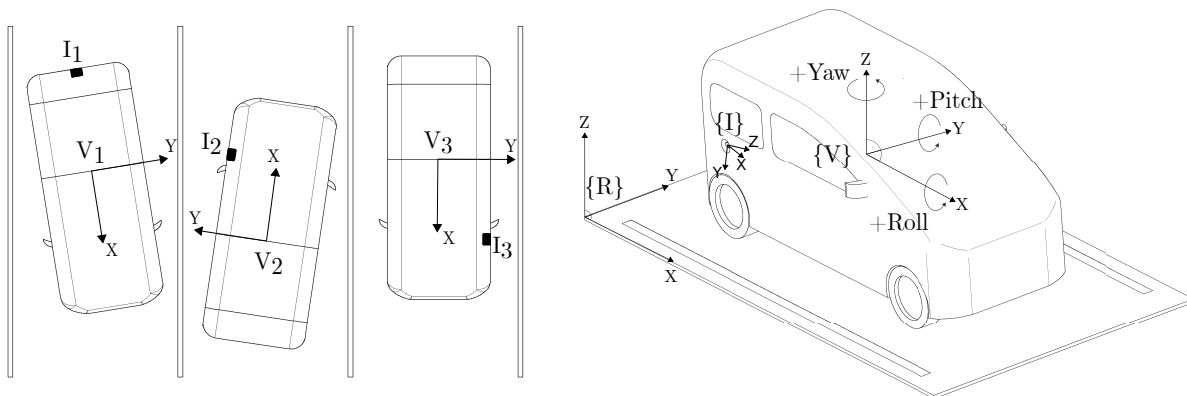


Figure 2.33.: Left: Vehicle parking processes result in different inlet positions (I_1 , I_2 and I_3). Right: Exemplary representation of reference coordinate systems of vehicle $\{V\}$, inlet $\{I\}$ and charging lot $\{R\}$.

2.7.3. Parking accuracy

Manual parking accuracy was recorded in a study for inductive charging. The study examines how exactly 100 participants park perpendicular to the road at three typical marked parking lots (figure 2.34, image 1, 2 and 3). The participants did not know that they were tested. In the second phase of the study, the participants were informed about measuring the accuracy of their parking process. Over an exemplary charging pad with the dimensions of 77 cm by 58 cm, 10 subjects parked on an area with no markings with the NISSAN Leaf test EV. The drivers were not versant with the vehicle. In the vehicle, an instructor was present, for helping in case of problems. The accuracy of parking was recorded, without orientation options like markers

2. State-of-the-art and boundary conditions

for adjusting. In practice, this would apply very often, especially in public. In the first test phase, most of the 100 participations parked forward, with a hatchback vehicle without parking sensors. The mean displacement from the centre of the car and the centre of the parking bay was recorded with 12.12 cm in lateral Y -direction, and 23.73 cm in longitudinal X -direction with 0.018 degrees mean angle. In the second test phase, where the charging pad was mounted at the vehicle front position, a mean displacement of 0.54 cm in lateral Y -direction and -66.68 cm in longitudinal X -direction was recorded. Moreover, the test results show a mean angle of 2 degrees from the centre of the vehicle to the centre of the charging pad and a mean displacement of 7.33 cm in Y -direction and -34.05 cm in X -direction with a mean angle of 0.18 degrees. Two inductive systems with different parking tolerances have been considered. The first enables misalignments of 15 cm in X -direction and 15 cm in Y -direction, whereas the second enables 10 cm in X -direction and 20 cm in Y -direction misalignment. The results show parking misalignments of up to 280 cm in the longitudinal direction and up to 60 cm in the lateral direction. Only in 5% off both parking studies were accurate enough that charging would be possible considering the two types of inductive charging systems. The test results are shown in table 2.5, [BWY⁺15].



Figure 2.34.: Beginning from left, image 1, 2 and 3: Parking bays for testing the parking accuracy of test drivers. Image 4: Charging pad and parking conditions for testing the parking accuracy over a charging par without parking aids, [BWY⁺15].

Table 2.5.: Parking position accuracy results from a study with 100 participants, [BWY⁺15].

	Mean	Standard Deviation (SD)
1st Test		
Y-direction [cm]	12.12	8.74
X-direction [cm]	23.73	29.12
Angle (°)	0.018	2.27
2nd test: Charging pad front position.		
Y-direction [cm]	0.54	7.21
X-direction [cm]	-66.86	60.81
Angle (°)	2	2.14
2nd test: Charging pad middle position.		
Y-direction [cm]	7.33	15.07
X-direction [cm]	-34.05	92.09
Angle (°)	0.18	5.64

2.7.4. Vehicle parking aids

Various studies analysed the parking accuracy of manual parking processes and the influence of parking aids for inductive charging. Birrel [BWY⁺15] describes parking offsets without aids from 120 cm to 280 cm in longitudinal and 20 cm to 60 cm in the transversal direction. Other studies show the increase of parking accuracy by parking aids, [BB11], [BWY⁺15] and [SMC⁺13]. Barth investigated the influence of non-electronic parking aids and their combination, e.g. *Marker* (figure 2.35, position 1), *Marker + mirror* (figure 2.35, position 1 and 2), *Marker + bump* (figure 2.35, position 1 and 3) and *Marker + mirror + bump*. Tests were done with 28 participants, in which each had only one parking attempt without repetition. The parking processes were carried out from three different directions, similar as they are common in practice. With the aid-combination *Marker + mirror + bump*, a parking position accuracy of less than 10 cm and an angular error of 2.5° has been achieved. Positioning in the lateral direction is particularly interesting, as compensation can only be made by manoeuvring through at least 2 movements. Additional adjustments to correct the lateral offset would reduce the time benefit of wireless charging as compared to conductive charging. Moreover, it is uncomfortable for the customer. The misalignment due to angle error was neglected for the accuracy since this has little influence on the energy efficiencies of inductive charging.

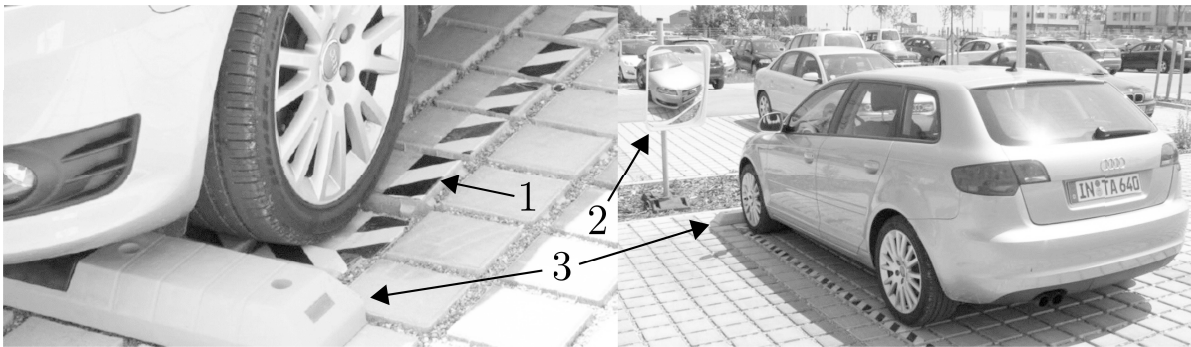


Figure 2.35.: Left: Detail view of marker and bump parking aids. Right: Position of marker, bump and mirror on a test parking lot, [BB11].

Table 2.6 and 2.7 shows the study results. Sufficient parking accuracy for a maximum 5% loss of efficiency and a 90% power loss of the maximum achievable inductive power transfer could be achieved with the non-electronic parking aid bump. However, without parking aids, parking misalignment is significantly greater than the wireless charging system tolerances. After completing the experiment, the participants were asked, which of the four aid instruments they would prefer. 85% chose the combination of mirror and bump, [BB11].

A study from 2013 tested parking aids such as audio systems, cameras and RFID sensors. The optimal travel direction was calculated and displayed to the driver by a standard market monitoring system. Parking accuracy increased after several tests. During non-aided parking, the drivers had to stop the vehicle at the centre of driving lines using only painted lines as a reference. The mean deviation by the use of markers was 13.3 cm in longitudinal and 9.3 cm in transversal direction. With support by means of audio and video system, a much

2. State-of-the-art and boundary conditions

better positioning was achieved with 7.0 and 7.9 cm. The test results are shown in table 2.8, [SMC⁺13].

Table 2.6.: Parking position accuracy achieved by 90% of the subjects grouped into longitudinal, transversal and angle deviation, [BB11].

Park assistant	Middle charging pad position (worst value / standard deviation)	Front charging pad position (worst value / standard deviation)
Longitudinal deviation (vehicle X-axis)		
Marker	83 cm / 21 cm	82 cm / 20 cm
Marker + mirror	15 cm / 3 cm	12 cm / 3 cm
Marker + bump	21 cm / 5 cm	17 cm / 4 cm
Marker + mirror + bump	8 cm / 2 cm	7 cm / 2 cm
Transversal deviation (vehicle Y-axis)		
Marker	27 cm / 7 cm	22 cm / 5 cm
Marker + mirror	11 cm / 2 cm	6 cm / 1 cm
Marker + bump	21 cm / 5 cm	17 cm / 4 cm
Marker + mirror + bump	7 cm / 2 cm	5 cm / 1 cm
Angle deviation (vehicle Z-axis rotation)		
Marker	5°	5°
Marker + mirror	3°	3°
Marker + bump	4.5°	4.5°
Marker + mirror + bump	2.5°	2.5°

Table 2.7.: Parking accuracy test results with middle charging pad position and straight forward parking, [BB11].

Park assistant	Longitudinal deviation (vehicle X-axis) [cm]		Transversal deviation (vehicle Y-axis) [cm]	
	Worst value	SD	Worst value	SD
Marker	59	17	15	4
Marker + mirror	11	3	3	1
Marker + bump	2	1	10	3

Table 2.8.: Parking accuracy test results with parking aids from [SMC⁺13].

Park assistant	Number of tests	Longitudinal deviation (vehicle X-axis) [cm]		Transversal deviation (vehicle Y-axis) [cm]	
		Mean	SD	Mean	SD
Markers (lines)	53	13.3	9.8	9.3	8.1
Visual system aided stop	39	11	8.6	11.6	7.9
Audio/visual system aided stop	39	7.0	4.5	7.9	4.7

Figure 2.36 shows a the study result summary of [BB11] and [SMC⁺13]. The aids *marker + bump* significantly reduce positional deviations in the longitudinal direction (figure 2.36, left). Audio and video systems improve the parking position accuracy significantly (figure 2.36, right).

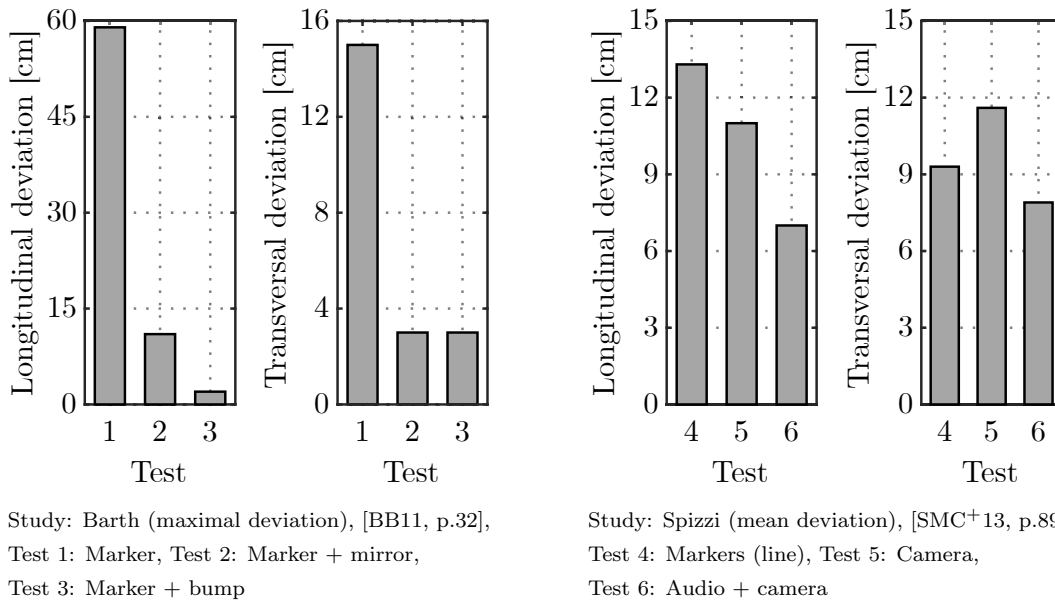


Figure 2.36.: Results of longitudinal and transversal deviations of parking tests with parking position additives, [WHB19a]

Barkow developed a guiding and positioning system to support parking above an inductive charging pad. The components used to determine the position are camera, RFID system and vehicle geometry data. The system calculates the optimal path to the destination, which is shown to the driver via a display. In figure 2.37, position 1 and 2 show the demonstrator vehicle positioning system and the charging pad integrated on a charging lot. The requirements of the system is a position determination with an accuracy of under 1 cm. This has to be achieved during vehicle movements at the last 5 meters. The RFID system achieves an accuracy of 5 cm, the camera system between 12 cm and 6 cm. The combined sensor data achieve an accuracy of less than 1 cm, [BKHC15].



Figure 2.37.: Charging pad and positioning system of [BKHC15].

ACCS has to compensate the variable vehicle parking position by sensor- and actuator systems. Even inlet position varieties due to different EV loads or the suspension wear has to be taken

into account. The ACCS working range is impacted by the charging station- and EV charging socket position and the parking accuracy. The required parking accuracy or the influence of parking aids for ACCS systems are not published yet. State-of-the-art are parking accuracy findings for vehicle positioning on parking lots and over inductive charging pads. In studies, the longitudinal and angular offset from the vehicle centre in relation to parking lot centre as well as the inductive charging pad centre (EV) in relation to the secondary pad (lot) were recorded. Parking over charging pads show significantly higher misalignments in y -direction. Parking aids and their combination increase the parking accuracy in all test surveys.

Parking over a charging pad differs from parking next to an ACCS. The pad disappears under the vehicle when passing. The pad is out of view, which makes positioning more difficult. An ACCS is located beside the EV. When entering the charging lot, the ACCS is visible for the driver until the final position is reached. In this way, vehicle parking and positioning corresponds to a petrol station parking process. This distinction means that the WPT parking accuracy results are restricted useable for ACCS. However, parking aids-related findings are useful. Their positive impact can also be transferred to ACCS-systems and enables the decremental of the range requirements.

2.8. Robotics for automated charging

ACCS requires a complex mechatronics system. In the following, the field of robotics is analysed for an ACCS actuator system. This includes the investigation of robot types, control and components as well as research regarding working range, kinematics and performance.

Robots are used for accurate and recurring movements, where they perform complicated tasks with high precision. In the past, robots are mainly used in industrial applications in the field of production and manufacturing. They are increasingly conquering private households as mowing, play and service robots. However, the requirements have to be differentiated: Especially concerning precision and repeatability, as well as work tasks, there are application differences. Industrial robots operate in a structured environment and framework with very clear tasks. Home robots, e.g. for mowing or vacuum cleaning, have low accuracy requirements and demands on repeatability. Robots are realised as a mechatronics system because they combine mechanic, kinematic, electronic and computer science. Therefore, robot development requires interdisciplinary mechatronics thinking.

Figure 2.38 shows the connection and relationship of central robot components as well as different robot control development possibilities, e.g. the realization of cognitive and intelligent robot systems. A robot system consists of an input, processing and output unit. The perception (*Input*) is typically carried out by sensors. Their information is processed and prepared for the output that carries out actions through actuators. Intelligent robot systems differ from conventional ones in terms of autonomy, cooperation or proactivity, which are operated by intrinsic intelligence in the *Brainware*. The monitoring of the execution also falls within the scope of duties of *Brainware*, [Hau13].

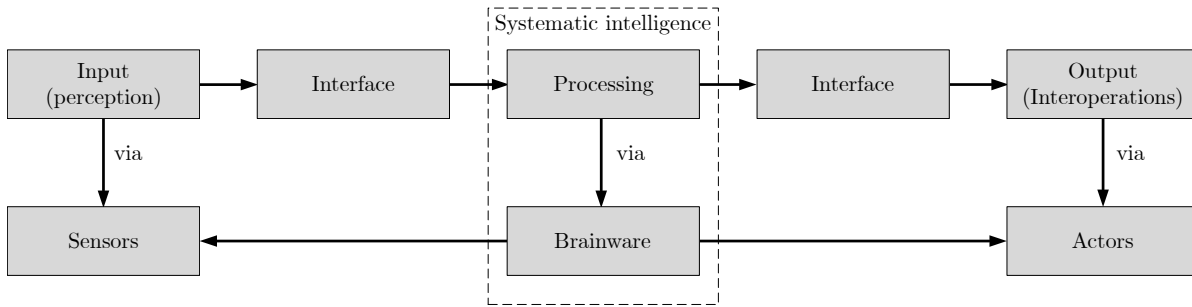


Figure 2.38.: Input-processing-output-principle with intelligence, [Hau13].

2.8.1. Architecture and kinematic

A typical robot architecture consists of manipulators and control unit. The end effectors do the work. Robot arms, joints and shifting axes are responsible for their positioning. Typical end-effector types are grippers, cutting tools, suckers, test and measuring tools, screwdrivers, paint spray guns, spot welding guns etc. Kinematics describes the movement of the robotic systems components. The most important kinematic types are portal, joint-arm, *Selective Compliance Assembly Robot Arm* or *Selectively Compliant Articulated Arm* (SCARA), parallel and swing-arm robots. Each robot type has advantages and disadvantages in a different field, which can be summarized as follows, [HMA10]:

- Portal robot: Often operates in working-free spaces across other production line machines, with a line plane working area.
- Joint-arm robot: Rotary axes lead to high movability. The most flexible robot type is often referred as universal robot, because of the movement capabilities similar to those of human arms.
- SCARA robot: Limited working range, high accuracy and velocities. They are specifically designed for robot boxes.
- Parallel robot: All drive axes work parallel. Possible are up to 6 axes with high velocities. In comparison to serial robot structures, the significant advantage is stiffness and low torques for workload holding.
- Swing-arm robot: The unique arrangement of the first two axes enables high working speeds and assembly forces. Disadvantageous is a small working area.

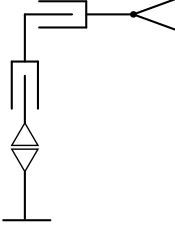
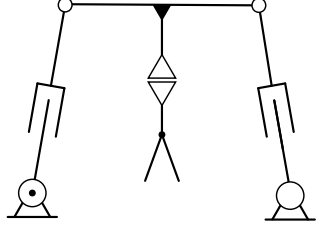
In this context, the robot choice depends on the application and work task requirements. Table 2.9 shows serial and parallel robot architectures and a comparison of the most important criteria. Due to the different arrangements of actuators and joints, properties, e.g. stiffness or inertia forces, vary significantly.

A robot system consists of axes that can be separated in main and minor axes. Main or basis axes determine the workspace and the positioning of the end effector. In a joint-arm robot, the axes 1 to 3, also called *large axes*, execute macro movements. In principle, linear and rotary axes can be main axes. In relation to the main axes, minor axes cause small changes in position.

2. State-of-the-art and boundary conditions

Minor axes, also called *hand axes* or *small axes*, are required for the micro-movements in the gripping area. These are mostly rotational movements, [HMA10].

Table 2.9.: Properties of serial and parallel robot systems, [HMA10]

Criteria	Serial structure	Parallel structure
		
Stiffness	Low	High
Measuring error in the structure	Cumulative	Averaging
Object to machine mass	Small	Large
Inertia forces	Large	Small
Relation of working space to design space	Large	Small
Working range manoeuvrability	Large	Limited
Calibration	Easy	Complex

The performance of a robotic system is described by the application technology view by characteristic data or performance features. Especially for industrial robots, these have been laid down in detail and are needed to be able to select robots that meet the requirements and to compare robots of different manufactures. Comprehensive representations can be found in the standard DIN EN ISO 9283 [ORG99] and the VDI Guideline 2861, sheet 2, [ING88]. The parameters are divided into four groups, [HMA10]:

- Geometric parameters such as mechanical system boundaries, layout and working area.
- Load parameters: Nominal load, payload, nominal torque, nominal or mass moment of inertia.
- Kinematic parameters: Speed of the end effector, acceleration, overshoot, delay time, travel time, cycle time.
- Accuracy values: Repeatability of pose and repeatability of trajectory.

Accuracy of the pose repeatability should not be confused with absolute accuracy. For the application of robots, it is essential how exact one programmed target point actually and repeatedly can be reached. Nevertheless, even in case of poor absolute accuracy of a robot system, it is possible to achieve a good repeat accuracy, [HMA10]. Table 2.10 shows the properties and performances of selected robot systems that were considered for use as charging robot in the present investigations. The serial kinematic robot systems with up to 7 axes show big differences regarding payload, range, position repeatability and weight.

Based on the robot system principle in figure 2.38, an ACCS system includes sensors for the vehicle and inlet recognition. The ACCS systematic intelligence (*Brainware*) consists of sensor

data processing and robot control. Due to the variable vehicle position, the inlet position (*Sensors*) and the actuator path (*Actors*) have to be updated by the ACCS systematic intelligence at each parking process. The ACCS actuator system is responsible for cable handling. Number and arrangement of joints and arms define robots mechanical properties like stiffness, motion flexibility, forces, speed and accuracy. The selection of an ACCS actuator system requires the elaboration and definition of the cable handling requirements, to fulfil range, motion and kinematics demands.

Table 2.10.: Properties and performance parameters of selected robot systems.

	ABB-YUMI	FANUC CR-35iA	KUKA LBR IIWA 14 R820	UNIVERSAL ROBOTS UR 10	YASKAWA MOTOMAN SIA20D	COMAU RACER 5-0.80
Payload [kg]	0.5	35	14	10	20	5
Range [mm]	500	1813	820	1,300	910	809
Axes	7	6	7	6	7	6
Positioning repeatability [mm]	0.02	0.08	0.15	0.1	0.1	0.03
Max. velocity [m/s]	1.5	0.75	1.2	1	2.44	2.54
Arms	2	1	1	1	1	1
Collaborating	Yes	Yes	No	Yes	Yes	No
Temperature working range [C°]	0-45	5-45	0-40	0-50	0-45	5-45
Weight [kg]	38	990	29.9	17	640	32
Costs [Euro]	ca. 40,000	ca. 35,000	35,000	30,000	ca. 30,000	ca. 15,000

2.8.2. Robot control

For the resent robot control application, it is sufficient to consider the robot movement as a rigid kinematic chain. Transformation equations for the respective coordinate systems can be used to describe the motion of the rigid bodys. The number of independent robot motions in relation to a fixed world coordinate system are referred to as *Degree Of Freedom* (DOF). A freely movable body in space has 6 DOF: 3 DOF for the position X , Y and Z and 3 DOF for the orientation R_x , R_y and R_z . The definition of coordinate systems is essential for robot programming. The end effector motion (trajectory) requires the control of robot arms. The trajectory consists of a chain of moves of each joint. The joints cause a linear movement or a rotation between two neighbouring members. For the description of the *Tool Centre Point* (TCP), two possibilities are common: The representation in joint-coordinates (TCP= (θ_1, θ_2)) or in cartesian world-coordinates (TCP= (X, Y)). If the robot is connected to other machines, the definition of the TCP in world-coordinates is useful. In this *neutral* form, the internal kinematic and design of the robot does not have to be known. Figure 2.39 shows an example of a robot application that is defined in world coordinates with the representation of the world coordinate frame (figure 2.39, Basis), gripper frame, (figure 2.39, TCP), object or user frame (figure 2.39, W) and reference frame (figure 2.39, REF). Forward transformation is used for the determination of the cartesian position in world coordinates (pose) from the axes variables. Backward transformation enables the determination of the axes variables from the given pose.

Exemplary the latter is used for robot control to calculate the joint angles for a given TCP, [HMA10].

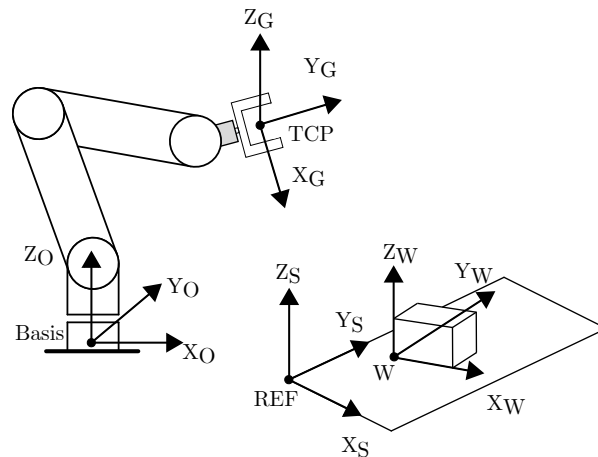


Figure 2.39.: Example of the TCP definition in a world coordinate system. Each component has its reference frame. The frames allow the positions and orientation determination to each other, [HMA10].

In the robotics field, it is common to describe the position and orientation of an object as pose. The description of 3D-poses can be done in different ways. Two applications are typical: On the one hand, to describe the pose of one coordinate system to another - for example, the position and orientation of the charging inlet in relation to the camera or a robot-based coordinate system. On the other hand, the use of mathematical transformation description of coordinates between coordinate systems. The transformation of the charging inlet coordinates into camera coordinates is an example. In comparison to the description of the object position in relation to a reference coordinate system, the description and formulation of the orientation are more difficult. In general, there are no fixed rules for the rotation sequences. Equation 2.1 describes the orientation formulation of an object, also referred in literature as *Roll-Pitch-Yaw* (RPY) convention, [HMA10]. The rotation chain can be read in two ways. Read from left, the rotations are based on the new or local coordinate system. Read from right, the rotations are based on the origin or unchanged coordinate system, [MVT17c]. Figure 2.40 represents an example of a right-handed RPY coordinate system and a *read from left* RPY rotation convention. The RPY convention starts with the γ -rotation via the new Z -axis, which represents the Z -axis of the origin coordinate system (figure 2.40, Step 1). Secondly, a rotation by the new Y' -axis is done by β (figure 2.40, Step 2). At last, the coordinate system rotates by α via the new X'' -axis (figure 2.40, Step 3).

In the robotics field, it is common to describe the position and orientation of an object as pose. The description of 3D-poses can be done in different ways. Two applications are typical: On the one hand, to describe the pose of one coordinate system to another - for example, the position and orientation of the charging inlet in relation to the camera or a robot-based coordinate system. On the other hand, the use of a mathematical transformation description of coordinates between coordinate systems. The transformation of the charging inlet coordinates into camera coordinates is an example. In comparison to the description of the object position

in relation to a reference coordinate system, the description and formulation of the orientation are more difficult. In general, there are no fixed rules for the rotation sequences. Equation 2.1 describes the orientation formulation of an object, also referred in literature as *Roll-Pitch-Yaw* (RPY) convention, [HMA10]. The rotation chain can be read in two ways. Read from left, the rotations are based on the new or local coordinate system. Read from right, the rotations are based on the origin or unchanged coordinate system, [MVT17c]. Figure 2.40 represents an example of a right-handed RPY coordinate system and a *read from left* RPY rotation convention. The RPY convention starts with the γ -rotation via the new Z -axis, which represents the Z -axis of the origin coordinate system (figure 2.40, Step 1). Secondly, a rotation by the new Y' -axis is done by β (figure 2.40, Step 2). At last, the coordinate system rotates by α via the new X'' -axis (figure 2.40, Step 3).

$$Rot_{RPY}(\alpha, \beta, \gamma) = Rot(Z, \gamma) \cdot Rot(Y', \beta) \cdot Rot(X'', \alpha) \quad (2.1)$$

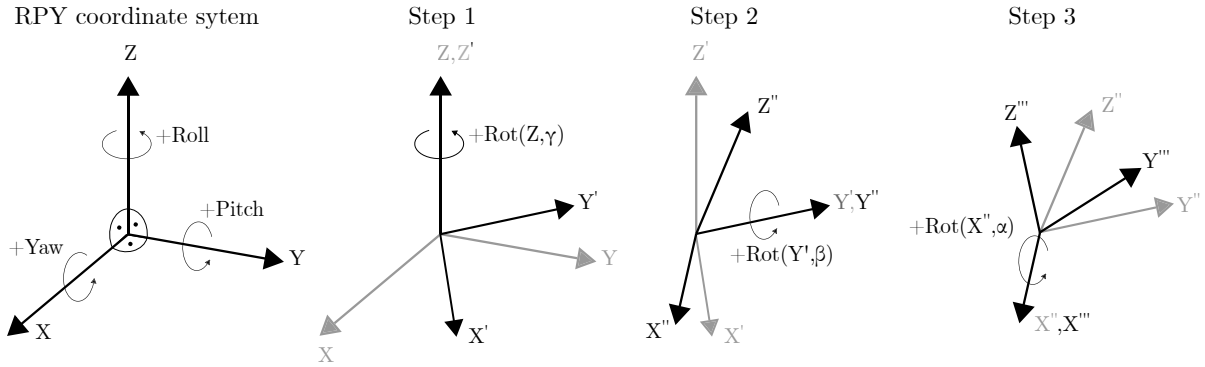


Figure 2.40.: RPY coordinate system and exemplary roll-pitch-yaw rotation convention, [Vin17] and [HMA10].

In many robotic control applications, the geometric description of poses is done by a *4 by 4 matrix* that is called *homogeneous matrix* or *frame*. Position and rotation coordinates of the base coordinate system are shifted and rotated around its zero points by means of a translation and rotation vector. The coordinate transformation thus consists of a translational and a rotational part. Cartesian coordinates and vectors describe the position. For the solution of the kinematic equations, vector and matrix computations are used, [HMA10]. Equations 2.2, 2.3, 2.4 and 2.5 describe the *homogeneous matrices* for a translation specified by the translation vector (equation 2.2), and rotations around X -, Y - and Z -axes defined by the rotation vectors, [Wüs04].

A translation in X -, Y - and Z -direction is defined as

$$Trans(x, y, z) = \begin{bmatrix} 1 & 0 & 0 & x \\ 0 & 1 & 0 & y \\ 0 & 0 & 1 & z \\ 0 & 0 & 0 & 1 \end{bmatrix}. \quad (2.2)$$

A rotation around X -axis by angle α is defined as

$$Rot(x, \alpha) = \begin{bmatrix} 1 & 0 & 0 & 0 \\ 0 & \cos\alpha & -\sin\alpha & 0 \\ 0 & \sin\alpha & \cos\alpha & 0 \\ 0 & 0 & 0 & 1 \end{bmatrix}. \quad (2.3)$$

A rotation around Y -axis by angle β is defined as

$$Rot(y, \beta) = \begin{bmatrix} \cos\beta & 0 & \sin\beta & 0 \\ 0 & 1 & 0 & 0 \\ -\sin\beta & 0 & \cos\beta & 0 \\ 0 & 0 & 0 & 1 \end{bmatrix}. \quad (2.4)$$

A rotation around Z -axis by angle γ is defined as

$$Rot(z, \gamma) = \begin{bmatrix} \cos\gamma & -\sin\gamma & 0 & 0 \\ \sin\gamma & \cos\gamma & 0 & 0 \\ 0 & 0 & 1 & 0 \\ 0 & 0 & 0 & 1 \end{bmatrix}. \quad (2.5)$$

From the α , β and γ rotation sequence it is possible to obtain the 3 by 3 rotation matrix by matrix multiplication (equation 2.6), [Haa17]. Translation and rotation matrix in one matrix form the transformation matrix T (equation 2.7). Matrix multiplications are not commutativity. Therefore, it is important to keep the order of the angle rotations sequence. However, the rotation is commutative for infinitesimally small rotation angles α . Then $\cos \alpha \approx 1$ and $\sin \alpha \approx \alpha$. This border case is from practical importance, because small rotations often occurs, [Jäh12].

$$R_{RPY}(\alpha, \beta, \gamma) = \begin{bmatrix} \cos\gamma\cos\beta & \cos\gamma\sin\beta\sin\alpha - \sin\gamma\cos\alpha & \cos\alpha\sin\beta\cos\gamma + \sin\alpha\sin\gamma \\ \sin\gamma\cos\beta & \sin\gamma\sin\beta\sin\alpha + \cos\alpha\cos\gamma & \sin\gamma\sin\beta\cos\alpha - \cos\gamma\sin\alpha \\ -\sin\beta & \cos\beta\sin\alpha & \cos\beta\cos\alpha \end{bmatrix} \quad (2.6)$$

$$T_{RPY}(\alpha, \beta, \gamma) = \begin{bmatrix} \cos\gamma\cos\beta & \cos\gamma\sin\beta\sin\alpha - \sin\gamma\cos\alpha & \cos\alpha\sin\beta\cos\gamma + \sin\alpha\sin\gamma & x \\ \sin\gamma\cos\beta & \sin\gamma\sin\beta\sin\alpha + \cos\alpha\cos\gamma & \sin\gamma\sin\beta\cos\alpha - \cos\gamma\sin\alpha & y \\ -\sin\beta & \cos\beta\sin\alpha & \cos\beta\cos\alpha & z \\ 0 & 0 & 0 & 1 \end{bmatrix} \quad (2.7)$$

The ACCS actuator requires a connector path control. Figure 2.41 shows an ACCS components world-coordinate system concept for charging lot (figure 2.41, $\{REF\}$), actuator (figure 2.41, $\{B\}$), connector (figure 2.41, $\{TCP\}$), inlet (figure 2.41, $\{I\}$) and sensor (figure 2.41, $\{S\}$). The TCP is placed at the charging connector. The vehicle's charging inlet, sensor and charging lot represents a further system component that has its own reference coordinate system. The coordinate systems are linked with each other. In this context, the component position and orientation description in world-coordinates is advantageous.

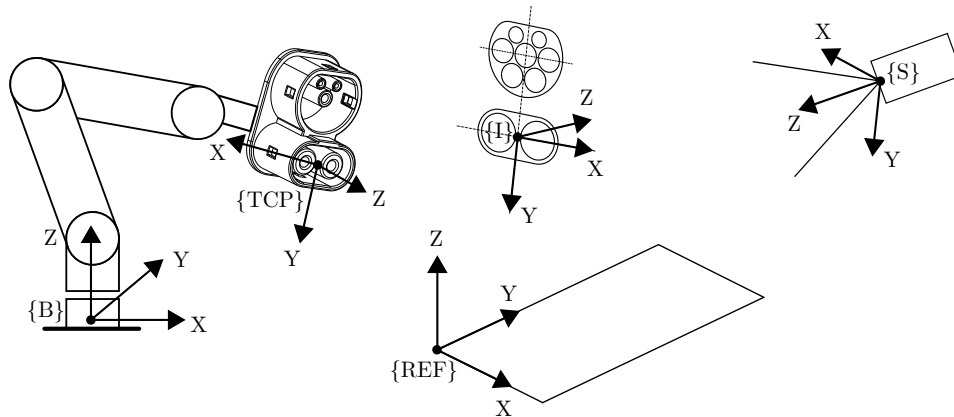


Figure 2.41.: Components coordinate system concept for the ACCS prototype.

The path control deals with the robot motion sequence for reaching a position. Robot motion concepts are *Point-to-Point* (PTP), Asynchronous and Synchronous PTP, as well as Cartesian (continuous) path control. In a simple PTP path control, the targeted points are reached by moving the axes to their position and angle target-values. The target values are calculated by backward transformations. TCP path and speed are uncontrolled and result from the individual axes and the system kinematic. With an Asynchronous PTP control, all axes start simultaneously with maximum speed and reach the target one after the other. With Synchronous PTP control, all axes start and stop simultaneously. PTP control has the disadvantage of unpredictable movements and an end-effector path that deviates from the ideal line. Many applications require a precise straight-line end-effector path, e.g. for welding applications, [Wüs04].

Figure 2.42 shows the Cartesian path control concept that enables robot movements in straight lines by means of the ACCS cable handling. For controlled cable handling and linear connector

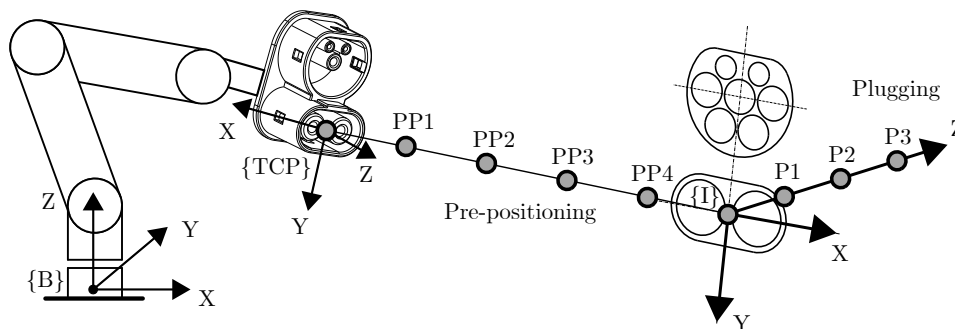


Figure 2.42.: ACCS prototype connector trajectory path concept.

plugging in inlet's Z -direction, Pre-Positioning (PPi) and Plugging (Pi) movements are carried out in straight lines. The TCP pre-positioning path is described with calculated interpolation points (figure 2.42, PP1 to PP4) between the start- and endpoint (figure 2.42, $\{TCP\}$ and $\{I\}$). For each intermediate position, a robot position must be found, i.e. a set of joint angles that brings the TCP to the desired target. A number of interpolation points are calculated for the desired path and passed through by the end-effector TCP point. The movement between the points can be done with PTP control. If the points are very close together, one can speak of continuous control, [Wüs04].

2.8.3. Safety

Human safety is the most important criterion and also the biggest hurdle in the planning and design of automated systems. It must be impossible for an automated device or robot to injure humans, [Elk13]. Many standards and guidelines support the development of safety concepts. The connection to the *Information Technology* (IT) infrastructure of a company and the legal requirements represent further hurdles for the introduction of cooperating work systems. All machines in industrial environments require a legal and safety-compliant design in accordance with the Machinery Directive 2006/42/EC before they can be placed on the market. Standards uniformly used in Europe support the implementation of these requirements with numerous approaches. The underlying standards are divided into three classes. EN ISO 12100, Class A describes important design principles for safe design and risk assessment processes and is necessary for all machines. Class B contains general design guidelines applicable to many machines. Class C contains standards for risk reduction for special machines, such as *Human robot collaboration* (HRC) applications, [MMN⁺16].

At industrial applications, an unexpected start-up and loss of control over a machine are the two most common reasons for unintentional contact between humans and robots. By far the most common cause of a collision is with hands, followed by the head and upper extremities. The greatest danger always emanates from clamping points. A free impact becomes dangerous only at high speeds combined with a large moving mass. One-third of trapped hands results in open injuries and severe bruising. Every 10th incident even results in a fracture. If the robot was able to recognize a person in its work area, accidents could be avoided. An even higher priority accident prevention requires systems used in public areas. Endangered persons cannot be trained as skilled workers, but like small children playing in the worst-case scenario, who can hardly be controlled by their parents, [MMN⁺16].

Regulations describe the general requirements, which are defined by standards. If a robot complies with these requirements, it is considered safe. Additional devices such as attachments, end effectors and aggregates, must be included in the overall safety system and rather define the system's safety. Guidelines and rules for the work with robots, without separating safety devices for isolation (collaborative work) were introduced in 2007 with the standard EN ISO 10218-1. This allows new working processes where humans and robots work together. From a safety point of view, this was previously impossible, [HMA10]. A list of relevant norms and guidelines can be found in the Appendix table A.4.

Collaborative robots are mostly lightweight joint-armed robots with safety technology. The DIN ISO/TS 15066 standard forms the robot requirements as well as the working environment. Human contact is regulated with force-limits to prevent massive injuries. The force impact is separated in the level of force/pressure and the duration of the action. Figure 2.43 represents forces and pressures to which humans may be exposed without suffering severe damage. Exemplary pressures are 250 N/m^2 for the tight that endures the biggest pressure. The robot has to avoid areas such as head, chest and genitals, which are the most sensitive, [INT16].

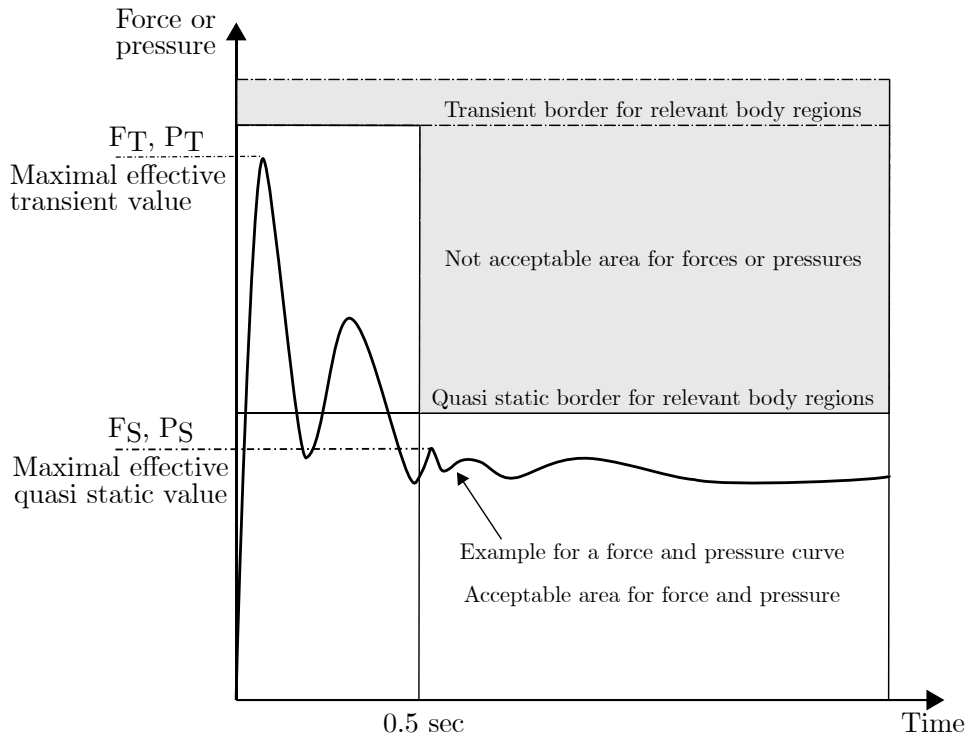


Figure 2.43.: Accepted collaborative robot forces and pressures for humans according to the duration of the action, [INT16].

For the ACCS cable handling, the use of a collaborative actuator system is advantageous. The force limitation capability prevents inlet and vehicles damages and enables working in the robot working range without safety fences. The robot proximity in tests supports the evaluation and optimization process of robot movements.

2.9. Sensor technologies for automated charging

Due to the very new technology, state-of-the-art research delivers no detail information about ACCS sensor technologies and detection processes requirements. Some vehicle detection sensor concepts are customized for one specific conductive charging technology. That means that the detection system can only be applied to that charging system, e.g. the ultrasound-based micro-navigation system of the concept of VOLTERIO [VOL18b]. The target of the present research activities was to find an interoperable sensor system for a large number of different vehicles.

2. State-of-the-art and boundary conditions

This section investigates potential vehicle-external and vehicle-internal sensor technologies for the position determination of vehicles at a charging lot and the exact 3D-pose estimation of the charging inlet.

The objectives can be divided into two separate tasks: On the one hand, the detection and classification of vehicles that enter the charging lot. Standard proposals for ACD charging, e.g. ISO 15118, [INT18a] define vehicle registration and authentication by wireless communication. Nevertheless, an additional vehicle authentication process would supply robustness, redundancy and safety. The second task includes the charging inlet position (pose) detection with high demands on the sensor system due to accuracy. By separating detection objectives, it is possible to define two working range and accuracy areas for the sensor requirements that are shown in 2.44. For locating a vehicle that enters, (figure 2.44, 1) or its positioned (figure 2.44, 2) on the charging lot, a maximal working distance of 10 m and an accuracy of 1 mm to 100 mm is defined (figure 2.44, area I). The 10 m working range is based on the maximal expected distance from the prototype-mounted sensor to the end of the charging lot. The upper accuracy range of 100 mm is defined by the goal to estimate vehicle distance to the robot in an acceptable accuracy. Fulfilment of the lower accuracy border of 1 mm would increase sensor costs. For the 3D-pose detection of the charging inlet, an accuracy from 0.01 to 1 mm and a working range based on the maximal expected distance of the inlet to the sensor of up 3 m (figure 2.44, area II) is defined. The upper accuracy range of 1 mm is defined by the requirements on the exact 3D-inlet pose detection and the lower range for costs reasons. The sensor system should enable inlet detection also slightly out of the ACCS actuator range to ensure corrections of potential vehicle parking misalignments.

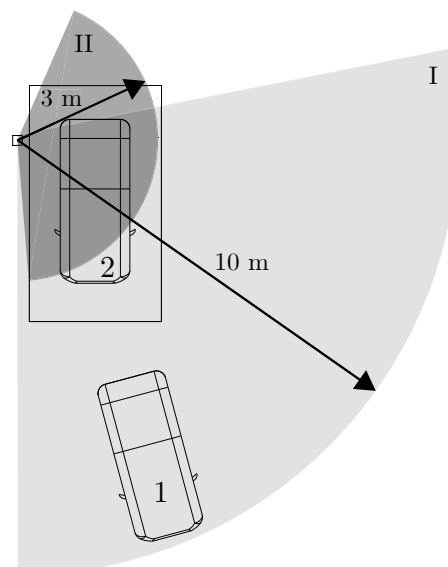


Figure 2.44.: Exemplary representation of a vehicle in the near and at the charging lot. Grey areas (I and II) illustrate the defined sensor working ranges for vehicle- and inlet detection.

2.9.1. Positioning sensors

Especially in the field of robotics, a large variety of sensors is available. Simple detector technologies are mostly sufficient for basic robotic applications, e.g. to detect the presence of an object. Accurate robot end-effector path control requires special and expensive sensors. For the position determination of objects, different sensor technics, e.g. laser including *Light Detection and Ranging* (LIDAR), vision systems, ultrasonic systems of radio technologies, e.g. *Wireless Local Area Network* (WLAN), Bluetooth, or *Radio Frequency Identification* (RFID) can be used. Because of the high variety of sensor systems, a full listing of all technologies is very comprehensive. Figure 2.45 shows the coverage and accuracy of different sensor position technologies. *Mautz*, [Mau12] categorized the sensors into 13 different technical groups.

The goal is to find sensor technologies that fulfil range and accuracy requirements under reasonable cost boundaries. In this way, the areas *Inlet* (figure 2.45, Inlet) and *Vehicle* (figure 2.45, Vehicle) indicate potential sensor systems for the present prototype sensor application under the consideration of range and accuracy limits (figure 2.44). For vehicle localization there are camera, magnetic, sound, infrared and *Ultra-Wide Band* (UWB) systems. For the inlet detection, there are tactile and combined polar, cameras and magnetic systems. Other sensor technologies, e.g. WLAN or RFID, can not satisfy the requirements due to insufficient accuracy and limited range. Due to the different technical operation modes and functionalities, a closer look at the selected sensor systems is necessary.

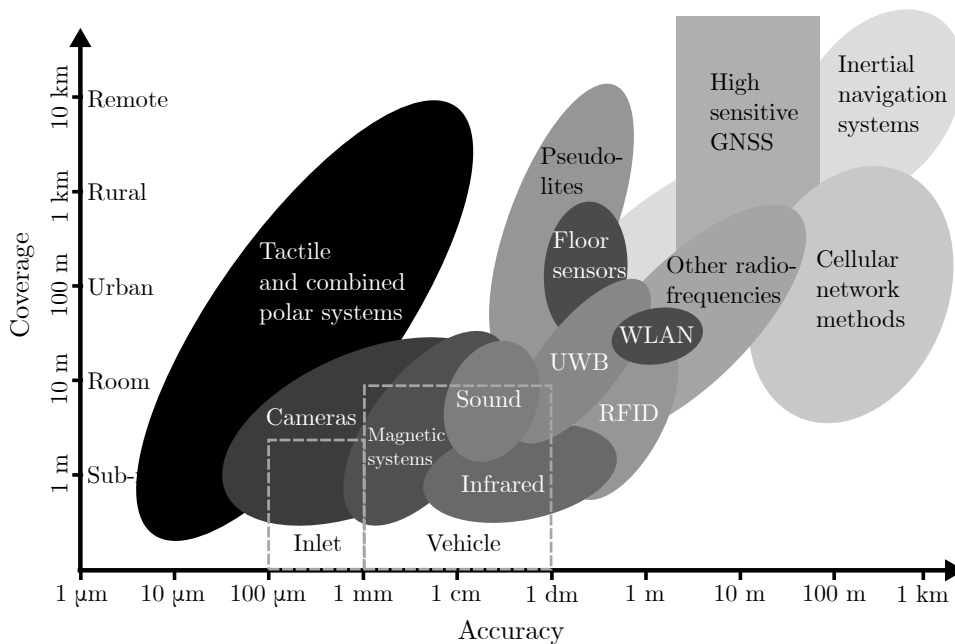


Figure 2.45.: Defined charging prototype sensor operating ranges for vehicle- and inlet detection according to different sensor technologies, which are categorized by *Mautz*, [Mau12].

UWB systems

Ultra-Wide Band (UWB) position sensors are based on radio technology and are used for short ranges. Several hundred MHz bandwidth and nanoseconds time resolution enables ranging and positioning at cm level. Commercial systems with transmitter and receiver achieve an accuracy of 150 mm on a range of up to 50 m. For more precise applications, a multiple transmitter and receiver infrastructure provides higher accuracy, [Mau12]. This setup is beneficial and useful for indoor applications. Disadvantageous is the requirement of a dedicated transmitter-receiver infrastructure, which prevents mass-market applications. Therefore, UWB can be only found in the industry today.

Sound systems

Sound systems work with acoustic waves and can be used for various object detection applications. The distance determination is done by *Ultra Sound* (US) pulses, which are sent by an emitter and received by an US receiver. The coverage area of up to 10 m is limited due to the strong decay of the acoustic waves with a typical carrier frequency of 1 kHz to 100 kHz. Disadvantages are frequency changes due to the *Doppler shift effect* as well as strong dependency on the temperature. Exemplary, a temperature change of 1° C over a distance of 10 m leads to a deviation in the distance estimation of 2 mm, [Mau12].

Infrared systems

The *Infrared Light* (IR) position technology can be divided into three different systems; active beacons, infrared imaging using artificial and natural radiation light sources, [Mau12] and [Sch10]. Artificial systems use an IR-light source that is not visible for the human eye, and a *Charged Coupled Device* (CCD) sensor that operates in the non-visible area and captures the IR-points. The IR-camera emits a structured light signal onto objects. The CCD-sensor determines the 3D-surface by detecting the displacement of the light spots on the object's surface. One major disadvantage is the light influence on signals. However, infrared lasers that emit strongly focused infrared radiation are used in very precise measuring systems, [Sch10].

Magnetic systems

The position detection process at magnetic fields is carried out by the combination of the produced electric and magnetic fields. The two sources of electromagnetic fields are static charges, which generate electric fields and currents that produce magnetic fields, [Mau12] and [Sch10]. The *Near Field Electromagnetic Ranging* (NFER) uses the characteristics of radio waves with an electromagnetic source. The distance to the electromagnetic source is determined by the phase shift between the electric and magnetic field of the electromagnetic field. An advantage of this technology is that it does not require a direct connection between transmitter and receiver. Walls can be penetrated, but large receivers are required because the receiver has to have a size of a quarter of the wavelength, [Mau12].

Tactile and combined polar systems

Tactile and combined polar systems provide very high accuracy of 0.01 mm on few meters and are mainly used in the field of environmental surveying. One disadvantage is the high price

of several 10,000 dollars for such systems, [Mau12]. *Light Detection and Ranging* (LIDAR) systems emit a light beam with a typical wavelength of 905 nm. The runtime of the light enables the distance to an object calculation, [Bal16]. The expensive technology allows accurate detection even at long distances and a good resolution of measurement of objects. Many LIDAR systems have only one laser, which is beamed by a rotating mirror to the object of interest. E.g. the VELODYNE HDL-64E-LIDAR sensor has 64 lasers with more than 1.3 million data points per second and a range from 1.2 m up to 120 m with an accuracy of 2 cm, [HHEM16].

Cameras

The position measurement accuracy of camera (vision) sensors is in the millimetre range. The technology can be divided into local sensors that detect moving objects and mobile sensors where a mobile camera is used for localization, [Mau12]. Cameras for object recognition and position detection are increasingly popular. However, even today, some tasks are difficult to realize in practice. Especially at changing light conditions, a scene can be captured very differently, but the quality of the recorded image plays an essential role for further image processing, [Li14]. That is one reason why results need long computing time, and some tasks are impossible to solve, [BB15].

An approach for the 3D-interpretation of objects by using cameras is shape-based 3D-matching. All image acquisition techniques project the three-dimensional space in one way or another onto a two-dimensional image plane (CCD-Sensor). Therefore, the image acquisition can be simplified as a projection from the three-dimensional into the two-dimensional space. This leads to the loss of a coordinate and a significant loss of information, [Jäh12]. Shape-based 3D-matching uses contours e.g. a *Computer Aided Design* (CAD)-model of known objects to estimate their position and orientation (pose) in a camera image, [MVT17d]. Figure 2.46 shows the process of shape-based 3D-matching in HALCON, [MVT17d]. The process consists of the following steps: First, a 3D-CAD-model of the observed object is created and converted in a HALCON readable CAD format, e.g. *Drawing Interchange File Format* (DXF), *Polygon File Format* (PLY) or *Standard Triangulation/Tesselation Language* (STL). Next, the approach-specific HALCON 3D-model is created by having access to the CAD-model. A 3D-shape model is generated by computing different views of the 3D-object model. The range and field of view depending on the application and is specified by the user. Virtual cameras are placed around the 3D-object model, and the 3D-contour is projected into the lens plane of each camera position. The 3D-shape model stores 2D-representations for each view. The pose range should be restricted as much as possible to avoid runtime and storage problems. For the generation of correct model views, the camera parameters are needed, which can be obtained by the camera calibration process. In the next step, the 3D-object model can be deleted, for decreasing memory. After the image acquisition and region of interest specifications are defined, the shape model is used for searching the objects 3D-pose in an image. In the matching process, the 2D-shape representations are used to find the best matching view. Possible visualization of HALCON supports the interpretation of the results, [MVT17d]. If the approach-specific 3D-model is not needed anymore, it can be deleted in the last step of the shape-based 3D-matching process, [MVT17a].

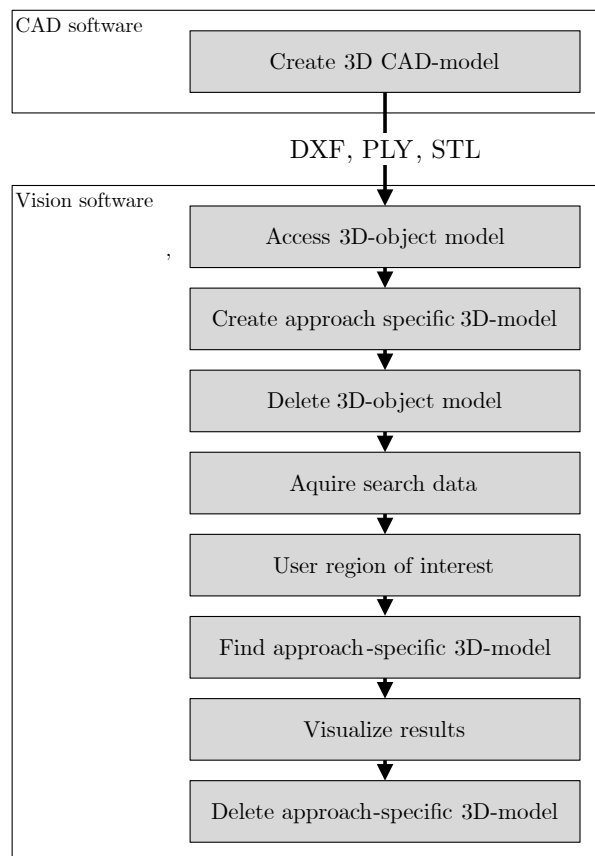


Figure 2.46.: Process steps of shape-based 3D-matching.

[Kol93] and [LSS08] provide examples for the pose estimation of vehicles. The authors use synthetic 3D-models to detect vehicles in a scene recorded by 2D-images. In further works, complex 3D-models are used to detect vehicles and motorcycles in traffic scenes, [JHB11] and [HMP⁺13]. Figure 2.47 shows examples of the comparison of 2D-images with 3D-vehicle data. The quality of the recorded image plays an important role in further image processing. A scene can be recorded very differently, especially by changing light conditions, [Li14].

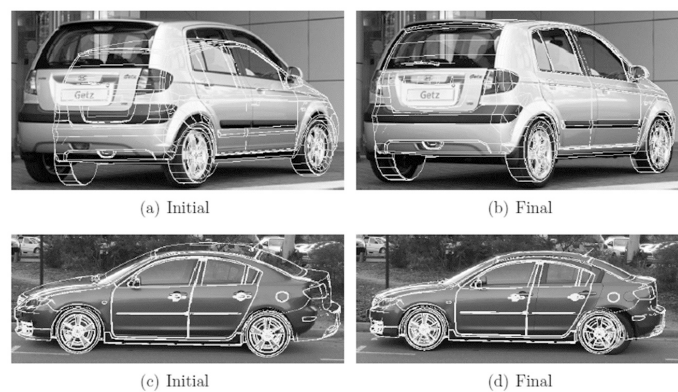


Figure 2.47.: 3D-position detection by 2D-camera and 3D vehicle data, [JHB11].

2.9.2. 3-dimensional imaging sensor technologies

The detection of *3-Dimensional* (3D)-scenes is enabled by different technologies. In the following, different 3D-imaging sensor technologies, e.g. 3D-vision, structured light and *Time-of-Flight* (ToF) systems are described.

Stereo vision

The technical question is, how to calculate 3D-positions and rotations of objects from the captured *2-dimensional* (2D)-images. One approach includes the use of two cameras (stereo-vision) that take up the same environment or an object from two different positions with a certain distance to each other. The depth estimation of a point of an object works by comparison of the separately recorded images where the same point appears with a displacement. One challenge for the depth calculation is that the point in image 1 must also be found in image 2. Compared to other 3D-imaging sensors, stereo-vision is very cost-effective, [Li14] and increasing computer performances improve the 3D-camera technology, [Mau12]. A stereo vision system with two cameras with 1280 pixels horizontal and 720 pixels vertical resolution achieves a mean distance error of 0.12 mm with a standard deviation of 1.26 mm by an object distance of 350 mm, [SSS17].

Structured light

Structured light systems observe the environment by a use of fixed infrared grid. The 3D-environment distorts the structured grid. The infrared-sensible CCD-sensor captures every light point, and the determination of the distance to the points on the observed object can be calculated by a comparison of the distorted and fixed infrared grid. A high image resolution can be achieved, but the sensitivity to ambient light represents main disadvantage. That is why this technique is more suitable for indoor applications, [Li14]. A well-known and cost-efficient representative of the structured light technology is the MICROSOFT Kinect V1, which achieves an accuracy of 10 mm at a distance of 2 m, [Mau12].

Time-of-Flight

A ToF-camera works by illuminating an object with light and perceiving the reflected light, which has the effect that the ambient light reduces the *Signal to Noise Ratio* (SNR). The phase shift between transmitted and reflected light is measurable and enables the determination of the distance to the object. Conventionally, solid-state lasers or *Light Emitting Diodes* (LED) operate with light in the range of 850 nm, which is not visible for the human eye, [Li14]. ToF-cameras can be modelled as pinhole cameras, and standard camera calibration techniques, e.g. for the distortion adjustment can be used. The depth accuracy can vary from a few centimetres up to several meters, [HHEM16].

Table 2.11 represents a comparison of 3D-imaging technologies regarding different considerations and common application areas. 3D-stereo vision technologies are cheap but have disadvantages in terms of depth information and low light conditions. In comparison to structured light technologies, ToF-cameras are less sensitive to environmental lighting conditions and

have lower resolution, but this area is rapidly improving. ToF-sensors with single laser scanning technology can cover a distance of kilometres, in contrast to structured-light 3D-imaging, [Li14].

Table 2.11.: Comparison of 3D-imaging technologies according to [Li14].

Considerations	Stereo vision	Structured light	Time-of-Light
Software complexity	High	Medium	Low
Material cost	Low	High	Medium
Compactness	Low	High	Low
Response time	Medium	Slow	Fast
Depth accuracy	Low	High	Medium
Low light performance	Weak	Good	Good
Outdoor application	Good	Weak	Good
Power Consumption	Low	Medium	Scalable
Range	Limited	Scalable	Scalable
Applications			
Game		x	x
3D-movie	x		
3D-scanning		x	x
User interface control			x

2.9.3. Vehicle-integrated sensors

Nowadays, vehicles include a number of sensors for recording and interpreting the environment, and the development of these technologies is increasingly pushed to meet the requirements of autonomous driving.

Since 2016, TESLA vehicles are equipped with sensors, which have the capability to perform driving functions. The sensor system includes eight cameras with 360° surround-view and 250 meter range, 12 ultrasound sensors and one forward operating radar sensor. Autonomous driving functions are automatic emergency braking, collision warning, lane holding and active cruise control. The automated driving functions of the vehicles are continuously updated according to development status, safety requirements and legal framework conditions. Exemplary, the vehicle drives entirely by itself in a autonomous call mode to move from a parking position to a person in a certain distance for pick-up purpose, [TES20a].

The company WAYMO operates fully driverless taxis in the Phoenix East Valley area in the USA. The taxis are fitted with several sensors. LIDAR, vision as well as radar sensors observe the environment with a 360° field of view. The LIDAR system contains a Short-, Mid- and Long-Range LIDAR sensor and detects objects in dark and bright light conditions. Besides environmental monitoring, additional cameras detect colour objects, e.g. traffic lights. The radar system can handle bad weather conditions such as rain and fog and recognizes, e.g. the speed of objects around the car. Supplemental sensors such as microphones and GPS-sensors detect relevant sounds, e.g. s a sirens and identify their location, [WAY20] and [WAY17]. The control software was trained with road images and a big dataset of driving scenarios. The

sensor data analysis is supported by a 130 square kilometres 3D-road-map with a resolution of down of a centimetre, [THE20].

The use of vehicle-internal sensors could be advantageous for the present approach of automated charging, too. The vehicle sensor functionalities correspond to the described technologies such as ultrasonic, vision, infrared and laser sensors. Figure 2.48 shows an overview of vehicle-internal sensor technologies as well as a classification into their physical principles, [Bal16]. Environmental sensors scan objects and obstacles and provide information about their location, dimension, speed or acceleration, also called autonomous locating. When information of obstacles is sent to the vehicle, for example, with *Vehicle-to-X* (V2X) communication technologies, [Bal16] it is called cooperative location.

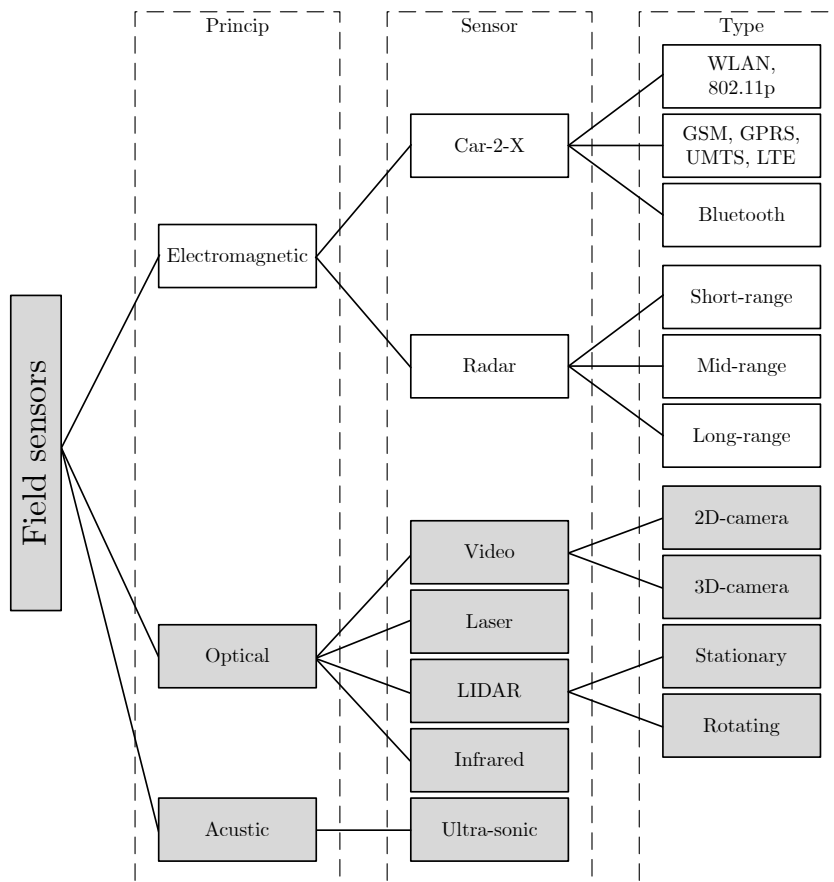


Figure 2.48.: Overview of vehicle-internal sensor technologies classified into their physical principle, according to [Bal16].

In practice, each sensor technology has specific advantages and disadvantages, that are comparable with the investigated sensor technologies in the previous section. 3D-cameras can classify near objects with specific software algorithm, but the results to distant areas under low light and bad weather conditions are relatively unreliable and not precisely. Ultrasonic sensors work in a close vehicle range of up to 4.5 m to assist during the parking process, [BS13]. A radar emits radio waves that are reflected by objects. The object distance is calculated by the waves running time. *Long-Range-Radar* (LRR) enables the detection of faraway objects but can not

interpret a traffic sign. *Short-Range-Radar* (SRR) sensors have an operating range of 25 cm up to 50 m, and the measuring accuracy lies in the range of centimetres. In this way, a combination of sensor systems is often used to compensate for sensor-specific weaknesses, [Bal16].

Figure 2.49 shows the defined working range for vehicle and charging inlet position detection for ACCS related to vehicle-internal sensors. Sensor systems based on electromagnetic principles such as WLAN, GSM, Bluetooth can not fulfil the accuracy and coverage requirements. Potentially sensors are ultrasound, cameras, SRR as well as infrared and laser. The sensors observe the ACCS charging station environment and locate the vehicle's position on the ACCS charging station. Vehicle parking aid cameras, also called top- or surround view system, detect markers and determines the vehicle position by vision matching algorithm. Usually, the cameras are integrated in the vehicle front, rear as well as in the left and right side area. Infrared, laser, ultrasound as well as SRR determine the position by obstacles, e.g. pillars on the ACCS charging station. A sensor combination improves the results. Disadvantageous are the required markers and obstacles. Both have to have a defined position on walls and floors, and obstacles may lead to complicating vehicle parking. Furthermore, the standardised infrastructure integration of those sensor aids is challenging to implement. Due to the different vehicle types and vehicle equipment, standardisation is difficult. Sensors position, function and accuracy differ, and vehicle specific calibration of the systems is required.

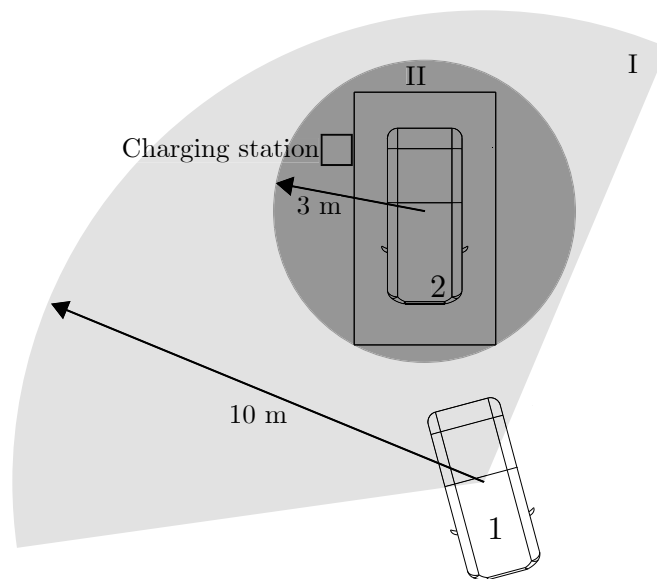


Figure 2.49.: Exemplary representation of a vehicle-internal sensor working range for ACCS. Grey areas (I and II) illustrate the defined sensor working ranges for vehicle- and inlet detection.

The state-of-the-art analysis of sensors includes an overview of position sensor technologies for the determination of the car and the inlet position detection on a charging lot, supporting successful charging processes by robot-based systems. A predefined ACCS sensor operating range and accuracy enable a preselection of potential sensor systems. The ACCS prototype should provide charging of different EV types. Due to the different sensor hardware and functionality in different vehicles, and the demand on an interoperable charging process, it

was decided that the ACCS prototype object position detection should be conducted by use of vehicle-external sensors only. Nevertheless, vehicle-internal sensors are a potential future possibility for ACCS object position determination, especially for involvement of cars with autonomous driving and parking functions. A selection of suitable vehicle-external sensors is made in the chapter prototype development.

2.10. Conclusion of the technology benchmark

The first part of this chapter analyses the state-of-the-art of charging technologies and automated charging systems. Conductive charging is the most common charging method today. Another way of EV charging is inductive charging by charging coils, with the disadvantageous limited charging power, electromagnetic compatibility and power losses due to charging pad misalignments. Battery swapping enables very fast energy provision for EVs. OEMs in China already operates swapping stations, with steadily growing numbers of units. Critical is the standardisation for a large number of different vehicle manufacturers. In this way, ACCS seems to provide a high potential for effective and comfortable charging of electric cars. There remain some challenges that need to be addressed for the implementation of ACCS. Publications of state-of-the-art ACD-S systems using standardised charging connectors provide less information about the automated cable connection process implementation and functionality. Some concepts consist of a robot or mechanical device for performing the cable motion sequence and a sensor system for vehicle charging inlet detection. Furthermore, concepts describe devices for compensating position and angle misalignments of charging connector and -inlet during plugging. An automated charging system should be able to charge EVs independent from the type of car or charging connector. In this context, the integration of specific adapters, e.g. for underbody charging systems has disadvantages. Furthermore, adapters are costly, and their standardisation is a challenge. The EV market is growing, and electric propulsion systems increasingly replace internal combustion engines. ACCS is able to address BEVs as well as petrol- and diesel PHEVs. In Europe, the mandatory standards for BEVs and PHEVs are Type 2 and CCS Type 2. In comparison to the ACD-U, the ACCS vehicle integration is more straightforward and does not impact the EV chassis packaging. This reduces technical effort and costs. A significant advantage of automated charging processes using established standards is the suitability of the existing charging infrastructure, which can also be applied for manual charging. To use the full benefits of automated charging systems, standardised and future preferred connectors with the ability for fast charging should be taken into account. In this context, the development of a future-proof ACCS should focus on CCS Type 2, which is the most widely supported charging standard in Europe and many other countries. EV charging systems are further developed over the next years to reduce charging session durations through higher charging power and to enhance the charging comfort through automatization. This means advantages regarding costs and vehicle adaptations. Automated charging has the potential to improve E-mobility significantly. Nevertheless, not only as backup solution manual EV-charging must be possible and charging sockets have to be on board. Inductive charging and ACD-U can not replace the technology for manual charging. For ACD-S that are not based

on standard connectors, it is challenging to develop new standards that also enable a manual cable connection. The investigated EVs show a variety of the charging socket positions and charging lid types as well as sophisticated safety and locking mechanisms. Considering typical long-distance travelling scenarios and the potential EV use, one crucial factor represents the provision of HPC, e.g. during travel brakes of about 15 minutes at motorway service areas. There is a big gap between the existing and desired charging infrastructure today. Studies indicate that the charging location choice is influenced by charging station availability and usability as well as the costs for electric energy. In this context, ACCS, autonomous parking functions and V2X communication technologies bring drivers comfort to another level. The vehicle can be left at a transfer area and can drive autonomously to the next free parking and charging lot. The combination with ACCS enables battery refuelling without user intervention.

A comparison of automated inductive and conductive charging, as well as battery swapping, highlights the state-of-the-art advantages and disadvantages of each technology. Table 2.12 and 2.13 represent the characteristics of the charging types in terms of technical, commercial, economical and user criteria. Conductive charging considers both standardized and non-standardized systems. Significant differences can be found in the possible charging capacities and charging times. In terms of efficiency, however, there are advantages for conductive systems and battery swapping, especially in case of inaccurate positioning at inductive charging pads. Charging pads on the floor and under the vehicle as well as and swapping stations have advantages in terms of accessibility and vandalism - securing an ACD-S system is more complicated. Rain, snow and dirt, as well as the prevention of stumbling, represent challenges of floor-side systems. Automated charging needs a sufficiently accurate positioning of the vehicle in relation to the automated charging device. Therefore, certain vehicle parking conditions must be fulfilled for the start of the charging process. At all systems, infrastructure requirements must be met, e.g. integration into a car park. ACD systems are (still) difficult to assess. In terms of compatibility and influences on the vehicle, the use of standard connector systems offers significant advantages. Systems at the vehicle underbody require space and mean additional weight. The use of standardized battery packs has disadvantageous regarding vehicle integration and provide challenges for the application in a large number of different vehicle types.

The second part of this chapter investigates the manual EV cable-based charging process and derives ACCS tasks and -restrictions. The manual charging process includes vehicle- and charging socket pre- and post-processing, cable handling and battery charging. Opening and closing lids and safety covers as well as connecting and disconnecting the cable indicate ACCS challenges. An interoperable ACCS that can handle a large number of EV types requires high automation effort. Communication standards for ACD are in development today. These standards cover the entire automated charging communication procedure and have to be coordinated and aligned with charging operation steps and processes. The further, ACD development will be considered in the standard guidelines to ensure interoperable, robust and comfortable automated charging. An automated charging device has to compensate the variable vehicle parking position. Published works provide less information about range and robustness as well as required vehicle parking accuracy. They do not describe parking and automated charging processes in a sufficient and comprehensible way. An important part of the automated charg-

ing process represents the proper positioning of the car in relation to the charging device or charging station. Because manual parking is not accurate enough, inductive charging requires positioning aids. The best results achieved mirrors, bumps as well as audio and video systems. The impact of parking aids on automated conductive charging systems is not published yet.

Table 2.12.: Comparison of automated inductive and conductive charging as well as battery swapping in terms of technical criteria.

Technical criteria			
	Inductive charging	Conductive charging	Battery swapping
Charging loads			
	<ul style="list-style-type: none"> - State of the art: AC 1-phase (230 V, 16 A): 3.7 kW, Series: Wireless charging BMW, [BMW18] - Perspective: 7.7 kW (WPT2), 11 kW (WPT3), 22 kW (WPT4), [oAE17] 	<ul style="list-style-type: none"> - VDE-AR-2009: AC 1-phase (230 V, 16 A): 3.7 kW, AC 3-phase (400 V, 16 A / 32 A / 63 A): 11.1 kW / 22.2 kW / 43.6 kW - State-of-the-art: 350 kW, [ION19] and [ELE19] - Charging power up to 500 kW (1000 V, 600 A), [CON17] 	Unlimited charging capacity by replacing the entire battery unit
Efficiency			
	<ul style="list-style-type: none"> - Depends on the positioning accuracy and the gap between charging pads, [BKHC15], actual: 80 to 87%, [BMW19] - 85% aligned, [oAE17] 	<ul style="list-style-type: none"> - 3.6 kW: 91% [Tob16] - 50 kW: 94% [Hor18] 	Corresponds to the conductive charging efficiency
Charging time			
Advantage	Frequent charging may have a positive impact on battery life because of the lower depth of discharge, [BB11].	<ul style="list-style-type: none"> - Significantly faster charging possible - 350 kW: 4 min / 100 km - 500 KW: 3 min / 100 km 	84 kWh battery pack swapping in 10 minutes, [NIO20]
Disadvantage	<ul style="list-style-type: none"> - Long charging time - 3.6 kW: 407 min / 100 km - 11 kW (expected household power connection): 133 min / 100 km - Max. 22 kW (public or buffered home charging) - Time for parking position alignment. 	Time for parking position alignment	Time for EV positioning and battery swapping (EV pre- and post-processing).
Compatibility			
Advantage	No mechanical contacts	Use of existing connector standards enables high compatibility and flexible charging loads.	Vehicle fleet optimized batteries, [NIO20]
Disadvantage	Different charging pad technologies and not uniform charging pad position at vehicles	<ul style="list-style-type: none"> - Hanging cables in (semi-) public spaces - Creepage current at wetness- and vandalism 	Vehicle fleet limited
Vehicle			
Advantage	Floor mounted pads effects only the EV underbody.	<ul style="list-style-type: none"> - Less vehicle package impacts for ACD-S - Minimal integration effort by use of cable standards 	- No aged battery packs
Disadvantage	<ul style="list-style-type: none"> - Vehicle adaptations and vehicle integration - Additional weight of charging pad 	Systems with non-standard connectors require vehicle adaptations and/or additional devices.	<ul style="list-style-type: none"> - Limited battery compatibility - Vehicle integration - Limited vehicle packaging
Safety			
Advantage	No exposed contacts	No significant electromagnetic fields	<ul style="list-style-type: none"> - Closed and not accessible swapping station - Vandalism resistant
Disadvantage	<ul style="list-style-type: none"> - Electric field intensity has to safety criteria and has to be validated. - Dirt, pollution and snow could influence charging. - Risk of stumbling 	<ul style="list-style-type: none"> - Hanging cables in (semi-) public spaces - Creepage current at wetness - Vandalism 	Charging station size and dimension

2. State-of-the-art and boundary conditions

Table 2.13.: Comparison of automated inductive and conductive charging as well as battery swapping in terms of commercial, economic and user practice criteria.

Commercial, economic and user criteria			
	Inductive charging	Conductive charging	Battery swapping
Manual parking and charging			
Advantage	Contactless devices enable vehicle movements (different payloads).	Enables parking position tolerances (depends on charging system range)	Swapping station compensates vehicle parking misalignments.
Disadvantage	Accurate positioning requires guided parking process and limits user-friendliness.	Parking guide for systems with limited working range	Swapping station entrance parking procedure
Comfort and user friendliness			
Advantage	No disturbing mechanical parts when parking	- High charging capacities - Conductive charging standards - ACCS allows manual cable charging	Controlled battery unit exchange
Disadvantage	- Demand for high parking accuracy. - Driver needs to be guided by a system.	Parking accuracy depends on the system range.	Driver has to leave the vehicle.
Infrastructure			
Advantage	Space requirements	Possible combination with existing charging stations	Secured and fenced charging area
Disadvantage	Limited application possibilities.	Space requirements and integration	Space requirements and integration
Costs			
Advantage	Due to the lower wear and vandalism a high infrastructure life expectancy	Combination with existing charging stations	For user various battery purchase and rental options
Disadvantage	- Vehicle and infrastructure integration - Higher charging losses lead to additional costs in operation.	Especially at (semi)-public locations costs for operating (e.g. vandalism and wear)	- Charging station plant - Infrastructure integration

In summary, the state-of-the-art ACCS analysis determines the following main challenges:

1. Effective localization of the charging inlet position.
2. Control of the robot or mechanical device.
3. Compensation of vehicle charging socket and connector positioning tolerances.

The last part of this chapter analyses robot and sensor technologies for ACCS. Number and arrangement of joints and arms define the robot's mechanical properties like stiffness, motion flexibility, forces, speed and accuracy. DOF define the independent motions to a fixed coordinate system. The robot type choice depends on the application and work task requirements. Robot control requires understanding of the input processing output procedure. Perceptions are carried out by sensors, and system intelligence is performed by the brainware. The definition of coordinate systems in a robot system is essential for robot programming. If the robot is connected to other systems, it is useful to describe the end effector motion (TCP) in Cartesian world coordinates. A further advantage is that for existing robotic systems the internal robot kinematic does not have to be known. Automated systems have to ensure safe operation. Especially for robots in public areas, e.g. automated charging at rest stops stations, accident prevention requires more attention in comparison to robots in factories. Collaborative robots ensure safe operation in the near of people, by limited forces and speeds. For vehicle recognition and charging inlet position detection, vehicle-external and vehicle-internal sensor technologies were investigated. There is a large number of different position sensors with physical-specific

behaviour regarding different criteria, e.g. object classification or environmental influences. In this context, vehicle-external, UWB, sound, infrared, magnetic, tactile and combined polar as well as camera systems fulfil predefined ACCS operating range and accuracy demands. Potential technologies vehicle-internal sensors are sound systems, cameras, laser, infrared as well as radar.

3. Prototype development

This chapter deals with the development of an ACCS prototype. The first part of the chapter develops and derives ACCS requirements from defined use cases, the manual charging process, as well as boundary conditions and demands. Subsequently, an ACCS system design serves as the basis for the prototype component requirements derivation. The second part of the chapter describes the development of the object recognition sensor technique, robot control as well as charging- and data processes. The last part of this chapter presents the ACCS prototype and hardware components in detail.

3.1. Requirements

The elaboration of ACCS requirements leads to the derivation of prototype tasks and functions, which define the prototype component demands and specifications. The requirements are developed by ACCS use cases, vehicle parking and automated charging process, as well as ACCS boundary conditions and demands. Furthermore, requirements for further ACCS development are defined.

3.1.1. Use cases

The ACCS prototype use cases define requirements for the charging lot layout and ACCS positioning as well as EV parking and address the most common charging socket positions and parking scenarios with typical charging lot dimensions. Figure 3.1 shows the ACCS prototype use cases. Use case I (figure 3.1, left) enables ACCS of EVs with front, left- as well as rear, right-mounted charging socket positions (figure 3.1, left, S1 and S2). EV with front, right- and rear, left-mounted charging sockets are considered in Use case II (figure 3.1, right, S3 and S4). In both cases, the charging lots can be entered by EVs from both sides, front or backwards. The EV charging sockets have to be positioned next to the ACCS prototype inside the marked stripes. The vehicle parking position accuracy influences ACCS requirements such as working range, kinematics and sensor technology. Manual vehicle parking tests show high parking position misalignments. Advantageous are simple parking processes with less infrastructure and vehicle impact. The targets of the research activities are comfortable and user-friendly parking processes and the avoidance of parking aids. Prototype test scenarios include different vehicle types and in- and outdoor locations. In this context, the ACCS should be compact and transportable. Sensors have to work in different light situations. Table 3.1 shows the derived and developed ACCS use case requirements.

Table 3.1.: ACCS prototype use case requirements.

Requirement	Type	Designation
Typical charging lot layout and size dimensions	Technical	R1
Easy and user-friendly vehicle parking and -positioning	Technical	R2
Simple parking aids	Technical	R3
Compact and transportable for testing at different locations	Technical	R4
Capability of handling different light situations	Technical	R5

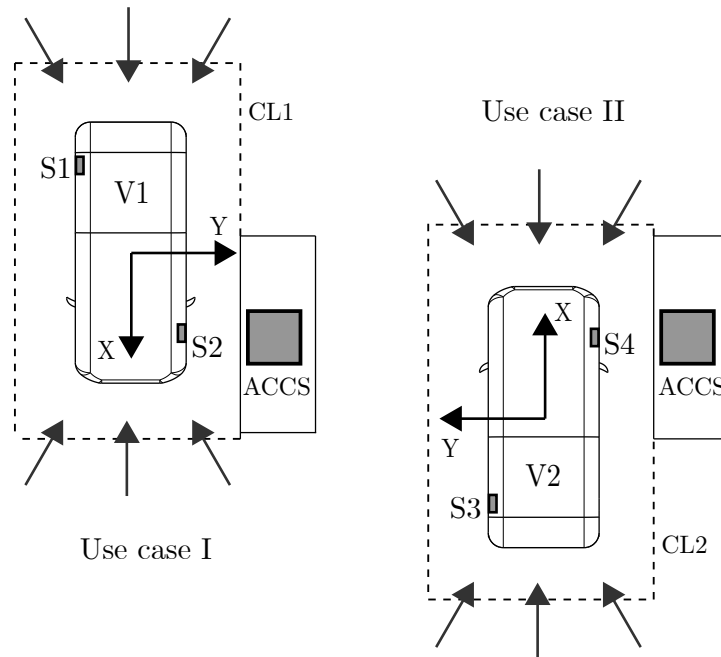


Figure 3.1.: ACCS prototype use cases for different charging socket positions and parking scenarios. Left: Use case I for front, left as well as rear, right EV charging socket positions (S1 and S2). Right: Use case II for front, right as well as rear, left charging sockets (S3 and S4).

3.1.2. Charging process

An ACCS substitutes the manual charging processes. In this context, the manual charging process with standardized technologies in figure 3.2 serves as basis for the prototype function derivation.

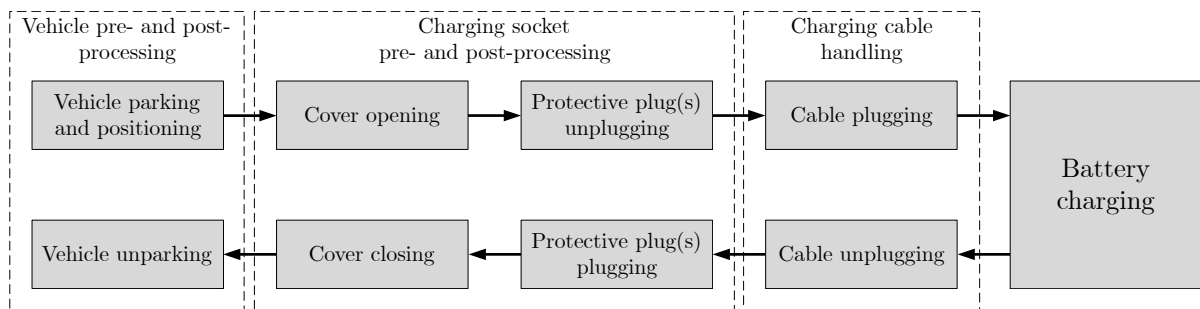


Figure 3.2.: Manual EV charging process with standardized cable technologies.

In the following, the ACCS prototype functional and technical requirements, as well as restrictions, are elaborated based on the manual cable process steps.

Vehicle pre- and post-processing

The driver performs the process steps *Vehicle parking and positioning* and *Vehicle unparking*. The automated cable connection requires EV positioning in an ACCS-reachable area. In this context, EV parking impacts the ACCS position and working range. An EV classification function supports the prototype system. EV type-related parameters, e.g. the charging socket height, assists the inlet position detection process.

Charging socket pre- and post-processing

The process steps *Cover opening*, *Protective plug(s) unplugging*, *Protective plug(s) plugging* and *Cover closing* present a challenge and complicate an ACCS system. The handling of charging covers, as well as protective or safety plugs, is complicated. A further challenge is the system variety for different EV types. An Audi e-tron and a TESLA Model 3, represented in chapter 2.4, open the charging cover automatically and do not need security plugs. Due to comfort, it is expected that other vehicle manufacturers will implement these functions in the future too. For the present investigations, it was defined that ACCS *Charging socket pre- and post-processing* functions are not required to be performed by the charging robot prototype.

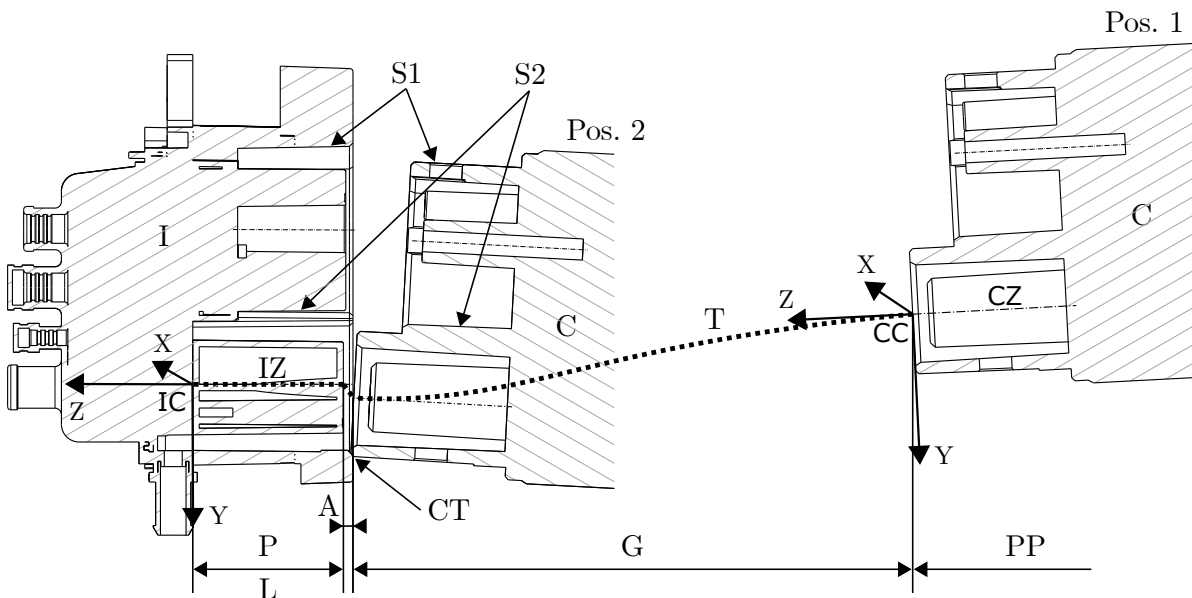


Figure 3.3.: Sectional view of the CCS Type 2 charging inlet and -connector manual charging plugging process CAD-model.

Charging cable handling

The main ACCS functions are the *Charging cable handling* steps *Cable plugging* and *Cable unplugging*. *Cable plugging* requires a start trigger, which is initiated by the driver. Challenge lays in the inlet position detection and charging cable plugging automation. The phase *Pre-positioning* (figure 3.3, PP) requires charging cable moving next to the charging socket.

Different vehicle charging socket positions lead to a required large ACCS working range. The phases *Guiding*, *Alignment* and *Plugging* (figure 3.3, G, A and P) lead to high ACCS sensor and actuator demands. For example, in case of manual connection, force reduction and cable tilting can be addressed by twisting and shaking of the plug. On the one hand, the imitation of human handling behaviour by a mechatronic system could be a solution for a safe and reliable connection. On the other hand, this implementation results in a further increase of the complexity of the entire system.

Battery charging

For standardized charging cables, the sub-processes and steps *Battery charging* are controlled by communication standards, e.g. ISO 15118. The standard controls the electric energy transfer start and stop by locking or unlocking the charging connector from the EV inlet. For prototype development and testing, electric energy exchange- as well as communication functions for energy transfer managing are not defined as a target..

Due to automated socket access mechanism as well as standardized battery charging procedures, the ACCS functions are reduced to vehicle parking and cable handling procedures. Table 3.2 shows the ACCS prototype requirements of the vehicle- and charging socket pre- and post-processing- as well as cable handling steps.

Table 3.2.: ACCS prototype requirements of the charging process.

Requirement	Type	Designation
Vehicle detection and classification	Functional	R6
Automated cable plugging start trigger	Functional	R7
Inlet position detection	Functional	R8
Guiding, alignment as well as plugging and unplugging of the charging cable	Functional	R9
Charging of different EV types	Functional	R10
Compensation of vehicle parking misalignments	Functional	R11
Manually or automatically charging inlet as well as safety caps handling	Restrictive	R12

3.1.3. Boundary conditions and demands

The ACCS prototype boundary conditions and demands are defined by the following criteria.

Charging standard

For ACCS, the capability of high power charging with CCS, CHAdeMO, or TESLA connectors is advantageous. Standard charging connectors enable handling of a large number of EVs with one system and do not require additional vehicle adaptations. CCS Type 2 combines two charging standards and is the most common charging method for BEVs, PHEVs and REEVs in Europe. Furthermore, it covers charging from 1 kW AC up to 500 kW DC charging power. In this context, the CCS Type 2 charging standard is defined for the present prototype development.

Electric vehicles

The avoidance of EV and charging socket changes or adaptations ensures cost-efficiency. ACCS should not affect the vehicle package. An ACCS prototype requirement is the avoidance of vehicle adaptations and vehicle architecture changes of interventions. In this way, the prototype must be able to charge all vehicles equipped with CCS Type 2 connectors at the European market.

Safety

Mechanical systems have to ensure safe operation in the near of peoples. For ACCS prototype tests and the avoidance of people injuries, it must be ensured that the system reacts and stops immediately. Furthermore, safety functions prevent vehicle damages. Table 3.3 shows the ACCS prototype requirements, derived from the boundary conditions and demands.

Table 3.3.: ACCS prototype requirements of boundary conditions and demands.

Requirement	Type	Designation
Handling of the CCS Type 2 charging standard	Technical	R13
Avoidance of EV and charging inlet adaptations and vehicle packaging architecture interventions	Technical	R14
Safety for ACCS development and -charging tests with trained persons	Technical	R15

3.1.4. Supporting ACCS requirements

Charging station usability is an essential customer demand. Implementation of registration, authentication and payment functions into ACCS supports user-friendliness and utilization. The ISO 15118 communication standard proposal, [INT18a] offers these functions and can be implemented to ACCS. ACCS prototype tests do not require communication between EV and ACCS, but it is recommended to use existing communication standards for further development. ISO 15118 EV and charging station data exchange takes place by wireless communication. In this context, the prototype development includes the implementation of wireless communication functions.

Further ACCS development has to take into account automated parking functions. This means the implementation of vehicle charging lot guiding functions as well as the fulfilment autonomous vehicle parking accuracy demands. ACCS installation and operation at different public and private locations should be as easy as possible. ACCS size and communication functions have to fulfil infrastructure demands, e.g. parking facilities communication techniques

Table 3.4.: Supporting ACCS requirements.

Requirement	Type	Designation
Easy registration as well as automated authentication and payment	Functional	SR1
Consideration of communication standards to fulfil V2X- and V2G-communication technologies	Functional	SR2
Ready for integration into public- and private locations as wells as serving of autonomous parking EVs	Functional	SR3

and future customer services. Table 3.4 shows the supporting requirements for a successful ACCS implementation in public and private areas.

3.2. System design

The ACCS prototype system design includes the functional concept and basic layout. The system design delivers the concept for the subsequently performed prototype component requirements definition and development.

3.2.1. Functional concept

Figure 3.4 shows the ACCS prototype functional concept. The system consists of 4 connected categories. The category *Object* considers the items that have to be handled by the prototype. The category *Process* includes the prototype process steps that are derivate from the ACCS requirements in chapter 3.1. The steps *Vehicle parking* and *Vehicle unparking* covers the activities for guiding the test drivers at parking and leaving the charging lot (requirements *R2* and *R3*). The following step *Vehicle detection* recognizes the vehicle on the charging lot (*R6*). The test driver executes the cable *Charging start trigger* (*R7*). The procedure *Inlet position detection* covers the inlet position detection (*R8*). The steps *Cable plugging* and *Cable unplugging* consists of all activities for guiding, alignment and plugging the charging cable (*R9*). *Devices* execute the processes. The system control performs the device control (*Intelligence*).

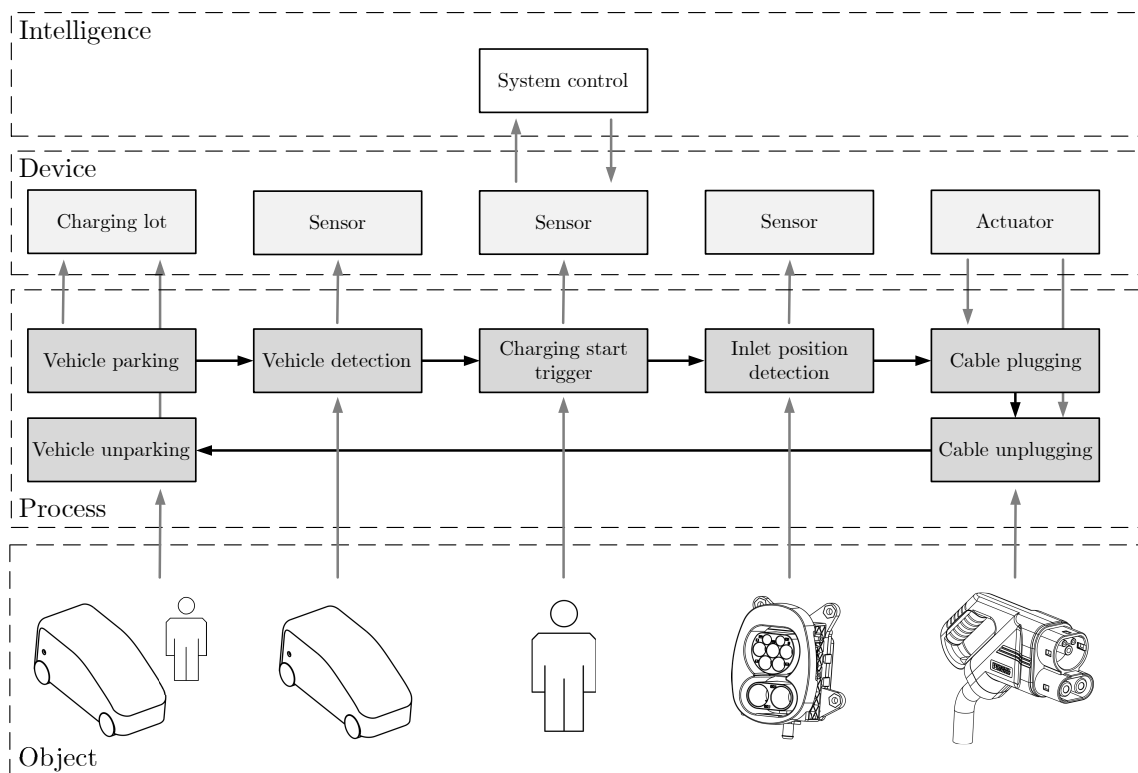


Figure 3.4.: Functional ACCS prototype system design.

In this context, the objects deliver the device- and system control requirements. The device *Charging lot* defines the environment for the parking process that is impacted by test driver and EV. *Sensors* detect the objects vehicle, inlet and test driver. The system control gathers sensors data and performs data processing. The *Intelligence* controlled actuators are responsible for cable handling.

3.2.2. Basic layout

Figure 3.5 shows the ACCS prototype basic layout. The layout is developed to fulfil the functional processes (figure 3.4, *Process*) Use case 1 (figure 3.1) and the ACCS requirements of chapter 3.1. The prototype position (figure 3.5, left, ACCS) is next to the expected EV charging sockets (figure 3.5, left, I). For the fulfilment of different charging socket positions, the lot can be entered from both sides ($R2$, $R3$ and $R10$). The lot (figure 3.5, left, M) is marked for supporting the vehicle positioning ($R3$). A and AP show the actuator working range and possible place for the actuator base mounting position. The working range covers different charging socket positions, positioning misalignments as well as different heights and enables charging of different vehicle types ($R10$ and $R11$). The possible actuator base position is due to the compact size of the ACCS prototype ($R4$). S_I and SP_I show the sensor working range for covering the charging socket position and the possible area for sensor positioning. S_V and SP_V show working range and the sensor position area for vehicle recognition. As with at the actuator, sensors positioning is limited to the ACCS size.

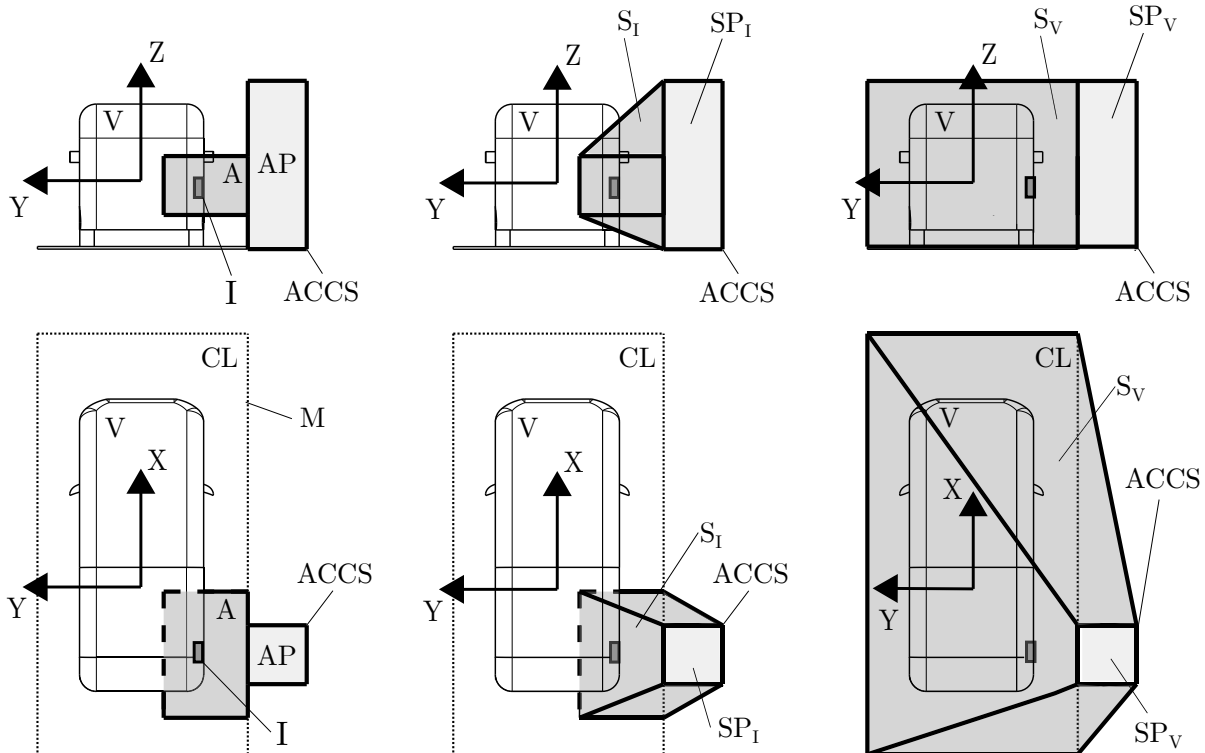


Figure 3.5.: ACCS prototype basic layout with working range and possible mounting area of actuator, as well as charging socket- and vehicle sensor.

Figure 3.6 shows the prototype components and defined coordinate systems. A reference coordinate system is used to define the relations of the components to each other. Sensors S_V and S_I detect vehicle $\{V\}$ as well as inlet $\{I\}$ position. The system control guides the connector $\{C\}$ to the charging inlet $\{I\}$. The connector frame S_I is defined at the front of the CCS Type 2 connector face between the DC pins. Charging lot $\{L\}$ and the actuator base $\{B\}$ represent the reference coordinate systems.

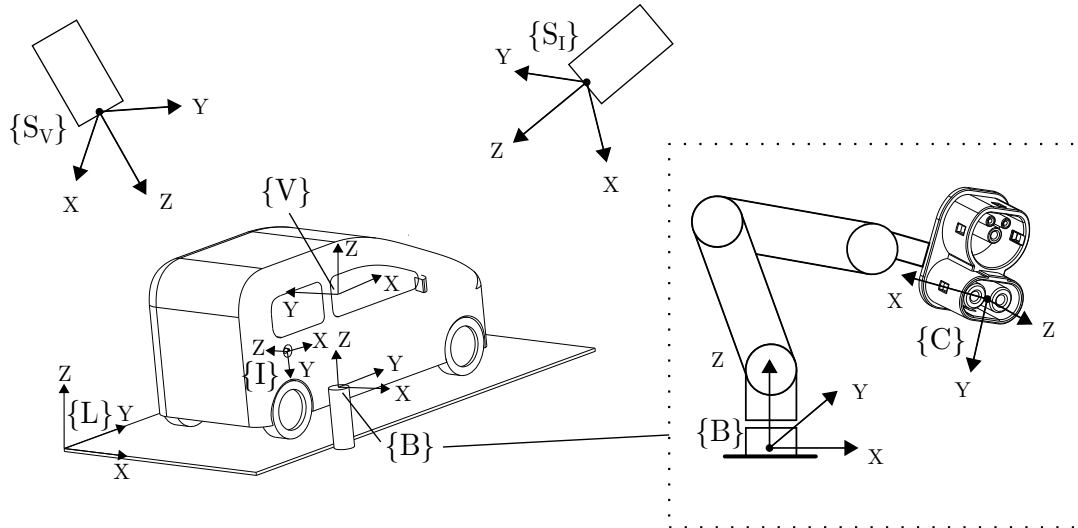


Figure 3.6.: ACCS prototype component coordinate systems layout.

3.3. Component requirements

Figure 3.7 shows the ACCS components that consist of *Charging lot*, *Vehicle detection sensor*, *Charging start trigger sensor*, *Inlet position detection sensor* as well as *Actuator* and *System control*. Table 3.5 shows the prototype components with the assigned ACCS requirements and

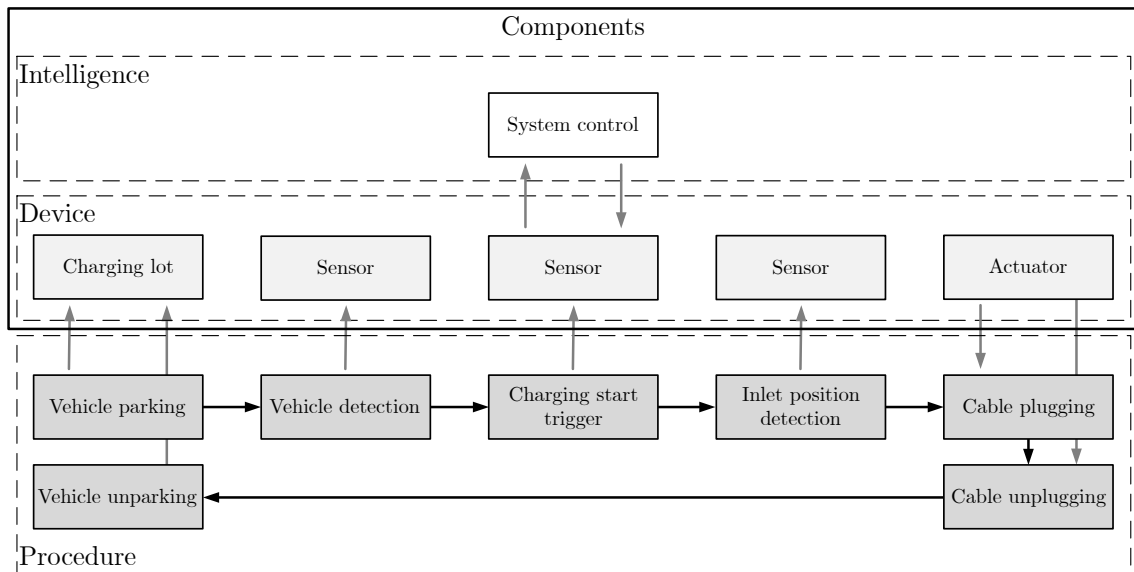


Figure 3.7.: Functional design model with representation of the ACCS components.

objects. In the following, component demands and -specifications are derivatives and developed based on the ACCS requirements, -objects and -working tasks.

Table 3.5.: Connection of ACCS prototype components, -requirements and -objects.

Component	ACCS prototype requirement designation	Object
Charging lot	R1, R2, R3, R4	Driver, Vehicle
Vehicle detection sensor	R5, R6, R10	Vehicle
Charging start trigger sensor	R7	Driver
Inlet detection sensor	R5, R8, R13, R14	Charging socket
Actuator	R9, R11, R12, R13, R14, R15	Charging cable
System control	R5, R6, R7, R8, R9, R10, R11, R12, R13, R14, R15	Devices

3.3.1. Charging lot

For the fulfilment of parking tests close to practice as possible, the defined charging lot has typical dimensions of 5 m length and 2.3 m width, [PJWZ09] (*R1*). Lot dimensions and environmental space impact ACCS size and -positioning. In this context, small and compact ACCS prototype dimensions are advantageous and support prototype transportability. Therefore, the ACCS ground area is limited by the EN 13698 standard pallet size of 1200 mm length and 800 mm width (0.96 m^2), [EPA20]. The charging station high has less impact on the vehicle entrance or environment, but is limited to 2.5 meters (*R4*).

High EV parking accuracy decreases ACCS requirements. Bumps and markers are effective parking aids as well as easy integrable and cost efficient. Bumps reduce parking comfort, and their charging lot position has to be specified for each vehicle type. Furthermore, standardisation is difficult. Markers are easy to integrate and cost-efficient. Typical lot dimensions and unrestricted vehicle entering by widespread and proven markers enables easy and user-friendly EV parking (*R2* and *R3*). Furthermore, the charging lot is unrestricted accessible from several directions, as no parking aids, e.g. obstacles are necessary (*R2*). The avoidance of vehicle-integrated parking aids supports the demand for vehicle adaption prevention and charging of different vehicle types (*R14* and *R10*).

Table 3.6.: ACCS prototype charging lot requirements.

Requirement	Type	Designation
Charging lot dimensions: 5 m length and 2.3 m width	Technical	RL1
ACCS prototype dimensions: max. 1.2 m to 0.8 m and 2.5 m height	Technical	RL2
Parking aids: Marker	Restriction	RL3

3.3.2. Vehicle detection sensor

EV position and -type classification supports the subsequent socket position recognition process due to additional information, e.g. height of charging socket and vehicle dimensions (*R6*, *R8* and *R9*). The upper vehicle position detection accuracy is limited to 5 cm in the vehicle *X*-, *Y*- and *Z*-axis. Important are cost-efficiency and easy ACCS integration. Due to costs, the

3. Prototype development

sensor accuracy is limited to 1 mm. Vehicle adaptations should be avoided (*RV14*), and the sensor system has to work at different light- and weather conditions (*RV5*).

Figure 3.8, left, shows the maximal vehicle sensor working range R_1 with 5.5 m. Concerning cost and development effort, the use of vehicle-internal sensors would be advantageous. This saves infrastructure cost for external sensors, associated hardware and software equipment as well as expensive vehicle adaptations. An ACCS communication link, e.g. ISO 15118, enables the transmission of vehicle data. Figure 3.8, right, show the vehicle sensor working area S_V . Sensors scan the charging station from the vehicle's point of view. For a vehicle position estimation, the sensors need to be suitably placed, and the lot requires arranged obstacles or markers, e.g. for laser, vision, ultrasound or radar systems. Only a few meters around the car are from interest. The vehicle-internal sensor detection range is limited to 10 meters. Table 3.7 shows the derived vehicle detection sensor requirements.

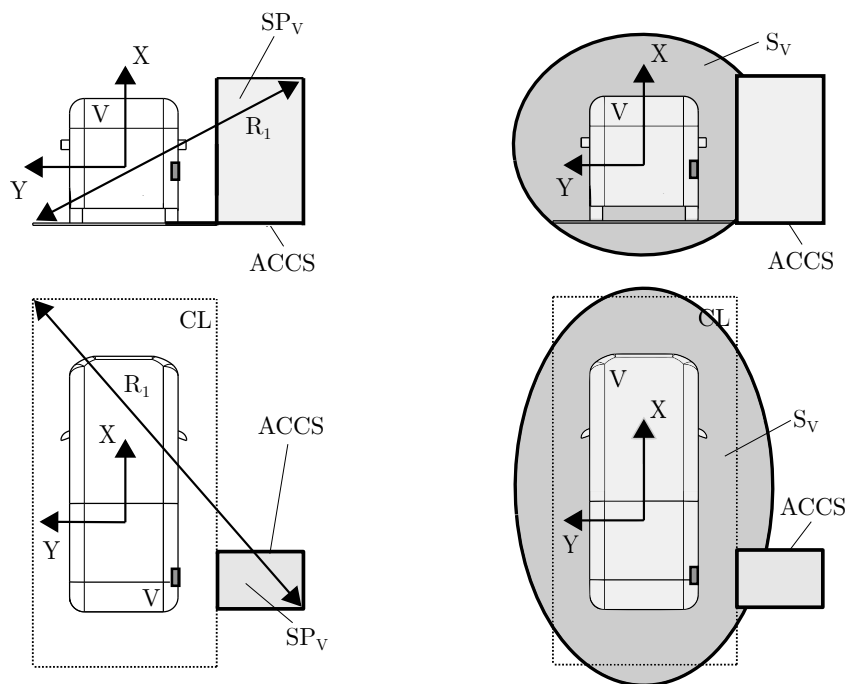


Figure 3.8.: Requirements on vehicle classification.

Table 3.7.: ACCS prototype vehicle detection requirements.

Requirement	Type	Designation
Vehicle type classification	Technical	RV1
Position detection accuracy: 1 mm to 5 cm	Technical	RV2
Working range: 5.5 m	Technical	RV3
Easy charging station integration	Technical	RV4
Cost efficient	Economical	RV5
Functionality at different light conditions	Technical	RV6
Functionality at bad weather conditions	Technical	RV7
Avoidance of vehicle adaptations	Restrictive	RV8
Vehicle-internal sensor detection range: 0 m to 10 m	Technical	RV9

3.3.3. Charging start trigger

A parked vehicle, opened charging lid and unplugged security caps ($R12$) enable ACCS cable plugging. For the present investigations, a located and accessible inlet serves as trigger for starting the ACCS cable connection process. Due to the inlet position detection function, information about the start trigger can be delivered by the inlet detection sensor system after identified inlet position.

Table 3.8.: ACCS prototype charging start trigger requirements.

Requirement	Type	Designation
Inlet position detection	Technical	RT1

3.3.4. Inlet detection sensor

Figure 3.9, left, represents exemplary inlet pose $\{I\}$, charging lot $\{R\}$ and actuator base reference coordinate $\{A\}$ systems. The variable vehicle parking position $\{V\}$ leads to translational and rotational position displacements in relation to $\{A\}$ and $\{R\}$. An inlet detection sensor has to determine the inlet 3D-position (figure 3.9, right, $\{I\}$) in its 6 degrees of freedoms.

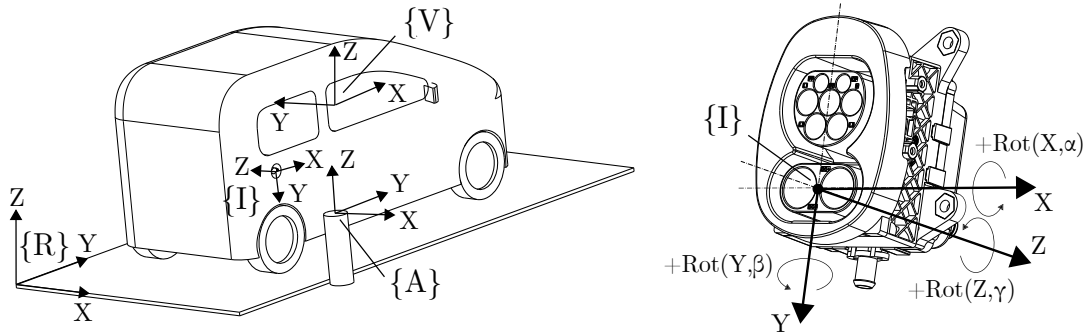


Figure 3.9.: Left: Exemplary representation of vehicle- and inlet positions at the ACCS prototype charging lot. Right: Inlet 3D-position frame-model.

Manual cable plugging consists of the 4 phases *Pre-positioning*, *Guiding*, *Aligning* and *Plugging* (chapter 2.6). Figure 3.10 shows the ACCS cable connection process. In comparison to the manual cable plugging, ACCS is carried out without cable position corrections at first inlet and connector contact (Pos. 2). Controlled automated corrections for connector and inlet alignments are difficult and require a complex mechatronic position compensation system. An ACCS system has to fulfil the accuracy requirements, so that subsequent cable docking and insertion is possible. Figure 3.11, 1 to 5, show the corresponding connector- and inlet edges that have to slide over each other for a successful connection. The ACCS prototype plugging concept consists of the phases *Pre-positioning* and *Plugging*. After determined charging inlet position, the cable pre-position phase starts from moving the charging connector to the charging inlet front. The resulting connector position in front of the charging inlet is influenced by inlet sensor- and actuator accuracy. Figure 3.10 shows the charging connector CAD-model in the phases *Pre-positioning* (figure 3.10, PP) and *Plugging* (figure 3.10, P). *Pre-positioning* starts

3. Prototype development

with the charging connector Pos.1 and ends at Pos.2. The connector position (CC) depends on the inlet sensor results and actuator accuracy. The exemplary Pos. 2 shows 1.5° X -axis angle misalignment and 0.4 mm translational misalignment in Y -direction based on the inlet coordinate system.

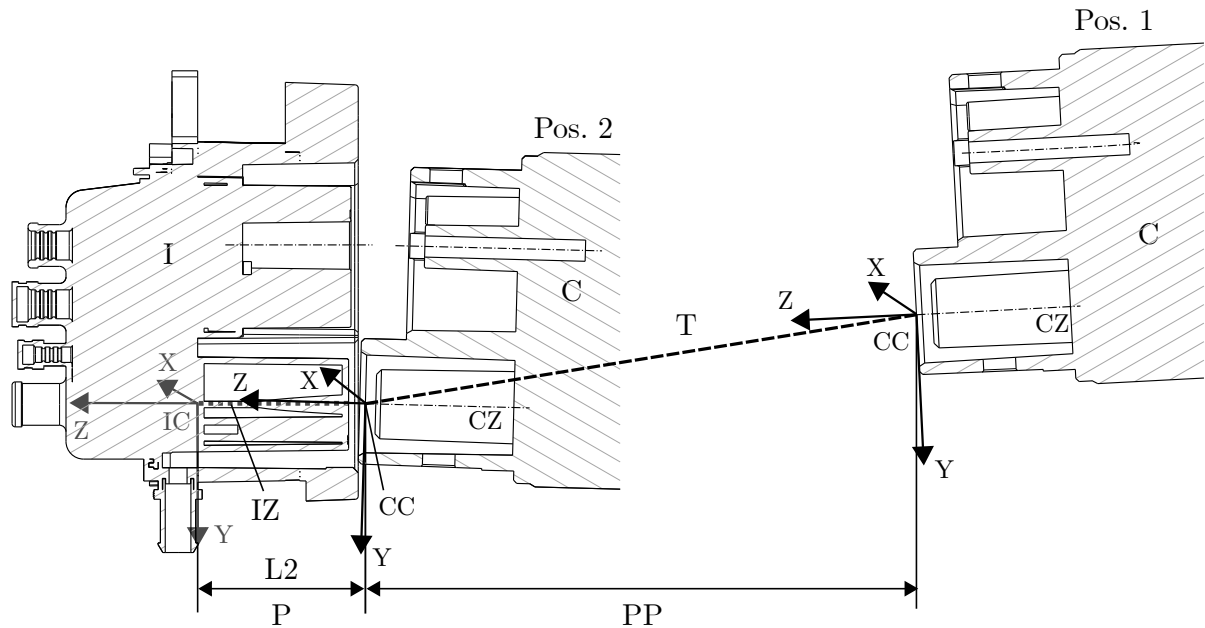


Figure 3.10.: ACCS charging cable plugging process by CAD-model sectional view of CCS charging inlet and -connector.

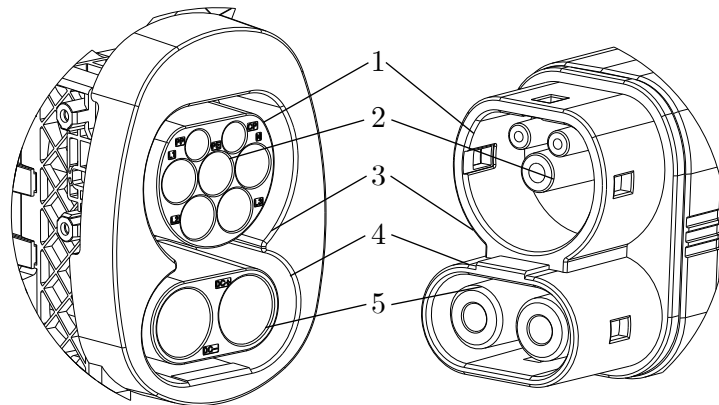


Figure 3.11.: Corresponding CCS Type 2 inlet and connector contact edges and surfaces.

In the following, the inlet sensor requirements are defined under consideration of the maximal misalignment where inlet and connector merging is possible. Figure 3.12 shows the overlaid sectional CAD-model views of inlet (figure 3.12, left, (A-A)) and connector (figure 3.12, right, (B-B)) at plug-in length of the inner connectors (figure 3.11, 2). Figure 3.12, middle, shows minimal connector and inlet gaps of ± 0.69 mm in X -direction and ± 0.66 mm in Y -direction. In this context, the prototype position accuracy in X - and Y -direction is specified with ± 0.6 mm.

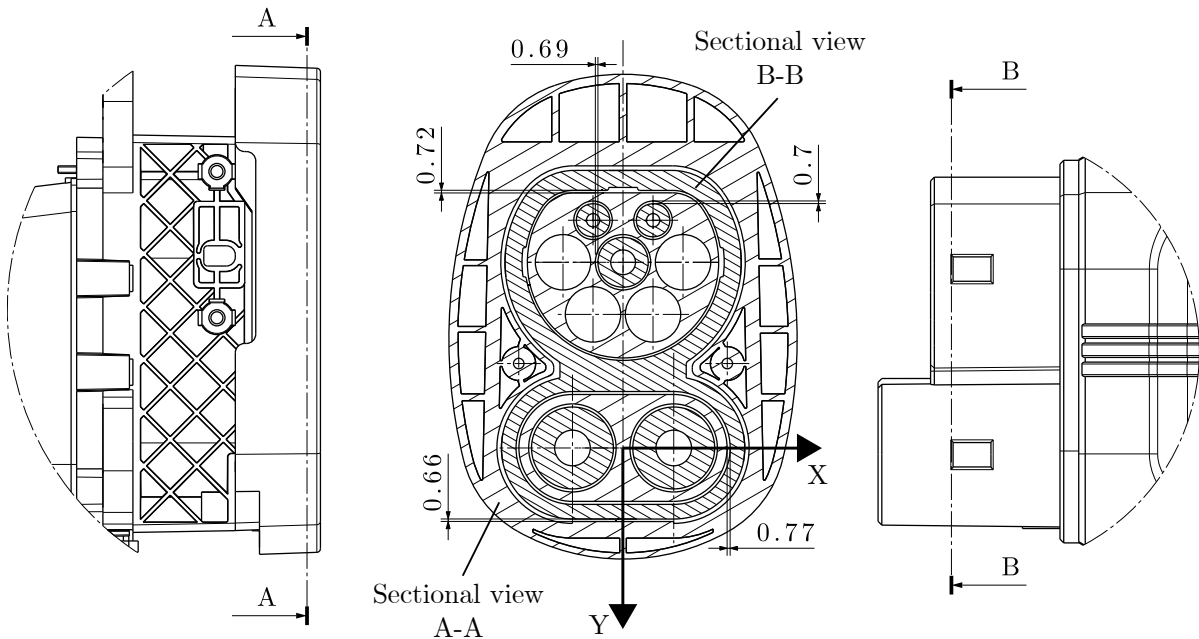


Figure 3.12.: Left: Inlet CAD-model side view. Middle: Overlaid inlet and connector CAD-model sectional views representing the connection partners clearance. Right: Connector CAD-model side view.

The process-accuracy in inlet Z -direction is defined by the connector insertion length requirements. Figure 3.13 shows the connector locking grooves and a sectional view of CCS Type 2 inlet and connector in plugged position. A full inserted connector leads to a 0.7 mm clearance of connector and locking mechanism. Connector insertion by an actuator and locking requires an ACCS prototype accuracy in inlet Z -direction of 0.7 mm.

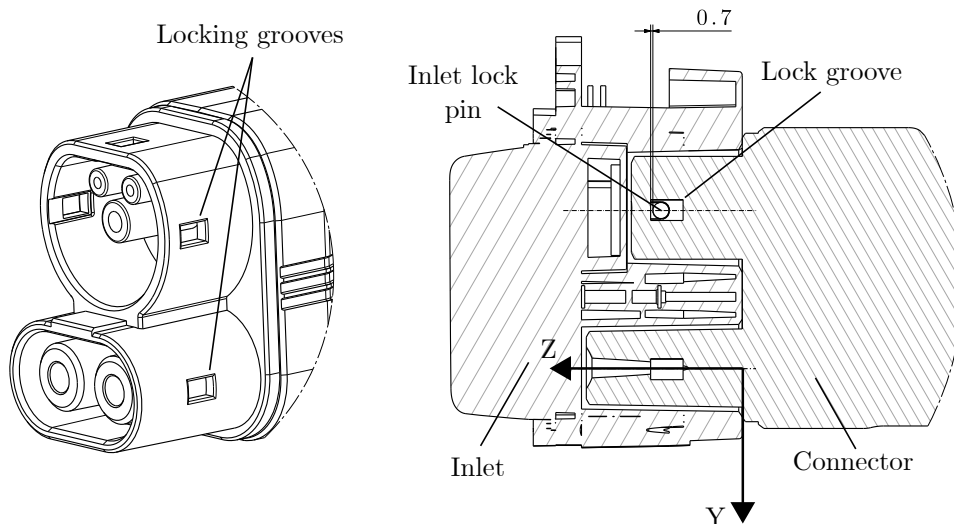


Figure 3.13.: Left: CCS Type 2 connector CAD-model. Right: CAD-models sectional views of connected CCS Type 2 inlet and connector.

In the following, the connector pre-positioning angle requirements in inlet X -, Y - and Z -axis rotation are defined under consideration of the maximal connector angle displacement. Figure

3.14 shows a plugged connector with an insertion length of 26.3 mm. The full insertion length is given with 48.5 mm. High angle misalignments lead to connector tilting. Angle misalignments decrease with insertion length. It is assumed that connector tilting is prevented after half reached insertion length. The maximal angle misalignment is given by the contacting surfaces and results in 3° angle misalignment in the shown position. Figure 3.15 shows the CAD-model sectional view of inlet and plugged connector. By an insertion length of 25 mm, a Y -axis displacement of 4° is given. Figure 3.16 shows the possible connector Z -axis angle displacement at the half-length plugged position. The angle until contact is given with 1.5° . In plugged and by the locking mechanism fixed position, there is no clearance between inlet and connector. As one requirement, the ACCS prototype actuator system has to compensate the position as well as angle misalignments. Actuator requirements and connector insertion process are developed in detail in chapter actuator requirements (chapter 3.3.5).

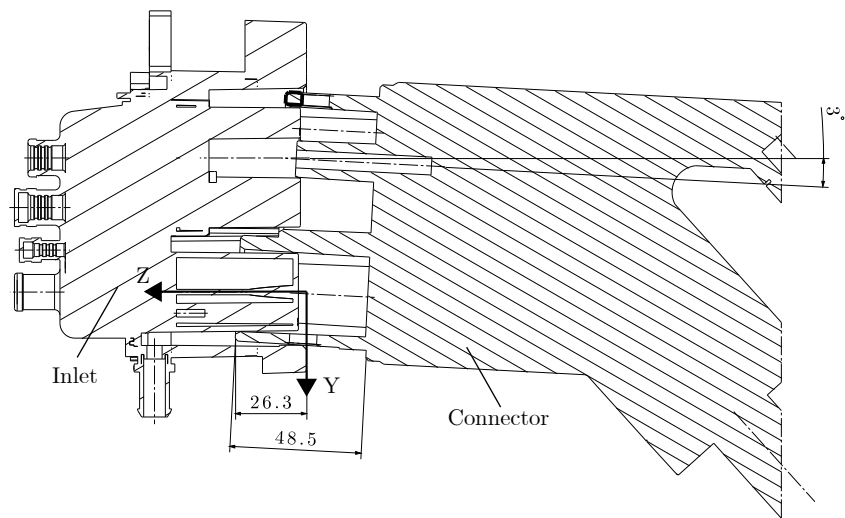


Figure 3.14.: CAD-model sectional view of connected inlet and connector with a X -axis rotation displacement of 3° .

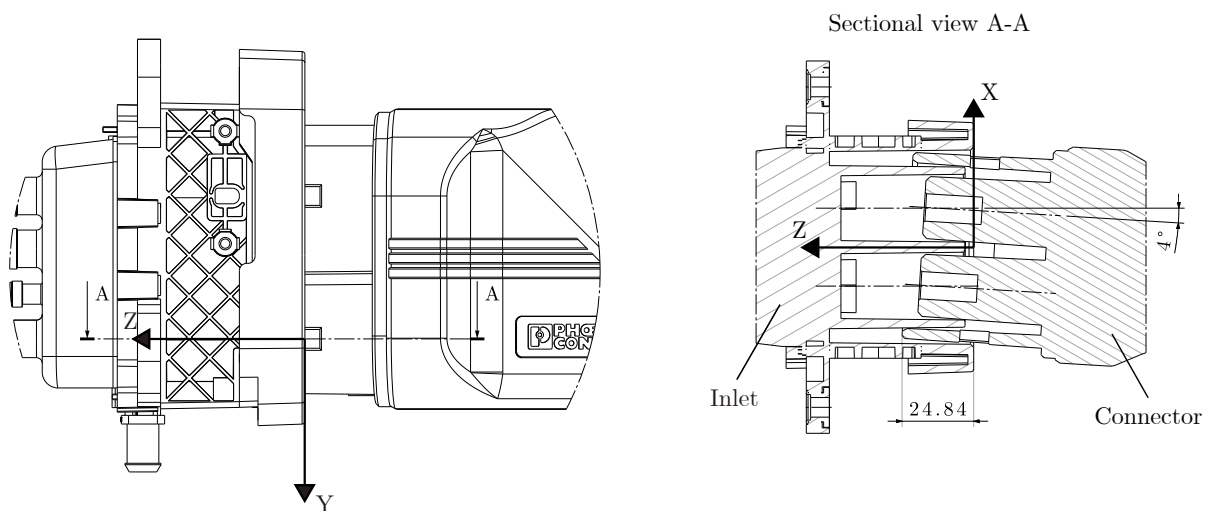


Figure 3.15.: Left: Side view of connected inlet and connector CAD-models. Right: Sectional view A-A of with a Y -axis rotation displacement of 4° .

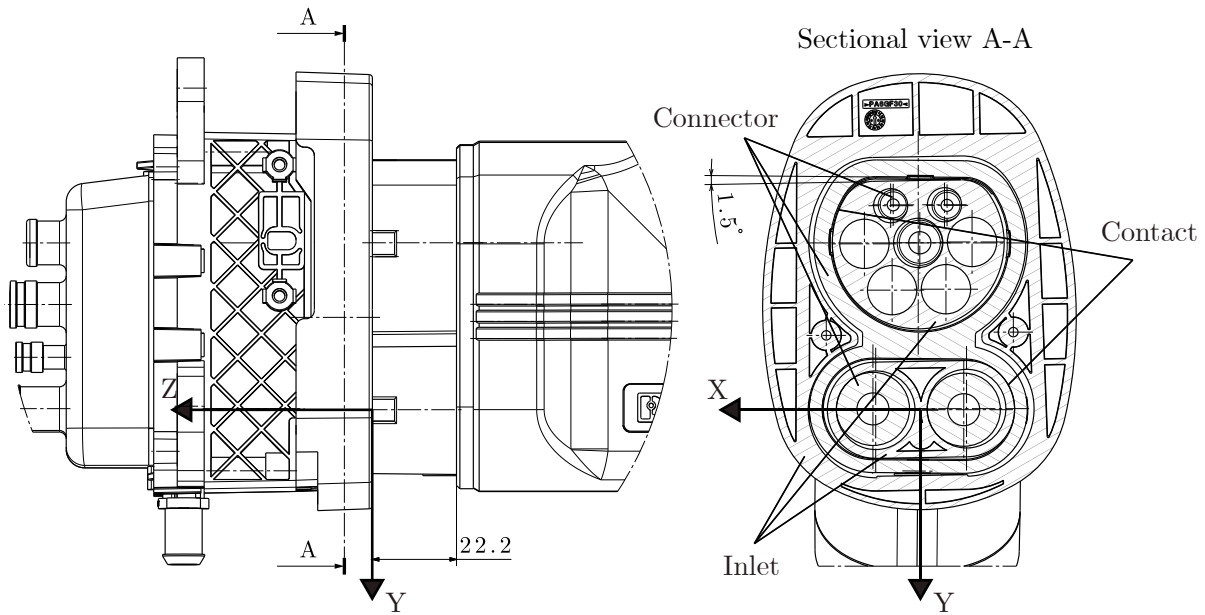


Figure 3.16.: Left: Side view of inlet and connector CAD-models in plugged position. Right: Sectional view A-A of with a Z -axis rotation displacement of 1.5° .

Sensor range

The vehicle parking accuracy and resulting charging inlet position tolerances define the inlet sensor working range. In this context, the sensor working range is influenced by the vehicle parking accuracy in vehicle X - and Y -direction as well as the charging socket height. In the following, the parking accuracy findings of manual parking without inductive charging devices of chapter 2.7.3 are used. Manual parking shows mean parking misalignments of 12.12 cm in Y -direction and -23.73 cm in X -direction and an angular misalignment of 0.018° .

The mean or expected value μ , as well as standard deviation σ results, and the assumption of a normal distributed parking position, enables the development of the inlet parking accuracy area. An assumed normal distributed distribution leads to an inlet area of 68.3%, as well as 95.5%, [J. 16] of all test drivers. Figure 3.17 shows the position accuracy area for 68.3% (figure 3.17, A) and 95.5% (figure 3.17, B) of all parking events. Area A corresponds to two times the standard deviations σ_x and σ_y , area B four times σ_x and σ_y and leads to a parking accuracy area of 116.48 cm in X - and 34.96 cm in Y -direction. The mean angle accuracy of 0.018° and a standard deviation of 2.27° and a 95.5% probability lead to an inlet angle from -4.52° up to 5.56° . For a 68.3% probability, the range is given from -2.25° up to 2.29° . Based on representative EV-fleet findings (figure 2.2), the inlet height is defined between 70 and 100 cm.

Figure 3.18, left and right, shows the top- and back view of the ACCS prototype layout model. The sensor range depends on sensor mounting position and maximal inlet parking misalignments. The inlet area (figure 3.18, I) is located parallel to the ACCS prototype X -direction and symmetric to the middle axis (figure 3.18, A). The maximal sensor working range SR_{\max} is given by

3. Prototype development

$$SR_{max} = \sqrt{SR_{max,X}^2 + SR_{max,Y}^2 + SR_{max,Z}^2} \quad (3.1)$$

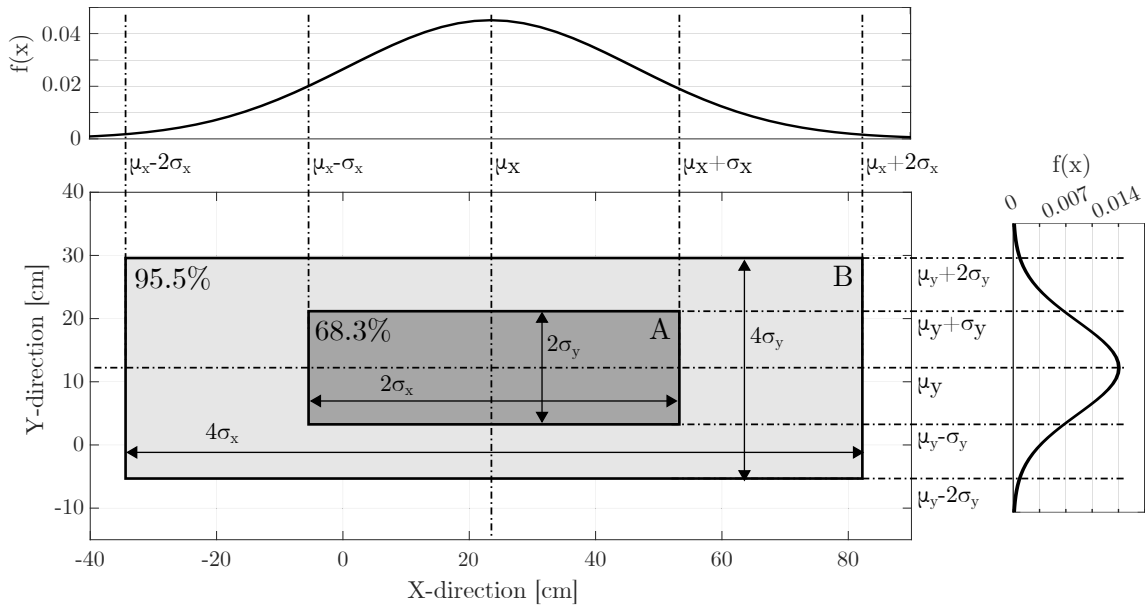


Figure 3.17.: Inlet positioning accuracy area represents 68.3% and 95.5% of parking tests.

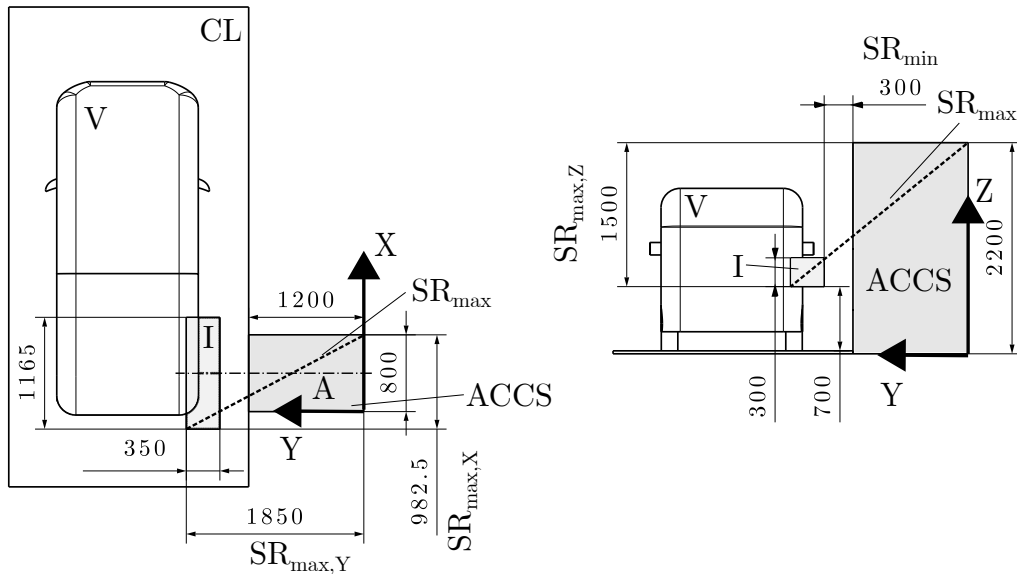


Figure 3.18.: ACCS prototype CAD-models represent inlet parking accuracy area and inlet sensor working range demands.

The minimal working range SR_{min} (figure 3.18, right, SR_{min}) is given with 300 mm and is defined by the minimal clearance of charging inlet and prototype. The minimal working range is reduced by 150 mm safety distance between actuator and vehicle if the inlet detection sensors are mounted on the actuator system.

Vehicle adaptations

An interoperable inlet position detection process is advantageous. The sensor system should be applicable to various vehicle types. The avoidance of charging inlet-, socket- as well as vehicle adaptations or modifications is essential for fulfilling automated charging by use of standard connectors (in case of the present investigations the CCS type 2).

Different light performance

ACCS has to work at different environmental conditions, e.g. parking garages or rest stop stations. Prototype tests are carried out in- and outdoor under different light conditions. Sensor requirements are robustness at different and changing light conditions, e.g. bright and dark light as well as shadows.

Costs

Cost is an ACCS prototype criterion. Sensor cost-efficiency requirements include the hardware for sensors as well as effort for charging station- and vehicle integration and adaptations. In the present investigations, automotive and industrial standard components came to use to involve state-of-the-art components for reasonable costs. This provides a good basis for subsequent further development of the technology for mass production applications.

Charging station integration

The sensor prototype integration impacts ACCS design and sensor data processing. The system has to fulfil ACCS prototype design and layout demands as well as unrestricted observation of the object of interest.

Weather robustness

Besides light conditions, weather conditions, e.g. rain or snow influence sensor results. Sensor robustness due to difficult weather conditions is important.

Table 3.9.: ACCS prototype inlet sensor detection requirements.

Requirement	Type	Designation
6 DOFs position detection capability	Technical	RI1
0.54 mm <i>X</i> -direction accuracy	Technical	RI2
0.54 mm <i>Y</i> -direction accuracy	Technical	RI3
0.64 mm <i>Z</i> -direction accuracy	Technical	RI4
2.9° <i>X</i> -rotation accuracy	Technical	RI5
3.9° <i>Y</i> -rotation accuracy	Technical	RI6
1.4° <i>Z</i> -rotation accuracy	Technical	RI7
Working range from 150 mm up to 2600 mm	Technical	RI8
Avoidance of vehicle and inlet adaptations	Restrictable	RI9
Cost-efficient	Restrictable	RI10
Working at different light conditions for testing in- and outdoor	Technical	RI11
Easy ACCS prototype integration	Restrictable	RI12
Weather robustness for testing in- and outdoor	Technical	RI13

Table 3.9 shows the inlet sensor requirements. Sensor and actuator accuracy are responsible for the resulting connector position. Based on the robot findings in table 2.10, an actuator position repeatability of 0.1 mm is assumed. The position repeatability corresponds to the cube diagonal D_c . Assuming an equally axes accuracy, the actuator accuracy in X -, Y - and Z -direction is given with $D_c/\sqrt{3}$ and leads to 0.058 mm. The actuator X - Y - and Z -rotation accuracy is assumed with 0.1° .

3.3.5. Cable handling actuator

The actuator is responsible for charging cable moving, plugging and -unplugging. In the following, the requirements are developed by the combination of evaluation criteria proposals according to [HMA10] and the prototype requirements (R9, R10 and R11).

Kinematics- and range requirements

The actuator is responsible for the trajectory path (figure 3.19, T), that handles the connector position and rotation movements until reaching Pos. 2. Cable type and charging socket position impact the trajectory path. In the phase *Plugging* (figure 3.19, P), the connector and inlet Z -axis align during the insertion length (figure 3.19, L2) until connector- and inlet coordinate system (figure 3.19, CC and IC) are equal. The actuator compliance requirements corresponds to the translational and rotational inlet sensor accuracy definitions. Alternatively, the compliance can be realized with position compensation devices presented in chapter 2.2.1.

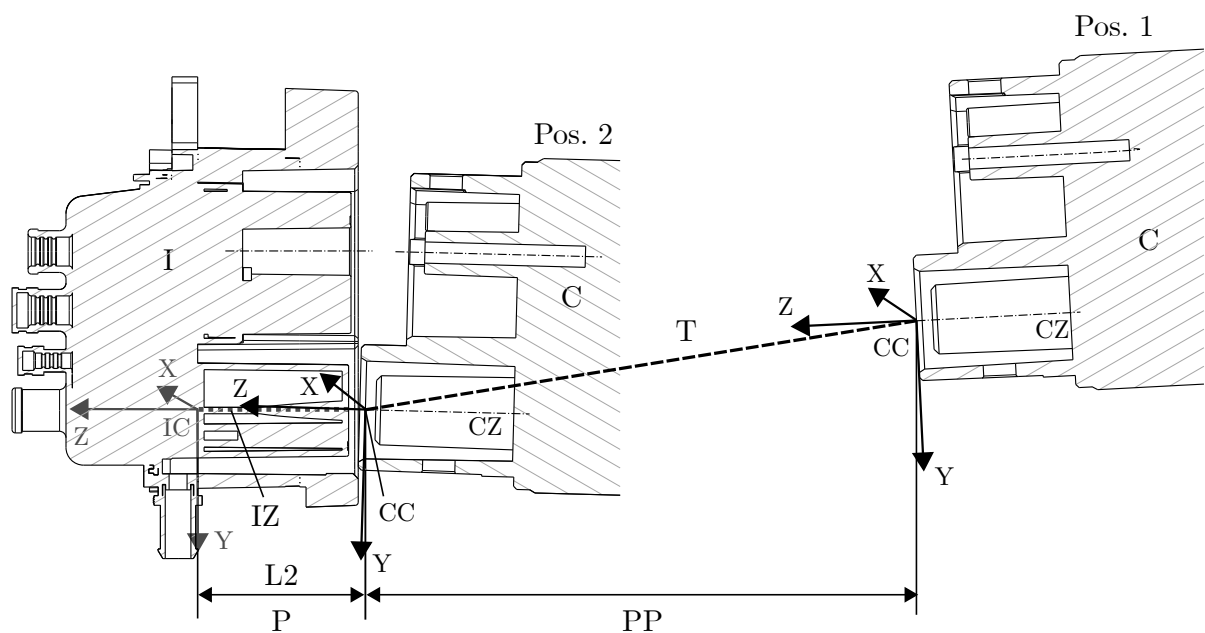


Figure 3.19.: ACCS charging cable plugging process by a sectional view of CCS Type 2 charging inlet and -connector CAD-models.

Figure 3.20 shows the ACCS prototype actuator working range model. The working range depends on actuator base mounting position and maximal inlet parking misalignment. For reducing the working range requirements, the actuator base is defined at the ACCS centre axis

(figure 3.20, A) with 150 mm clearance to prototype outer dimensions. The maximal working range AR_{max} is defined as

$$AR_{max} = \sqrt{AR_{max,X}^2 + AR_{max,Y}^2 + AR_{max,Z}^2} = 1132 \text{ mm.} \quad (3.2)$$

The minimal working range AR_{min} (figure 3.20, right, AR_{min}) is given with 450 mm and corresponds to the minimal distance of 300 mm between charging inlet and ACCS base and 150 mm clearance. The maximal working radius $AR_{max,R}$ is given with 105° .

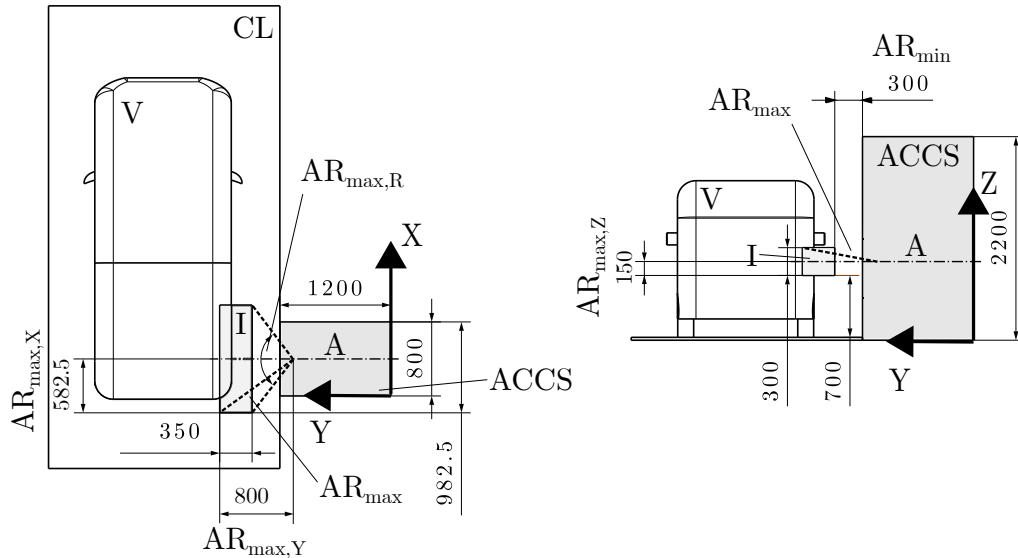


Figure 3.20.: ACCS prototype layout model with representation of charging inlet area and actuator range requirements.

Figure 3.21 shows the ACCS prototype *Pre-positioning* cable path model. The path prevents a sagging cable that could grind on the floor or a stretched cable that leads to high tensile forces.

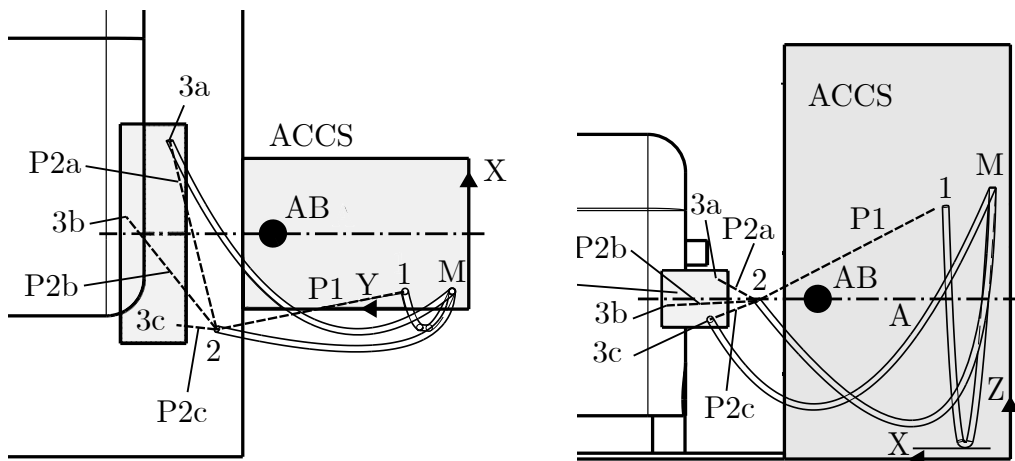


Figure 3.21.: Actuator cable path model for the phase *Pre-positioning*. Left: Charging lot and ACCS prototype top view. Right: Back view of the ACCS charging station.

Position 1 (figure 3.21, 1) indicates the cable home position. Position 2 provides guiding the cable around the actuator base AB. Positions 3a, 3b and 3c show exemplary inlet positions. The cable trajectory paths with reference in the actuator TCP in the phases *Pre-positioning* (P1, P2a, P2b and P2c) and *Plugging* occur in straight lines. The TCP corresponds to the defined connector coordinate system CC. The process needs to run through in reverse order for cable unplugging and returning the charging cable to waiting position.

Capacity and forces

The actuator capacity and force requirements are separated in the phases *Pre-positioning* and *Plugging*. Figure 3.22, left, shows the connector forces model for the phase *Pre-positioning*. Without touching the ground, the cable is mounted at its ends at the charging station and the actuator head (figure 3.22, A). The actuator head tool weight m_T is estimated with 1 kg, the cable length L_{CCS} with 5 meters. α is given with 135° . Technical data of the CCS Type 2 cable are given in table 2.3.

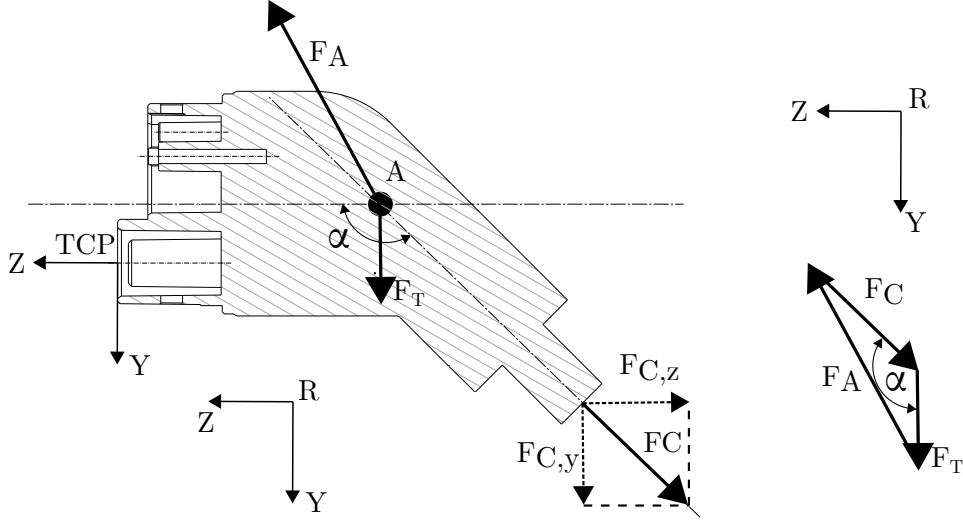


Figure 3.22.: Actuator force model for the cable phase *Pre-positioning*. Left: Forces on actuator head reference TCP. Right: Force model to determine the actuator force F_A .

The actuator force F_A is obtained by the tool force F_T and the cable force F_C direction of action. $F_{C,y}$ is given by

$$F_{C,y} = q_{l,CCS} \cdot \frac{L_{CCS}}{2} \cdot g = 58.12 \text{ N}, \quad (3.3)$$

with a cable weight per meter $q_{l,CCS}$, cable length L_{CCS} and the gravitational acceleration g . The horizontal cable force $F_{C,z}$ in TCP Z-direction due to cable moving, pulling, accelerating and twisting is estimated as equal to $F_{C,y}$.

$$F_{A,z} = F_{C,z} = 58.12 \text{ N} \quad (3.4)$$

$$F_{A,y} = m_T \cdot g + F_{C,y} = 67.93 \text{ N} \quad (3.5)$$

$$F_A = \sqrt{F_{A,y}^2 + F_{A,z}^2} = 89.40 \text{ N}. \quad (3.6)$$

Figure 3.23 shows the simplified model for the actuator forces due to cable plugging. The maximal plugging force F_P for a CCS Type connector is indicated with 100 N, [CON16a]. The actuator force F_A is given by

$$F_{A,z} = F_P + \cos(\alpha - 90) \cdot F_C = F_I + F_{C,z} = 158.12 \text{ N} \quad (3.7)$$

$$F_{A,y} = F_T + \sin(\alpha - 90) \cdot F_C = F_T + F_{C,y} = 67.93 \text{ N} \quad (3.8)$$

$$F_A = \sqrt{F_{A,z}^2 + F_{A,y}^2} = 172.09 \text{ N}. \quad (3.9)$$

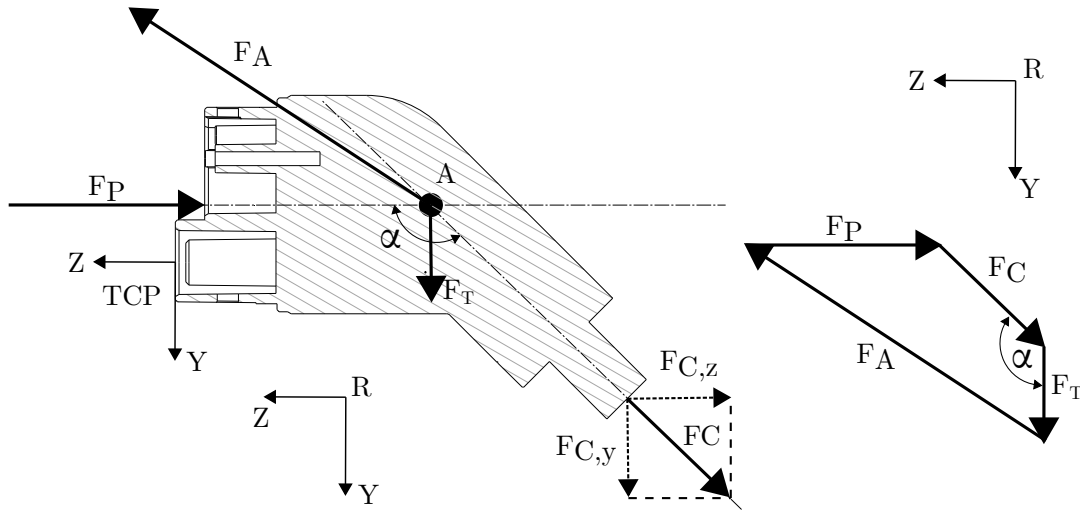


Figure 3.23.: Actuator force model for the *Plugging* cable phase. Left: Forces on the actuators head. Right: Force model to determine the actuator force F_A .

Accuracy

The actuator has to fulfil the accuracy requirements in the robot head tool coordinate point *TCP*. Derived from state-of-the-art robots (table 2.10) and ACCS prototype sensor demands (table 3.9), 0.1 mm actuator position repeatability and 0.1° angle rotation accuracy are defined. During the phase *Plugging*, the actuator compensates the position and angle misalignment of connector and inlet. The compliance requirements correspond to the connector positioning accuracy demands for the phase *Pre-positing* in translational and rotational directions.

Safety

Actuator safety functions support the ACCS development and -charging tests with test drivers. Functions, e.g. collaboration or force-controlled actuator stops, avoid human violations or vehicle damages. An ACCS actuator with collaborative features does not need a specific safety installation, e.g. fences or barriers and makes the prototype handling during the tests simpler.

Velocity, size and weight

A compact and easily transportable ACCS prototype supports charging tests at different locations. Actuator size and weight impact the ACCS prototype design and layout. Requirements are defined as 300 kg maximal actuator weight and dimensions that fit into the ACCS prototype. Actuator velocity plays a subordinate role, but cable movement and connection tests should be performed with the appropriate speed of minimal 0.05 m/s.

Table 3.10.: ACCS prototype actuator requirements.

Requirement	Type	Designation
Kinematic movement capability in 6 DOFs	Technical	RA1
$\pm 582\text{mm}$ working range in ACCS X -translational direction	Technical	RA2
450 mm to 800 mm working range in ACCS Y -translational direction	Technical	RA3
± 150 mm working range in ACCS Z -translational direction	Technical	RA4
1132 mm working range	Technical	RA5
105° working radius	Technical	RA6
0.1 mm position repeatability in X -, Y - and Z -translational direction	Technical	RA7
0.1° angle accuracy in X -, Y - and Z -rotational direction	Technical	RA9
0.6 mm compliance in X -translational direction	Technical	RA10
0.6 mm compliance in Y -translational direction	Technical	RA11
0.7 mm compliance in Z -translational direction	Technical	RA12
3° compliance in X -rotational direction	Technical	RA13
4° compliance in Y -rotational direction	Technical	RA14
1.5° compliance in Z -rotational direction	Technical	RA15
Trajectories in straight lines	Technical	RA16
70 N payload capacity	Technical	RA17
100 N plugging force	Technical	RA18
180 N max. load	Technical	RA19
0.05 m/s min. velocity	Technical	RA20
Max. dimensions: Base area 1200 to 800 mm, height 2200 mm	Technical	RA21
500 kg max. weight	Technical	RA22
Collaborative and force controlled safety functions	Technical	RA23

3.3.6. System control

The system control handles the charging process, sensor data processing, actuator control and the data exchange between the component interfaces. Sensor data processing includes vehicle detection, inlet position detection as well as charging start trigger. The cable trajectories in the phases *Pre-positioning* and *Plugging* occurs are defined as straight lines. A continuous trajectory path control enables straight movements. Furthermore, the TCP path between start- and target point is known.

Table 3.11.: ACCS prototype system control requirements.

Requirement	Type	Designation
Sensor data processing	Technical	RC1
Vehicle and inlet detection algorithm in X -direction	Technical	RC2
Continuous TCP trajectory path control	Technical	RC3

3.4. Sensor system selection

The following chapter deals with the selection of the ACCS prototype sensor systems. Figure 3.24 shows suitable sensor technologies for vehicle- (figure 3.24, Vehicle) and inlet (figure 3.24, Inlet) detection, based on the range and accuracy requirements ($RV2$ and $RV3$ as well as $RI2$ - $RI4$). Appropriate vehicle recognition sensors for the present prototype development are camera-, magnetic-, sound- and infrared systems. Tactile and combined polar- and camera system fulfil the inlet detection requirements with higher precision.

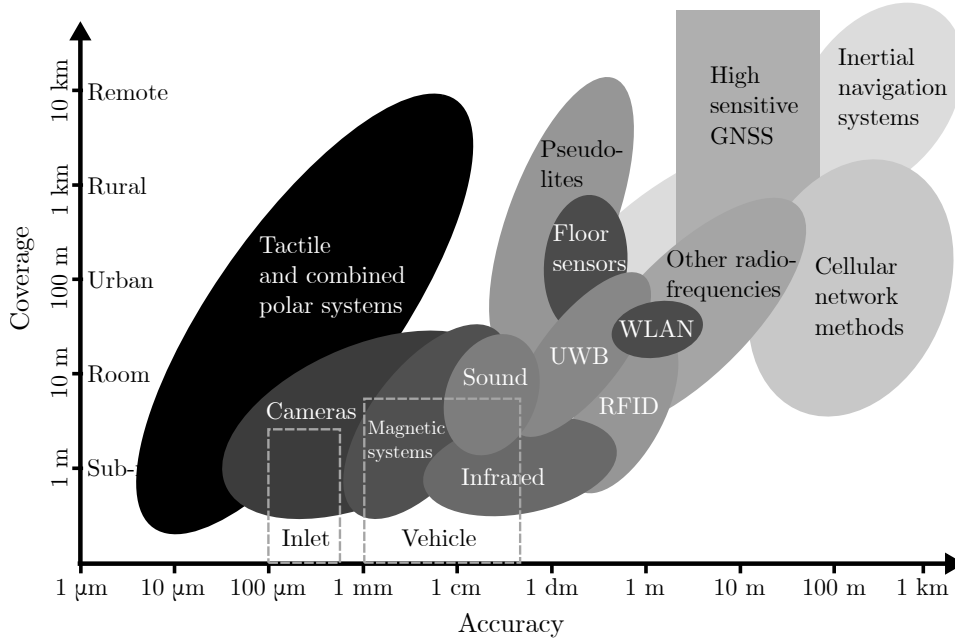


Figure 3.24.: Preselection of ACCS vehicle and inlet detection sensor technologies.

An evaluation consisting of a benefit analysis also called *point value method*, *point evaluation method* or *scoring model* serves as basis for the further sensor technologies selection. The theoretical basis is the *additive multi attributive value function*. This assigns a value to each alternative depending on its attribute characteristics [FEL10]. The *additive multi attributive value function*, for calculating the total value of an alternative is given by

$$S(A) = \sum_{c=1}^N W_c \cdot R_c(A_c). \quad (3.10)$$

*Indices explanation: S ... score, A ... alternative,
W ... weighting, R ... rating, c ... criteria*

Score $S(A)$ for each alternative A is calculated from the sum of the products of individual weighting W_k and rating $R_k(A_k)$ per criteria. In a benefit analysis, particular attention has to be paid to the criteria formulation. The selection of wrong criteria can lead to result distortions, e.g. the definition of irrelevant targets and objectives. The analysis should contain criteria appropriate to the situation, and the criteria should take all essential aspects into account, [Hal62].

3.4.1. Vehicle detection with vehicle-external sensors

The evaluation criteria are derived from the vehicle detection requirements (table 3.7). Table 3.12 shows the vehicle detection evaluation criteria and their weighting. The weighting defines the importance of the ACCS criterion.

Table 3.12.: Sensor evaluation criteria and their weighting for vehicle detection and classification.

Criteria	Designation	Weighting [%]
Parking position accuracy	RV2	20
Material costs	RV5	20
Different light performance	RV6	20
Vehicle classification	RV1	10
Charging station integration	RV4	10
Weather robustness	RV7	10
Vehicle adaption	RV8	10

Figure 3.25 shows the vehicle-external sensor technologies score results for vehicle detection and classification. Detailed information about the rating criteria of each technology is shown in Appendix table A.7. Positioning systems using magnetic and electromagnetic fields are not very precise and require vehicle adaptations because an additional sensor or electromagnetic field source is needed. Structured light sensors achieve medium results in all criteria. A disadvantage compared to other sensor systems is the restricted outdoor usability. Ultrasonic sensors as well as 2D- and 3D-cameras achieve best evaluation results. Ultrasonic sensors are cheap; however, it is challenging to determine the type or brand of the vehicle with this technology. Cameras are cost-efficient and with stored vehicle geometry data, not only the vehicle position can be determined, but also a vehicle type classification is possible. Due to camera size, prototype integration is easy. However, robustness under different weather conditions cannot be guaranteed. Laser technologies are well-suited for vehicle detection and

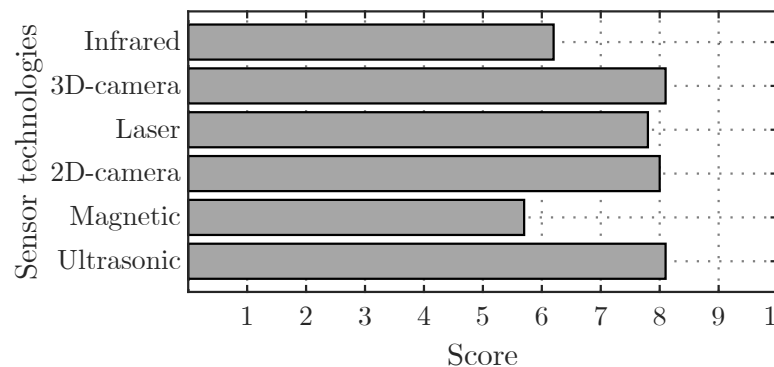


Figure 3.25.: Evaluation score results for vehicle-external sensor technologies for vehicle position detection and classification.

classification under different weather and light conditions, but their price is a main disadvantage.

3.4.2. Vehicle position detection with vehicle-internal sensors

Table 3.13 shows the vehicle-internal sensor evaluation criteria. Except from the criteria *vehicle adaption and classification*, the evaluation considerations for the vehicle-external sensor system can be assumed for vehicle-internal sensors.

Table 3.13.: Criteria and their weighting for vehicle-internal sensor systems.

Criteria	Designation	Weighting [%]
Parking position accuracy	RV2	25
Material costs	RV5	25
Different light performance	RV6	20
Charging station integration	RV4	15
Weather robustness	RV7	15

Figure 3.26 shows the benefit analyses score results of vehicle-internal sensor technologies. The criteria rating is shown in Appendix table A.8. Today's vehicles have various camera systems, e.g. for mid-range distances and top-view-camera systems that include up to 8 cameras around the car. These systems are suitable for the determination of the vehicle charging lot position by detecting markers on the ground. Snow or other adverse weather conditions could lead to bad results, which represents a disadvantage of this technology. Ultrasound sensors are not sufficiently accurate and require the existence of obstacles. The evaluation considers costs as well as light and weather robustness. Ultrasound sensors are also installed in many vehicles as standard parking aids. *Short-Range-Radar* (SRR) show disadvantageous regarding costs and vehicle integration. A cost-effective and robust solution is provided by the combination of ultrasound sensors with 2D-cameras.

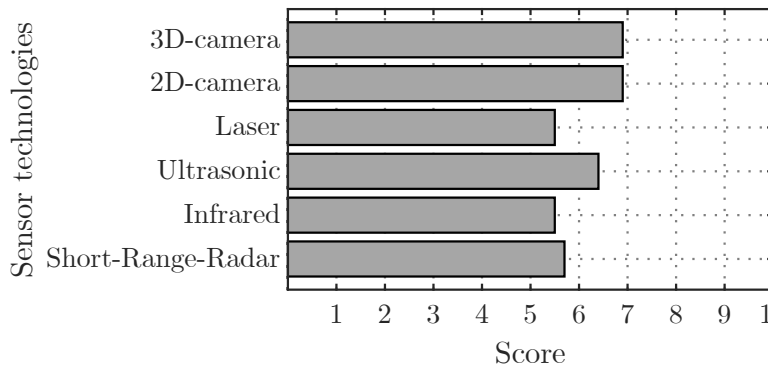


Figure 3.26.: Evaluation score results for different vehicle-internal sensors.

3.4.3. Inlet position detection

Suitable technologies, under consideration of accuracy and working range (figure 3.24), are laser as well as camera systems. The inlet recognition has special requirements on a sensor. Evaluation criteria and their weighting are shown in table 3.14.

Table 3.14.: Criteria weighting for inlet 3D-pose detection sensor systems.

Criteria	Designation	Weighting [%]
Inlet 3D-pose detection	RI1-RI7	30
Vehicle adaption	RI9	20
Light performance	RI11	15
Material costs	RI10	15
Charging station integration	RI12	10
Weather robustness	RI13	10

Figure 3.27 shows the sensor evaluation results. The evaluation criteria rating is presented in detail in Appendix table A.9. Laser systems, achieve very high accuracy of up to 0.01 mm on few meters, but this skill goes hand in hand with rising costs. 2D- and 3D-cameras achieve high evaluation score results. Cameras are cost-efficient, with adequate accuracy. Due to ACCS prototype integration, 2D-cameras require less space in comparison to 3D-cameras. 2D-camera sensors are best suited for the ACCS prototype vehicle recognition- and inlet position detection application. The 2D-camera specifications are defined in the following section.

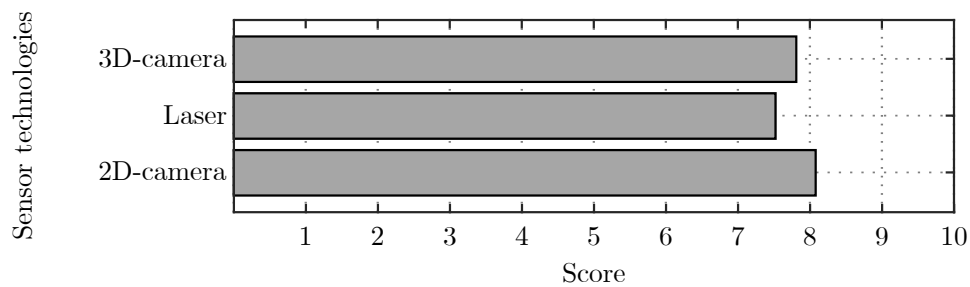


Figure 3.27.: Evaluation score results for inlet position detection sensor technologies.

3.4.4. 2D-camera specifications

The 2D-camera specifications are defined for shape-based 3D-matching methods for enabling inlet detection in 6 DOF. An ACCS prototype requirement is the ability to detect the CCS type 2 standardized inlet in such a way, that no specific modifications and adaptations are necessary. Figure 3.28, A, shows the standardized inlet, [COM14a] area for the shape-based 3D-matching detection by 2D-camera images.

Figure 3.29 shows the projected inlet shapes I_X , I_Y and I_Z in a 2D-image based on the connector insertion X -, Y - and Z -axes rotation requirements $RI5$, $RI6$ and $RI7$. Table 3.15 shows the horizontal and vertical 2D-camera image accuracy demands AC_h and AC_v due to length changes in comparison to the inlet shape without rotation.

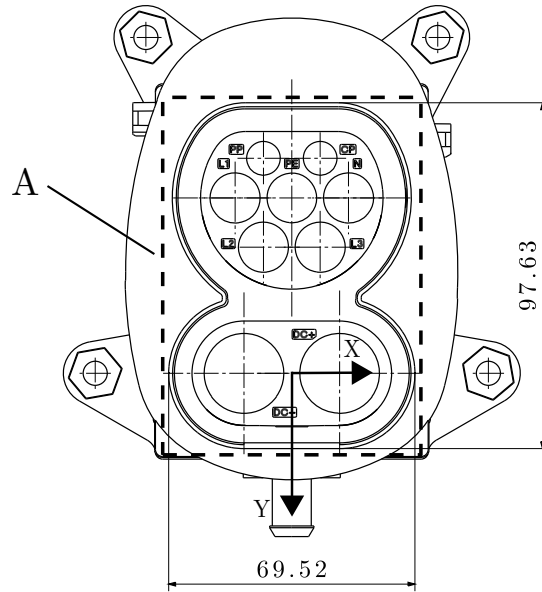


Figure 3.28.: CCS Type 2 inlet area for ACCS prototype shape-based 3D-matching.

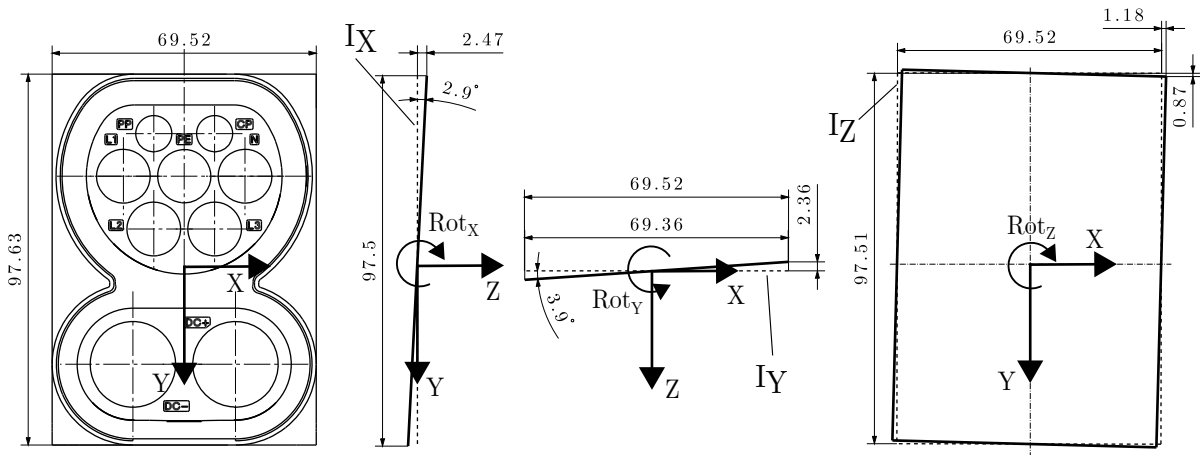
Figure 3.29.: Projected inlet shape and dimensions in an image due to X -, Y - and Z -axis rotation in relation to the 2D-camera.

Table 3.15.: 2D-camera accuracy due to inlet rotation angles in relation to the 2D-camera.

Requirement	Designation	2D-camera accuracy AC_h [mm]	2D-camera accuracy AC_v [mm]
2.9° X -rotation accuracy	RI5	-	0.13
3.9° Y -rotation accuracy	RI6	0.16	-
1.4° Z -rotation accuracy	RI7	1.18	0.87

To meet the accuracy demands with a horizontal 2D-camera pixel resolution P_h and lens angle of view α_h as well as vertical pixel resolution P_v and lens angle of view α_v , the maximal object distance D is given by

$$D \leq D_h, D \leq D_v. \quad (3.11)$$

The horizontal distance D_h is calculated by

$$D_h \leq \frac{AC_h \cdot P_h}{2 \cdot \tan(\alpha_h/2)} \quad (3.12)$$

and the vertical distance D_v is calculated by

$$D_v \leq \frac{AC_v \cdot P_v}{2 \cdot \tan(\alpha_v/2)}. \quad (3.13)$$

The inlet Z -direction accuracy requirement $RI4$ results in the horizontal and vertical 2D-image accuracy demands AC_h and AC_v , that are given by

$$AC_h = 2 \cdot RI4 \cdot \tan(\alpha_h/2) \quad (3.14)$$

and

$$AC_v = 2 \cdot RI4 \cdot \tan(\alpha_v/2). \quad (3.15)$$

Table 3.16 shows the maximal object distance with 1280 pixels horizontal and 1024 pixels vertical 2D-camera resolution, as well as 66.1° horizontal and 50.8° vertical lens angle of view, [IDS19] and [TAM19]. In comparison to translational requirements, the inlet rotations lead to higher 2D-camera demands. In this context, the Y -rotation accuracy requirement limits the 2D-camera to inlet distance to 138 mm.

Table 3.16.: ACCS prototype inlet detection 2D-camera requirements.

Requirement	Designation	Max. distance [mm]
0.54 mm X -direction accuracy	RI2	533
0.54 mm Y -direction accuracy	RI3	584
0.64 mm Z -direction accuracy	RI4	656
2.9° X -rotation accuracy	RI5	157
3.9° Y -rotation accuracy	RI6	138
1.4° Z -rotation accuracy	RI7	938

The horizontal and vertical 2D-camera accuracy AC_h and AC_v for the vehicle detection requirement RV3 with D_h and D_h object distance are given with

$$AC_h = \frac{2 \cdot D_h \cdot \tan(\alpha_h/2)}{P_h} \quad (3.16)$$

and

$$AC_v = \frac{2 \cdot D_v \cdot \tan(\alpha_v/2)}{P_v}. \quad (3.17)$$

Table 3.17 shows the horizontal and vertical accuracy AC_h and AC_v for a 2D-camera with 1280 pixels horizontal P_h and 1024 pixels vertical P_v resolution P_v , and a lens with 60.1° horizontal α_h and 46.6° vertical angle of view α_v , [IDS19] and [TAM19]. Selected 2D-cameras and lenses

fulfil the ACCS prototype inlet- and vehicle detection accuracy- and range requirements and thus provide the basis for proper sensors for the ACCS object detection process.

Table 3.17.: ACCS prototype vehicle detection 2D-camera requirements.

Object distance (RV3)	Designation	Accuracy [mm]
D_h : 5.5 m	RV3	AC_h : 4.97
D_v : 5.5 m	RV3	AC_v : 4.63

3.5. Recognition process

Figure 3.30 shows the vehicle, charging start trigger as well as inlet position recognition process. The process steps *Recognition I* and *Recognition II* are carried out by the same 2D-camera system and include *Vehicle recognition* as well as *Basic inlet position-* and *Charging start trigger* detection. An additional 2D-camera system is responsible for the *Advanced inlet position detection* in the process step *Recognition III*.

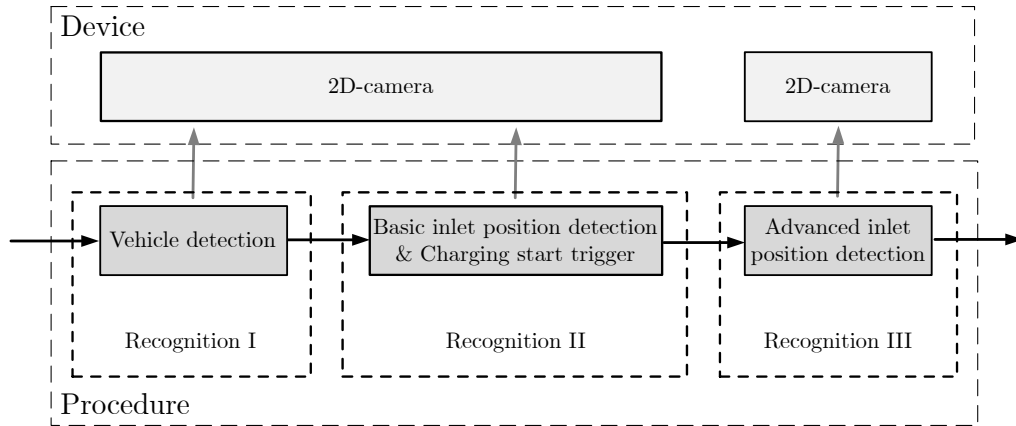


Figure 3.30.: Recognition process including devices and procedures for vehicle-, charging start trigger- and inlet 3D-position detection recognition.

Figure 3.31, left, shows the charging socket and inlet sensor working range S_{CS} . Additionally to the charging socket, the 2D-camera FoV covers the wheel fender. Fender- and charging cover area (figure 3.31, right, F and CS) indicate markant geometric shapes and visible edges in a camera image. Two 2D-cameras observe the vehicle fender contour and classify the vehicle by shape-based 3D-matching processes. In the present approach, the contour of the vehicle fender is used for the vehicle type classification by the use of shape-based 3D-matching algorithms. Optional, the registration and authentication of the vehicle type can be managed by wireless communication technologies [INT18a]. If the vehicle is recognized and identified, the system goes on to the next step.

The determination of $\{I\}$ is divided into the process steps *Recognition II* and *Recognition III*. Field of view (figure 3.32, FoV1, FoV2 and FoV3), position and orientation of each camera are positioned with respect to the ACCS component requirements and 2D-camera specifications.

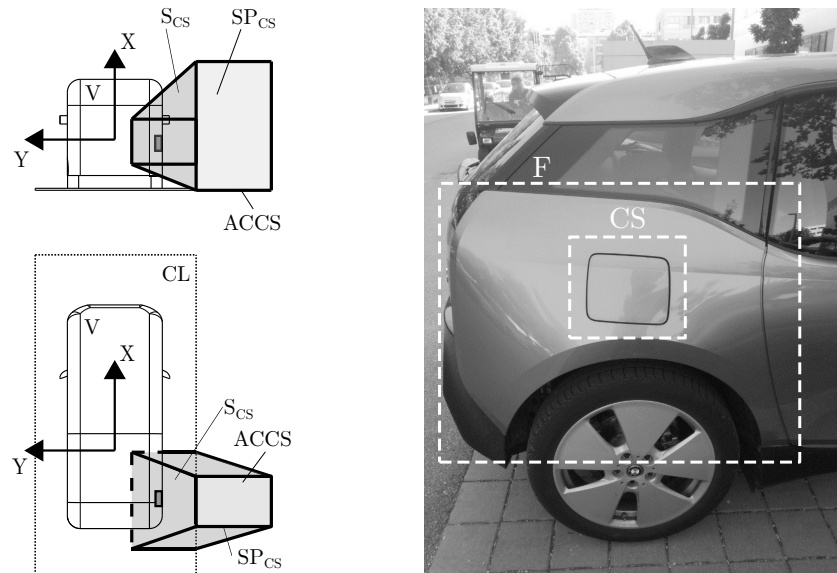


Figure 3.31.: Left: Charging socket sensor working range concept. Right: 2D-image of a rear, right vehicle wheel fender and charging cover.

Camera 1 and Camera 2 (figure 3.32, frame $\{C1\}$ and $\{C2\}$) are mounted on the ACCS and are responsible for the process steps *Recognition I* and *Recognition II*. The position of Camera 2 is at the height of Camera 1 and extends the field of view in ACCS Y-axis (figure 3.32, D1 and D2) to cover the vehicle fender. According to the ISO 15118 communication standard proposal, the charging start signal is initiated from the vehicle and sent by a communication channel to the charging station. This means that the vehicle, respectively the driver, has to initiate the charging process, [INT18a]. In case of the present prototype, the trigger to start charging is defined as the opened charging lid. When it is fully open, the charging inlet is completely visible for Camera 1 and 2. In the case of bad lighting conditions, the frame LEDs (figure 3.32, L) are supporting the matching process. After 10 seconds of unsuccessful search, the lights are switched on. For robot control in process step *Recognition III*, only the translational

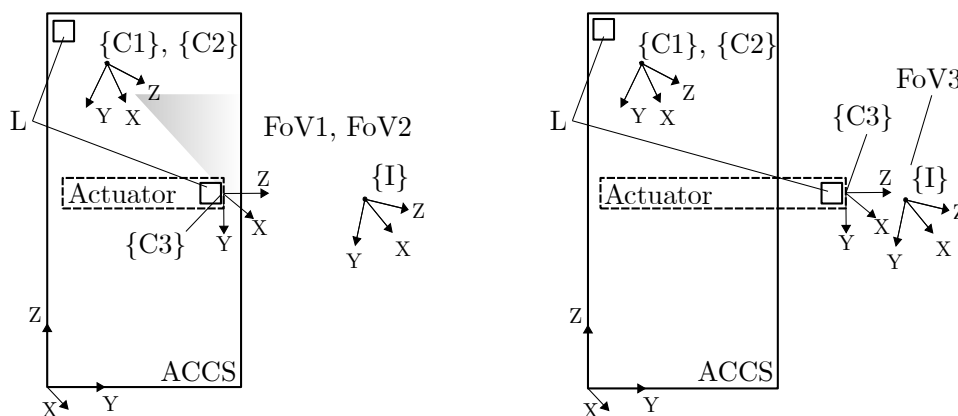


Figure 3.32.: ACCS concept side view with an exemplary representation of an inlet frame and the field of view of the 2D-vision sensors, [WHB19c]. Left: Field of view of Camera 1 and Camera 2 at process step *Recognition II*. Right: Field of view of Camera 3 at process step *Recognition III*.

components X , Y and Z of the frame $\{I\}$ are from interest - the rotation components R_x , R_y and R_z are not relevant. According to the camera specifications, maximal object distance and equitations 3.14 to 3.17 the basic inlet position accuracy is given with 2.37 mm in horizontal (camera X -direction), 2.17 mm vertical (camera Y -direction) and 2.51 mm camera Z -direction. With the given charging inlet basic position information, the robot positions itself in front of the inlet with a distance of less than 138 mm. During the process *Recognition III* Camera 3 (figure 3.32, frame $\{C3\}$) is responsible for the exact detection of $\{I\}$. In contrast to the previous process *Recognition II*, the exact values of the X -, Y - and Z -coordinates and the R_x -, R_y - and R_z -rotations are from interest, [WHB19c].

3.6. Charging process

Figure 3.33 shows a flow chart of the ACCS prototype charging process sequences. The process can be divided into two primary activity fields. This includes the activities responsible for object recognition (dashed lines) and the activities for robot control (full lines). In the following, the individual process steps are explained, [WHB19c]:

1. *Waiting*: If the prototype station is in *standby mode*, the robot waits in the start position for a charging task. The environment is continuously recorded by Camera 1 and 2.
2. *Recognition I*: The system checks the charging station occupancy by Camera 1 and 2. If an object enters the charging lot, the system begins to identify the object. If the vehicle is recognized and identified, the system goes on to the next step.
3. *Recognition II*: Subsequently, step *Recognition II* starts searching for the position of the charging inlet. When the charging inlet is found, the position data are compared with stored data of the vehicle. The next step starts when the charging inlet is recognized within the pre-defined working range of the robot.
4. *Sensor positioning*: In this step, the robot moves along a pre-defined path and positions to the front of the charging inlet for optimal field of view conditions.
5. *Recognition III*: This step is responsible for the accurate charging inlet 3D-position (pose) detection by use of Camera 3. If the charging inlet pose is detected accurately and robustly, the data are processed and transformed for the subsequently performed robot movements. Frame and head LEDs start after 10 seconds matching procedure without positive results.
6. *Dock and connect*: The connector is moved directly in front of the charging inlet face and aligns with its axis, which represents the plug-in direction. In the next step, the robot inserts the connector until the end position is reached and the charging process starts.
7. *Disconnect and undock*: This step includes the withdrawal of the connector and closing of the charging lid. After charging, the robot plugs-out the connector. Charging lid closing

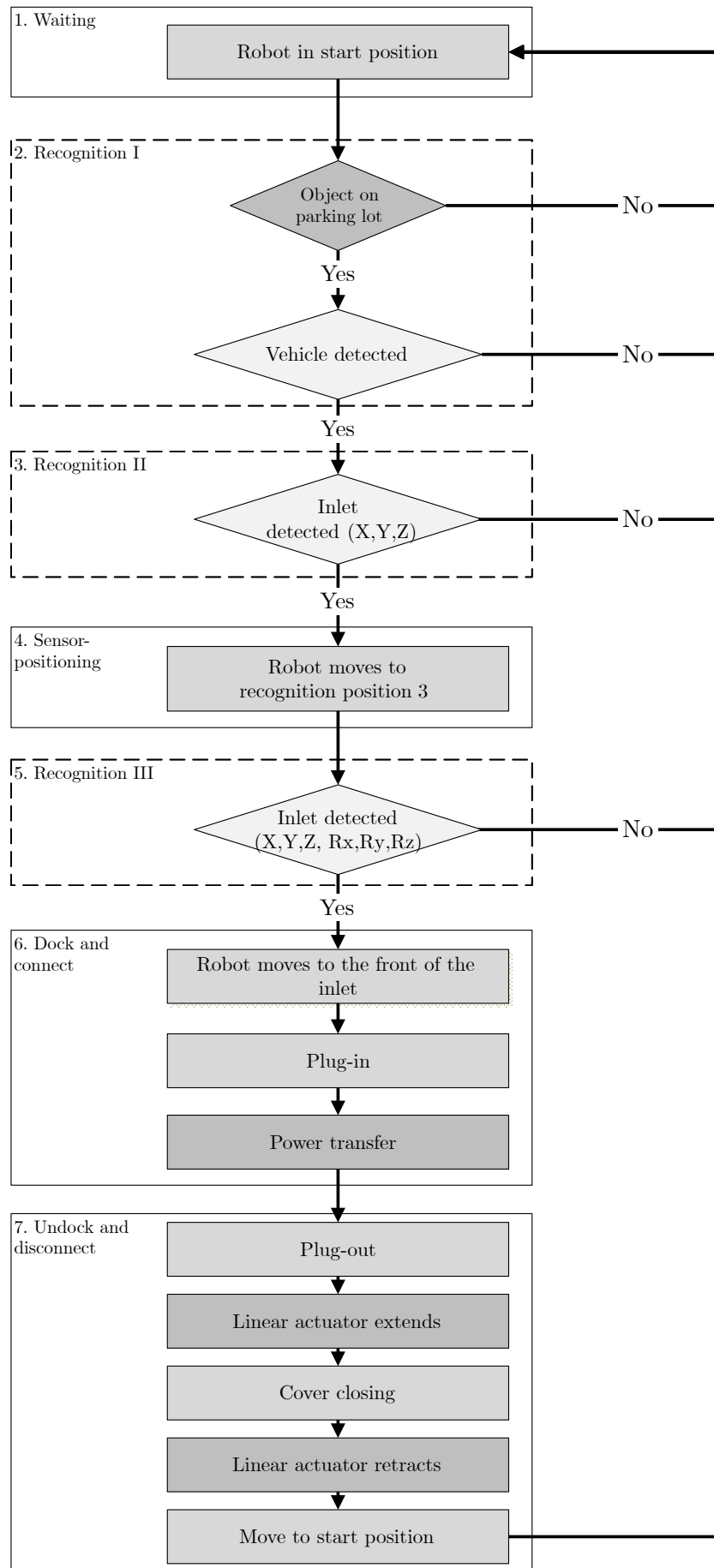


Figure 3.33.: Steps of the automated charging process.

is done manually, by the car itself or automatically by pre-defined robot movements. Different vehicle types have dissimilar lid kinematics. Therefore, the closing process requires different robot-arm movements for successful lid closing and avoidance of collisions with vehicle components. In the case of the exemplary test vehicle, a linear actuator at the robot head extends and retracts before and after the charging lid closing operation. After the charging lid is closed, the robot arm moves to the start position and waits for the next charging task.

3.7. Object detection

The sensor evaluation results lead to a camera-based inlet and vehicle detection system. This section deals with the 2D-camera and shape-based 3D-matching procedures for the objects position determination.

3.7.1. Vehicle detection

The prototype charging process starts by checking the charging lot occupancy with Camera 1 and 2. The prototype activates charging inlet position detection after recognized and classified the EV type. But also without knowing the EV type inlet detecting, robot guiding and cable are possible. Nevertheless, vehicle position information supports the ACCS robustness, exemplary, for evaluating the determined charging inlet position of Camera 3. EV classification is done by vehicle-specific distinctive contours and structures and shape-based 3D-matching. Figure 3.34 shows the rear right fender of the test vehicle BMW i3 as well as different views of the 3D-CAD model. The model acts as a template for the shape-based 3D-matching process in HALCON, [MVT17d]. A match provides information about the vehicle type and the vehicle position. No vehicle adaptations, e.g. transmitter, RFID, or sensors, are necessary in this case.

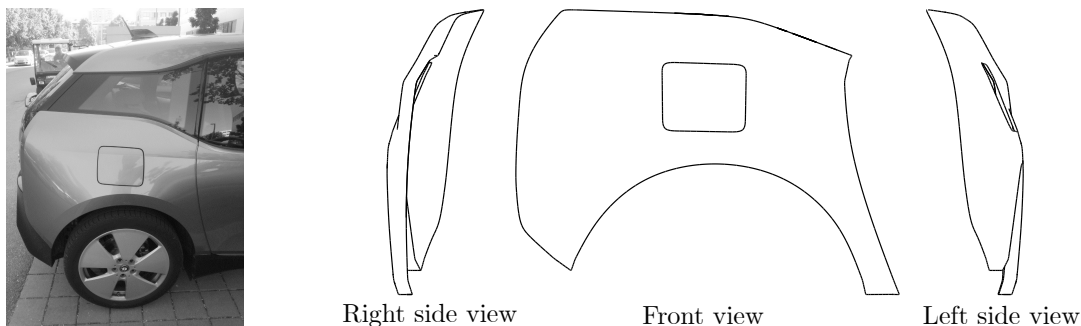


Figure 3.34.: Left: Rear, right wheel fender of a BMW i3. Right: Different views of the fender 3D-CAD model for shape-based 3D-matching.

3.7.2. Inlet detection

Successful and good matching results require a suitable 3D-CAD model for the shape-based 3D-matching model generation. One challenge is the development of an universal interoperable

3D-shape-model for the CCS Type 2 standard. The geometric shape of the inlet is standardized by IEC 62196-3:2014, [COM14a]. The standard defines the parts Type 2 connector (figure 3.35, left, position 1), DC connector (figure 3.35, left, position 2) and socket frame (figure 3.35, left, position 3) within the market border (figure 3.35, left, position 4). The universal matching-model considers the area inside the border. Image processing results are driven by striking events in an image. Matching processes are based on contour detection (edges) in an image. Object edges can be captured by the contours. The stronger contours appear and are pronounced in an image, the better they can be captured. Thus it is important to select and define suitable shapes for the 3D-CAD-model, on the one hand, to ensure the inlet detection, on the other hand, to support good 3D-matching results.

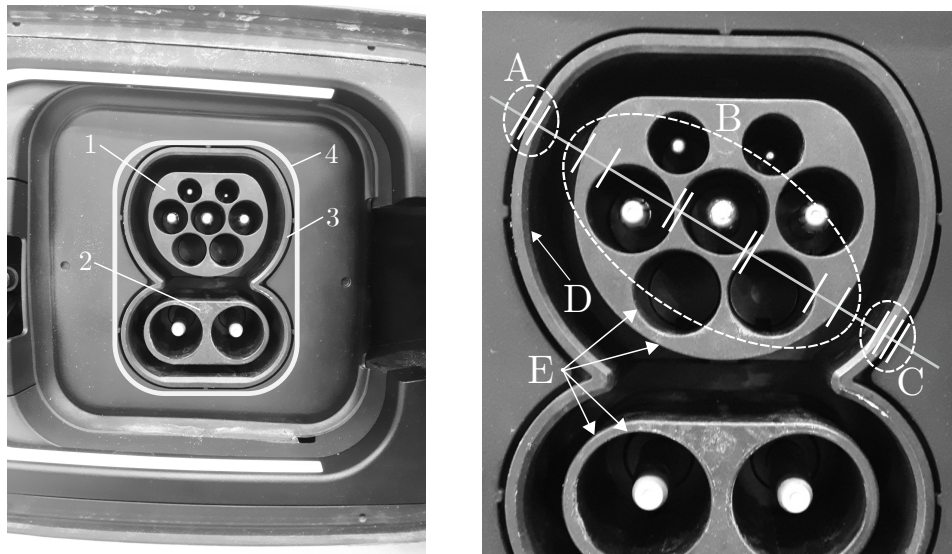


Figure 3.35.: Left: Picture of a test vehicle's CCS Type 2 inlet. Right: Example of detected edges (orthogonal lines in relation to the examination line) by using grey value curve analyses.

Edges in an image can be described as those places where the intensity of the light is limited to a small space or changed greatly along a clear direction. The stronger the intensity changes, the stronger is the reference to an edge at the corresponding position. The strength of the change in relation to the distance is nothing more than the first derivation. This is an important approach for the determination of edges, [BB15] and [SR14].

Before creating the matching model, an investigation of relevant and striking inlet edges and contours is beneficial and results in better matching results. Figure 3.35, right, shows detected edges along a diagonal line through the standard inlet by using the pixels of a greyscale camera image. The greyscale image with a colour depth T of 8 Bit/pixel possesses 256 values from 0 to 255. 0 defines the lowest grey value (minimum brightness, black), 255 the highest grey value (maximum brightness, white), [BB15].

The grey value function and its first derivation of the diagonal line (figure 3.35, right) with a length of 875 pixels and a width of 2 pixels is shown in figure 3.36. Both functions indicate the quality of the inlet edge detection, and it is possible to develop a suitable matching

model proposal on the basis of the edge detection results. However, different light and shadow conditions cannot be estimated completely. By a defined grey value derivation amplitude of ± 20 along the line, fifteen edges (figure, 3.35, right) were found in the example. At region B and C (figure 3.35, right), all edges along the defined line of the connector Type 2 region and the outer socket frame were found. At region A (figure 3.35, right), the defined greyscale gradient was not reached, and the fourth edge was not detected (figure 3.36, right). Reducing the gradient amplitude of ± 5 would detect the missing edge, but with the disadvantage that other unwanted edges or fragments would also be recognized. Only striking differences of grey values lead to good results. Light and shadow can have a significant influence on the image. Edges can disappear or be caused by shadows.

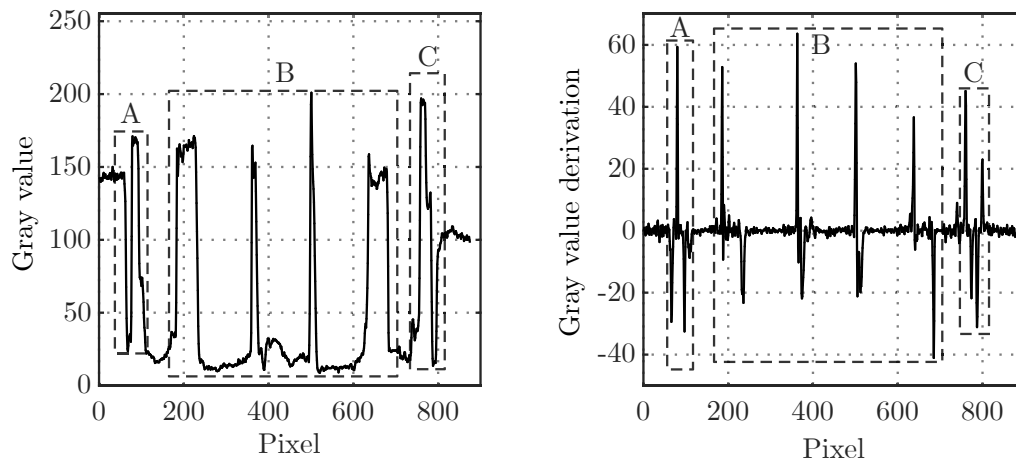


Figure 3.36.: Left: Gray value function applied on a pixel examination line. Right: First derivation of the gray value function.

Besides difficult light conditions, sloped or rounded geometric inlet surfaces complicate edge detection, due to different camera angles that distort or blur edges. Besides, light reflections, e.g. of sloped surfaces or inlet shape deviations from the standard, complicate the detection process and degrade matching results. The shape tolerances for the socket frame based on the standard are ± 0.1 mm at the 1.1 mm \times 45° bevel (figure 3.35, right, D) and ± 0.1 mm for the 0.6 mm radius at the CCS Type 2- and CCS DC-parts (figure 3.35, right, E), [COM14a].

Shapes with minimum contour deviations are represented at the 3D-CAD-model to reduce edge detection and light problems. The model was created by using the CCS Type 2 and CCS DC part (figure 3.35 1, 2 and 3). The standard CAD drawings determine the inlet shape geometry dimensions, [COM14a].

The inlet front surface CAD-model has been converted to a 3D STL file-format for further processing by use of the vision software HALCON [MVT17b]. Figure 3.37, left, shows the 3D-CAD-model with the defined reference coordinate system R_c . Position and orientation of the inlet in the captured camera image are related to R_c . An exemplary positive matching result and the inlet pose during tests is displayed in figure 3.37, right, M and $\{I\}$. $\{I\}$ is characterized by translational and rotational information in relation to the camera coordinate system of Camera 3.

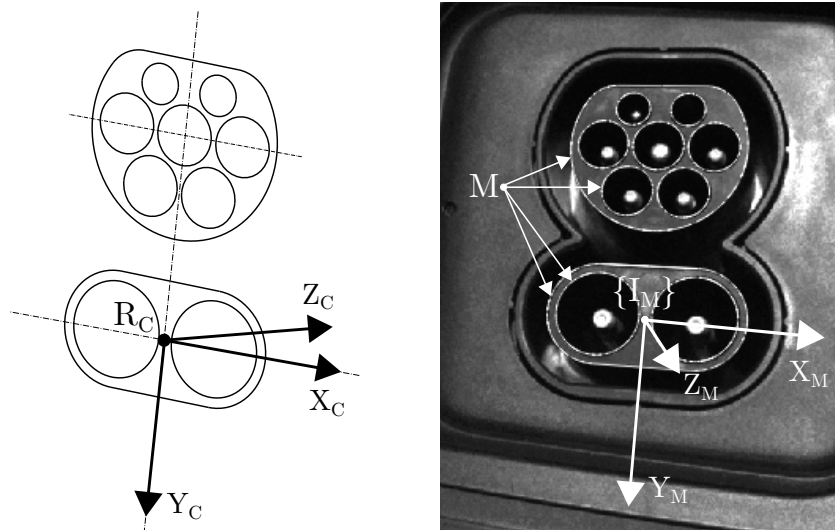


Figure 3.37.: Left: CAD-model as template for shape-based 3D-matching. Right: Matching result of an image from the robot-head mono camera.

Figures 3.38 and 3.39 show examples of inlet edge detection conditions due to shadows, dark light or reflections, with two different vehicles types. In comparison to the clearly visible contours in figure 3.38, right, the inlet of the other vehicle (figure 3.38, left) is mounted deeper in the car body, which results in shadows. Due to the low contrast difference, it is challenging to detect edges (figure 3.38, left, position 1 and 2). At position 2 edges are hardly visible any more.

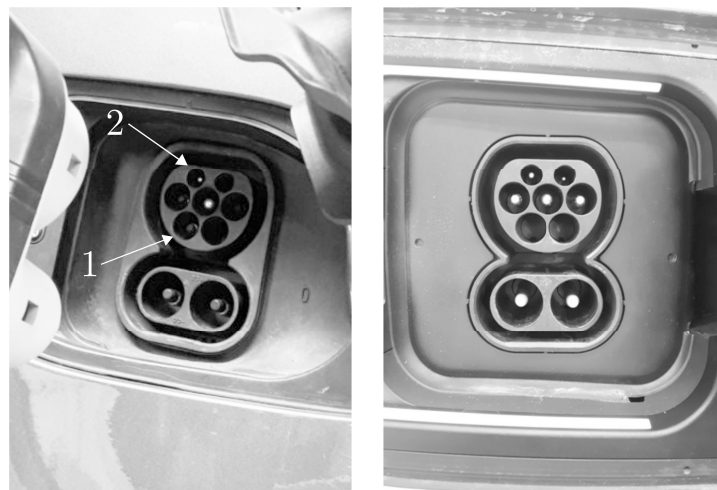


Figure 3.38.: Left: Example for shadow on the charging inlet. Right: Example of uniform light conditions that leads to a good image contrast.

Figure 3.39, left, shows an inlet image during the process *Recognition III* in case of dark environmental light conditions. The image does not fulfil the defined matching process parameter limits for a functional and robust inlet pose result. For better results, light support is served by LEDs. Figure 3.39, right, shows the scene by light support of the robot head LED. The

visibility of the inlets improves significantly. However, light reflections on surfaces and edges (position 1 and 2) can occur and worsen the matching outcomes.



Figure 3.39.: Examples of inlet camera images without and with LED light support.

3.8. Robot control

Figure 3.40 shows the defined coordinate systems (frames) at the charging station prototype, the robot head and an exemplary charging inlet. The robot base frame $\{B\}$ defines the stationary reference. The Z -axis of Camera 1 and Camera 2 define the cameras field of view direction. $\{B\}$, $\{C1\}$ and $\{C2\}$ are fixed frames, that means that they are not changing their position or orientation. Figure 3.40, right, shows the defined frames at the robot head. $\{T\}$ is located at the robot head mounting plate reference point, also called *Tool Centre Point* (TCP). The connector frame $\{C\}$ is defined at the centre of the CCS Type 2 connector DC component. Z -

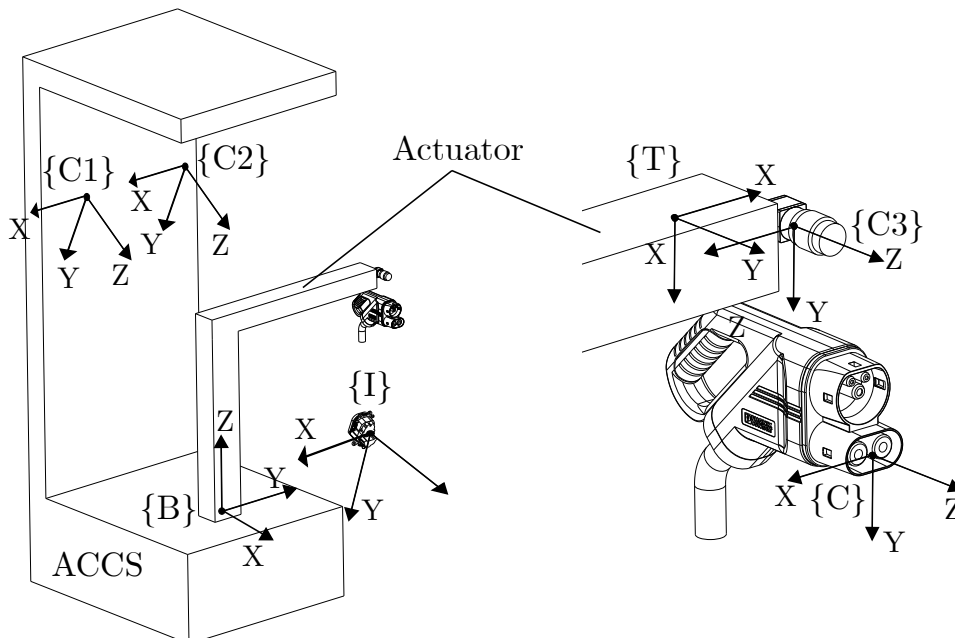


Figure 3.40.: Left: Coordinate systems (frames) of robot base $\{B\}$, Camera 1 $\{C1\}$ and 2 $\{C2\}$ and inlet $\{I\}$. Right: Robot head detail view with the frame representation of robot tool $\{T\}$, Camera 3 $\{C3\}$ and connector $\{C\}$.

axis of $\{C\}$ and $\{C3\}$ show in plug-in direction. $\{T\}$ is transferred to $\{C\}$, because they don't change their poses towards each other. This has the advantage that all robot control commands refer directly to $\{C\}$. The exemplary inlet frame $\{I\}$ varies at each vehicle parking position. For the coordinate system orientation definition, it is suitable that the inlet frame orientation aligns to the camera's frame orientation. An accurate docking positioning of the connector in front of the inlet requires an exact match of the frame $\{C\}$ and $\{I\}$. Table 3.18 describes the constant translation and rotation transformations between the prototype component frames and their references in RPY rotation convention, [WHB19c].

Table 3.18.: Constant translational and rotational transformations between robot system component frames.

	Reference	Translation			Rotation			Rotation convention
		X [m]	Y [m]	Z [m]	R_x [°]	R_y [°]	R_z [°]	
$\{C1\}$	$\{B\}$	0.41173	0.75323	0.98578	151.75	300.06	295.38	RPY
$\{C2\}$	$\{B\}$	-0.43321	0.75504	0.91142	189.96	296.68	261.99	RPY
$\{C3\}$	$\{C\}$	0.06432	0.14031	0.14416	0.43	0.54	0.70	RPY
$\{C\}$	$\{T\}$	0.0	207.5	126.49	0	-127.19	-127.19	RPY

Figure 3.41 shows the ACCS prototype control processes. The sectional performed robot movements are responsible for the charging connector frame pose $\{C\}$. Charging connector path control is managed by a *point-to-point* steering concept with a cartesian path control in combination with linear interpolation, [Wüs04], based on a modified MATLAB, [DMR⁺16] script code model from [Fer16]. An ARDUINO board, [ARD19] controls LEDs and a linear actuator performs additional tasks, e.g. charging lid closing. The ACCS prototype control processes as well as control data exchange are explained in detail in the section *Data processing*.

For emergency stops in case of problems or too high actuation forces, e.g. because of a collision or a misalignment, the robot force limit is defined with 250 Newtons. The robot path control considers the cable handling behaviour by preventing a sagging cable that could grind on the ground or a stretched cable that leads to high tensile forces on the robot head. Figure 3.42 shows examples of robot path computation based on three different inlet positions (figure 3.42, $\{5a\}$, $\{5b\}$ and $\{5c\}$), whereby the robot path during docking and plug-in operation are represented. It starts with the waiting position (figure 3.42, position 1). Position 2 is implemented because of cable-handling issues. Position 3 is calculated as a function of the obtained charging inlet pose from Camera 1 and Camera 2. The positions 4 to 6 are calculated by the inlet pose information from Camera 3. At step 5, the connector is fully aligned with the CCS Type 2 inlet's X -, Y - and Z -axis. Connector insertion happens between step 5 and 6. Exemplary charging inlet frames with reference to the robot base are shown in table 3.19. For plug-out and undocking, positions 4 to 6 need to run through in reverse order. The path for closing the charging lid by a linear actuator is specially developed for the test vehicle and is not described further here, [WHB19c].

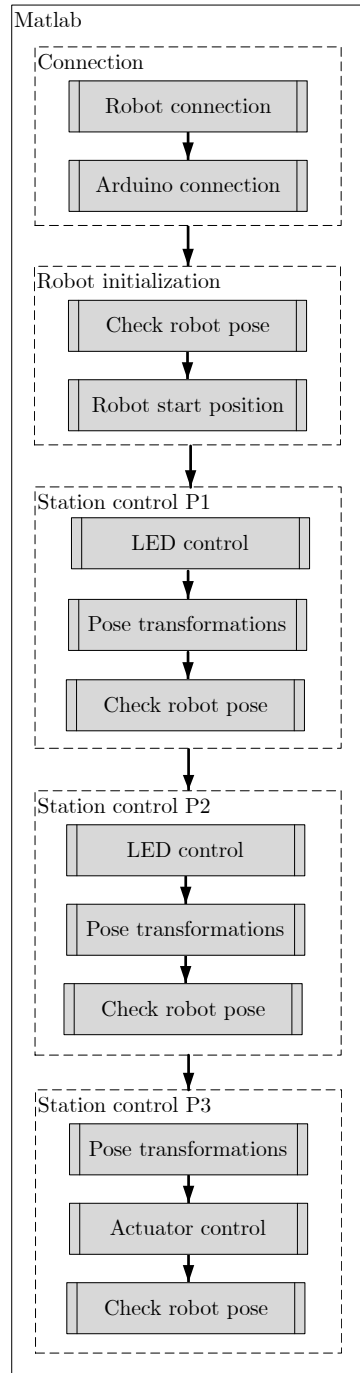


Figure 3.41.: ACCS prototype control processes in MATLAB.

Table 3.19.: Exemplary charging inlet positions with reference to the robot base $\{B\}$.

	Reference	Translation			Rotation			Rotation formulation
		X [mm]	Y [mm]	Z [mm]	R_x [°]	R_y [°]	R_z [°]	
$\{5a\}$	$\{B\}$	891.28	-425.74	-550.00	252	0.4	267	RPY
$\{5b\}$	$\{B\}$	805.87	85.91	-550.00	252	0.4	267	RPY
$\{5c\}$	$\{B\}$	622.62	782.53	-400.00	252	0.4	267	RPY

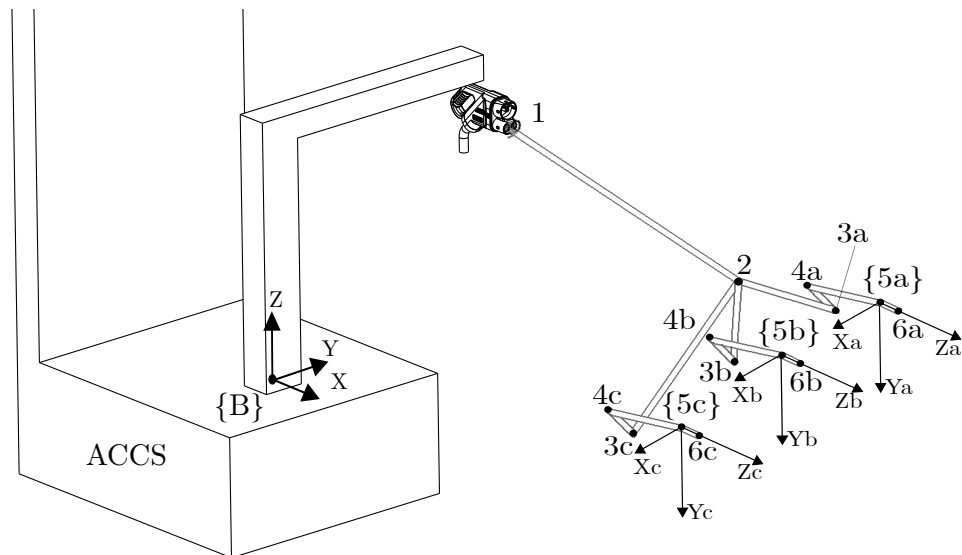


Figure 3.42.: Exemplary robot path during cable docking and plug-in for three various charging inlet positions, [WHB19c, p.10].

3.9. Data processing

Figure 3.43 shows the software environments that communicate with each other and controls the prototype data processing. The tasks and script-codes can be divided into the main, simultaneously running applications object recognition in HALCON, pose transformation and robot control in MATLAB, robot monitoring in Polyscope as well as LED and actuator control with Arduino. Data communication starts with the vehicle that enters the charging lot and ends with the robot waiting position.

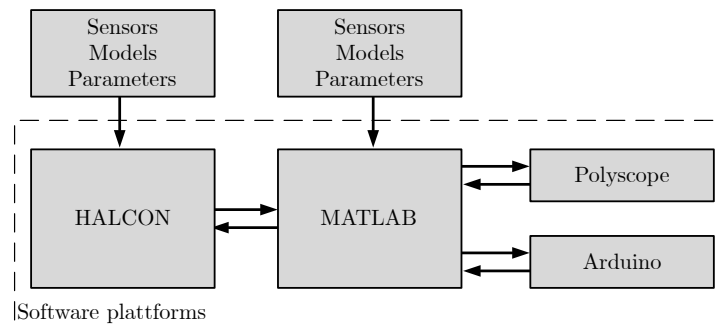


Figure 3.43.: Data processing architecture overview.

Figures 3.44 and 3.45 show the data communication process in detail. The data processing for the vehicle and inlet pose recognition is managed by the script code in HALCON (figure 3.44). The first process contains data initialization. This includes the import of camera parameters and static world coordinate frames of the charging station components, e.g. robot base and cameras. The further steps include the processes *Recognition I* (vehicle detection), *Recognition III* (simple inlet pose estimation) and *Recognition III* (extended inlet pose estimation). One input for the processes are the 3D-shape model (fender, inlet_V1 and inlet_V2) and the captured

images of 3 cameras. After positive matches of the objects of interest, pose transformations are done, and data are sent for further data processing to the MATLAB script code. This data consists of the translational and rotational parts ($T_x, T_y, T_z, R_x, R_y, R_z$). The process in HALCON starts from the beginning after the MATLAB process and completes the last step *Check robot pose and robot start position* (figure 3.45).

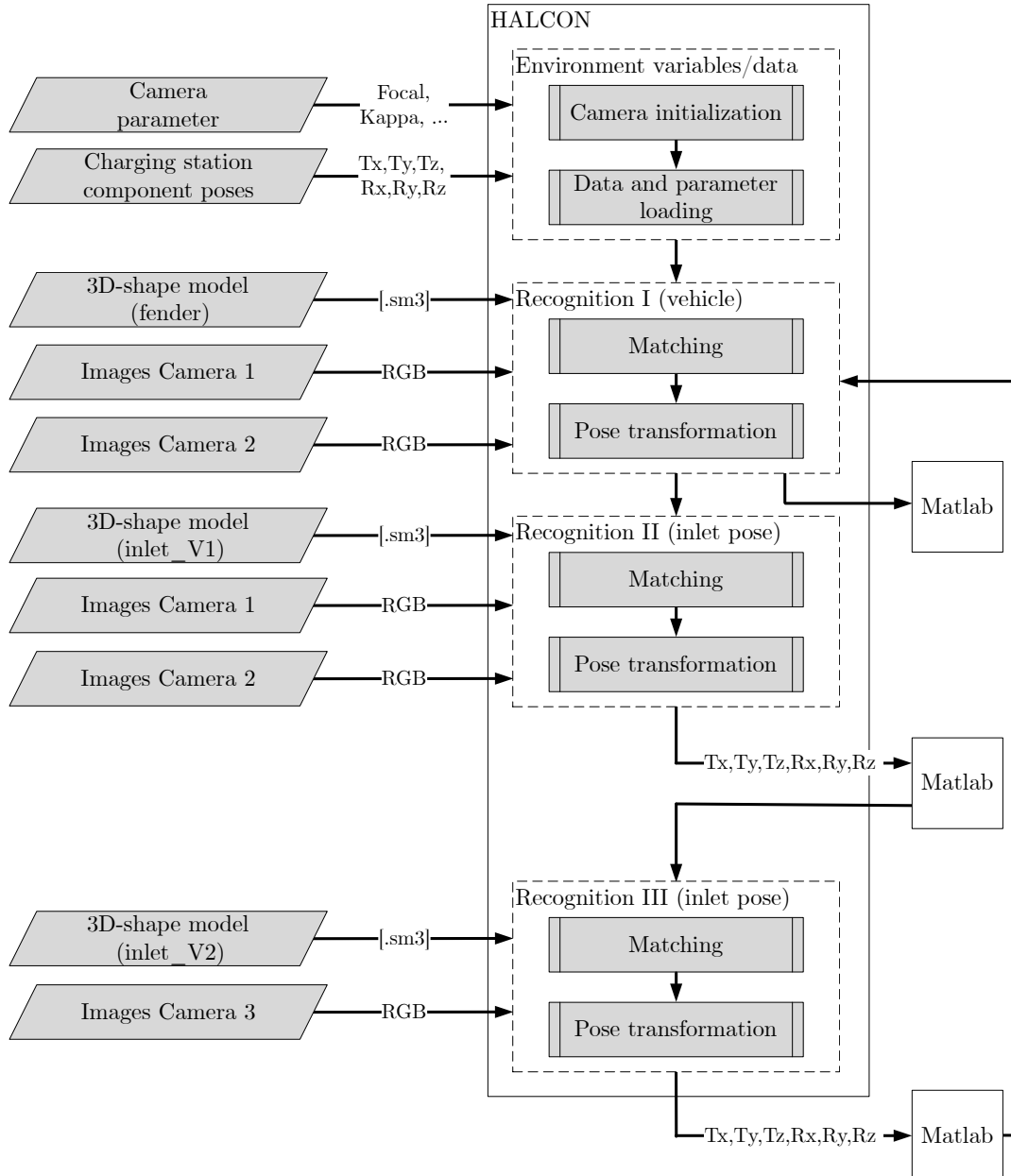


Figure 3.44.: Data processing in the HALCON script code.

The MATLAB script code manages the functions of the charging station prototype components. It starts with the creation of the robot and *ARDUINO* board connection by *Transmission Control Protocol* (TCP) and *Universal Serial Bus* (USB). After checked and loaded robot pose and inlet type parameters, the main processes *Station control P1*, *Station control P2* and *Station Control P3* are performed one after the other by robot control and *ARDUINO*

board. Parallel, the script code on the selected research robot UR-10, [ROB17] waits for new TCP targets and monitors the robot forces and moments during movements. In case of problems, the robot stops at defined maximal forces, velocities, accelerations and unwanted joint angles. In case of successful 3D-matching and after pose transformations, the MATLAB subprocesses *Station control P1* and *Station control P2* get the pose from HALCON and further transformations are done for the robot guidance (e.g. intermediate steps for the robot head path to the inlet front face). If it is not possible to get suitable inlet pose results, *Station con-*

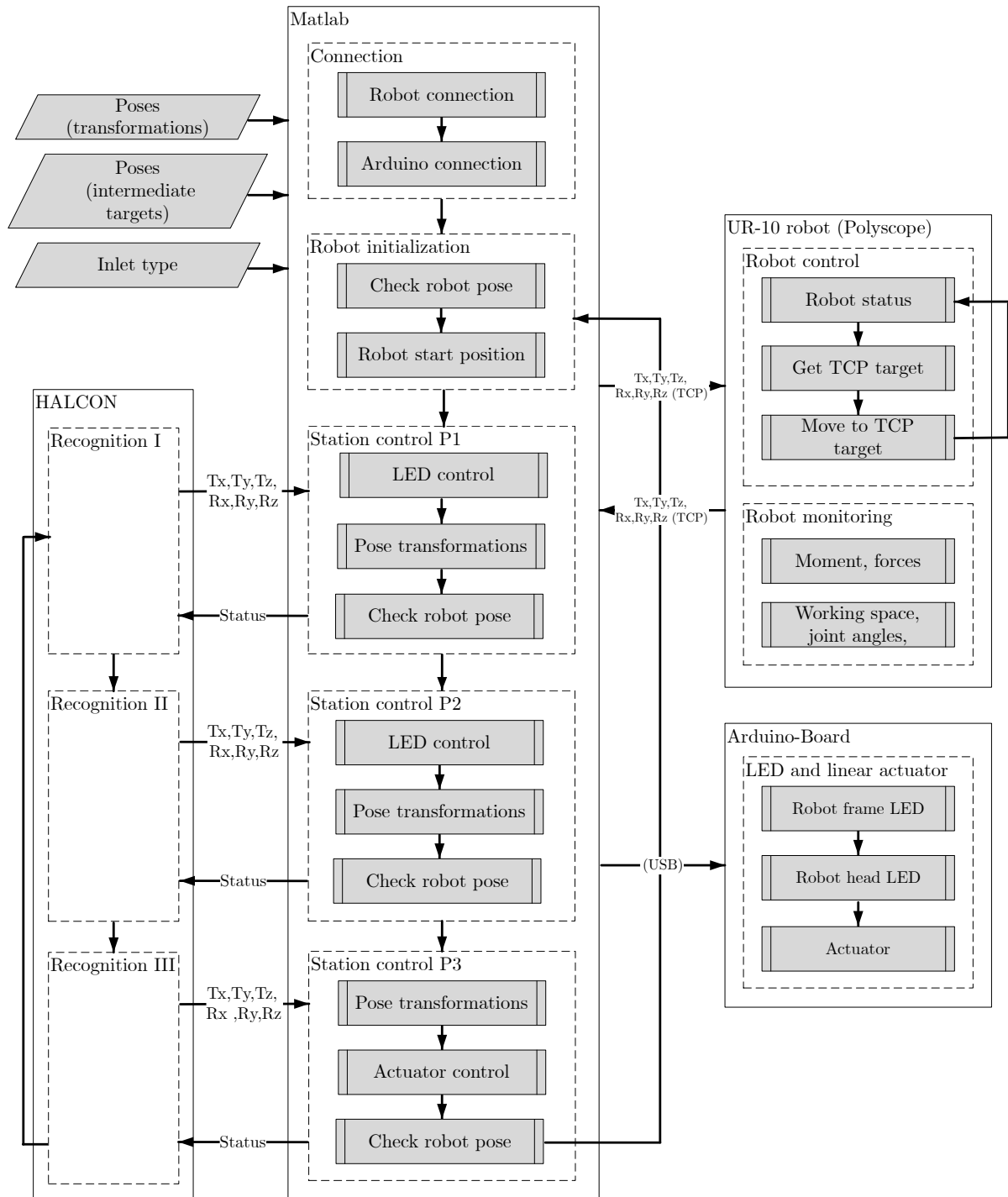


Figure 3.45.: Data processing in the MATLAB script code.

trol P1 or *Station control P2* switch on the LEDs by sending commands to the *ARDUINO* board. Besides LED control, the *ARDUINO* board controls the actuator for charging lid closing. *Station control P1* guides the robot head to the pose. *Recognition II* starts after successfully reached position. Therefore the MATLAB script checks the robot pose by TCP communication with the UR-10 script code that is based on the programming language PYTHON, [VR90]. *Station control P2* is responsible for cable plug-in and requires the precise inlet pose of the detection process *Recognition III*. After charging, *Station control P3* performs the TCP frame transformations for charging lid closing and robot waiting position.

3.10. Connector system

The ACCS charging connector insertion process indicates a challenge. In the course of the plug-in process, position deviations in three-dimensional space have to be expected due to tolerances of ACCS sensor results and actuator movements. Furthermore, manufacturing tolerances of plug and socket, as well as the coefficient of friction between both parts, influenced by material properties, but also by environmental conditions such as temperature, dirt, humidity, affects the plug-in procedure. In the case of a manual connector insertion, the human operator compensates these influencing variables and tolerances by hand with corresponding macro and micro-movements. For automated connector plugging, the sensor and robot systems have to be able to consider and compensate these influencing parameter accordingly.

For reducing ACCS sensor and robot requirements, a solution was developed to facilitate the connector insertion process and prevent connector tilting. Due to the new solution and the smart approach introduced, a patent application has been filed, [WHB19b]. The approach concerns the CCS Type 2 face shape to support automated plug docking, insertion and removal. This is achieved by a defined chamfering of certain connector surface elements. Figure 3.46 shows the CCS Type 2 connector face approach. However, the concept is not limited to this plug type, but can be transferred to other standardized vehicle couplings, e.g. CCS Type 1 (SAE-J1772 and IEC-62196-3), Type 1 (SAE J1772 and IEC 62196-2) and Type 2 (IEC 62196-2). Standard charging inlets are not impacted, and the solution does not require vehicle adaptations or modifications. In this context, the solution fulfils ACCS requirements.

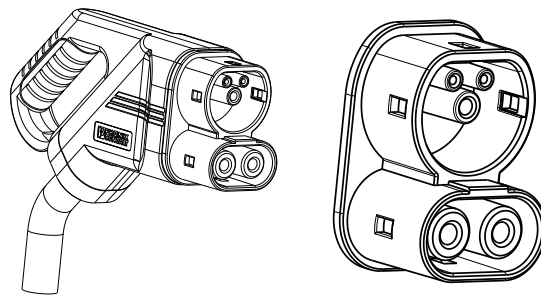


Figure 3.46.: Left: CCS Type 2 EV coupling (IEC 62196-3). Right: Replaceable face of the CCS Type 2 connector.

Figure 3.47 shows the concept's underlying geometric changes. Position 1 and 2 indicate the affected areas of the outer and inner contour of the connector face frame. A similar design of all available e-mobility plugs enables the concept to be transferred to other standardized vehicle couplings.

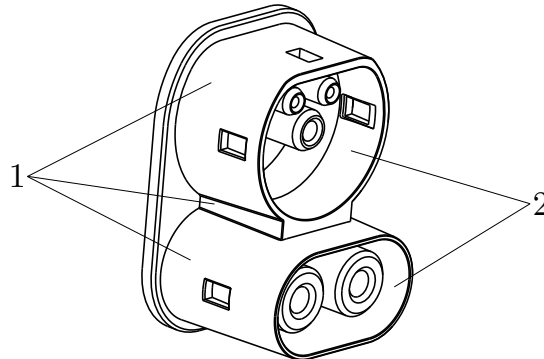


Figure 3.47.: Affected CCS Type 2 connector face areas by the modifications for easier cable plugging.

Figure 3.48 shows front and cross-sectional CAD-model views of the CCS Type 2 connector face. The circumferential outer contour of the face frame is formed in a pointed converging shape, and the inner contour is formed in a diverging shape in plugging direction. The shapes can be conical, parabolic or similar. Exemplary, the conical shape is defined with the inclination angles A , B , X and Y with value ranges between 1.5° and 4° . The dimensions $A1$ and $B1$ are less than 45 mm and for $X1$ and $Y1$ less than 30 mm. The geometric design shown as an example on the CCS Type 2 is also valid for other connector types and can be transferred to them.

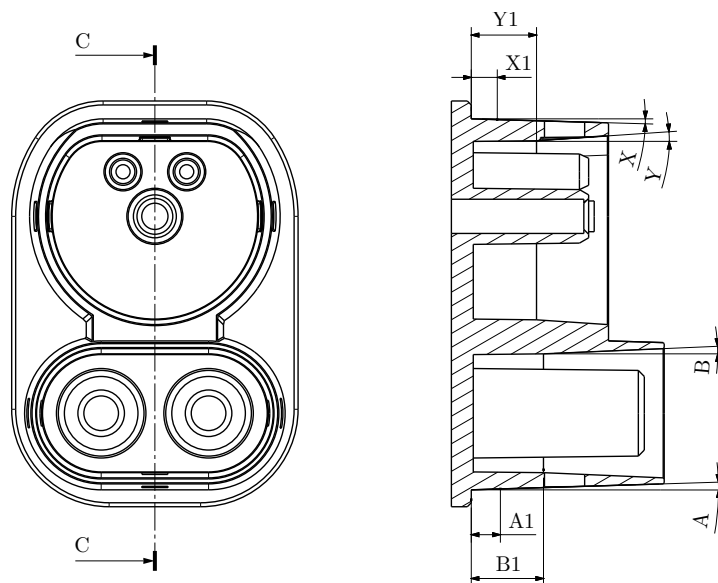


Figure 3.48.: Left: Front view of the CCS Type 2 face CAD-model. Right: Cross-sectional view (C-C) of the CCS Type 2 face CAD-model.

Table 3.20 shows the ACCS requirements with connector modifications. The requirements determination corresponds to the inlet position detection accuracy demands development in chapter 3.3.4 (figure 3.14, 3.15 and 3.16). The approach decreases the X - and Y -direction accuracy by 0.39 and 0.7 mm. The Z -direction accuracy demands are not affected since the chamfering contour does not influence this connector geometry direction. The electrical connector pins define the maximal the angle misalignment during insertion. In this context, the X -, Y - and Z -angle accuracy requirements correspond to the requirements without connector modifications. Besides better connector docking conditions, the solution enables easier connector plugging by reduced forces. More clearance leads to less friction between connector and inlet surfaces.

Table 3.20.: ACCS CCS Type 2 inlet detection requirements without and with connector modifications.

ACCS requirement	Without connector modification	With connector modification	Difference
X -direction accuracy	0.54 mm	0.93 mm	0.39 mm
Y -direction accuracy	0.54 mm	1.24 mm	0.7 mm
Z -direction accuracy	0.64 mm	0.64 mm	0 mm
X -rotation accuracy	2.9°	2.9°	0°
Y -rotation accuracy	3.9°	3.9°	0°
Z -rotation accuracy	1.4°	1.4°	0°

3.11. Communication

Once the vehicle has reached its charging position, the charging process should start automatically. The ACCS prototype does not require any communication between vehicle and charging station to start the charging process, to feed the cable into the charging socket or to disconnect the cable. Instead, the detection of the vehicles charging inlet activates the automated charging process. However, for series production and marked-ready compatibility, the implementation of the entire communication scheme between vehicle and charging system, according to ISO 15118 is recommended. The draft standards of ISO-15118-1 , [INT19] and ISO-15118-8, [INT18b] take the communication between the *Electric Vehicle Communication Controller* (EVCC) and the *Supply Equipment Communication Controller* (SECC) of ACD systems into account. In the following, the ISO standard draft communication implementation is discussed by the comparison of the standard draft and ACCS prototype process steps.

Figure 3.49 and table 3.21 show the comparison of the ACD standard draft- and ACCS prototype process steps. To check the vehicle and charging station compatibility, parameters are exchanged. Whether charging station and vehicle are compatible or not, is tested in the processes *Association* and *High Level Communication* (HLC), [INT19]. The ACCS prototype plugging process is carried out without a vehicle data exchange. According to the standard draft, communication between the charging station and the vehicle takes place via wireless communication. If an ACCS communicate via this standard, parameters can be proposed that support the charging procedure. Additional robustness, safety and redundancy of the system can be created.

3. Prototype development

Concerning the draft standard process steps *Fine Positioning, Parking, Plugging and Pairing*, ACD pairing should be started from the EV as soon as the parking position is reached. If the parking position is not reached, the driver is prompted to move to the (optimum) position. Pairing is successful when the vehicle has reached the correct parking position, [INT19]. For vehicle position detection, the standard and requirement proposals of WPT-charging, [INT18b] can be adopted to ACCS, e.g. the determination of the vehicle position by means of directional antennas. For the ACCS prototype, *Pairing* is implemented by the vehicle recognition step using a camera-based vision system.

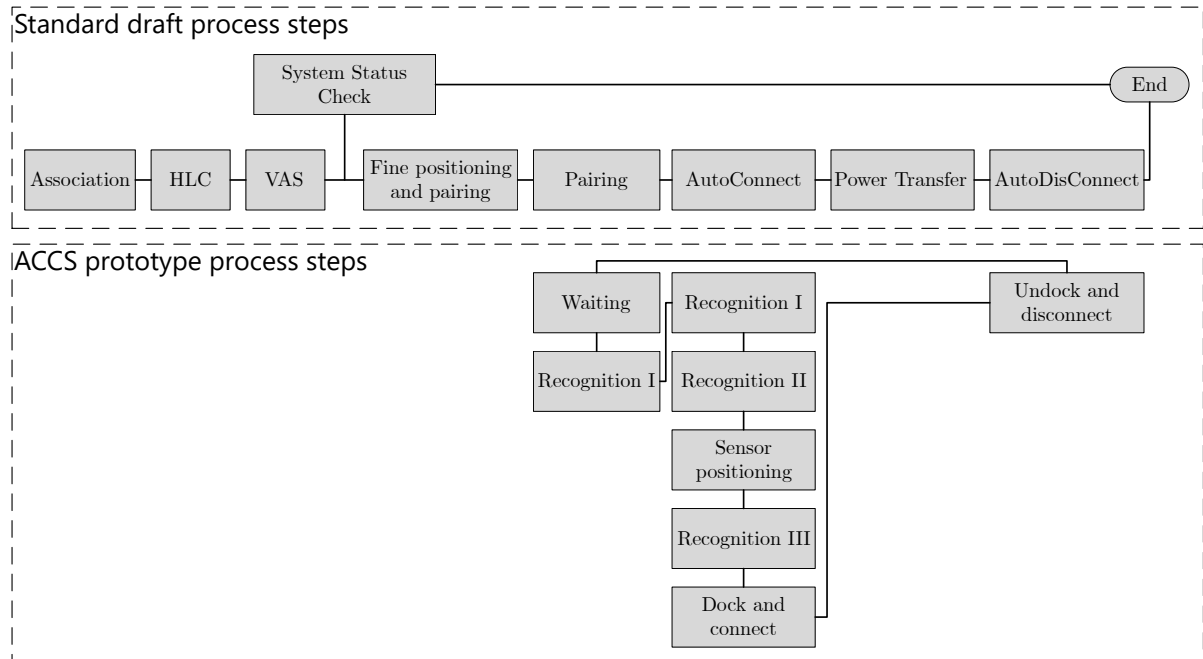


Figure 3.49.: Process steps comparison of the ACCS prototype and the ACD communication sequence draft of the ISO 15118, [INT18a] standard.

Table 3.21.: Process steps of the ACCS prototype charging process in comparison to ISO 15118, example sequence illustrating ACD energy transfer procedure.

Process	ACCS prototype	ISO 15118 (draft)
1	-	Association
2	-	High level communication (HLC)
3	-	Value added services (VAS)
4	Waiting	Fine positioning and pairing
5	<i>Recognition I</i> : Vehicle recognition	Pairing
6	<i>Recognition II</i> : Inlet detection (X, Y, Z)	AutoConnect
7	Sensor positioning	AutoConnect
8	<i>Recognition III</i> : Inlet detection (X, Y, Z, R_x, R_y, R_z)	AutoConnect
9	Dock and connect	AutoConnect
10	-	Power Transfer
11	Undock and disconnect	AutoDisconnect

EVCC and SECC exchange messages and data until the connection process *AutoConnect* is complete. The *Power Transfer* starts subsequently, [INT19]. The ACCS prototype does not require vehicle data, such as the charging lot position or analogue information for localization. Concerning functional safety, data of unexpected stops or incorrect positioning of the ACCS robot are required to stop cable docking, insertion and undocking. These failures and conditions are defined in [INT19] and can be adopted to ACCS with implemented wireless-communication.

For *AutoDisconnect*, the EV request the EV supply equipment to disconnect the ACD and bring it back to its home position. The *System Status Check* of [INT19] is performed throughout the whole energy transfer process and supports the supervision of the ACD in all unexpected situations, which may occur during energy transfer. As examples, unexpected events, e.g. the robot changes its position due to an external force or to vehicle moves, misalignments and vandalism as well as damages or malfunctions during the charging process can occur, which must be checked by the system during the entire charging process. The prototype performs the disconnection after a defined time. A system status check is not implemented. An ACCS series application should implement the ISO communication draft functions to ensure safety and compatibility. The ISO standard drafts for ACD systems can be applied and adapted to ACCS. For charging start, the following conditions must be met:

- Humans and vehicles must not be injured/damaged.
- The functionality of the components (e.g. charging lid mechanism) must be given.
- The charging station must not be damaged, and its functionality must be given.
- The charging lot is not occupied.

If one of these conditions does not apply, the charging process can not start. This corresponds to the requirements of the standard proposals, [INT19].

3.12. ACCS prototype

Figure 3.50 shows CAD-models of the ACCS prototype and prototype robot head tool. The station consists of robot (1), frame (2), cameras (3, 4), robot control box (5), (LED) (6, 7), actuator (8), CCS Type 2 connector (9), two adapters (10, 11), rubber damper (13) and a in the frame-integrated *ARDUINO UNO*, [ARD19] microcontroller board (12). As a basis for the prototype serves the collaborative robot UR10-CB3, [ROB17]. The prototype frame (2) has compact dimensions of 960 mm length, 820 mm width and 2140 mm height and is made of aluminium shape modules, [ITE20]. The 2D-cameras (3 and 4) are responsible for the identification of vehicles and inlet pose detection. Two LEDs (6) on the frame (2) and the LED (7) on the robot head tool are supporting the vision system in case of insufficient light conditions. The robot head is designed to fulfil the requirements of limited space. An additionally integrated actuator (8) enable closing of charging lids. Two adapters, whereas one is made of aluminium (11), the other one (10) is made of 3D-printed plastics to reduce weight, improving robot control and cable handling, are integrated and hold the parts in a

compact system that is connected with the robot. In the following, the prototype components are described in detail.

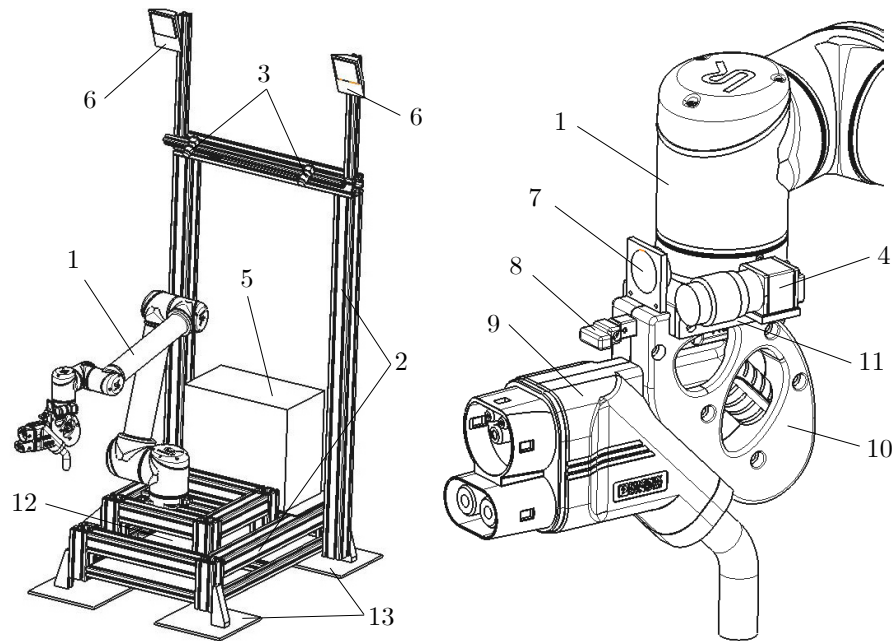


Figure 3.50.: Left: CAD-model of the charging station prototype. Right: CAD-model of the robot head tool with CCS Type 2 connector, camera, LED, actuator and adapters.

Robot system

Figure 3.51 shows a picture and the specifications of the collaborative research robot UNIVERSAL ROBOTS UR10-CB3. The robot meets the ACCS prototype actuator requirements developed in chapter 3.3.5 (table 3.10). It serves as the basis for the ACCS prototype robotic system and is responsible for charging cable handling. The serial 6-axes kinematics system has a range of 1.3 m, and a weight of 28.9 kg. 10 kg payload, position repeatability of ± 0.1 mm and 250 Newton maximal force fulfils the CCS Type 2 cable handling and plugging requirements. The X -, Y - and Z -translational direction stiffness K_x , K_y and K_z were determined by [RPBL18] by static forces and meets the connector plugging compliance requirements. The UR10-CB3 belongs to the new generation of collaborating robots with relatively simple handling, and the safety features allow people to be in a robot's working area. The robot enables a safe stop, e.g. when hitting an object or crossing safety limits such as force, impulses or speeds. Forces and impulses are measured via the energy consumption of the joint propulsion motors. Force torque control enables contact detection as a programmable resilience, [ROB17]. The robot control system software language is PYTHON, [VR90]. Communication interfaces such as TCP/IP 100 Mbit: IEEE 802.3u, 100BASE-TX Ethernet socket, MODBUS TCP and EtherNet/IP offer external robot control. An operating panel enables offline robot controlling and programming.



Specification	
Max. range	1300 mm
Max. payload	10 kg
Positioning repeatability	0.1 mm
Axes (DOFs)	6
Weight	28.9 kg
Max. velocity	1 m/s
Joint ranges	$\pm 360^\circ$
Max. speed	Base and shoulder: $120^\circ/\text{s}$, other joints: $180^\circ/\text{s}$
Temperature working range	$0\text{-}50^\circ\text{C}$
X-direction stiffness K_x	2.88 N/mm
Y-direction stiffness K_y	3.33 N/mm
Z-direction stiffness K_z	2.80 N/mm

Figure 3.51.: The collaborative 6-axes robot Universal Robot UR10-CB3 with technical specifications, [ROB17] and [RPBL18].

Figure 3.52, left, shows the 2D-camera UI-5240CP-C-HQ Rev.2 from IDS. The *Complementary Metal-Oxide Semiconductor* (CMOS) colour sensor has a resolution of 1280 to 1024 pixels (1.31 megapixels), [IDS19]. The camera type is used for the vehicle- as well as inlet position detection. Two cameras are mounted on the ACCS prototype frame, with the lens shown in figure 3.52, middle. One camera is fixed on the robot head tool. The lens for the robot head camera is shown in figure 3.52, right. Lens fields of view are selected due to the determined 2D-camera specifications in chapter 3.4.4 for vehicle recognition and inlet position detection.



Figure 3.52.: Left: IDS 2D-Camera UI-5240CP-C-HQ Rev.2. Middle: Lens model LENSAGON C3M0616V2 1/1.8": 6 mm focal length, 60.1° horizontal and 46.6° vertical angle of view, [LEN19]. Right: Lens model TAMRON M118FM06 1/1.8": 6 mm focal length, 66.1° horizontal and 50.8° vertical angle of view, [TAM19].

In the case of dark light conditions, the inlet position detection is supported by 3 LEDs. Two 35 Watt LEDs (figure 3.53, left) with 2700 Lumen nominal luminous flux and 6000 Kelvin light temperature, [GOO20], serve to illuminate the inlet during the *Recognition II*. The 1.5 Watt GENESIS SMD5050 LED with 30 mm outer diameter, 148.5 Lumen nominal flux and 5800 up to 6800 Kelvin light temperature, [GEN20] is responsible for the object illumination

3. Prototype development

in the inlet position *Recognition III*. After 10 seconds of unsuccessful inlet position detection, the LEDs starts to illuminate the inlet.



Figure 3.53.: Left: 35 Watt LED from Goobay, [GOO20]. Right: GENESIS SMD5050 round LED, [GEN20].

Figure 3.54, left, shows the linear actuator ACTUONIX P16-100-22-12-P, which represents the ACCS prototype seventh axis. The actuator has 100 mm stroke length and maximal 50 Newton force, [ACT17]. The actuator was implemented in the ACCS prototype for testing the automated charging lid closing. The power supply for LEDs on and off switching as well as the actuator extending and retracting are controlled by the *ARDUINO UNO REV3* board (figure 3.54, right). The ARDUINO is a cost-efficient and straightforward microcontroller board. It offers 14 digital input and outputs, 6 analogue inputs and a USB connection, [ARD19].



Figure 3.54.: Left: Linear actuator ACTUONIX P16-100-22-12-P, [ACT17]. Right: ARDUINO UNO REV3 microcontroller board, [ARD19].

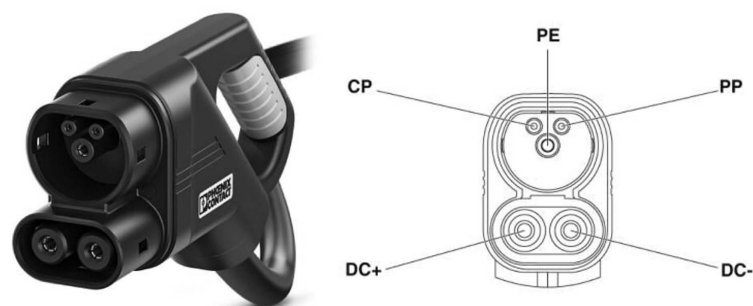


Figure 3.55.: CCS Type 2 EV-T2M4CC-DC200A charging cable from Phoenix Contact, [CON16a].

The used charging cable from Phoenix Contact complies with the IEC 62196-3 and ISO 15118 standards. It enables a charging capacity of up to 200 KW with 200 Ampere and 1000 Volt. The insertion and withdrawal forces are indicated as less than 100 N, [CON16a]. The ACCS prototype cable has a length of 5 meters, 32.1 mm outer diameter, 324 mm minimal bending radius and weights 11.85 kg. The exchangeable connector face shape has been adapted due to the ACCS cable connection concept represented in chapter 3.10.

3.13. Conclusion

This chapter dealt with the development of the ACCS prototype. The first part of the chapter elaborated ACCS requirements and defined charging use-cases, charging plug positions, as well as EV parking positions. ACCS requirements and manual charging process serve as a basis for the elaboration of the ACCS prototype tasks. The tasks consist of vehicle- and charging socket pre- and post-processing as well as charging cable handling. Developed functional demands as well as boundary conditions and -requirements, e.g. charging cable type or the avoidance of vehicle adaptations, are the basis for the subsequently performed ACCS system design.

The following section of this chapter dealt with the ACCS system design that consists of a functional concept and ground layout. The functional concept handles ACCS objects, process steps, as well as devices that are responsible for ACCS tasks. The ACCS prototype ground layout defines sensor- and actuator positions as well as component coordinate systems. The system design serves as a basis for the following development of the component requirements. Due to the inlet position detection and connector plugging, the most challenging requirements lie on ACCS sensors and actuators. Range requirements are elaborated by vehicle parking position accuracy tests and static methods. Essential prototype requirements are the capability of handling 6 DOFs as well as the accuracy of below 1 mm and 4 degrees.

In the subsequent section of this chapter, sensor systems are evaluated and selected as well as sensor specifications are defined. Regarding the ACCS prototype criteria, 2D-camera sensor achieved the best evaluation results. 2D-camera range and accuracy demands are reduced by a object recognition separation into the tasks vehicle classification, rough- as well as accurate inlet position detection. The inlet 3D-position detection approach includes the combination of 2D-cameras with shape-based 3D-matching algorithms and the CCS Type 2 inlet contour as a shape template.

The next part describes the development of the ACCS charging process, -robot control, -data processing, as well as a connector shape concept. The newly invented ACCS charging process sequence enables charging of different EVs with standard charging inlets. The ACCS prototype benefits from the introduced connector shape concept by reducing sensors-, mechanics- and kinematics requirements. The shape changes have little influence on the production costs of connector faces and are transferable to other EV charging standards. A vehicle-to-charging station communication is not implemented in the ACCS prototype. Charging infrastructure interoperability and customer comfort requires communication, e.g. for charging power control, payment and additional services. For the transferability of standardized communication

guidelines, the prototype charging process sequence is compared with the ISO 15118 ACD communication proposals, which cover the ACCS prototype communication requirements. In this way, ACD use cases, communication processes and data transfer can be assigned to ACCS. ACCS benefits from standards, e.g. the system status check, where all components are checked continuously during automated charging.

The last section of this chapter presents the ACCS prototype and -hardware components. The prototype contains a collaborative 6-axes robot and a vision-based vehicle- and inlet detection sensor system. Further functionality serves a seventh-axis for charging lid closing and LEDs for object illuminating. The limited robot force fulfils ACCS test safety requirements.

4. Prototype testing and evaluating

This chapter deals with tests and evaluation of the automated plug-in prototype. Targets are the assessment of the prototype functionality and operating range, maximal possible vehicle parking misalignments as well as parking and plugging of different EV types. The parking position of different test drivers and the corresponding prototype functionality behaviour is evaluated and analysed. The analysis includes recording and investigation of the charging inlet position in 6 DOFs- and ACCS cable plugging process. Furthermore, the automated plugging time duration and the LEDs behaviour at different parking positions and light conditions are recorded. Inlet detection- and plugging robustness tests include ACCS test scenarios with different vehicles and outdoor experiments.

4.1. Testing plan

The testing plan defines test targets, contents and restrictions. Table 4.1 shows the test EVs. A BMW i3 60 Ah (table 4.1, Vehicle 1), is used for detailed prototype functionality assessment. Further EV parking, cable connection and disconnection tests are made with BMW i3 94 Ah, HYUNDAI IONIQ Electro, TESLA Model 3 and VOLKSWAGEN e-Golf.

Table 4.1.: ACCS prototype test EVs, [BMW19], [HYU18a], [TES20b], [VOL18a].

Test vehicle	Type	Year	Security cap	Plug position and -height [cm]	Charging use case
1	BMW i3 60 Ah	2016	Plastic flap	Rear, right, 95	I
2	BMW i3 94 Ah	2017	Plastic flap	Rear, right, 95	I
3	VOLKSWAGEN e-Golf	2019	No flap	Rear, right, 88	I
4	HYUNDAI IONIQ Electro	2019	No flap	Rear, left, 97	II
5	TESLA Model 3	2019	No flap	Rear, left, 95	II

Figure 4.1 shows ACCS vehicle parking test cases. Parking case I (figure 4.1, left) describes charging lot parking next to the ACCS prototype for EVs with the charging socket on the rear, right side (figure 4.1, left, $V_{1,2,3}$). Parking case II represents vehicle positioning for charging sockets on the EV's rear, left side (figure 4.1, right, $V_{4,5}$). Markers signed the parking lot dimensions in both test cases. The prototype tests are divided into various scenarios that are listed as follow:

1. Charging process evaluation: Functional tests of the automated plugging process and determination of maximal possible vehicle parking misalignments with test vehicle 1. Misalignments are the maximal position and angle in relation to the charging station.

4. Prototype testing and evaluating

2. Parking and charging: This section investigates the prototype behaviour at EV parking, automated charging and unparking procedure. Practised and unpractised drivers park vehicle 1 for test situations as close to practice as possible.
3. Different vehicles: Inlet positions, their access as well as connector plugging varies for different vehicle types. The differences are due to loading situations, vehicle assembling, age-related wear or varying friction. For the evaluation of the interoperability of recognition and robot control function, the system is tested with vehicle 2, 3, 4 and 5.
4. Outdoor: Camera sensor systems are sensitive regarding changing lighting conditions. Ambient light is much brighter than in the laboratory halls. For the evaluation of the inlet position recognition robustness, outdoor experiments under different light conditions are carried out with vehicle 1.

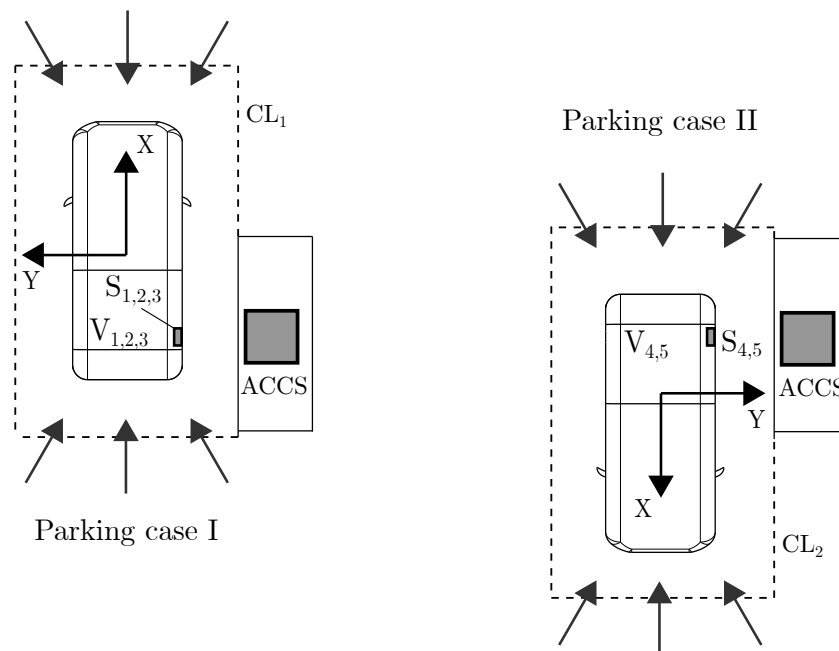


Figure 4.1.: ACCS prototype test case I and II for different EVs and charging socket positions.

Camera 1, 2 and 3 documented vehicle- and inlet positions. Besides, the robot control system collected data of robot head tool movements and -positions. The tests were limited to functional examination of sensors, actuators and control system as well as the investigation of vehicle parking processes. Thus the prototype tests were carried out under the following conditions:

1. During tests, no charging currents are transferred. As a result, the test vehicles release the charging cable lock, a few seconds after the connector end position is reached and the cable is able to be pulled out.
2. The protective flaps of the charging sockets are removed.
3. Manually or automatically charging lid opening and closing.

4. Floor markings support the driver's orientation while entering the charging lot and vehicle positioning.
5. The robot velocity during tests was limited down to 0.3 meter per seconds due to safety reasons.
6. No communication between vehicle and prototype

4.2. Charging process evaluation

The test series aim was to determine the robustness of the prototype cable plugging process at different vehicle positions. The test was carried out with test vehicle 1 and examined the robot behaviour at the maximum working range and with large vehicle angle offsets of up to $\pm 15^\circ$. Figure 4.2, left, exemplary depicts the relative position of vehicle $\{V\}$ and inlet $\{I\}$ in relation to robot base $\{B\}$ with an angular offset of 15° . Vehicle manoeuvring assistants enabled inlet positioning near to the robot range limit and with defined vehicle angle misalignment. The vehicle was lifted at each tire with the 4 manoeuvring assistants and placed to be at dropped down at predefined positions. Additionally, the height of the vehicle varied during the charging tests by different loading situations (position of the inlet regarding the robot Z -axis), achieved by different charge procedures by varying the number of vehicle occupants. The high variation of the inlet position contributed to the evaluation of the robustness of the recognition and control approach.

The maximum robot working range is defined by 1.3 m in robot X -axis and 1.45 m in robot Y -axis. The robot kinematic limits the minimum working area with a radius circle of 0.3 m. Charging requires inlet positioning between this border (figure 4.2, right). Furthermore, the robot range in X -direction decreases with the Y -distance of the inlet to the robot base and vice-versa. In the course of this test series, a total of 42 experiments with 6 basic positions with 7 angular offsets, each from -15° to $+15^\circ$ with 5° interval were carried out in the robot working area (figure 4.2, right). For the evaluation of the prototype function, the charging process was divided into 5 steps, [WHB19c]:

1. Docking (connector positioning in front of the charging inlet)
2. Plug-in until the end position of the charging inlet
3. Plug-out
4. Closing of the charging lid
5. Robot moving to the waiting position

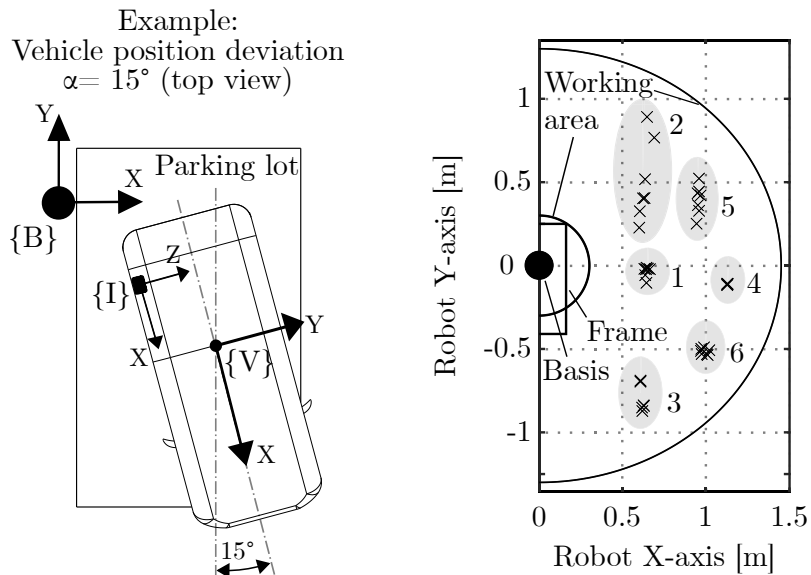


Figure 4.2.: Left: Exemplary presentation of the vehicle position with 15° angular deviation. Right: Representation of the inlet test positions to evaluate the functionality and robustness of the charging station prototype, [WHB19c].

The test results are shown in table 4.2. Docking, plug-in, plug-out as well as moving to the waiting position were carried out successfully in all 42 tests. Just two times, on test position 3, at 10° and 15° vehicle rotation angle in relation to the robot Z -axis, the charging lid was not sufficiently closed until its end position. The actuator could not completely close the lid due to its high relative position deviation. The inlet position regarding the robot X - and Y -axis were specified by the robot range limits and the angle deviation of the vehicle. That is why the inlet position varies along with the robot Y -axis, that is particularly visible at test basic position 2 (figure 4.2, right). In robot Z -axis the inlet mean position regarding the robot base was recorded with 52.64 cm with a standard deviation of 4.6 mm. This result shows the essential change in the height of the vehicle, which must not be neglected in the design of an automated charging system. The test shows, that even if the accuracy of the position sensor system decreases with increasing vehicle parking angles relatively to the robot system, the tests were carried out successfully with a high level of robustness, [WHB19c].

Table 4.2.: Summary of the plug-in motion experiment results, [WHB19c].

Process number	Process	Result	Annotation
1	Docking	42 times successful	-
2	Plug-in	42 times successful	-
3	Plug-out	42 times successful	-
4	Charging lid closing	40 times successful	Incorrect positioning of the actuator
5	Robot moving to waiting position	42 times successful	-

ACCS goal is a short charging duration, especially for ultra-fast public charging. Cable connection and disconnection should take a reasonable amount of (short) time in relation to power

transfer, that is requested with less than 20 minutes. For home charging with lower charging power, longer connection and disconnection processes can be tolerated. Nevertheless, short operating time leads to increased customer comfort.

Figure 4.3 shows box plots of the connecting and charging cable disconnecting duration (process number 1, 2, 3, 4 and 5) of the so-called *robustness tests* at the predefined basic positions. The connection and disconnection duration is defined by the robot movements and the inlet position *Recognition II* and *III*. Connection starts with opened charging lid (figure 3.33, *Recognition II*) and ends in the reached inlet end position. Disconnection starts by leaving the inlet end position, after a simulated charging process of 30 seconds and ends with the reached robot waiting position. Minimum and maximum connection time were 22 and 63 seconds. Due to the short distances of the robot head to the inlet, the connection at position 1 and 2 took the shortest time. The seven attachments in position 1, 2 and 4 were completed in less than 30 seconds with a scatter within 5 seconds. The connection time, especially of position 3 and 5, indicates a high distribution. At position 5 and a vehicle angle deviation of -15° , the charging process extended to 63 seconds due to the long matching procedures of *Recognition I* and *II*. 50% of the charging processes were carried out under 23 seconds. High distribution of the connection duration is mainly due to a long shape-based matching process to find the inlet position. In comparison, the temporal sequences of the robot movements are relatively constant and fluctuate only slightly, even with different angular ranges.

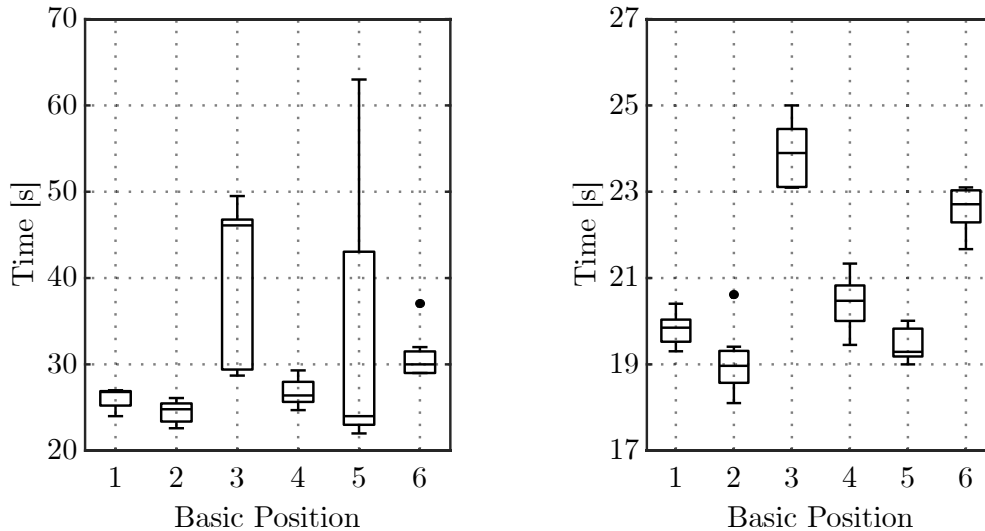


Figure 4.3.: Cable connection and disconnection time box plots for 6 basic vehicle positions. Left: Cable connection. Right: Cable disconnection.

Disconnection duration distribution is more constant at all test positions (figure 4.3, right) and the duration time is corresponding to the robot move distance. Position 3 and 6 indicate disconnection time of up to 25 seconds. In contrast, the minimum time was 18.1 seconds at position 2. One outlier was recorded with 20.6 seconds at position 2 with $+15^\circ$ vehicle angle deviation and a mean time of 19.6 seconds. With 13 seconds, the closing of the charging lid takes up a significant part of the time required for disconnection. The mean time of plug-in for

all 42 robustness tests was 30.3 seconds (SD=8.9 seconds) and for plug-out was 20.9 seconds (SD=1.9 seconds).

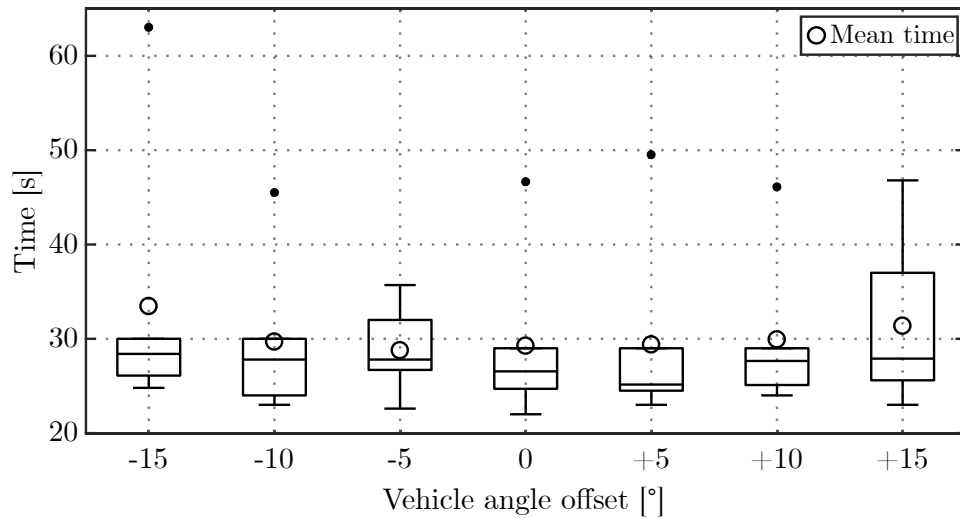


Figure 4.4.: Cable plug-in time box plot for various vehicle angle offsets.

As mentioned, the inlet pose recognition by shape-based 3D-matching requires time. Figure 4.4 shows box plots and mean values of the connection duration by different vehicle angle deviations from -15° up to $+15^\circ$, in 5-degree steps. The results show longer recognition processes at higher angular misalignments. Outlier indicates proportionally long matching durations due to low inlet edge contrast as a result of bad light conditions or shadows.

Table 4.3.: LEDs activation behaviour at different positions and vehicle angle misalignments.

	<i>Recognition II</i>	<i>Recognition III</i>	
Test position	Frame LEDs activation	Frame and head LEDs activation	Total
1	-	1	1
2	1	-	1
3	4	2	6
4	-	1	1
5	3	-	3
6	-	3	3
Vehicle angle	Frame LEDs	Frame and Head LEDs	
-15°	1	1	2
-10°	1	-	1
-5°	1	1	2
-0°	1	1	2
$+5^\circ$	1	-	1
$+10^\circ$	2	1	3
$+15^\circ$	1	3	4

3 LEDs support the image acquisition and matching process in case of bad light conditions. Table 4.3 shows the activation behaviour of the LEDs during the robustness tests grouped by basic test positions and vehicle angle deviation. Most light support indicates test position 3,

followed by position 5 and 6, and an angle deviation of $+15^\circ$. A summary of the lightning-related behaviour at different vehicle parking positions and angles can be found in the Appendix table A.10.

4.3. Parking and charging

The test series comprises the entire automated charging process, including driving in and parking the vehicle at the charging station, recognition of the vehicle and the inlet by the vision system, plug-in and plug-out of the charging cable, closing of the lid, leaving the charging station and finally taking the charging robot wait position. During the test, no instructor or other aids were used for guiding the test drivers with test vehicle 1. Figure 4.5 shows an exemplary section of the connection sequence of the charging robot. Documented were inlet poses, as well as the correct execution of the charging process.



Figure 4.5.: Exemplary section of the charging connecting sequence. Left: Robot during inlet 3D-pose detection with Camera 3. Middle: CCS Type 2 connector axis aligns with the vehicle charging inlet axis. Right: Robot during the cable insertion process.

Figure 4.6 shows 34 resulting positions of the inlet in robot X - and Y -axis of 12 different *practised* and *unpractised* drivers. 10 out of the 12 drivers did not have experiences with the test vehicle and the parking process at the charging station. The charging lot was marked with stripes on the floor to support the orientation of the test drivers. With a length of 5 m and a width of 2.3 m, usual parking lot dimensions were used, [PJWZ09]. The goal for the test persons was to park the vehicle in such a way that the inlet is within the working range of the charging robot. The area is given with 1.45 m in robot X -axis, 1.3 m in Y -axis and 1.05 m in Z -axis. The robot head extends or reduces the basic robot arm range of 1.3 m in the 3 main axis directions. After reached the parking position and opened the charging lid, the sensor system detected the inlet. The charging process was carried out according to the sequence described in chapter 4. In order to be able to represent parking situations as close to practice as possible, the vehicle was parked from various start positions and driving directions. The tests were carried out by parking forwards or backwards, as well as by straight entry into the charging station lot or after the previous turning. For the tests, the drivers were informed about the vehicles inlet location as well as the optimal vehicle parking position. The optimal inlet position is at the zero-line of the robot Y -axis. Parking aids were not used. In all 34 tests,

the inlet was placed in the robot working area, and the vehicle was charged automatically. An interesting fact is that there is also no significant difference between the achieved inlet position accuracy of practised and unpractised drivers.

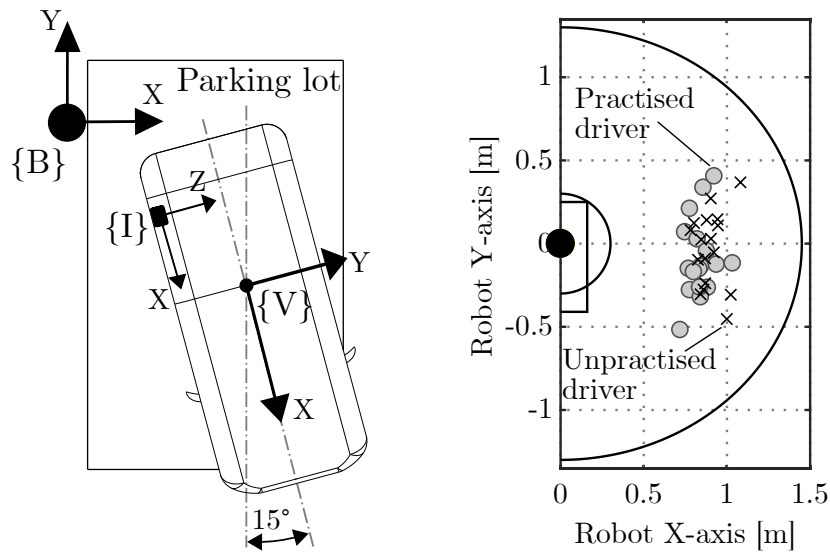


Figure 4.6.: Left: Example of a vehicle position deviation $\alpha = 15^\circ$ (top view) Right: Resulting inlet positions of 34 practised and unpractised test drivers.

Figure 4.7 shows box plots of the resulting inlet positions from the test series in transversal (robot X -axis) and longitudinal vehicle direction (robot Y -axis). The mean deviation of the inlet position in relation to the robot base after parking was 86.9 cm in the transversal direction with a SD of 8.32 cm and -5.92 cm in the longitudinal direction with a SD of 23.05 cm. 50% of the participants (2^{nd} to 3^{rd} quartile of the box plot) could park within a range of less than 9 cm deviation in transversal and 25 cm in the longitudinal direction.

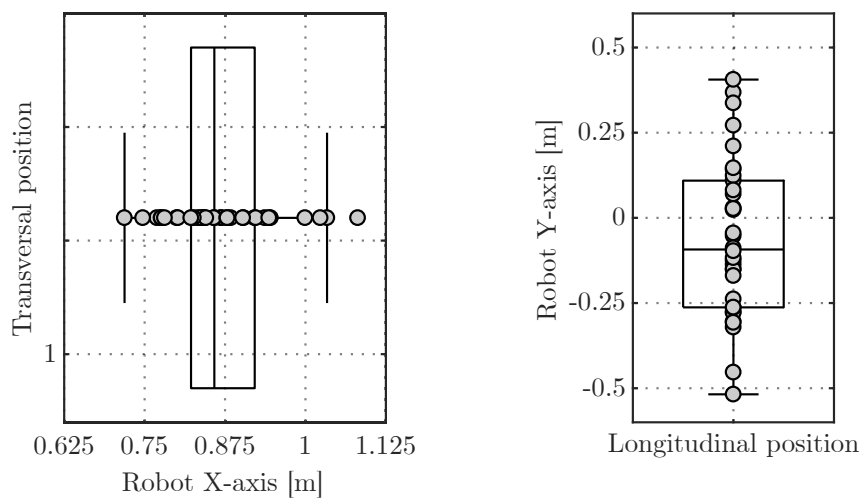


Figure 4.7.: Box plots of the resulting inlet positions of 34 test drivers. Left: Inlet position in robot X -axis. Right: Inlet position in robot Y -axis.

Figure 4.8 shows the vertical inlet position distribution and the angular deviation of the vehicles in relation to the robot base. The inlet has an installation-related angle deviation in relation to the vehicle Z -axis of -4.25° . In robot Z -axis the inlet mean distance was 49.7 cm with a SD of 8.6 mm. The average angular offset of the vehicles in relation to the vertical axis is recorded with -1.15° with a SD of 1.67° . For almost 60%, the angular offset was less than $\pm 2.5^\circ$. The maximum angular offset is recorded with -5.1° .

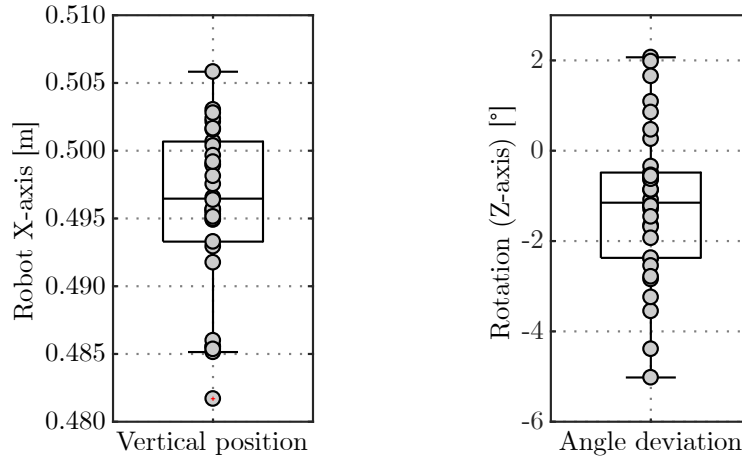


Figure 4.8.: Box plot of the resulting inlet Z -axis position and rotation deviation of 34 test drivers.

Figure 4.9 shows the charging processes connection and disconnection durations for 22 test drivers. Equal as in the *robustness tests* the connection starts with opened charging lid, and the disconnection ends with reached robot waiting position. The mean time for charging plug connection was 25.5 seconds with a SD of 2.67 seconds and for disconnection 22.1 seconds with a SD of 2.68 seconds. At disconnection, the robot stopped two times because of a communication delay between the software interfaces HALCON and MATLAB. The duration difference between the remaining connection test is within 4 seconds. With 13 seconds, charging lid closing consumes more than half of the disconnection time. The mean time for automated plug-in and plug-out for 22 tests is recorded with 47.6 seconds.

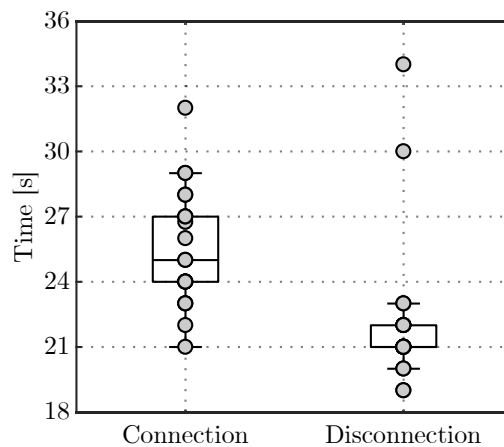


Figure 4.9.: Box plots of the automated connection and disconnection duration of 22 test drivers.

4.4. Different vehicles

Vehicle parking, cable plugging and cable unplugging tests have been carried out with test vehicle 2, 3, 4 and 5. The test series include driving in and parking the vehicle at the charging station, charging lid opening, inlet position recognition, plug-in and plug-out of the charging cable, leaving the charging station and finally taking the charging robot wait position. BMW i3 94 Ah and VOLKSWAGEN e-Golf were tested with parking case I - HYUNDAI IONIQ Electro and TESLA Model 3 with parking case II conditions. Test drivers parked the vehicle for- and backwards on the charging lot. The BMW i3 charging lids opened by a button in the centre console. TESLA Model 3 enables this function by the central touch screen inside the car. At Hyundai IONIQ Electro and VOLKSWAGEN e-Golf, the charging lid was opened and closed manually after parked EV and unplugged charging cable. During the test series, vehicle 2, 3, 4 and 5 have been parked, and the cable was automatically connected and disconnected successfully for several times.

Figure 4.10, left, shows the TESLA Model 3 charging socket. The automated charging lid and no security plugs enable unrestricted charging inlet access by the prototype. The inlet enables CCS Type 2 cable connection - but the inlet shape does not fulfil the CCS Type 2 standard dimensions. Figure 4.10, right, shows the charging inlet detail view. The inlet front surface contains a curvature (figure 4.10, right, C). For the shape-based 3D-matching inlet position detection process, the inlet CAD-model was bent by a curvature. The curvature was determined by inlet front surface measuring points (figure 4.10, right, P). The points lie on the height of the inlet pin-holes and -edges in inlet's Y -direction.

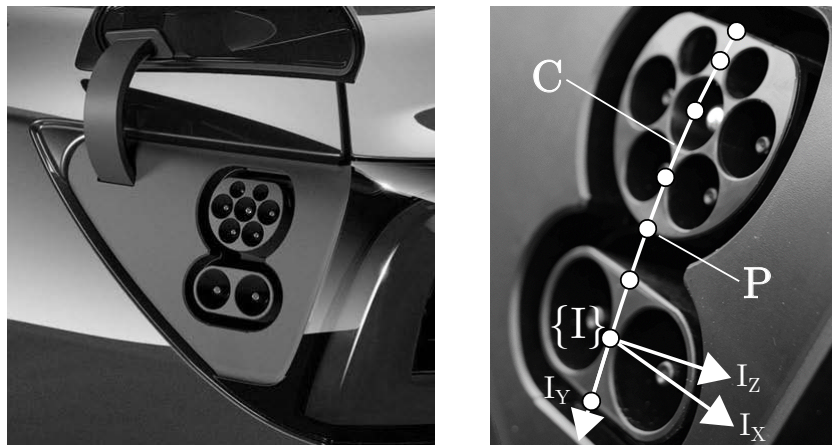


Figure 4.10.: Left: TESLA charging socket positioned at the vehicle rear, left side, [WAU20]. Right: Charging inlet detail view and representation of the inlet shape curvature [Sch20].

Figure 4.11 shows the test series scenario (figure 4.11, Step 1, Step 2 and Step 3) of subsequently charging of test vehicle 1 and 2 and a possible future scenario of automated vehicles series charging in large parking facilities, e.g. in shopping centres, rest stops or charging farms (figure 4.11, Future scenario). In the test series, vehicle 2 waits until vehicle 1 has finished charging and leaves the charging lot. When the charging station is free, vehicle 2 enters the

charging lot and the charging process starts again. The series charging test vehicles are shown in table 4.4. The charging lot was marked with adhesive tapes to simulate a parking lot with typical dimensions, [PJWZ09]. Practised and unpractised drivers directed the test vehicles to the charging station and parked the car near the charging station, according to their judgment without vehicle parking positioning adds. In comparison to the previously performed charging tests, vehicle parking was only performed by driving forward into the charging lot, in order to be able to fulfil the predefined scenario requirements. For the functionality of the automated charging station prototype, it doesn't matter if the cars parks front- or backwards, [WHB19c].

Table 4.4.: Test vehicle properties for the series charging scenario.

Vehicle	Vehicle type	Year	Charging inlet	Colour	Annotation
1	BMW i3 60 Ah	2016	CCS Type 2	Grey	Charging lid opens by a knob inside the car.
2	BMW i3 94 Ah	2017	CCS Type 2	Black	Charging lid opens by a knob inside the car.

The series tests support understanding and definition of requirements for the *Future scenario*, where a large number of cars can be charged subsequently on highly frequented places. The combination with autonomous driving functions can automate the whole parking and charging process. In the case of a larger number of vehicles, this process repeats until all vehicles are charged. During the test series, the EVs have been charged several times automatically without user intervention. The mean distance of the charging inlet in relation to the robot base after parking was 0.870 m in robot *X*-axis and 0.034 m in robot *Y*-axis with a SD of 0.081 m and 0.188 m. Seven unpractised test persons parked the inlet in a square area of 0.242 m in robot *X*-axis and 0.579 m in robot *Y*-axis.

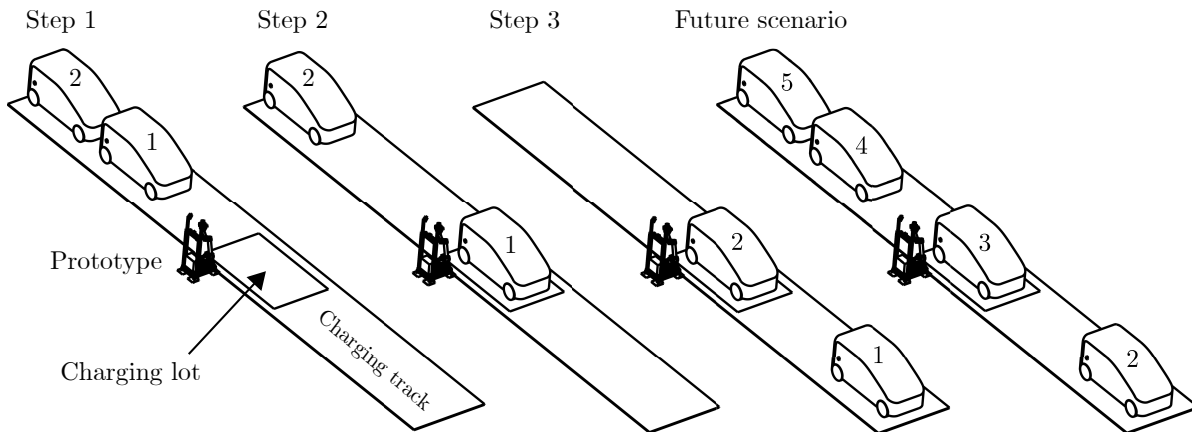


Figure 4.11.: Test case of subsequent charging of two different vehicles (Step 1, Step 2 and Step 3) and possible future scenario of charging a number of EVs.

4.5. Outdoor

Figure 4.12, left shows a parking lot at the campus of Graz University of Technology, with a EV charging station. The parking lot has a length of 5.3 m and a width of 2.5 m. A fixed charging station with up to 7.2 kW charging power enables charging two vehicles. For outdoor tests, the

prototype was placed in front of the charging station, and real-world environment tests with the BMW i3 test vehicle were done (figure 4.12, right). The parking process was started by driving the car from the left and right of the street and parking backwards into the charging bay. Several charging tests were done during typical daily traffic situations. In contrast to the laboratory hall, outdoors, the LEDs did not start at all test runs, [WHB19c]. Thus, at any time, ambient light was available sufficiently to represent the contours and outlines of the charging inlet with sufficient contrast for object recognition and identification. The inlet was placed in the robot's range, and the vehicle was charged several times successfully.



Figure 4.12.: Left: EV charging station at campus of Graz University of Technology. Right: Charging station outdoor test setup.

4.6. Conclusion

Four test scenarios were conducted to test and evaluate the ACCS prototype. The prototype was positively tested for high inlet position and angle misalignment in relation to the robot base. In all cases, the inlet position was detected with a sufficient accuracy, so that the automated plug-in process could start. The robot was able to carry out the plug-in and plug-out processes within its working range during all robustness tests. The compact robot head tool, including linear actuator, was able to close the charging lid in nearly all tests with the BMW i3. Higher angular misalignments lead to longer recognition processes.

Charging tests with test drivers show maximal parking angle misalignments of up to 5° , whereby 50% parked under $\pm 2.37^\circ$. The low vertical inlet position variances have low influences on the working range of the robot, but docking and plug-in motions have to be adjusted by the system. Without an instructor, the test drivers parked the inlet in an exactable area next to the robot. The findings show that the inlet was positioned in an area of approximately 1 m x 0.5 m relative to the charging robot. This area corresponds approximately to the parking tolerance at conventional fuel stations. For the fulfilment of easy and user-friendly parking, floor markings were used for supporting the driver's orientation while entering the charging lot. Parking guides, e.g. monitors or parking assistants, were not used. The view to the charger for positioning the vehicle proves to be advantageous, which was confirmed by the test drivers.

Without user intervention, test vehicle 1 and 2 have been charged several times automatically successfully. The results of seven unpractised test persons showed that the inlet was positioned

in an area of approximately 0.6 m x 0.25 m relative to the charging robot. In comparison to parking and charging tests from different directions and without a straight charging track, the drivers parked more accurate.

ACCS parking and plugging tests of 5 EV types with different charging socket positions at varying charging use cases were successfully accomplished. An adapted inlet position detection process enabled cable plugging of a not standardized charging inlet (at the TESLA Model 3).

Automated outdoor charging on a typical charging station were positively tested. In this test scenario, the test vehicle parked backwards into the charging bay. The support lights were not activated during several automated charging processes under different daylight conditions.

5. Conclusion and outlook

The final chapter discusses the thesis outcomes and findings and gives an outlook to possible research activities in the field of automatic EV charging with conductive standards.

5.1. Conclusion

The thesis introduces a novel method for charging of electric vehicles automatically and presents approaches that enable charging of different EV types without the requirement of complex vehicle adaptations. In this way, the results of the research activities highlight the promising possibilities of ACCS by use of robot-controlled systems and contribute to the further development of ACCS. The following items relate to the predefined thesis targets, which are explained in chapter 1.3.

The state-of-the-art research of ACD-U, ACD-S and ACCS systems gave less information about ACCS requirements and demands. Identified ACCS challenges are charging inlet position detection, the compensation of vehicle and charging device position misalignments and connector plugging. Further identified challenges are the variety of charging cap systems and charging socket positions. In this context, not-standardised charging inlet access, security caps and lids as well as inlet positions, increase the ACCS complexity additionally.

ACCS prototype boundary conditions and demands include the consideration of the European CCS Type 2 standard. The standard is compatible with the most common plug systems and achieves charging capacities up to 350 kW, [ION19]. For technical effort- and costs reduction of automated EV charging solutions, further prototype demands include the prevention of vehicle adaptations and -architecture related interventions. ACCS has to consider the EV parking process and local parking conditions. Strait forward accessible charging lots and easy to perform vehicle positioning are essential. In this context, boundary conditions for the development of an ACCS prototype are easy EV parking and the avoidance of vehicle positioning parking aids. In addition, the ACCS prototype testing with persons in the near area requires an actuator force limitation-based safety function.

Prototype functional requirements are derived from a cable-based manual charging process analysis, charging use cases definition as well as the gathering of ACCS boundary conditions and demands. The elaborated tasks serve as basis for the ACCS system design that includes the ACCS functional and ground layout concept. Using the system design approach, ACCS prototype component requirements, e.g. ACCS vehicle charging lot- and system dimensions, as well as vehicle charging lot entering specifications, are defined. Sensor and actuator accuracy

and range requirements depend on vehicle parking accuracy, the charging cable insertion process and the standardized inlet shape. In an ACCS vehicle parking misalignment elaboration, a positioning area of the vehicle's charging socket of 116.5 cm in vehicle-longitudinal and 35 cm in the lateral direction was defined, which fulfils 95.5% of all parking events. Sensor detection requirements are the capability of identification of the inlet position in 6 DOFs with approximately 0.5 mm translational and 1° rotational accuracy. The comparatively low required actuator stiffness during the connector insertion process indicates a particular task. Actuator payload and kinematics were derived from cable movement and handling requirements, considering, e.g. cable weight, -movement trajectories and -insertion force.

Requirements for ACCS development relate to customer demands and easy charging station use. Functions for automated registration, authentication and payment as well as the communication with autonomous parking vehicles by consideration of V2X- and V2G-communication technologies should be taken into account. In this context, the implementation of communication standards is essential.

Related to the research question, the goal was to develop a sensor and actuator system to investigate the possibility of using conductive standards for automated EV charging. Position sensor technologies were investigated regarding the vehicle and charging inlet position determination requirements and ACCS criteria, e.g. detection accuracy, kinematics system, light influences and costs. The prototype sensor system consists of three mono-cameras. Based on unmodified CCS Type 2 inlet shape, a 3D-inlet position detection system by the use of a shape-based 3D-matching algorithm was developed. Due to the requirements, the actuator system was chosen as a research robot with 6 DOFs, robot control- and robot position-dependent recognition as well as an adapted CCS Type 2 charging plug. An additional seventh axis enables closing of charging lids of selected test cars. A new invented ACCS procedure for charging of different EVs was developed, which the actuator and sensor system activities.

For fulfilling future ACCS infrastructure implementation, vehicle-to-charging station communication standard proposals were taken into account. For this purpose, the ACCS prototype charging procedures were compared with the ISO 15118 ACD standard proposal communication processes. Vehicle-to-charging system communication standards, e.g. ISO 15118 proposals, consider basis processes for ACD-S. The study shows that the represented ISO 15118 ACD communication process contents can be transferred as a basis for ACCS. However, the automated connection and disconnection communication procedures for ACCS are not regulated yet. For interoperable systems, ACCS systems have to be united and combined with the communication standards. This would support the ACCS compatibility with various EV types, reduce market entry barriers and save costs. The communication takes place wirelessly. Therefore, ACCS requires a wireless communication interface device.

Concerning the research question, whether EVs can be automatically charged by conductive standards, the following statements can be made based on the present research findings. Tests showed that the CCS Type 2 standard can be used for automated charging. The newly introduced approaches for inlet position detection as well as for automated connection and disconnection procedures are applicable on different EVs without influencing charging inlet shape and

design. One *still* limitation is the inlet access due to today's often non-automatically opening and closing charging lids as well as additional protective plastic flaps or rubber plugs. However, manufacturers provide new solutions in their latest models, that allow unrestricted inlet access. The prototype charging station enabled fully automated charging of electric vehicles without vehicle inlet adaptations at high vehicle parking misalignments, which was proven in the course of experiments with 12 test drivers. The parking accuracy was recorded in an area of 1 meter and 0.5 meter. The sensor system enabled sufficiently accurate inlet position estimation at different vehicles and under changing light conditions.

Vehicle parking and parking aid influences were tested with different test drivers and test scenarios. For easy and user-friendly parking, floor markings were used for supporting the drivers' orientation while entering the charging lot. Without any instruction, the test drivers parked the inlet properly in the robot's working area. The parking tests showed maximal vehicle parking angle misalignments of up to 5° - whereby 50% parked with an accuracy below $\pm 2.37^\circ$. The test drivers positioned the charging inlet in an area of approximately 1 m x 0.5 m. In comparison to parking and charging from different directions, parking straight into the charging lot was more easy to achieve for the test persons. Seven unpractised test persons parked the inlet in an area of approximately 0.6 m x 0.25 m. This resulting inlet positions area corresponds approximately to the parking tolerance at conventional fuel stations. As a result, the prototype charging system was able to plug-in the charging socket properly in all test cases. Parking guides, e.g. monitors or parking assistants, were not used in the tests. Floor markings indicated the prototype working range demands and test drivers did not need any other parking aids, e.g. sound or camera systems. During the tests, a visual driver's view to the prototype charging station supporting vehicle positioning proves to be advantageous, which was confirmed by the test drivers.

5.2. Outlook

The different types of tests with the prototype showed the feasibility of automated charging with conductive standards. In the following, recommendations for further ACCS development are given:

- a. The testing of a high number of various vehicles would generate more information. Further tests are recommended. On the one hand, this will deliver more data of kinematics, forces and movement requirements. On the other hand, more information about vehicle parking and inlet position accuracy will be determined. Parking test findings for inductive charging and the prototype show a dependency on the achievable parking accuracy and the resulting charging inlet position. Further tests have the potential to improve the definitions of ACCS specifications in terms of the required sensor system and kinematics system complexity.
- b. The study results are limited to manual vehicle parking. Future research activities should investigate the potential of integrating automated vehicle parking functions into the charg-

- ing process. Findings regarding the parking process and resulting position accuracy of different automated parking vehicles will support the further development of ACCS.
- c. Safety plays a crucial role at home and for public charging. To fulfil safety-related requirements, a framework must be created, which prevents accidents and damages to people and machinery. The collaborating features of the tested research robot enable prototype developing and testing without safety fences or barriers. For a serial application, specifically developed security processes and software have to be implemented and tested in addition to the application of appropriate protective devices.
 - d. EVs are not prepared for automated charging today. Especially the inlet access and additional security flaps and mechanism complicate ACCS. Standards for automated charging processes as well as automated inlet access, e.g. automatically opening and closing lids should be defined to enable improved interoperability of EVs and ACCS systems.
 - e. For an economically series implementation, the separate consideration and development of ACCS systems for home and public charging applications might be advantageous. This should be taken into account in further research activities and development processes of dedicated automated charging systems.

A. Appendix

A.1. Equations

Equation (2.1)

$$Rot_{RPY}(\alpha, \beta, \gamma) = Rot(Z, \gamma) \cdot Rot(Y', \beta) \cdot Rot(X'', \alpha) \quad (A.1)$$

Equation (2.2)

$$Trans(x, y, z) = \begin{bmatrix} 1 & 0 & 0 & x \\ 0 & 1 & 0 & y \\ 0 & 0 & 1 & z \\ 0 & 0 & 0 & 1 \end{bmatrix} \quad (A.2)$$

Equation (2.3)

$$Rot(x, \alpha) = \begin{bmatrix} 1 & 0 & 0 & 0 \\ 0 & \cos\alpha & -\sin\alpha & 0 \\ 0 & \sin\alpha & \cos\alpha & 0 \\ 0 & 0 & 0 & 1 \end{bmatrix} \quad (A.3)$$

Equation (2.4)

$$Rot(y, \beta) = \begin{bmatrix} \cos\beta & 0 & \sin\beta & 0 \\ 0 & 1 & 0 & 0 \\ -\sin\beta & 0 & \cos\beta & 0 \\ 0 & 0 & 0 & 1 \end{bmatrix} \quad (A.4)$$

Equation (2.5)

$$Rot(z, \gamma) = \begin{bmatrix} \cos\gamma & -\sin\gamma & 0 & 0 \\ \sin\gamma & \cos\gamma & 0 & 0 \\ 0 & 0 & 1 & 0 \\ 0 & 0 & 0 & 1 \end{bmatrix} \quad (A.5)$$

Equation (2.6)

$$R_{RPY}(\alpha, \beta, \gamma) = \begin{bmatrix} \cos\gamma\cos\beta & \cos\gamma\sin\beta\sin\alpha - \sin\gamma\cos\alpha & \cos\alpha\sin\beta\cos\gamma + \sin\alpha\sin\gamma \\ \sin\gamma\cos\beta & \sin\gamma\sin\beta\sin\alpha + \cos\alpha\cos\gamma & \sin\gamma\sin\beta\cos\alpha - \cos\gamma\sin\alpha \\ -\sin\beta & \cos\beta\sin\alpha & \cos\beta\cos\alpha \end{bmatrix} \quad (A.6)$$

Equation (2.7)

$$T_{RPY}(\alpha, \beta, \gamma) = \begin{bmatrix} \cos\gamma\cos\beta & \cos\gamma\sin\beta\sin\alpha - \sin\gamma\cos\alpha & \cos\alpha\sin\beta\cos\gamma + \sin\alpha\sin\gamma & x \\ \sin\gamma\cos\beta & \sin\gamma\sin\beta\sin\alpha + \cos\alpha\cos\gamma & \sin\gamma\sin\beta\cos\alpha - \cos\gamma\sin\alpha & y \\ -\sin\beta & \cos\beta\sin\alpha & \cos\beta\cos\alpha & z \\ 0 & 0 & 0 & 1 \end{bmatrix} \quad (\text{A.7})$$

Equation (3.1)

$$SR_{max} = \sqrt{SR_{max,X}^2 + SR_{max,Y}^2 + SR_{max,Z}^2} \quad (\text{A.8})$$

Equation (3.2)

$$AR_{max} = \sqrt{AR_{max,X}^2 + AR_{max,Y}^2 + AR_{max,Z}^2} \quad (\text{A.9})$$

Equation (3.3)

$$F_{C,y} = q_{l,CCS} \cdot \frac{L_{CCS}}{2} \cdot g \quad (\text{A.10})$$

Equation (3.5)

$$F_{A,y} = m_T \cdot g + F_{C,y} \quad (\text{A.11})$$

Equation (3.6)

$$F_A = \sqrt{F_{A,y}^2 + F_{A,z}^2} \quad (\text{A.12})$$

Equation (3.7)

$$F_{A,z} = F_P + \cos(\alpha - 90) \cdot F_C \quad (\text{A.13})$$

Equation (3.8)

$$F_{A,y} = F_T + \sin(\alpha - 90) \cdot F_C \quad (\text{A.14})$$

Equation (3.9)

$$F_A = \sqrt{F_{A,z}^2 + F_{A,y}^2} \quad (\text{A.15})$$

Equation (3.10)

$$S(A) = \sum_{c=1}^N W_c \cdot R_c(A_c) \quad (\text{A.16})$$

Equation (3.12)

$$D_h \leq \frac{AC_h \cdot P_h}{2 \cdot \tan(\alpha_h/2)} \quad (\text{A.17})$$

Equation (3.13)

$$D_v \leq \frac{AC_v \cdot P_v}{2 \cdot \tan(\alpha_v/2)} \quad (\text{A.18})$$

Equation (3.14)

$$AC_h = 2 \cdot RI4 \cdot \tan(\alpha_h/2) \quad (\text{A.19})$$

Equation (3.15)

$$AC_v = 2 \cdot RI4 \cdot \tan(\alpha_v/2) \quad (\text{A.20})$$

Equation (3.16)

$$AC_h = \frac{2 \cdot D_h \cdot \tan(\alpha_h/2)}{P_h} \quad (\text{A.21})$$

Equation (3.17)

$$AC_v = \frac{2 \cdot D_v \cdot \tan(\alpha_v/2)}{P_v}. \quad (\text{A.22})$$

A.2. Tables

Table A.1.: Overview of localization systems using sound waves with performance parameters. In comparison to other position technologies, properties and performance parameters of various sound systems are quite similar. The techniques can be separated into active and passive device systems. Active systems transmit scheduled ultrasonic pulses between mobile devices. A passive system includes a receiver that captures signals from fixed installed transmitters. The advantage is the anonymity of the receiver, [Mau12].

Name	Year	Accuracy	Active or passive device	Carrier frequency	Principle	Application
ACTIVE BAT, [HB02]	1997	3 cm	Active	40 kHz	Multilateration	Smart tracking
Alloulah, [MAM10]	2010	3 cm	Active	20-50 kHz	AAL, monitoring	Demonstration
Sato, [SNT ⁺ 11]	2011	4 cm	Active	40 kHz	Multilateration	Human motion
SONITOR TECHN., [TEC20]	2011	Subroom	Active	35-40 kHz	Disclosed	Hospitals, mines
HEXAMITE, [HEX20]	2011	0.9 cm	Active tags	40 kHz	Multilateration	3D-studio
Cricket, [Pri05]	2005	1-2 cm	Passive	40 kHz	Multilateration	Smart tracking
Schweitzer, [SS10]	2010	1 cm	Passive	35-65 kHz	Multilateration	WSN
Jiménez, [JSP ⁺ 09]	2009	1 cm	Passive	>25 kHz	Multilateration	Archeology
Reijnders, [RP07]	2007	Ecimeter	Echo	31-59 kHz	Echolocation	Rotot guidance
Wan, [WP10]	2010	0.5 cm	Echo	40 kHz	Body reflected	Person tracking
Filonenko, [FCC10]	2010	>1m	Active	17-22 kHz	Multilateration	LBS, guidance
Mandal, [MCH ⁺ 05]	2005	60 cm	Active	4 kHz	Multilateration	LBS, malls

Table A.2.: Performance characteristics of tactile and combined polar systems. Tactile systems measure the position of an object by touching them with a calibrated probe. Combined polar systems use rotating beams and *Time of Arrival* (ToA) principles or optical or mechanical encoders. Determined object angles and distances enable the creation of a complete 3D-scene, [Mau12].

Model	Resolution (HxV)	Range/accuracy	Field of View (FoV)	Frame rate	Points	Laser	Pulse width
HDL-64E, [VEL20]	0.08° x 0.4°	2-120m/2cm	360° x 26.8°	5-15 Hz	1,300,000	905 nm	10 ns
HDL-32E, [VEL20]	0.08° x 1.33°	2-120m/2cm	360° x 31.4°	5-20 Hz	700,000	905 nm	10 ns
VLP-16, [VEL20]	0.08° x 1.87°	2-100m/2cm	360° x 30°	5-20 Hz	300,000	905 nm	10 ns
TOYOTA, [CNK13]	0.05° x 1.5°	Not specified	170° x 4.5°	10 Hz	326,400	870 nm	4 ns

Table A.3.: Evaluation scores results of vehicle-external and -internal sensor technologies for the determination of the vehicle position on a charging lot and the charging inlet 3D-position.

Vehicle-external	Score	Vehicle-internal	Score	Inlet sensors	Score
Ultrasonic	8.1	Ultrasonic	6.4	2D camera	8.1
Magnetic	5.7	Laser	5.5	Laser	7.5
2D camera	8.0	2D camera	6.9	3D camera	7.7
Laser	7.8	3D camera	6.9		
3D camera	8.1	Infrared	5.5		
Infrared	6.2	Short-Range-Radar	5.7		

Table A.4.: Selection of standards and guidelines for robotics. Robots are flexible and complex mechatronic machines. Robot manufacturers have to ensure all directives and standards, which also exist for other electrical devices and controls as well as for software and mechanical machines. Depending on the application, specific standards must also be taken into account, e.g. when using robots in clean rooms, cells in the food sector or for the combination with laser applications. Furthermore, specific safety regulations apply to robots, [HMA10].

Norm	Description
EN ISO 12100-1	Safety of machines, terminology
EN ISO 12100-2	Safety of machines, technical specifications
EN 954-1	Safety of machines, safety-related parts of control systems; replaced by EN ISO 13849-1
EN ISO 13849-1	Safety of machinery - Safety-related parts of control systems - Part 1: General principles for design; will replace EN 954-1
EN ISO 13849-2	Safety of machinery - Safety-related parts of control systems - Part 2: Validation
EN 62061	Safety of machinery - Functional safety of safety-related equipment electrical, electronic and programmable electronic control systems
IEC 61508	Functional safety of safety-related electrical/electronic/programmable electronic systems
EN 60204	Electrical equipment of machines
EN 60204	EMV, Electromagnetic compatibility
EN 775	Operation of industrial robots, safety; will be replaced by EN ISO 10218-1
IEC 60204-1	Electrical equipment of machines
IEC 60529	Degrees of protection of the housings
EN ISO 10218-1	Operation of industrial robots, safety
EN ISO 10218-2	Industrial robots - safety requirements - Part 2: Robot system and integration (ISO 10218-2:2008); German version EN ISO 10218-2:2008
ISO 9787	Operation of industrial robots, coordinate systems and movement directions
ISO 9409-1	Operation of industrial robots, mechanical interface
ISO 9283	Industrial robots - Performance characteristics and associated test methods (ISO 9283:1998).

Table A.5.: Prototype requirements for standardized cable-based charging technologies.

Requirement	Type	Designation
Typical charging lot layout and size dimensions	Technical	R1
Easy and user-friendly vehicle parking and -positioning	Technical	R2
Simple parking aids	Technical	R3
Compact and transportable for testing at different scenarios	Technical	R4
Capability of handling different light situations	Technical	R5
Vehicle detection and classification	Functional	R6
Automated cable plugging start trigger	Functional	R7
Inlet position detection	Functional	R8
Guiding, alignment as well as plugging and unplugging of the charging cable	Functional	R9
Charging of different EV types	Functional	R10
Compensation of vehicle parking misalignments	Functional	R11
Manually or automatically charging inlet as well as safety caps handling	Restrictive	R12
Handling of the CCS Type 2 charging standard	Technical	R13
Avoidance of EV and charging inlet adaptations and vehicle packaging architecture interventions	Technical	R14
Safety for ACCS development and -charging tests with trained persons	Technical	R15

Table A.6.: Overview of of commercially depth cameras and range scanners based on *Time-of-Flight* (ToF) technologies with performance parameters. The manufacturers do not specify the depth accuracy. This is due to the accuracy dependence on various factors, e.g. object surface, illumination or frame rate, [HHEM16]

Camera	Resolution (HxV) [pixel]	Range [m]	Mult. cameras	Field of View (FoV)	Max. Frames Per Second (FPS)	Indoor/outdoor
SR4000, [IMA16]	176x144	0-5 or 0-10	Six cameras	43°x34°	30	Yes/no
SR4500, [IMA16]	176x144	0-9	Many cameras	43°x34°	30	Yes/no
DS311, [SOL20]	160x120	0.15-1 or 1.5-4.5	Not specified	57°x42°	60	Yes/no
DS325, [SOL20]	320x240	0.15-1	Not specified	74°x58°	60	Yes/no
E70, [FOT16]	160x120	0.1-10	Four cameras	70°x53°	52	Yes/yes
E40, [FOT16]	160x120	0.1-10	Four cameras	45°x34°	52	Yes/yes
Kinect V2, [MIC20]	512x424	0.8-4.2	Not specified	70°x60°	30	Yes/no

Table A.7.: Criteria rating of vehicle-external sensor systems. A suitable sensor system has been chosen by an evaluation with according to the listed criteria. Its weighting indicates the importance of each criterion.

Sensor	Criteria						
	Parking position (accuracy)	Material costs	Different light performance	Vehicle classification	Charging station integration	Weather robustness	Vehicle adaption
Ultrasonic	5	10	10	2	10	9	10
Magnetic	8	2	10	2	5	8	2
2D-camera	8	8	6	9	9	8	10
Laser	10	1	9	9	9	10	10
3D-camera	9	7	6	10	9	8	10
Infrared	6	6	3	8	9	6	10
	Weighting						
	20	20	20	10	10	10	10

Table A.8.: Criteria rating of vehicle-internal sensor systems. Vehicle sensors such as 2D- and 3D-cameras have been evaluated according the listed criteria regarding vehicle position determination on a charging lot.

Sensor	Criteria				
	Parking position detection accuracy	Material costs	Different light performance	Charging station integration	Weather robustness
Ultrasonic	3	10	10	4	9
Laser	10	1	8	4	8
2D-camera	8	8	4	7	6
3D-camera	9	7	4	7	6
Infrared	9	5	4	4	6
Short-Range-Radar (SRR)	7	3	10	4	8
	Weighting				
	25	25	20	15	15

Table A.9.: Criteria rating of selected sensor techniques for the charging inlet position detection. The most important criteria are inlet 3D-pose detection, costs, performance at different light conditions as well as necessary vehicle adaptations.

Sensor	Criteria					
	Inlet 3D-pose detection	Vehicle adaption	Different light performance	Material costs	Charging station integration	Weather robustness
2D-camera	8	10	6	8	9	8
Laser	10	10	9	1	8	10
3D-camera	9	10	6	6	7	8
	Weighting					
	30	20	15	15	10	10

Table A.10.: Summary of the prototype charging process LEDs behaviour evaluation. The results show the behaviour at different vehicle parking positions and angles in the different recognition processes II and III.

Test	Angle	<i>Recognition II</i>		<i>Recognition III</i>	
		Frame LEDs	Head LED	Frame LEDs	Head LED
1					
	-15	No	No	No	No
	-10	No	No	No	No
	-5	No	No	No	No
	0	No	No	Yes	Yes
	5	No	No	No	No
	10	No	No	No	No
	15	No	No	No	No
2					
	-15	No	No	No	No
	-10	No	No	No	No
	-5	No	No	No	No
	0	No	No	No	No
	5	No	No	No	No
	10	Yes	No	No	No
	15	No	No	No	No
3					
	-15	No	No	No	No
	-10	No	No	No	No
	-5	No	No	No	No
	0	Yes	No	No	No
	5	Yes	No	No	No
	10	Yes	No	Yes	Yes
	15	Yes	No	Yes	Yes
4					
	-15	No	No	No	No
	-10	No	No	No	No
	-5	No	No	No	No
	0	No	No	No	No
	5	No	No	No	No
	10	No	No	No	No
	15	No	No	Yes	Yes
5					
	-15	Yes	No	No	No
	-10	Yes	No	No	No
	-5	Yes	No	No	No
	0	No	No	No	No
	5	No	No	No	No
	10	No	No	No	No
	15	No	No	No	No
6					
	-15	No	No	Yes	Yes
	-10	No	No	No	No
	-5	No	No	Yes	Yes
	0	No	No	No	No
	5	No	No	No	No
	10	No	No	No	No
	15	No	No	Yes	Yes

A.3. Test objects and equipment



Figure A.1.: BMW i3 60 Ah, battery capacity 18.8 kWh, real range 130 km, energy consumption 14.5 kWh/100km, [DAT19]. The CCS Type 2 charging inlet of the vehicle serves as the main test object for ACCS prototype functionality. In addition, the vehicle was used for parking tests on the prototype charging lot.



Figure A.2.: BMW i3 94 Ah, battery capacity 27.2 kWh, real range 170 km, energy consumption 16 kWh/100km, [DAT19]. The EV was used as 2nd test object in the scenario of subsequently performed automated charging of different vehicles.



Figure A.3.: TESLA Model 3 standard version, battery capacity 53 kWh, WLTP range 409 km, energy consumption 14.1 kWh/100km, 0-100 km/h in 5.6 seconds, [TES20b]. The EV was the 4th ACCS prototype test EV. The EV offers automated charging lid opening and closing.



Figure A.4.: HYUNDAI IONIQ Elektro, battery capacity 38 kWh, WLTP range 294 km, energy consumption 13.8 kWh/100km, 0-100 km/h in 9.9 seconds, [HYU18a]. The vehicle served as the 5rd ACCS prototype test EV.



Figure A.5.: VOLKSWAGEN e-Golf, battery capacity 35.8 kWh, WLTP range 231 km, energy consumption 15.8 kWh/100km, [VOL18a]. The EV served as the 3rd ACCS prototype test EV.



Figure A.6.: The shunting aid enables easy vehicle moving. 4 shunting aids were used for lifting the test EVs to different cable-plugging test positions, [REA19].



Figure A.7.: Mobile workstation DELL Precision M4800. Software platform Windows 10 Pro, processor Intel Core i7 fourth generation, main memory 16 GB, graphics NVIDIA Quadro K1100M with 2 GB GDDR5 memory, hard disk storage 500 GB SATA with 6 Gbit/s, [DEL19]. The tasks of the work station include vision detection and robot control processes as well as test recording and documentation during the ACCS prototype tests.

List of Figures

1.1. Structure of work.	5
2.1. Functional objective and impact fields for automated EV charging with conductive standard technologies (ACCS).	7
2.2. EV charging in 1912. Left: Woman drives the EV into a charging station lot, [MOT19b]. Right: Women next to a charger from GENERAL ELECTRICS, [Dro19].	8
2.3. Selection of charging connector standards according to [EI18].	8
2.4. Left: Patent drawing of TESLA’s battery swap system, [TES15]. Right: Concept illustration of the BETTERPLACE battery swap facility, [Jer19].	11
2.5. ACCS concept with a KUKA robot arm, gripper and a CCS Type 2 connector, [VOL16].	12
2.6. Automated side coupler concept of the Technical University of Dortmund. The concept includes a special robot arm kinematic, which handles a standard charging plug, [DOR15].	13
2.7. Detailed view on the robot head concept with gripper and a Type 2 connector, [Ste18].	13
2.8. Image section during cable connection from a published video of TESLA’s charging snake, [TES16].	14
2.9. Charging assistant of FORWARDttc, [FOR19]. The system contains a new robot design with a CCS Type 2 connector developed for automated charging.	15
2.10. Drawings of selected patented ACD-S concepts. Left: Robot of [GMR ⁺ 16]. Middle: Robot arm coupled to a charging body, [EIL17]. Right: Moveable EV charging robot, [Zho15].	15
2.11. Left: Illustration of a patented coupling unit concept with a retractable guide from GM, [GMR ⁺ 16]. Right: Patent drawing of a connector system with a misalignment compensation module, [CON16b].	16
2.12. Left: ACD-U charging arm of VOLTERIO, [VOL18b]. Right: Matrix-charging from the company EASELINK, [EAS19].	17
2.13. Patent drawings of selected ACD-U concepts, [Bro18] and [MVD17].	18
2.14. Pantograph charging system for buses, [FRA19].	18
2.15. Percentage of numbers of plug-in electric vehicles in Austria, [AUS17].	20
2.16. Example of a typical EV component packaging, [VOL19a].	23

2.17. Examples of various EV charging and security cap systems. Beginning from the top, left: KIA Soul EV (2015), MERCEDES C350 Hybrid (2015), NISSAN Leaf (2010), PEUGEOT iON (2011), PORSCHE Panamera S Hybrid (2013) and BMW i8 (2015).	24
2.18. Left: CCS Type 2 connector. The connector contains seven pins - three pins for ground, proximity detection, control plot and two pins for DC power + and DC power -. Right: CCS Type 1 connector. Five pins are available for AC line 1, AC line 2, ground, proximity detection, control plot and two pins for DC power +, DC power -, [CON20] and [ELE19]	25
2.19. The big picture shows a possible stepwise development of CCS, [INI19].	26
2.20. ACD communication sequence draft of the ISO 15118 standard, [INT18a].	29
2.21. Number of charging stations in Europe from 2010 to 2019, [OBS20].	29
2.22. Driving range comparison in case of 15 minutes charging with different charging power levels.	30
2.23. Comparison of the required charging time for a driving range of 100 km with different charging power levels.	30
2.24. Evaluation of the current and target charging infrastructure with regard to various criteria, [VF17].	31
2.25. Shopping centre and rest stop concept for the year 2030 with customer-friendly comfort services, [WBH18].	32
2.26. Manual EV charging process with charging cables.	33
2.27. Top view of a charging lot model. Left: Backward parked EV and representation of the charging cable position. Right: Forward parked EV with representation of the charging cable position.	34
2.28. Left: Side view of a BMW i3 with closed charging socket cover. Middle: View of the CCS Type 2 inlet with unplugged Type 2 inlet plastic flap. Right: View of final cover position and unplugged plastic flaps.	34
2.29. Model of the charging cable plugging process by cut CAD-models of CCS charging inlet and -connector.	35
2.30. Left: Side view of the EV with an open charging lid and plugged charging cable. Middle: Side view of the EV during battery charging. Right: 11 kW charging station with two Type 2 charging cables.	36
2.31. Charging park concept with comfortable parking and charging lots, [VF17].	37
2.32. Development steps of the vehicle parking automation, [MOT19a], [Sys19], [Dum15] and [VOL19b]	38
2.33. Left: Vehicle parking processes result in different inlet positions (I_1 , I_2 and I_3). Right: Exemplary representation of reference coordinate systems of vehicle $\{V\}$, inlet $\{I\}$ and charging lot $\{R\}$	39
2.34. Beginning from left, image 1, 2 and 3: Parking bays for testing the parking accuracy of test drivers. Image 4: Charging pad and parking conditions for testing the parking accuracy over a charging par without parking aids, [BWY ⁺ 15].	40
2.35. Left: Detail view of marker and bump parking aids. Right: Position of marker, bump and mirror on a test parking lot, [BB11].	41

2.36. Results of longitudinal and transversal deviations of parking tests with parking position additives, [WHB19a]	43
2.37. Charging pad and positioning system of [BKHC15].	43
2.38. Input-processing-output-principle with intelligence, [Hau13].	45
2.39. Example of the TCP definition in a world coordinate system. Each component has its reference frame. The frames allow the positions and orientation determination to each other, [HMA10].	48
2.40. RPY coordinate system and exemplary roll-pitch-yaw rotation convention, [Vin17] and [HMA10].	49
2.41. Components coordinate system concept for the ACCS prototype.	51
2.42. ACCS prototype connector trajectory path concept.	51
2.43. Accepted collaborative robot forces and pressures for humans according to the duration of the action, [INT16].	53
2.44. Exemplary representation of a vehicle in the near and at the charging lot. Grey areas (I and II) illustrate the defined sensor working ranges for vehicle- and inlet detection.	54
2.45. Defined charging prototype sensor operating ranges for vehicle- and inlet detection according to different sensor technologies, which are categorized by <i>Mautz</i> , [Mau12].	55
2.46. Process steps of shape-based 3D-matching.	58
2.47. 3D-position detection by 2D-camera and 3D vehicle data, [JHB11].	58
2.48. Overview of vehicle-internal sensor technologies classified into their physical principle, according to [Bal16].	61
2.49. Exemplary representation of a vehicle-internal sensor working range for ACCS. Grey areas (I and II) illustrate the defined sensor working ranges for vehicle- and inlet detection.	62
3.1. ACCS prototype use cases for different charging socket positions and parking scenarios. Left: Use case I for front, left as well as rear, right EV charging socket positions (S1 and S2). Right: Use case II for front, right as well as rear, left charging sockets (S3 and S4).	70
3.2. Manual EV charging process with standardized cable technologies.	70
3.3. Sectional view of the CCS Type 2 charging inlet and -connector manual charging plugging process CAD-model.	71
3.4. Functional ACCS prototype system design.	74
3.5. ACCS prototype basic layout with working range and possible mounting area of actuator, as well as charging socket- and vehicle sensor.	75
3.6. ACCS prototype component coordinate systems layout.	76
3.7. Functional design model with representation of the ACCS components.	76
3.8. Requirements on vehicle classification.	78
3.9. Left: Exemplary representation of vehicle- and inlet positions at the ACCS prototype charging lot. Right: Inlet 3D-position frame-model.	79

3.10. ACCS charging cable plugging process by CAD-model sectional view of CCS charging inlet and -connector.	80
3.11. Corresponding CCS Type 2 inlet and connector contact edges and surfaces. . .	80
3.12. Left: Inlet CAD-model side view. Middle: Overlaid inlet and connector CAD-model sectional views representing the connection partners clearance. Right: Connector CAD-model side view.	81
3.13. Left: CCS Type 2 connector CAD-model. Right: CAD-models sectional views of connected CCS Type 2 inlet and connector.	81
3.14. CAD-model sectional view of connected inlet and connector with a X -axis rotation displacement of 3°	82
3.15. Left: Side view of connected inlet and connector CAD-models. Right: Sectional view A-A of with a Y -axis rotation displacement of 4°	82
3.16. Left: Side view of inlet and connector CAD-models in plugged position. Right: Sectional view A-A of with a Z -axis rotation displacement of 1.5°	83
3.17. Inlet positioning accuracy area represents 68.3% and 95.5% of parking tests. . .	84
3.18. ACCS prototype CAD-models represent inlet parking accuracy area and inlet sensor working range demands.	84
3.19. ACCS charging cable plugging process by a sectional view of CCS Type 2 charging inlet and -connector CAD-models.	86
3.20. ACCS prototype layout model with representation of charging inlet area and actuator range requirements.	87
3.21. Actuator cable path model for the phase <i>Pre-positioning</i> . Left: Charging lot and ACCS prototype top view. Right: Back view of the ACCS charging station.	87
3.22. Actuator force model for the cable phase <i>Pre-positioning</i> . Left: Forces on actuator head reference TCP. Right: Force model to determine the actuator force F_A	88
3.23. Actuator force model for the <i>Plugging</i> cable phase. Left: Forces on the actuators head. Right: Force model to determine the actuator force F_A	89
3.24. Preselection of ACCS vehicle and inlet detection sensor technologies.	91
3.25. Evaluation score results for vehicle-external sensor technologies for vehicle position detection and classification.	92
3.26. Evaluation score results for different vehicle-internal sensors.	93
3.27. Evaluation score results for inlet position detection sensor technologies.	94
3.28. CCS Type 2 inlet area for ACCS prototype shape-based 3D-matching.	95
3.29. Projected inlet shape and dimensions in an image due to X -, Y - and Z -axis rotation in relation to the 2D-camera.	95
3.30. Recognition process including devices and procedures for vehicle-, charging start trigger- and inlet 3D-position detection recognition.	97
3.31. Left: Charging socket sensor working range concept. Right: 2D-image of a rear, right vehicle wheel fender and charging cover.	98

3.32. ACCS concept side view with an exemplary representation of an inlet frame and the field of view of the 2D-vision sensors, [WHB19c]. Left: Field of view of Camera 1 and Camera 2 at process step <i>Recognition II</i> . Right: Field of view of Camera 3 at process step <i>Recognition III</i>	98
3.33. Steps of the automated charging process.	100
3.34. Left: Rear, right wheel fender of a BMW i3. Right: Different views of the fender 3D-CAD model for shape-based 3D-matching.	101
3.35. Left: Picture of a test vehicle's CCS Type 2 inlet. Right: Example of detected edges (orthogonal lines in relation to the examination line) by using grey value curve analyses.	102
3.36. Left: Gray value function applied on a pixel examination line. Right: First derivation of the gray value function.	103
3.37. Left: CAD-model as template for shape-based 3D-matching. Right: Matching result of an image from the robot-head mono camera.	104
3.38. Left: Example for shadow on the charging inlet. Right: Example of uniform light conditions that leads to a good image contrast.	104
3.39. Examples of inlet camera images without and with LED light support.	105
3.40. Left: Coordinate systems (frames) of robot base $\{B\}$, Camera 1 $\{C1\}$ and 2 $\{C2\}$ and inlet $\{I\}$. Right: Robot head detail view with the frame representation of robot tool $\{T\}$, Camera 3 $\{C3\}$ and connector $\{C\}$	105
3.41. ACCS prototype control processes in MATLAB.	107
3.42. Exemplary robot path during cable docking and plug-in for three various charging inlet positions, [WHB19c, p.10].	108
3.43. Data processing architecture overview.	108
3.44. Data processing in the HALCON script code.	109
3.45. Data processing in the MATLAB script code.	110
3.46. Left: CCS Type 2 EV coupling (IEC 62196-3). Right: Replaceable face of the CCS Type 2 connector.	111
3.47. Affected CCS Type 2 connector face areas by the modifications for easier cable plugging.	112
3.48. Left: Front view of the CCS Type 2 face CAD-model. Right: Cross-sectional view (C-C) of the CCS Type 2 face CAD-model.	112
3.49. Process steps comparison of the ACCS prototype and the ACD communication sequence draft of the ISO 15118, [INT18a] standard.	114
3.50. Left: CAD-model of the charging station prototype. Right: CAD-model of the robot head tool with CCS Type 2 connector, camera, LED, actuator and adapters.	116
3.51. The collaborative 6-axes robot Universal Robot UR10-CB3 with technical specifications, [ROB17] and [RPBL18].	117
3.52. Left: IDS 2D-Camera UI-5240CP-C-HQ Rev.2. Middle: Lens model LENSAGON C3M0616V2 1/1.8": 6 mm focal length, 60.1° horizontal and 46.6° vertical angle of view, [LEN19]. Right: Lens model TAMRON M118FM06 1/1.8": 6 mm focal length, 66.1° horizontal and 50.8° vertical angle of view, [TAM19].	117

3.53. Left: 35 Watt LED from Goobay, [GOO20]. Right: GENESIS SMD5050 round LED, [GEN20].	118
3.54. Left: Linear actuator ACTUONIX P16-100-22-12-P, [ACT17]. Right: ARDUINO UNO REV3 microcontroller board, [ARD19].	118
3.55. CCS Type 2 EV-T2M4CC-DC200A charging cable from Phoenix Contact, [CON16a].	118
4.1. ACCS prototype test case I and II for different EVs and charging socket positions.	122
4.2. Left: Exemplary presentation of the vehicle position with 15° angular deviation. Right: Representation of the inlet test positions to evaluate the functionality and robustness of the charging station prototype, [WHB19c].	124
4.3. Cable connection and disconnection time box plots for 6 basic vehicle positions. Left: Cable connection. Right: Cable disconnection.	125
4.4. Cable plug-in time box plot for various vehicle angle offsets.	126
4.5. Exemplary section of the charging connecting sequence. Left: Robot during inlet 3D-pose detection with Camera 3. Middle: CCS Type 2 connector axis aligns with the vehicle charging inlet axis. Right: Robot during the cable insertion process.	127
4.6. Left: Example of a vehicle position deviation $\alpha = 15^\circ$ (top view) Right: Resulting inlet positions of 34 practised and unpractised test drivers.	128
4.7. Box plots of the resulting inlet positions of 34 test drivers. Left: Inlet position in robot X -axis. Right: Inlet position in robot Y -axis.	128
4.8. Box plot of the resulting inlet Z -axis position and rotation deviation of 34 test drivers.	129
4.9. Box plots of the automated connection and disconnection duration of 22 test drivers.	129
4.10. Left: TESLA charging socket positioned at the vehicle rear, left side, [WAU20]. Right: Charging inlet detail view and representation of the inlet shape curvature [Sch20].	130
4.11. Test case of subsequent charging of two different vehicles (Step 1, Step 2 and Step 3) and possible future scenario of charging a number of EVs.	131
4.12. Left: EV charging station at campus of Graz University of Technology. Right: Charging station outdoor test setup.	132
A.1. BMW i3 60 Ah, battery capacity 18.8 kWh, real range 130 km, energy consumption 14.5 kWh/100km, [DAT19]. The CCS Type 2 charging inlet of the vehicle serves as the main test object for ACCS prototype functionality. In addition, the vehicle was used for parking tests on the prototype charging lot.	147
A.2. BMW i3 94 Ah, battery capacity 27.2 kWh, real range 170 km, energy consumption 16 kWh/100km, [DAT19]. The EV was used as 2 nd test object in the scenario of subsequently performed automated charging of different vehicles.	147

A.3. TESLA Model 3 standard version, battery capacity 53 kWh, WLTP range 409 km, energy consumption 14.1 kWh/100km, 0-100 km/h in 5.6 seconds, [TES20b]. The EV was the 4 th ACCS prototype test EV. The EV offers automated charging lid opening and closing.	147
A.4. HYUNDAI IONIQ Electro, battery capacity 38 kWh, WLTP range 294 km, energy consumption 13.8 kWh/100km, 0-100 km/h in 9.9 seconds, [HYU18a]. The vehicle served as the 5 rd ACCS prototype test EV.	148
A.5. VOLKSWAGEN e-Golf, battery capacity 35.8 kWh, WLTP range 231 km, energy consumption 15.8 kWh/100km, [VOL18a]. The EV served as the 3 rd ACCS prototype test EV.	148
A.6. The shunting aid enables easy vehicle moving. 4 shunting aids were used for lifting the test EVs to different cable-plugging test positions, [REA19].	148
A.7. Mobile workstation DELL Precision M4800. Software platform Windows 10 Pro, processor Intel Core i7 fourth generation, main memory 16 GB, graphics NVIDIA Quadro K1100M with 2 GB GDDR5 memory, hard disk storage 500 GB SATA with 6 Gbit/s, [DEL19]. The tasks of the work station include vision detection and robot control processes as well as test recording and documentation during the ACCS prototype tests.	149

List of Tables

2.1. Selection of BEVs in the year 2019 in Austria.	21
2.2. Examples of various EVs and their charging- and security cap system.	25
2.3. Technical data of different charging cables, [CON20].	27
2.4. Contents and description of the ISO 15118 standard parts, [INT13].	28
2.5. Parking position accuracy results from a study with 100 participants, [BWY ⁺ 15].	40
2.6. Parking position accuracy achieved by 90% of the subjects grouped into longi- tudinal, transversal and angle deviation, [BB11].	42
2.7. Parking accuracy test results with middle charging pad position and straight forward parking, [BB11].	42
2.8. Parking accuracy test results with parking aids from [SMC ⁺ 13].	42
2.9. Properties of serial and parallel robot systems, [HMA10]	46
2.10. Properties and performance parameters of selected robot systems.	47
2.11. Comparison of 3D-imaging technologies according to [Li14].	60
2.12. Comparison of automated inductive and conductive charging as well as battery swapping in terms of technical criteria.	65
2.13. Comparison of automated inductive and conductive charging as well as battery swapping in terms of commercial, economic and user practice criteria.	66
3.1. ACCS prototype use case requirements.	70
3.2. ACCS prototype requirements of the charging process.	72
3.3. ACCS prototype requirements of boundary conditions and demands.	73
3.4. Supporting ACCS requirements.	73
3.5. Connection of ACCS prototype components, -requirements and -objects.	77
3.6. ACCS prototype charging lot requirements.	77
3.7. ACCS prototype vehicle detection requirements.	78
3.8. ACCS prototype charging start trigger requirements.	79
3.9. ACCS prototype inlet sensor detection requirements.	85
3.10. ACCS prototype actuator requirements.	90
3.11. ACCS prototype system control requirements.	90
3.12. Sensor evaluation criteria and their weighting for vehicle detection and classifi- cation.	92
3.13. Criteria and their weighting for vehicle-internal sensor systems.	93
3.14. Criteria weighting for inlet 3D-pose detection sensor systems.	94
3.15. 2D-camera accuracy due to inlet rotation angles in relation to the 2D-camera. .	95
3.16. ACCS prototype inlet detection 2D-camera requirements.	96
3.17. ACCS prototype vehicle detection 2D-camera requirements.	97

3.18. Constant translational and rotational transformations between robot system component frames.	106
3.19. Exemplary charging inlet positions with reference to the robot base $\{B\}$	107
3.20. ACCS CCS Type 2 inlet detection requirements without and with connector modifications.	113
3.21. Process steps of the ACCS prototype charging process in comparison to ISO 15118, example sequence illustrating ACD energy transfer procedure.	114
4.1. ACCS prototype test EVs, [BMW19], [HYU18a], [TES20b], [VOL18a].	121
4.2. Summary of the plug-in motion experiment results, [WHB19c].	124
4.3. LEDs activation behaviour at different positions and vehicle angle misalignments.	126
4.4. Test vehicle properties for the series charging scenario.	131
A.1. Overview of localization systems using sound waves with performance parameters. In comparison to other position technologies, properties and performance parameters of various sound systems are quite similar. The techniques can be separated into active and passive device systems. Active systems transmit scheduled ultrasonic pulses between mobile devices. A passive system includes a receiver that captures signals from fixed installed transmitters. The advantage is the anonymity of the receiver, [Mau12].	142
A.2. Performance characteristics of tactile and combined polar systems. Tactile systems measure the position of an object by touching them with a calibrated probe. Combined polar systems use rotating beams and <i>Time of Arrival</i> (ToA) principles or optical or mechanical encoders. Determined object angles and distances enable the creation of a complete 3D-scene, [Mau12].	142
A.3. Evaluation scores results of vehicle-external and -internal sensor technologies for the determination of the vehicle position on a charging lot and the charging inlet 3D-position.	142
A.4. Selection of standards and guidelines for robotics. Robots are flexible and complex mechatronic machines. Robot manufacturers have to ensure all directives and standards, which also exist for other electrical devices and controls as well as for software and mechanical machines. Depending on the application, specific standards must also be taken into account, e.g. when using robots in clean rooms, cells in the food sector or for the combination with laser applications. Furthermore, specific safety regulations apply to robots, [HMA10].	143
A.5. Prototype requirements for standardized cable-based charging technologies.	144
A.6. Overview of of commercially depth cameras and range scanners based on <i>Time-of-Flight</i> (ToF) technologies with performance parameters. The manufacturers do not specify the depth accuracy. This is due to the accuracy dependence on various factors, e.g. object surface, illumination or frame rate, [HHEM16]	144
A.7. Criteria rating of vehicle-external sensor systems. A suitable sensor system has been chosen by an evaluation with according to the listed criteria. Its weighting indicates the importance of each criterion.	144

A.8. Criteria rating of vehicle-internal sensor systems. Vehicle sensors such as 2D- and 3D-cameras have been evaluated according the listed criteria regarding vehicle position determination on a charging lot. 145

A.9. Criteria rating of selected sensor techniques for the charging inlet position detection. The most important criteria are inlet 3D-pose detection, costs, performance at different light conditions as well as necessary vehicle adaptations. . . . 145

A.10. Summary of the prototype charging process LEDs behaviour evaluation. The results show the behaviour at different vehicle parking positions and angles in the different recognition processes II and III. 146

Bibliography

- [ABB18] ABB. TOSA flash-charging e-bus. Available at <https://new.abb.com>, 2017. Accessed on 10.9.2018.
- [ACT17] ACTUONIX. Technical data linear actuator ACTUONIX P16-100-22-12-P-LAC. Available at <https://s3.amazonaws.com/actuonix/Actuonix+L16+Datasheet.pdf>, 2019. Accessed on 4.2.2017.
- [ARD19] ARDUINO. Technical data ARDUINO UNO. Available at <https://store.arduino.cc/arduino-uno-rev3>, 2019. Accessed on 2.1.2019.
- [AUS17] STATISTIK AUSTRIA. Anzahl der Neuzulassungen von Elektroautos in Österreich von 2008 bis 2016. Available at <https://de.statista.com/statistik/daten/studie>, 2016. Accessed on 30.5.2017.
- [AUS18] STATISTIK AUSTRIA. Kraftfahrzeuge - Bestand Österreich. Available at <https://www.statistik.at>, 2018. Accessed on 31.10.2018.
- [AUS19] PORSCHE AUSTRIA. Product information AUDI e-tron. Available at <https://www.audi.at/media>, 2018. Accessed on 11.1.2019.
- [Bal16] P. Balzer. Fahrzeugumfeldsensorik: Überblick und Vergleich zwischen Lidar, Radar, Video. Available at <https://www.cbcity.de/fahrzeugumfeldsensorik-ueberblick-und-vergleich-zwischen-lidar-radar-video>, 2016. Accessed on 15.11.2016.
- [Bau18] U. Baumann. Plug-in-Hybridmodelle kabellos laden - Induktives Ladesystem von BMW ab 3.200 Euro. Available at <https://www.auto-motor-und-sport.de/>, 2018. Accessed on 31.10.2018.
- [BB11] H. Barth and M. Braun. Abschlussbericht zum Verbundvorhaben - Kontaktloses Laden von Elektrofahrzeugen (W-Charge). Technical Report 1, Fraunhofer IWES, Kassel, 27 October 2011.
- [BB15] W. Burger and M.J. Burge. *Digitale Bildverarbeitung: Eine algorithmische Einführung mit Java*. Springer Vieweg, Berlin and Heidelberg, 3. edition, 2015.
- [BH12] H. Brunner and M. Hirz. Neugestaltung der Automobile. Report 1: Urbaner Personenverkehr – Rahmenbedingungen für neue Fahrzeugkonzepte. Institute of Automotive Engineering, University of Technology Graz. Graz, 2012.
- [BKHC15] A. Barkow, J. Küfen, J. Hudecek, and F. Christen. Positionierungssystem für induktives laden. in proceedings of atz-automobiltechnische zeitschrift, volume 117, issue 7-8. pages 46–51. Springer, July 2015.

- [Bla20] S. Blanco. Chinas NIO making EV battery swapping work. Available at <https://www.sae.org/news/2019/01/nio-ev-battery-swapping>, September 2019. Accessed on 19.2.2020.
- [BMW18] BMW. BMW Wireless Charging. Available at <https://www.bmw.de>, 2018. Accessed on 17.1.2018.
- [BMW19] BMW. Technical data BMW i3 and BMW i3s. Available at <https://www.bmw.de/de/neufahrzeuge/bmw-i/i3/2017/technische-daten.htmltab-0>, 2019. Accessed on 4.11.2019.
- [BNRH13] K. Bozem, A. Nagl, V. Rath, and A. Haubrock. Elektromobilität: Kundensicht, Strategien, Geschäftsmodelle: Ergebnisse der repräsentativen Marktstudie FUTURE MOBILITY. Springer-Verlag, Wiesbaden, 1. edition, 2013.
- [BOS13] BOSCH. Chassis Systems Control - Fahrerassistenzsysteme: Wie viel Unterstützung wünschen deutsche Autofahrer? Report. Robert BOSCH GmbH. Germany, 2013.
- [Bro18] W. Brown. Method and apparatus for automatic charging of an electrically powered vehicle, US patent number 9,873,347. Grant 23 January 2018.
- [BS13] H.H. Braess and U. Seiffert. Vieweg Handbuch Kraftfahrzeugtechnik. ATZ/MTZ-Fachbuch. Springer Vieweg, Wiesbaden, 7. edition, 2013.
- [Böt19] U. Böttger. Autonomer Ladeassistent für Elektrofahrzeuge. Available at <https://industrieanzeiger.industrie.de/themen/robotics-award>, 2019. Accessed on 4.4.2019.
- [BWY⁺15] S. Birrell, D. Wilson, C. P. Yang, G. Dhadyalla, and P. Jennings. How driver behaviour and parking alignment affects inductive charging systems for electric vehicles. volume 58, pages 721–731. Elsevier, 2015.
- [CHA18] CHARGELOUNGE. CHARGE LOUNGE - charge future. Available at <http://www.chargelounge.eu>, 2019. Accessed on 7.11.2018.
- [CNK13] H. Matsubara S. Kato C. Niclass, M. Soga and M. Kagami. A 100-m range 10-frame/s 340 96-pixel time-of-flight depth sensor in 0.18-cmos. In *IEEE Journal of Solid-State Circuits*, 2013.
- [COM14a] INTERNATIONAL ELECTROTECHNICAL COMISSION. IEC 62196-3:2014: Plugs, socket-outlets, vehicle connectors and vehicle inlets - Conductive charging of electric vehicles - Part 3: Dimensional compatibility and interchangeability requirements for d.c. and a.c./d.c. pin and contact-tube vehicle couplers, International Standard, July 2014.
- [COM14b] INTERNATIONAL ELECTROTECHNICAL COMISSION. IEC61851-23:2014: Electric vehicle conductive charging system - Part 23: DC electric vehicle charging station, International Standard, March 2014.

- [COM14c] INTERNATIONAL ELECTROTECHNICAL COMMISSION. IEC61851-24:2014: Electric vehicle conductive charging system - Part 24: Digital communication between a d.c. EV charging station and an electric vehicle for control of d.c. charging, International Standard, March 2014.
- [CON16a] PHOENIX CONTACT. Technical data PHOENIX CONTACT CCS Type 2 connector. Available at <https://www.phoenixcontact.com>, 2016. Accessed on 5.8.2016.
- [CON16b] PHOENIX CONTACT. Steckverbinderteil mit einer Ausgleichseinrichtung. Patent number DE 10 2015100452 A1. Grant 14 January 2016.
- [CON17] PHOENIX CONTACT. High Power Charging - CCS-based fast charging with up to 500 A. Phoenix Contact GmbH and Co. KG. 16 August 2017.
- [CON20] PHOENIX CONTACT. Technical data PHOENIX CONTACT charging cables. Available at <https://www.phoenixcontact.com>, 2020. Accessed on 2.2.2020.
- [DAT19] ELECTRIC VEHICLE DATABASE. Technical data of BMW i3 with 60 Ah battery. Available at <https://ev-database.org/car/1004/BMW-i3-60-Ah>, 2019. Accessed on 29.10.2019.
- [DEL19] DELL. Technical specifications DELL Workstation Precision M4800. Available at <https://www.dell.com/>, 2014. Accessed on 10.8.2019.
- [DMR⁺16] G. Dalong, N.D. Mckay, M. Reiland, S. Foucault, M. Lacasse, T. Laliberte, B. Mayer-St-Onge, A. Lecours, C. Gosselin, and D. Milburn. Robotically operated vehicle charging station, 23 February 2016. US Patent 9,266,440.
- [DOR15] TECHNISCHE UNIVERSITÄT DORTMUND. Ladesystem der TU-Dortmund betankt Elektroautos automatisch. Available at <http://www.e-technik.tu-dortmund.de>, 2015. Accessed on 20.6.2015.
- [Dro19] W. Dron. This is what charging an electric car looked like in 1912. Available at <https://www.driving.co.uk>, 2018. Accessed on 1.3.2019.
- [Dum15] B. Dumaine. Robot garage parks your car. Available at <http://nicolasrapp.com/wp-content/uploads/2013/03/parking.jpg>, 2013. Accessed on 1.4.2015.
- [EAS19] EASELINK. EASELINK - The new standard for automatic charging. Available at <http://easelink.com>, 2019. Accessed on 1.10.2019.
- [ECO16] ECOMENTO. Elektroautoprojekt Better Place meldet Insolvenz an. Available at <https://ecomento.de>, May, 2013. Accessed on 19.5.2016.
- [EI18] EV-INSTITUTE. Plug-In Around the EV World. EV-INSTITUTE (EVI). Available at <http://ev-institute.com/images/>, 2018. Accessed on 2018.
- [EIL17] W. E-In and Hon Hai Precision Industry Co Ltd. Battery charging system and apparatus and method for electric vehicle. US Patent 9,662,995. 2017.

- [ELE19] ELECTRIFY AMERICA. News and Updates. Available at <https://www.electrify-america.com/news-updates>, 2019. Accessed on 15.1.2019.
- [ELE20] ELECTREK. EV battery swapping is dead in US, but China wants to make it happen. Available at <https://electrek.co>, Januray 17, 2020. Accessed on 19.2.2020.
- [Elk13] N. Elkmann. Sichere Mensch-Roboter-Kooperation: Normenlage, Forschungsfelder und neue Technologien. *Journal of Zeitschrift für Arbeitswissenschaft*. volume 67, pages 143–149. Springer, 2013.
- [ENE12] FORSCHUNGSSTELLE FÜR ENERGIEWIRTSCHAFT. Alltagstauglichkeit des induktiven Ladens. Technical report, Forschungsstelle für Energiewirtschaft e.V. (FfE), Munich, Germany, Februar 2012.
- [ENE19] US DEPARTEMENT OF ENERGY. Timeline: History of the electric car. Available at <https://www.energy.gov/timeline/timeline-history-electric-car>, 2019. Accessed on 1.3.2019.
- [EPA20] EPAL. EPAL EUROPALETTE (EPAL) - The pallet system. Available at <https://www.epal-pallets.org/eu-de/>, 2020. Accessed on 2.2.2020.
- [E.V19] CHARIN E.V. Position Paper of Charging Interface Initiative e.V. Automatic Connection Device Interface for automatic conductive charging. Berlin, 2019.
- [FCC10] V. Filonenko, C. Cullen, and J. Carswell. Investigating Ultrasonic Positioning on Mobile Phones. In *Proceedings of the 2010 International Conference on Indoor Positioning and Indoor Navigation (IPIN)*, 2010.
- [FEL10] M. Weber F. Eisenführ and T. Langer. Rationales Entscheiden. Springer, Berlin, 5. edition, 2010.
- [Fer16] A. Fereshteh. UR5 Control Using Matlab. Matlab Script Code. Available at <https://www.mathworks.com>, 2015. Accessed on 10.9.2016.
- [FOR19] FORWARDTTC. KUKA AG case study - Ladeassistent für Elektrofahrzeuge. Available at <https://www.forward-ttc.de>, 2019. Accessed on 2.7.2019.
- [FOT16] FOTONIC. FOTONIC E-series product specifications, 2016.
- [FRA18] FRAUNHOFER-INSTITUT FÜR VERKEHRS- UND INFRASTRUKTURSISTEME (IVI). EDDA-Bus - Schnellladefähiger Batteriebus für den Linienbetrieb in Städten. Available at <https://www.edda-bus.de/>, 2018. Accessed on 7.11.2018.
- [FRA19] FRAUNHOFER-INSTITUT FÜR VERKEHRS- UND INFRASTRUKTURSISTEME (IVI). Schnellladefähiger Elektrobus - Das Docking-Prinzip. Available at <https://www.ivi.fraunhofer.de>, 2019. Accessed on 7.7.2019.
- [GEN20] GENESIS. Technical manual LED GENESIS SMD5050. Available at <https://www.conrad.at>, 2020. Accessed on 4.2.2020.

- [GMR⁺16] D. Gao, N. McKay, M. Reiland, S. Foucault, M. Lacasse, T. Laliberte, B. Mayer-St-Onge, A. Lecours, C. Gosselin, D. Milburn, et al. Robotically operated vehicle charging station. US Patent 9,266,440, Grant 5 December 2016.
- [GOI20] GOINGELECTRIC. GOINGELECTRIC Wiki - Ladung und Ladestecker. Available at <https://www.goingelectric.de/wiki/Ladung-und-Ladestecker>, Accessed on 2.1.2020.
- [GOO20] GOOBAY. LEDs light manual. Available at <https://www.conrad.at>, 2020, Accessed on 4.2.2020.
- [GT12] B. Geringer and W. Tober. Batterieelektrische Fahrzeuge in der Praxis - Kosten, Reichweite, Umwelt, Komfort. Österreichischer Verein für Kraftfahrzeugtechnik, 2. edition, October 2012, Vienna, Austria, 2012.
- [GT15] B. Geringer and W. Tober. Plug-In Hybridfahrzeuge in der Praxis: Energiebedarf und Reichweite. Österreichischer Verein für Kraftfahrzeugtechnik (ÖVK), 2015, Vienna, Austria, 2015.
- [Haa17] F. Haas. Industrieroboter. Script. volume 4. Institute of Production Engineering, University of Technology Graz. Graz, 2017.
- [Hal62] A. Hall. A methodology for systems engineering. Van Nostrand, Princeton N.J., 1962.
- [Hal20] B. Halvorson. NIO is providing a fully charged battery in 3 minutes for free, in China. Available at <https://www.greencarreports.com>, August 2019. Accessed on 19.2.2020.
- [Hau13] M. Haun. Handbuch Robotik: Programmieren und Einsatz intelligenter Roboter. Springer Vieweg, Berlin and Heidelberg, 2. edition, 2013.
- [HB02] R. Harle and A. Beresford. The Bat System - Ubiquitous Computing in Action. Laboratory for Communications Engineering University of Cambridge., 2002.
- [HEX20] HEXAMITE. HEXAMITE 3D ultrasound positining systems. Available at <http://www.hexamite.com>, 2020. Accessed on: 30.05.2020.
- [HH11] S. Hollar and E. Hollar. System to automatically recharge vehicles with batteries, US Patent 7,999,506. Grant 16 August 2011.
- [HHEM16] R. Horaud, M. Hansard, G. Evangelidis, and C. M  nier. An overview of depth cameras and range scanners based on time-of-flight technologies. In *Proceedings of Machine vision and applications*, pages 1005–1020. Springer Berlin Heidelberg, 16 June 2016.
- [Hir17] W. Hirschl. Untersuchungen zum Zeit-, Wege- und CO2-Sparpotentials durch Autonomes Parken. Bachelor Thesis. Institute of Automotive Engineering, University of Technology Graz. Graz, 2017.

- [HJE⁺11] R. Horvath, B. Jensen, N. Elsmo, H. Rusk, and D. Andrews. Automated electric plug-in station for charging electric and hybrid vehicles. US Patent 12,586,047. Grant 17 March 2011.
- [HMA10] S. Hesse, V. Malisa, and A. Almansa. Taschenbuch Robotik - Montage - Handhabung. Fachbuchverlag Leipzig im Carl-Hanser-Verlag, München, 2010.
- [HMP⁺13] M. Hödlmoser, B. Micusik, M. Pollefeys, M. Liu, and M. Kampel. Model-based vehicle pose estimation and tracking in videos using random forests. In *2013 International Conference on 3D Vision-3DV 2013*, pages 430–437. IEEE, 2013.
- [Hor18] J. Horn. Infrastruktur für elektrische Fahrzeuge, June 4, 2018.
- [HY00] K. Hayashi, K. and Uchibori and A. Yamamoto. Battery charging apparatus for electric vehicles. US Patent 6,157,162. Grant 5 December 2000.
- [HYU18a] HYUNDAI. Technical data and specifications HYUNDAI IONIQ Electro. Available at <https://www.hyundai.at>, 2019. Accessed on 10.09.2018.
- [HYU18b] HYUNDAI. Technical data and specifications HYUNDAI KONA. Available at <https://www.hyundai.at>, 2019. Accessed on 28.11.2018.
- [IDS19] IDS. Technical data of the UI-5240CP Rev.2 camera. Available at <https://de.ids-imaging.com/store/ui-5240cp-rev-2.html>, 2014. Accessed on 10.8.2019.
- [IMA16] MESA IMAGING. SR4000 and SR4500 User Manual. Zürich, 2016.
- [ING88] VEREIN DEUTSCHER INGENIEURE. VDI 2861: Assembling and handling; characteristics of industrial robots; designation of coordinates. Technical Guideline. VEREIN DEUTSCHER INGENIEURE (VDI) and Gesellschaft Produktionstechnik. VDI-Verlag, Düsseldorf, 1988.
- [INI19] CHARGING INTERFACE INITIATIVE. The functional-temporal CCS Step Model. Charging Interface Initiative e. V. (CharIn). Available at <https://www.charinev.org>, 2019. Accessed on 15.2.2019.
- [INS10] DEUTSCHES CLEANTECH INSTITUT. E-Mobilität: CleanTech-Branche; Treiber im Fokus, volume 4. 2010.
- [INT13] INTERNATIONAL STANDARD ORGANIZATION. ISO 15118-2013: Road vehicles - Vehicle to grid communication interface Part 1-8:. International Standard, Technical Committee: ISO/TC 22/SC 31. 2013.
- [INT16] INTERNATIONAL STANDARD ORGANIZATION. ISO 15066:2016-02, Robots and robotic devices - Collaborative robots. International Standard, 1. edition, Technical Committee : ISO/TC 299, 2016.
- [INT18a] INTERNATIONAL STANDARD ORGANIZATION. ISO 15118-1: Road vehicles - vehicles to grid communication interface, Part 1-8. Standard Draft, Technical Committee: ISO/TC 22/SC 31. 2018.

- [INT18b] INTERNATIONAL STANDARD ORGANIZATION. ISO 15118-8:2018: Road vehicles - Vehicle to grid communication interface - Part 8: Physical layer and data link layer requirements for wireless communication. International Standard, Technical Committee: ISO/TC 22/SC 31. 2018.
- [INT18c] INTRASOL. E-Ladepark - Tankstelle der Zukunft - Kundenfreundlich. Leistungsstark. Zukunftssicher. Available at <https://www.amperio.eu/wp-content/uploads/>, 2019. Accessed on 15.11.2018.
- [INT19] INTERNATIONAL STANDARD ORGANIZATION. ISO 15118-1:2019: Road vehicles - Vehicle to grid communication interface - Part 1: General information and use-case definition. International Standard, Technical Committee: ISO/TC 22/SC 31. 2019.
- [ION19] IONITY. THE POWER OF 350 KW. Available at <https://ionity.eu>, 2019. Accessed on 15.1.2019.
- [ITE20] ITEM. Der item MB Systembaukasten. Available at <https://at.item24.com>, 2020. Accessed on 18.2.2020.
- [J. 16] J. Hedderich, and L. Sachs. *Angewandte Statistik: Methodensammlung mit R*. Springer Verlag, 2016.
- [JAG18] JAGUAR. Technical data and specifications JAGUAR i-Pace. Available at <https://www.jaguar.at/jaguar-range/i-pace>, 2018. Accessed on 2.12.2018.
- [Jäh12] B. Jähne. *Digitale Bildverarbeitung und Bildgewinnung*. Springer-Verlag, Berlin and Heidelberg, Germany, 7. edition, 2012.
- [Jer19] B. Jerew. Sad News: Battery Swapping Company Better Place Goes Bankrupt. Available at <https://www.greenoptimistic.com>, May 27, 2013. Accessed on 10.09.2019.
- [JHB11] S. Jayawardena, M. Hutter, and N. Brewer. A novel illumination-invariant loss for monocular 3d pose estimation. In *2011 International Conference on Digital Image Computing: Techniques and Applications*, pages 37–44. IEEE, 2011.
- [JSP⁺09] A. Jimenez, F. Seco, C. Prieto, J. Roa, and K. Koutsou. A Survey of Mathematical Methods for Indoor Localization. In *6th IEEE International Symposium on Intelligent Signal Processing (WISP 2009)*, Budapest, Hungary. 2009.
- [KH09] M. Kloess and R. Haas. Entwicklung von Szenarien der Verbreitung von PKW mit teil- und vollelektrifiziertem Antriebsstrang unter verschiedenen politischen Rahmenbedingungen. ELEKTRA-Project final Report. Institute of Energy Systems and Electrical Drives, Energy Economics Group, University of Technology Vienna, Vienna, Austria, 31 August 2009.
- [KH15] S. Kümmell and M. Hillgärtner. Inductive charging comfortable and nonvisible charging stations for urbanised areas. In *E-Mobility in Europe*, pages 297–309. Springer, 28 April 2015.

- [Kle11] F. Kley. Ladeinfrastruktur für Elektrofahrzeuge: Entwicklung und Bewertung einer Ausbaustrategie auf Basis des Fahrverhaltens. ISI-Schriftenreihe "Innovationspotenziale". Fraunhofer Verlag, Stuttgart, 2011.
- [Kol93] D. Koller. Moving object recognition and classification based on recursive shape parameter estimation. In *Proc. 12th Israel Conf. Artificial Intelligence, Computer Vision*, volume 2728, page 2, 1993.
- [LEN19] LENSAGON. Technical data of the lens LENSAGON C3M0616V2. Available at <https://www.lensation.de/product/C3M0616V2/>, 2014. Accessed on 10.8.2019.
- [LFK15] W. Leal Filho and R. Kotter. E-Mobility in Europe: Trends and good practice. Green energy and technology. Springer, London, 2015.
- [Li14] L. Li. Time-of-Flight Camera - An Introduction. Texas Instruments, Texas. Mai 2014.
- [LSS08] J. Liebelt, C. Schmid, and K. Schertler. independent object class detection using 3d feature maps. In *2008 IEEE Conference on Computer Vision and Pattern Recognition*, pages 1–8. IEEE, 2008.
- [MAM10] M. M. Alloulah and Hazas M. An efficient CDMA core for indoor acoustic position sensing. In *Indoor Positioning and Indoor Navigation (IPIN)*, 2010. pages 1–5. IEEE Publishing, September 2010.
- [MAN18] CENTER OF AUTOMOTIVE MANAGEMENT. Entwicklung der Elektromobilität bis 2030. Available at <https://auto-institut.de/studienvorjahre.htm>, 2018. Accessed on 1.11.2018.
- [Mau12] R. Mautz. Geodätisch-geophysikalische Arbeiten in der Schweiz: Indoor Positioning Technologies, volume 86 of *Geodätisch-geophysikalische Arbeiten in der Schweiz*. Zürich, 2012.
- [MCH⁺05] A. Mandal, C. Givargis, A. Haghighat, R. Jurdak, and P. Baldi. Beep: 3D Indoor Positioning Using Audible Sound. In *Proceedings of the Consumer Communications and Networking Conference (CCNC 2005), IEEE Xplore*, 2005.
- [MED19] TIMEBANDIT MEDIA. Mein Elektroauto. Available at <http://www.meinelektroauto.com>, 2015. Accessed on 1.2.2019.
- [MIC20] MICROSOFT. Kinect for Windows. Available at: <https://developer.microsoft.com>, 2020. Accessed on 01.04.2020.
- [MMN⁺16] A. Markis, H. Montenegro, M. Neuhold, A. Oberweger, C. Schlosser, C. Schwald, F. Sihl, W. and; Ranz, T. Edmayr, P. Hold, and G. Reisinger. *Sicherheit in der Mensch-Roboter-Kollaboration: Grundlagen, Herausforderung, Ausblick*. TÜV AUSTRIA Holding AG and Fraunhofer Austria Research GmbH, 10 October 2016, Vienna, Austria, 2016.

- [MOT19a] THE OLD MOTOR. Vertical Parking Lots. Available at <http://theoldmotor.com>, 2019. Accessed on 2.1.2019.
- [MOT19b] GENERAL MOTORS. GENERAL MOTORS and the electric car: 100 years of invention and innovation. Available at <https://artsandculture.google.com>, 2019. Accessed on 1.3.2019.
- [MSH19] D. Mehta, P. Sapun, and A. Hamke. In-depth: eMobility 2019, Statista Mobility Market Outlook. Technical Report. Statista, Hamburg, February 2019.
- [MVD17] J. Mardall and C. Van Dyke. Charging station providing thermal conditioning of electric vehicle during charging session. US Patent 9,527,403. Grant 27 December 2017.
- [MVT17a] MVTEC. HALCON Solution Guide I - Basics. HALCON Manual, Version 12.0.2, Edition 5a. MVTec Software GmbH, München, Germany, 2017.
- [MVT17b] MVTEC. HALCON Solution Guide III-C 3D Vision. HALCON Manual, Version 12.0.2, Edition 7a. MVTec Software GmbH, München, Germany, 2017.
- [MVT17c] MVTEC. HALCON/HDevelop Reference Guide 13.0.2. HALCON Manual, Version 13.0.2, Edition 14a. MVTec Software GmbH, München, Germany, 2017.
- [MVT17d] MVTEC. HALCON Version 13.0.1, Vision Software, MVTec Software GmbH. MVTec Software GmbH, München, Germany, 2017.
- [NIO20] NIO. NIO Power Swap. Available at <https://www.nio.com>, 2020. Accessed on 19.2.2020.
- [NIS18] NISSAN. Technical data NISSAN Leaf. Available at <https://www.nissan.at>, 2019. Accessed on 2.12.2018.
- [NPE10] NPE Nationale Plattform Elektromobilität. Zwischenbericht der Nationalen Plattform Elektromobilität, January 10 2010.
- [oAE17] Society of Automotive Engineers. SAE J2954: Wireless Power Transfer for Light-Duty Plug-In Electric Vehicles and Alignment Methodology J2954 201711. International Standard, 17 November 2017.
- [OBS20] EUROPEAN ALTERNATIVE FUELS OBSERVATORY. Total number of infrastructure 2019. Available at <https://www.eafo.eu>, 2020. Accessed on 5.1.2020.
- [ORG99] INTERNATIONAL STANDARD ORGANIZATION. ISO 9283:1998: Manipulating industrial robots – Performance criteria and related test methods. International standard, Technical Committee ISO/TC 184 and CEN/TC 310 . 1999.
- [P. 18] P. Komarnicki and J. Haubrock. Elektromobilität und Sektorenkopplung. Springer Vieweg, Heidelberger Platz 3, 14197 Berlin, Germany, 2018.

- [Pan15] J. Pan. Robotersystem für das automatisierte Betanken von Elektrofahrzeugen. Bachelor Thesis. Institute of Automotive Engineering, University of Technology Graz, Graz, Austria 2015, 2015.
- [PGKW13] P. Plötz, T. Gnann, A. Kühn, and M. Wietschel. Markthochlaufszszenarien für Elektrofahrzeuge: Langfassung ; Studie im Auftrag der acatech - Dt. Akademie der Technikwissenschaften und der Arbeitsgruppe 7 der Nationalen Plattform Elektromobilität (NPE). Fraunhofer-Institut für System- und Innovationsforschung (ISI), Karlsruhe, 2013.
- [PJWZ09] A. Pech, K. Jens, G. Warmuth, and J. Zeininger. *Parkhäuser - Garagen: Grundlagen, Planung, Betrieb*, volume 18 of *Baukonstruktionen*. Springer, Wien, 2. edition, 2009.
- [Pri05] N. Priyantha. The Cricket Indoor Location System. In *Proceedings of the 2011 International Conference on Indoor Positioning and Indoor Navigation (IPIN)*, PhD Thesis, Massachusetts Institute of Technology. 2005.
- [Ran20] C. Randall. BJEV plans to build 3,000 battery swapping stations. Available at <https://www.electrive.com>, September 2019. Accessed on 19.2.2020.
- [REA19] REAL. COSTWAY shunting aid. Available at <https://www.real.de>, 2019. Accessed on 5.1.2019.
- [Rec16] K. Rechberger. EVs und Schnellladen bei Porsche. Report. Porsche AG. 27 April 2016.
- [REN19] RENAULT. Technical data RENAULT ZOE. Available at <https://www.renault.at>, 2019. Accessed on 30.1.2019.
- [Res18] Research project KoMoT. KoMoT - Comfortable Mobility by Technology Integration. Funded by the Austrian research funding association (FFG) and the Austrian Federal Ministry of Transport, Innovation and Technology (bmvit). Project partners: Magna Steyr Engineering, KEBA AG, Institute of Automotive Engineering, University of Technology Graz, Graz, 2018.
- [ROB17] UNIVERSAL ROBOTS. Technical data Universal Robot UR10. Available at <https://www.universal-robots.com>, 2017. Accessed on 3.7.2017.
- [RP07] J. Reijnders and H. Peremans. Biomimetic Sonar System Performing Spectrum Based Localization. In *IEEE Transactions on Robotics*, volume 23, 2007.
- [RPBL18] L. Roveda, N. Pedrocchi, M. Beschi, and Tosatti L. High-accuracy robotized industrial assembly task control schema with force overshoots avoidance. volume 71, pages 142–153. Elsevier, 2018.
- [Sch10] M. Schmidt. Positionsbestimmung in Gebäuden. Freie Universität Berlin, Januar 2010.

- [Sch13] H. Schrieber. Laden ohne Kabel - Laden leicht gemacht: Ein Hamburger Unternehmer zeigt, wie die Stromübertragung bei Elektroautos ohne Kabel funktioniert. Induktion heißt das Zauberwort. Available at <https://www.autobild.de/artikel/schriebers-stromkasten-teil-86-1206801.html>, 2019. Accessed on 27.6.2013.
- [Sch17] M. Schöttle. Ende der Henne-Ei-Diskussion. In *Proceedings of ATZelektronik*, volume 4, 1 August 2017.
- [Sch20] S. Schaal. TESLA erhöht die Ladeleistung im Model 3 auf 200 kW. Available at <https://www.electrive.net>, 2020. Accessed on 01.02.2020.
- [SMC⁺13] S. Spizzi, L. Marengo, G. Campatelli, R. Barbieri, A. Meneghin, R. Ceravolo, L. Zanotti, C. Surace, R. Johannson, G. Geulen, M. Dierkes, L. Homer, and J. Fiedler. Unplugged Deliverable 3.1? Technical feasibility of en-route charging. Technical report, 30 December 2013.
- [SNT⁺11] T. Sato, S. Nakamura, K. Terabayashi, M. Sugimoto, and H. Hashizume. Design and Implementation of a Robust and Real-time Ultrasonic Motion-capture System. In *Proceedings of the 2011 International Conference on Indoor Positioning and Indoor Navigation (IPIN)*. Guimarães, Portugal. Sept. 21-23, 2011.
- [SOL20] SONY DEPTHSENSING SOLUTIONS. DS311 and DS325 datasheets. Available at: <https://www.sony-depthsensing.com>, 2020. Accessed on 2020.
- [SR14] H. Süße and E. Rodner. Bildverarbeitung und Objekterkennung: Computer Vision in Industrie und Medizin. Springer Vieweg, Wiesbaden, 2014.
- [SS10] H. Schweinzer and S. Syafrudin. LOSNUS: An Ultrasonic System Enabling High Accuracy and Secure TDoA Locating of Numerous Devices. In *Conference on Indoor Positioning and Indoor Navigation (IPIN), Campus Science City, ETH Zurich, Switzerland.*, 15 September, 2010.
- [SSB⁺14] A. Siegrist, P. Schnabl, S. Burkhart, P. De Haan, and R. Bianchetti. Elektromobilität - Studie Ladeinfrastruktur Region Basel. Final Report. Zürich, 10 October 2014.
- [SSS17] A. Sophian, W. Sediono, and M. Salahudin. Evaluation of 3D-Distance Measurement Accuracy of Stereo-Vision Systems. pages 5946–5951, 10-12 May 2017. Vienna, Austria, 2017.
- [Ste18] M. Steinebach. Der Weg ist das Ziel: Automatischer Tankwart für Elektrofahrzeuge. Available at <https://www.tu-chemnitz.de/tu/pressestelle/aktuell/7039>. 2015. Accessed on 12.3.2018.
- [Sto15] J. Stocker. Kelag und Tesla: Die größte und leistungsfähigste E-Tankstelle in Österreich. Available at <http://www.ots.at/presseaussendung/OTS20150618OTS0297>, 2015. Accessed on 29.12.2015.
- [Sys19] Serva Transport Systems. RAY Parking. Available at <https://serva-ts.com/de/home-de-2/>, 2019. Accessed on 9.11.2019.

- [TAM19] TAMRON. Technical data lens M118FM06. Available at <https://www.tamron.biz>, 2014. Accessed on 10.8.2019.
- [TEC20] SONITOR TECHNOLOGIES. Ultrasound positioning- 20 years of industry leading innovation. Available at <https://www.sonitor.com>, 2011. Accessed on: 30.05.2020.
- [TES15] TESLA. Battery swapping system and techniques. US Patent 0,307,068, 29 October 2015.
- [TES16] TESLA. Charger prototype finding its way to Model S. Available at <https://www.youtube.com/watch?v=uMM0IRfX6YI>, 2015. Accessed on 6.8.2016.
- [TES20a] TESLA. All Tesla Cars Being Produced Now Have Full Self-Driving Hardware. Available at <https://www.tesla.com>, 2020. Accessed on 25.5.2020.
- [TES20b] TESLA. TESLA homepage. Available at <https://www.tesla-motors.com/deAT/>, 2020. Accessed on 31.1.2020.
- [THE20] THE VERGE. I took a ride in WAYMO's fully driverless car. Available at <https://www.youtube.com>, 2019. Accessed on 25.5.2020.
- [Tob16] W. Tober. Praxisbericht Elektromobilität und Verbrennungsmotor: Analyse elektrifizierter Pkw-Antriebskonzepte. Report ÖVK. Springer Vieweg, Wiesbaden, 2016.
- [VEL20] VELODYNE LIDAR. VELODYNE LIDAR surround sensor systems. Available at <https://velodynelidar.com/products>, 2020. Accessed on 30.05.2020.
- [VF17] M. Vogt and K. Fels. Bedarfsorientierte Ladeinfrastruktur aus Kundensicht: Handlungsempfehlungen für den flächendeckenden Aufbau benutzerfreundlicher Ladeinfrastruktur : Schaufenster Elektromobiltät - eine Initiative der Bundesregierung. Report. Deutsches Dialog Institut GmbH, Frankfurt am Main, March 2017.
- [Vin17] J. Vince. Mathematics for Computer Graphics. Springer Verlag, London, 5. edition, 2017.
- [VLO18] VKW VLOTTE. VKW VLOTTE Ladestationen in Vorarlberg - Das leistungsfähige VLOTTE Ladenetz der illwerke vkw. Available at <https://www.vlotte.at/vkw-vlotte-ladestationen-in-vorarlberg.html>, 2018. Accessed on 7.11.2018.
- [VOL16] VOLKSWAGEN. e-smartConnect: VOLKSWAGEN is conducting research on an automated quick-charging system for the next generation of electric vehicles. Available at <https://www.volkswagen-newsroom.com/>, 2015. Accessed on 1.2.2016.
- [VOL18a] VOLKSWAGEN. Technical data and specifications VOLKSWAGEN e-Golf. Available at <https://www.volkswagen.at/e-golf/infomaterial>, 2019. Accessed on 28.11.2018.
- [VOL18b] VOLTERIO. Redefining charging for e-mobility, Available at www.volterio.com, 2018. Accessed on 10.9.2018.

- [VOL19a] VOLKSWAGEN. Neue Elektroplattform von Audi und Porsche (PPE). Available at <https://www.auto-motor-und-sport.de>, 2019. Accessed on 10.11.2019.
- [VOL19b] VOLVO. Kein lästiges Parkplatzsuchen mehr: VOLVO stellt das selbstparkende Auto vor. Available at <https://www.media.volvocars.com>, 2013. Accessed on 1.2.2019.
- [VR90] G. Van Rossum. Python programming language. Stichting Mathematisch Centrum (CWI), Amsterdam, Nederland, 1990.
- [WAU20] WAUTOWORLD. TESLA Model 3 Europe is coming with a CCS2 charge port, Model S and X adapter also in the works. Available at <https://www.xautoworld.com>, 2020. Accessed on 01.02.2020.
- [WAY17] WAYMO. Waymo Safety Report - On the Road to Fully Self-Driving, 2017.
- [WAY20] WAYMO. We are building the World's Most Experienced Driver. Available at <https://waymo.com>, 2020, Accessed on 27.5.2020.
- [WBH18] B. Walzel, H. Brunner, and M. Hirz. Autonomes Parken und Laden von E-Fahrzeugen. In *Berichte des des Österreichischen Vereins für Kraftfahrzeugtechnik (ÖVK)*. 2018.
- [WFO10] H. Wallentowitz, A. Freialdenhoven, and I. Olschewski. *Strategien zur Elektrifizierung des Antriebsstranges: Technologien, Märkte und Implikationen*. Vieweg + Teubner, Wiesbaden, 1. edition, 2010.
- [WH18] B. Walzel and M. Hirz. Smart Parking - Neue Fahrzeugkonzepte und Technologien welche die Parksituation verbessern. Technical Report 3. Institute of Automotive Engineering, University of Technology Graz, Graz, Austria 2018, 2018.
- [WHB16] B. Walzel, M. Hirz, and H. Brunner. Anforderungen an die Tankstelle im Jahr 2025. In *Proceedings of 14. Symposium Energieinnovation: Energie für unser Europa*, 10-12 Februar 2016, Graz, Austria, 2016.
- [WHB19a] B. Walzel, M. Hirz, and H. Brunner. Automated Charging of Electric Vehicles with Conductive Charging Standards. In *40. Internationales Wiener Motorensymposium, 2019*, volume 2, pages 462–476, 15-17 Mai 2019. Vienna, Austria, 2019.
- [WHB19b] B. Walzel, M. Hirz, and H. Brunner. Verfahren zum automatisierten Herstellen einer Steckverbindung zum Laden von Elektrofahrzeugen. Patent pending Germany 126 377.8, 18 October 2019.
- [WHB19c] B. Walzel, M. Hirz, and H. Brunner. Robot-Based Fast Charging of Electric Vehicles. In *WCX SAE World Congress Experience*, 2 April 2019. Detroit, Michigan, 2019.
- [WP10] E. Wan and A. Paul. A Tag free Solution to Unobtrusive Indoor Tracking Using Wallmounted Ultrasonic Transducers. In *Proceedings of the 2010 International Conference on Indoor Positioning and Indoor Navigation (IPIN)*, 2010.

- [Wüs04] K. Wüst. Grundlagen der Robotik. Universities lecture script. Technische Hochschule Mittelhessen, Germany. April 2004.
- [Zho15] W. Zhou. Vehicle charge robot. US Patent 9,056,555 B1. 16 June 2015.